

University of Bath



PHD

The catalytic dehydration of alcohols.

Olaofe, O.

Award date:
1982

Awarding institution:
University of Bath

[Link to publication](#)

General rights

Copyright and moral rights for the publications made accessible in the public portal are retained by the authors and/or other copyright owners and it is a condition of accessing publications that users recognise and abide by the legal requirements associated with these rights.

- Users may download and print one copy of any publication from the public portal for the purpose of private study or research.
- You may not further distribute the material or use it for any profit-making activity or commercial gain
- You may freely distribute the URL identifying the publication in the public portal ?

Take down policy

If you believe that this document breaches copyright please contact us providing details, and we will remove access to the work immediately and investigate your claim.

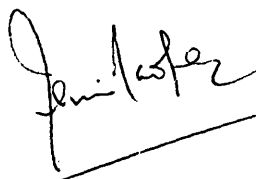
THE CATALYTIC DEHYDRATION OF ALCOHOLS

Submitted by: O. Olaofe
for the degree of Ph.D.
of the University of Bath
1982

COPYRIGHT

Attention is drawn to the fact that copyright of this thesis rests with its author. This copy of the thesis has been supplied on condition that anyone who consults it is understood to recognise that its copyright rests with its author and that no quotation from the thesis and no information derived from it may be published without the prior written consent of the author.

This thesis may be made available for consultation within the University Library and may be photocopied or lent to other libraries for the purpose of consultation.



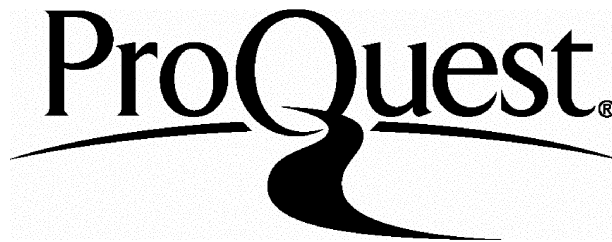
ProQuest Number: U334154

All rights reserved

INFORMATION TO ALL USERS

The quality of this reproduction is dependent upon the quality of the copy submitted.

In the unlikely event that the author did not send a complete manuscript and there are missing pages, these will be noted. Also, if material had to be removed, a note will indicate the deletion.



ProQuest U334154

Published by ProQuest LLC(2015). Copyright of the Dissertation is held by the Author.

All rights reserved.

This work is protected against unauthorized copying under Title 17, United States Code.
Microform Edition © ProQuest LLC.

ProQuest LLC
789 East Eisenhower Parkway
P.O. Box 1346
Ann Arbor, MI 48106-1346

UNIVERSITY OF BATH		
LIBRARY		
34	- 5OCT 1982	PRO
PHD		

ACKNOWLEDGMENT

I am greatly indebted to Dr. Po-Lock Yue for supervising this work. His suggestions, co-operation and useful assistance are sincerely appreciated.

I thank Prof. W.J. Thomas very much for providing the equipment used in this study.

Many thanks to Mr. T. Walton, Mr. L. Steel and other technical staff for their useful assistance during the experimental work and to fellow students for their useful discussions.

I gratefully acknowledge the financial support provided under the Commonwealth Scholarship Scheme.

Finally, I am most grateful to my wife - Mrs. F.K. Olaofe and son, Temitope for their encouragement and moral support throughout my studies.

CONTENTS

NOMENCLATURE

SUMMARY

CHAPTER 1	MECHANISM, THERMODYNAMICS AND KINETICS	Page
	OF THE PRODUCTION OF LIGHT OLEFINS AND	
	ETHERS FROM THE DEHYDRATION OF ALCOHOLS	1
1.1	Introduction	1
1.1.1	Layout of the Thesis	3
1.2	Reaction Mechanisms	5
1.2.1	Mechanism for the Formation of	
	Olefin	5
1.2.2	Mechanism for the Formation of	
	Ether	6
1.3	Chemical Reaction Thermodynamic	
	Equilibrium Constant	8
1.4	Review of Kinetic and Product	
	Selectivity Studies	9
1.4.1	The Reaction Scheme	9
1.4.2	Kinetics and Product selectivity	11
1.5	Catalyst	14
1.5.1	Zeolites	14
1.5.2	Ion-exchange Resin	15
1.6	Principal Conclusions in	
	Literature	16

CHAPTER 2	EXPERIMENTAL, APPARATUS AND OPERATION	19
2.1	Introduction	19
2.2	Selection of Reactor	20
2.3	Basic Principles and Features of CSGSR	23
2.4	Experimental Equipment	28
2.4.1	Feed Preparation Unit	28
2.4.1.1	Nitrogen Supply	28
2.4.1.2	Alcohol supply	29
2.4.2	Evaporation Unit	30
2.4.3	Reactor Unit	32
2.4.3.1	Continuous Stirred Gas Solid Reactor	32
2.4.3.2	Packed Tubular Reactor	35
2.4.4	Sample Analysis	37
2.4.5	Effluent Treatment	40
2.4.6	Safety Aspects	41
2.4.7	Operation Procedures	42
2.5	Selection of Reaction Conditions	44
CHAPTER 3	MODELLING OF THE DEHYDRATION REACTION KINETICS	47
3.1	Introduction	47
3.2	Transport and Kinetic Processes	49

3.3	Power Function Rate Expression	50
3.3.1	Power Function Model	51
3.4	Hougen-Watson Approach	52
3.4.1	Reaction Steps	55
3.4.2	Equilibrium Considerations	56
3.4.3	Adsorption of Alcohol as Rate Controlling Step	58

CHAPTER 4	RESULTS AND DISCUSSION OF THE KINETIC DATA ON THE CATALYTIC DEHYDRATION OF ALCOHOLS IN A CSGSR	61
-----------	--	----

4.1	General Considerations	61
4.1.1	Introduction	61
4.1.2	Main Side Reactions	62
4.1.3	Mass and Heat Transfer Effects	63
4.1.4	Mathematical Estimation of Chemical Constants	64
4.1.5	Preliminary Discrimination and Simplification of Hougen- Watson Rate Expression	64
4.2	Results and Discussion of the Dehydration of alcohols over zeolites	68
4.2.1	Kinetic Data	68
4.2.2	Kinetic Expression	69
4.2.2.1	Empirical Power Law	69

4.2.2.2	Hougen-Watson Rate Expression	73
4.2.2.2.1	Kinetic Expression for the Formation of Olefin	74
4.2.2.2.2	Kinetic Expression for the Formation of Ether	78
4.3	Results and Discussion of the Dehydration of Isopropanol and Ethanol over Synthetic Cation Exchange Resin	84
4.3.1	Introduction	84
4.3.2	Kinetic Rate Expression	91
4.3.2.1	Power Function Rate Expression	91
4.3.2.2	Hougen-Watson Rate Expression	95
4.3.2.2.1	Rate of Formation of Olefin	95
4.3.2.2.2	Rate of Formation of Ether	98
4.3.2.2.2.1	Formation of Di-isopropyl Ether	98
4.3.2.2.2.2	Formation of Di-ethyl Ether	100
4.4	Conclusions	103

CHAPTER 5 MECHANISM, SELECTIVITY, REACTIVITY OF
ALCOHOLS AND ACTIVITY OF ZEOLITES 106

5.1	Alkene Product Distribution	106
5.1.1	Introduction	106
5.1.2	The Effect of Partial Pressure of Alcohol	108

5.1.3	The Effect of Reaction Temperature	109
5.1.4	Discussion	111
5.1.4.1	Product Distribution	111
5.1.4.2	Reaction Mechanism	117
5.2	Activity of Zeolites	122
5.3	Selectivity	125
5.3.1	Geometrical Shape Selectivity	
	Selectivity	125
5.3.2	Molecular Shape Selectivity	126
5.3.3	Thermal Selectivity	128
5.4	Reactivity of Alcohols	129
5.5	Conclusions	134
CHAPTER 6 MODELLING OF CATALYTIC BED REACTOR		136
6.1	Introduction	136
6.2	Mathematical Description of Catalytic Packed Bed Reactor	137
6.3	Chemical Reactions Rates	140
6.4	Solution of the Mathematical Model	141
6.4.1	Ideal Plug Flow Reactor	141
6.4.2	One-Dimensional Plug Flow with Axial Dispersion Term	142
6.4.3	Two-Dimensional Pseudo Homogeneous Model	144

6.5	Results and Discussion	145
6.6	Summary	148
CHAPTER 7	CONCLUSIONS AND RECOMMENDATIONS	149
7.1	Conclusions	149
7.2	Recommendations	151
APPENDIX 1	HOUGEN-WATSON TYPE RATE EQUATION	A1
APPENDIX 2	POWER FUNCTION RATE EXPRESSION	A14
APPENDIX 3	EFFECTS OF INTRA-PARTICLE MASS AND HEAT TRANSPORT	A15
APPENDIX 4	TABLES OF EXPERIMENTAL KINETIC DATA AND ESTIMATED PARAMETERS	A17
APPENDIX 5	THE PERCENTAGE DISTRIBUTION OF BUTENE	A61
APPENDIX 6	THE EFFECTS OF EXTERNAL MASS AND HEAT TRANSPORT	A68
	TABLES A6.1 AND A6.2	A72
REFERENCES		A76

NOMENCLATURE

A	reactant (Alcohol) or constant	-
A_0	frequency factor, units same as the corresponding kinetic constant.	
a	reaction order with respect to A or constant	-
a_i	parameters or constant	-
B	constant	-
Bi	Biot number $(\frac{\alpha_w d_t}{G_m C_p d_p})$	-
$Bo_{m,a}$	axial Peclet group number for mass diffusion $(Ud_p/D_{e,a})$	-
$Bo_{m,r}$	radial Peclet group number for mass diffusion $(Ud_p/D_{e,r})$	-
b_i	constant or parameter	-
C	constant	-
C_j	molar concentration of component j in the mixture	Kgmol m^{-3}
CS_j	molar concentration of component j chemisorbed on the catalyst active site	Kgmol m^{-3}
c_i	parameters or constant	-
\bar{C}_p	mean heat capacity	$\text{J Kg}^{-1} \text{K}^{-1}$
D_e	effective pore diffusivity	$\text{m}^2 \text{s}^{-1}$
$D_{e,a}$	axial effective diffusivity	$\text{m}^2 \text{s}^{-1}$
$D_{e,r}$	radial effective diffusivity	$\text{m}^2 \text{s}^{-1}$

d_p	particle diameter	m
d_t	reactor diameter	m
E	component (Ether)	-
E_R	reaction activation energy	KJ Kgmol ⁻¹
e	reaction order with respect to component E	-
F	total mass flowrate	Kgmol s ⁻¹
G_m	superficial mass flow rate	Kg m ⁻² s ⁻¹
ΔH_A	heat of adsorption	KJ Kgmol ⁻¹
ΔH_j	heat of formation of component j	KJ Kgmol ⁻¹
ΔH_R	heat of reaction	KJ Kgmol ⁻¹
h	step size	-
I	inerts	-
K_{eq}	thermodynamic equilibrium constant	Kgmol m ⁻³ or -
K_j	adsorption equilibrium constant	m ³ Kgmol ⁻¹
k_a	forward adsorption constant	Kgmol s ⁻¹
k_d	backward adsorption constant	Kgmol s ⁻¹
K_{Ri}	forward kinetic constant of reaction i	Kgmol Kg _c s ⁻¹
k_{-i}	backward kinetic constant of reaction i	Kgmol Kg _c s ⁻¹
l	reactor length	m
LHM	Langmuir-Hinshelwood mechanism	-
l	grid position number at the wall	-
l_o	reactor length	m
M	molecular weight	Kg Kgmol ⁻¹
\bar{M}	mean molecular weight	Kg Kgmol ⁻¹

m	order of reaction or grid position number	-
N_T	total number of mole	Kgmol
n	order of reaction or grid position number	-
O	component (Olefin)	-
o	order of reaction with respect to component O	-
P	pressure	$N\ m^{-2}$
$Pe_{h,a}$	axial Peclet group number for the heat transfer $(\frac{G_m C_p d_p}{\lambda_{e,a}})$	-
$Pe_{h,a}$	radial Peclet group number for heat transfer $(\frac{G_m C_p d_p}{\lambda_{e,r}})$	-
P_j	partial pressure of component j in a reaction system	$N\ m^{-2}$
Pr	Prandtl number $(\bar{C}_p / \mu \lambda_g)$	-
P_t	total pressure	$N\ m^{-2}$
Re	Reynolds number $(\frac{G_m d_p}{\mu})$	
R_g	gas constant (8.310)	$KJ\ Kg\ mol^{-1}\ K^{-1}$
R_j	net rate of formation or disappearance of component j	$Kg\ mol\ Kg^{-1}\ s^{-1}$
R_o	tube diameter	m
REMI	Rideal-Eley mechanism based on dual sites	
REM2	Rideal-Eley mechanism based on single site	-

r	radius of reactor	m
r_j	net rate of adsorption-desorption process of component j	Kgmol s ⁻¹
r_j	net rate of formation or disappearance of component j	Kgmole Kg s ⁻¹
S	selectivity (R_O/R_E) or speed	- or RPM
S	number of vacant active site	-
S_0	total number of active site	-
SR1	surface reaction controlling based on single site	-
SR2	surface reaction controlling based on dual sites	-
SSR	sum of squares of residual	-
T	temperature	K
T_w	wall temperature	K
t	time	s
U	superficial velocity	m/s
V_j	volume	m ³
W	component (Water)	-
W_g	total weight of catalyst	Kg
w	reaction order with respect to component W	-
X	dimensionless variable	-
x_j	fractional conversion to component j	-
x	variable	

x_j	mole of component j in the mixture	Kgmole
Y	dimensionless parameter	-
Z	dimensionless parameter	-

Greek Symbols

α_w	wall heat transfer co-efficient	$\text{KJ m}^{-1} \text{s}^{-1}$
β	kinetic parameter	$\text{Kgmole Kg}^{-1} \text{s}^{-1}$
ϵ	void fraction or deviation	-
θ	dimensionless parameter (T/T_0)	-
$\lambda_{e,a}$	axial effective thermal conductivity	$\text{KJ m}^{-1} \text{s}^{-1} \text{K}^{-1}$
$\lambda_{e,r}$	radial effective thermal conductivity	$\text{KJ m}^{-1} \text{s}^{-1} \text{K}^{-1}$
μ	dynamic viscosity	$\text{Kg m}^{-1} \text{s}^{-1}$
ρ_b	catalyst bulk density	Kg m^{-3}
ρ_f	fluid density	Kg m^{-3}
ρ_m	catalyst material density	Kg m^{-3}
ρ_p	particle density	Kg m^{-3}

r	radial direction	-
s	surface	-
t	total or true or tube	-
W	water	-
w	at the wall	-

SUMMARY

The vapour phase dehydration of ethanol, isopropanol and n-butanol over zeolites 13X, 4A and ZNa and the synthetic cation exchange resin Dowex 50-X-8 has been studied in a continuous stirred gas solid reactor covering a wide range of experimental conditions.

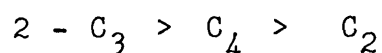
Both principal products, ether and olefin were produced. The kinetic data procured have been satisfactorily correlated both with the empirical power function and the Hougen-Watson type of rate expressions. For the former type of correlation, reaction orders, activation energies and pre-exponential factors for both simultaneous reactions were established for each zeolite and each alcohol. The kinetic data on the dehydration of alcohol over the synthetic cation exchange resin were also satisfactorily correlated by power function rate equations. But the activation energies and pre-exponential factors obtained were markedly different from those for zeolites because of the effect of the adsorption process.

Qualitative and statistical considerations were used to discriminate among different Hougen-Watson models. The rate expression based on surface reaction controlling was found to satisfactorily fit the kinetic data. The kinetic and adsorption parameters in the Hougen-Watson rate expression have been satisfactorily correlated as functions of reaction temperature.

The activity and selectivity of the zeolites have been systematically investigated. The activity pattern was explained in terms of surface area, pore size and acidic and basic strength. The importance of geometrical shape on selectivity was clearly demonstrated.

The synthetic cation exchange resin was found to be suitable for the exclusive production of di-ethyl ether from the dehydration of ethanol. However both di-isopropyl ether and propene were formed from the dehydration of isopropanol under the reaction conditions studied.

The sequences of the reactivity and activation energy of the alcohols were explained in terms of an inductive effect and a positively charged intermediate complex. The order of reactivity of alcohols for all the catalysts used was



Activation energies and pre-exponential factors were satisfactorily correlated with an empirical relationship called the 'compensation effect'. Molecular shape selectivity, that is selectivity of the same catalyst between two molecules of different shapes, was assessed.

Product distribution from the dehydration of n-butanol was investigated to gain insight of the reaction mechanism. The formation of 2-alkenes (cis-2-butene and trans-2-butene)

in the absence of isomerization reactions during the catalytic dehydration of n-butanol over zeolites is unambiguous evidence in favour of a positively charged intermediate, indicating that the reaction proceeds via a E1 type of mechanism. Experimental data also showed the preferential formation of cis-2-butene over that of trans-2-butene.

Fixed bed reactor behaviour was simulated using one and two dimensional pseudo-homogeneous isothermal models to test the adequacy of the rate expressions established for the dehydration of isopropanol over zeolite 13X. Experimental conversion data were gathered from a packed tubular reactor. The experimental data agreed fairly well with the predictions of the models.

CHAPTER 1

MECHANISM, THERMODYNAMICS AND KINETICS OF THE PRODUCTION

OF LIGHT OLEFINS AND ETHERS FROM THE DEHYDRATION OF

ALCOHOLS.

CHAPTER 1

MECHANISM, THERMODYNAMICS AND KINETICS OF THE PRODUCTION OF LIGHT OLEFINS AND ETHERS FROM THE DEHYDRATION OF ALCOHOLS.

1.1 Introduction

Reaction kinetic studies provide some of the vital information which are needed for the design of catalytic reactors. A more thorough understanding of the reaction routes, mechanisms and a knowledge of reliable kinetic models can lead to better and safer process development and design.

The purpose of this work is to study the kinetics of the production of light olefins and ethers from alcohols over selected solid catalysts. Such studies would lead to the development of useful kinetic model equations and the selection of better catalysts for the alcohol-based chemical industries.

Although the catalytic dehydration of some alcohols over solid catalysts have been reported in literature (1-6), doubts still exist on reaction routes and mechanism. Kinetic data for some solid catalysts are still within very limited reaction conditions. In the

case of the dehydration of n-butanol, product distribution has not been studied in great detail. The present investigation is therefore focused on some of the controversial or missing aspects so as to supplement, confirm or contradict what is known in literature.

Light olefins ($C_2 - C_5$) are basic and important industrial products which are produced at an annual rate of millions of tons in Western Europe (7). They are valuable starting raw materials for the production of high octane alkylates and other commercially useful chemicals. For example, ethylene is used for the production of poly-vinyl chloride (PVC), ethylene glycols, ethylene oxides, etc.

Conventionally, light olefins are produced via steam cracking of naphtha. In some developing countries where there are scant petroleum sources, there may however be abundant supply of alcohols from fermentation processes. The production of olefins can be achieved economically by the catalytic dehydration of alcohols in small plants. This method of olefin production has already been achieved in India, Pakistan, Peru, Brazil, Australia and East Germany (8).

Ethers can be produced commercially from alcohols by passing evaporated alcohol over solid catalyst in a fixed

bed or a mixture of alcohol and acid through a tubular reactor. The latter method has problems with separation of products, unreacted alcohol and acid solution catalysts, as well as problems of corrosion of process equipment. Hence the study of the former process is of more practical interest.

It is hoped that the present study will make some small contribution towards the development of processes for producing olefins and ethers by the catalytic dehydration of alcohols.

1.1.1 Layout of the Thesis.

This thesis discusses theoretical and experimental work on the catalytic dehydration of alcohols.

Chapter one reviews the literature in the field of dehydration of alcohols over solid catalysts. Attention is paid to ethanol, isopropanol and n-butanol over solid catalysts of interest.

Chapter two discusses the experimental equipment and operation. The basic principles of the continuous stirred gas solid reactor, CSGSR, analysis procedure and safety considerations were discussed.

The modelling of dehydration reaction kinetics according to the empirical power function law and the

Hougen-Watson approach is presented in chapter 3.

The kinetic data from the CSGSR on the dehydration of alcohols are fully discussed in chapter 4. This chapter is divided into three sections; general considerations, results and discussion of alcohols over zeolites and results and discussion of isopropanol and ethanol over synthetic exchange resin.

Chapter 5 considers the use of product distribution for mechanistic studies, the importance of geometrical and molecular shapes on selectivity, the influence of zeolite properties on catalytic activity and the reactivity of alcohols.

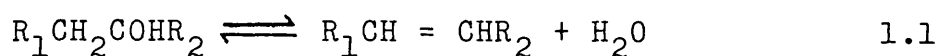
Chapter 6 reports the simulation of the behaviour of an isothermal tubular reactor. The predictions of pseudo-homogeneous isothermal models are compared with the experimental conversion data procured from an isothermal fixed bed reactor.

Whenever appropriate, a summary or major conclusions are presented at the end of a chapter. Major conclusions of the present work and recommendations for further studies are also presented in chapter 7.

1.2 Reaction Mechanisms

1.2.1 Mechanism for the Formation of Olefin.

The catalytic dehydration of alcohol to olefin is a typical example of elimination reactions which can be represented as



The mechanisms of elimination reactions, with particular reference to the catalytic dehydration of alcohol in solution and in vapour phase, have been extensively reviewed by Pines and Manassen (1), Venuto and Landis (2) and Emmett (3) and have been discussed in (10). Noller et al. (11, 12) have also given an extensive review of elimination reactions over polar catalysts.

Three different types of mechanisms have been proposed for the elimination reactions, which lead to the formation of a double bond, in an organic molecule. They are called E1, E2 and E1cB mechanisms.

The dehydration reaction via E1 mechanism is a two-step process. The C-X bond is broken first and an intermediate carbenium ion is produced. The E2 type of mechanism involves the simultaneous abstraction of hydrogen atom from the β -carbon atom by the basic site and the abstraction of electronegative species from the α -carbon atom by the paired acidic site. E1cB (cB = conjugate base) is referred

to as 'step wise E2 mechanism'. It is also a two step mechanism, but C-H bond is broken first and an intermediate carbanion is formed.

The type of mechanisms that an elimination reaction may follow depends on the following factors (10, 11, 12).

- a) The easier the electronegative species X can be removed, the more the mechanism shifts towards E1 type. The ease of removal of the electronegative species is a function of the heterolytic C-X bond, dissociation energy and substituted group at α and β carbon atoms.
- b) The type of catalyst site involved: Catalyst surface with higher electron pair acceptor or that which is capable of losing a proton favours the E1 type mechanism.
- c) Reaction temperature: Increasing reaction temperature shifts the elimination reaction mechanism towards the E1 type.

1.2.2 Mechanism for the Formation of Ether.

The catalytic dehydration of alcohol to ether can proceed according to two types of mechanism:

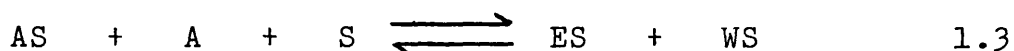
- a) Langmuir-Hinshelwood mechanism (LHM).
- b) Rideal-Eley mechanism (REM).

LHM is the reaction of two adjacently chemisorbed alcohol molecules on the catalyst active sites. LHM can be considered to proceed according to



This type of mechanism has been proposed by Jain and Pillai (13).

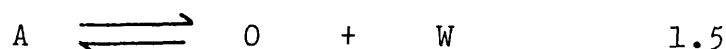
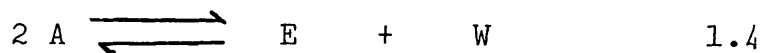
The Rideal-Eley mechanism proposes that a chemisorbed alcohol molecule reacts with an alcohol molecule in the gaseous phase in the presence of a vacant active site adjacent to the adsorbed molecule. This can be written as



There is still no conclusive experimental work to discriminate between these mechanisms for the formation of ether. Most conclusions on reaction mechanisms for the formation of ether are based on kinetic analysis. But kinetic analysis is not necessarily a useful method for the elucidation of the mechanism of a reaction. An interesting discussion on this has been given by Knozinger et al (18). A powerful tool for mechanistic studies is the use of deuterated reactant or product distribution. The former has been reported by Thomke et al (19,20). The latter is used in this study.

1.3 Chemical Reaction Thermodynamic Equilibrium Constant.

The principal simultaneous chemical reactions involved in the dehydration of alcohols can be represented by the following equations:



Reactions 1.4 and 1.5 are exothermic and endothermic respectively. Therefore the thermodynamic equilibrium constant of reaction 1.4 or 1.5 decreases or increases with increasing temperature according to Van't Hoff law. In the present work these constants K_{eq} have been estimated at various temperatures using the thermodynamic data (Gibbs free energy) of Stull et al (22). When correlated as a function of temperature, the equilibrium constant followed the form

$$\ln K_{eq} = \ln a + b/T \quad 1.6$$

The values of a and b are summarised in Table 1.1. Figures 1.2 and 1.3 show the temperature dependence of K_{eq} for the dehydration of alcohols to ethers and olefins, respectively. The correlated equation, obtained in the present study, using Stull et al (22) data, for the dehydration of ethanol to di-ethyl ether agrees perfectly well with the equation of Kabel and Johanson (21).

Table 1.1 Thermodynamic Equilibrium Constants for the
Dehydration of Ethanol, n-Propanol, Isopropanol
and n-Butanol to Ethers or Olefins.

$$K_{eq} = a_i \text{Exp}(b_i/T)$$

Alcohol	Product	a	b x10 ⁻³
Ethanol	olefin	5.4 10 ⁶	-5.6
	ether	3.1 10 ⁻²	2.8
n-Propanol	olefin	9.5 10 ⁶	-4.4
	ether	2.1 10 ⁻²	2.1
Isopropanol	olefin	48 10 ⁶	-6.2
	ether	1.1 10 ⁻²	1.7
n-Butanol	olefin	9.7 10 ⁶	-4.0
	ether	2.4 10 ⁻²	3.0

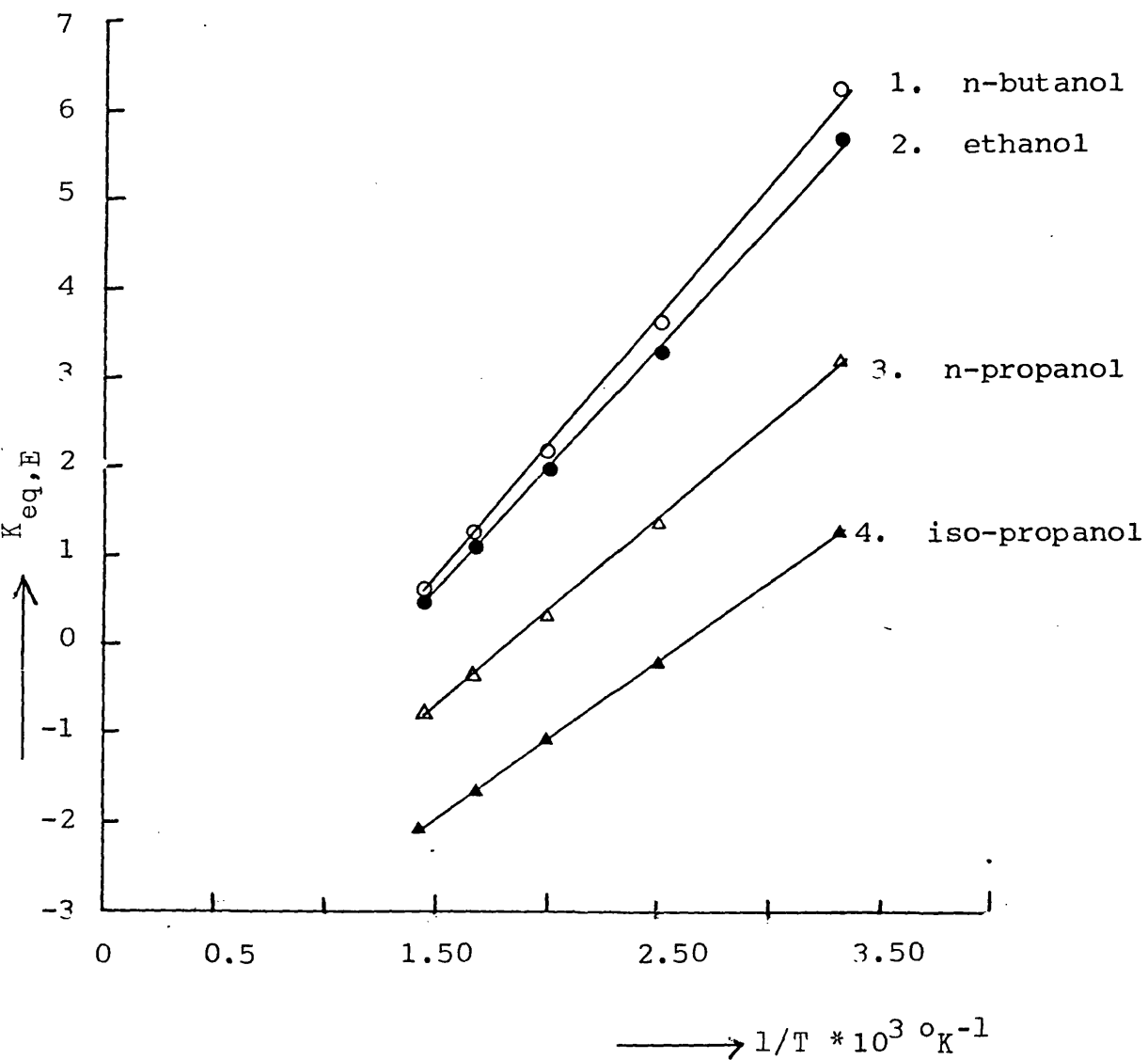
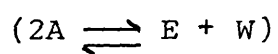


FIGURE 1.2 Temperature Dependence of the Thermodynamic Equilibrium Constant for the Dehydration of Alcohols to Ethers



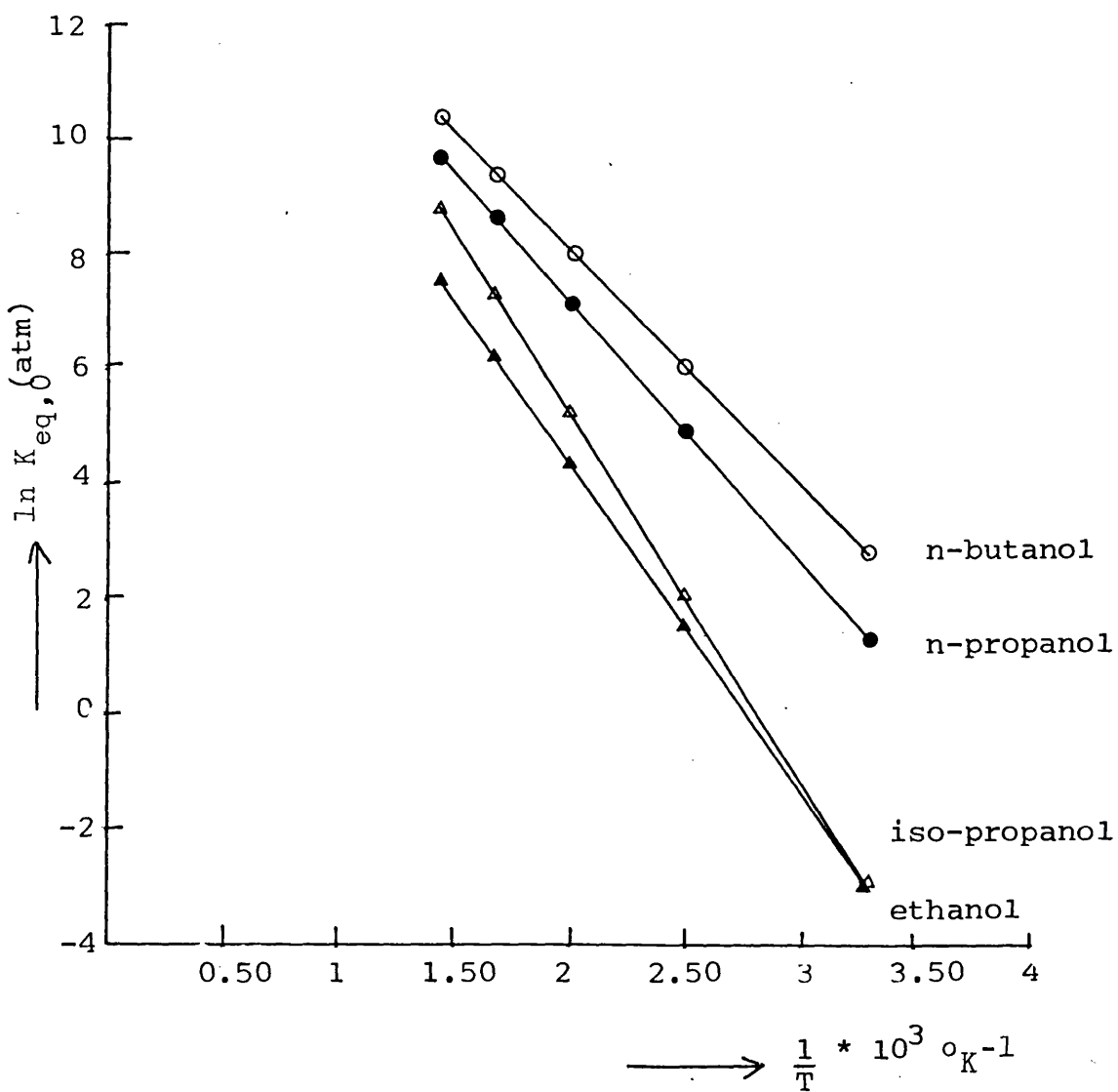
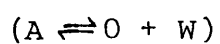
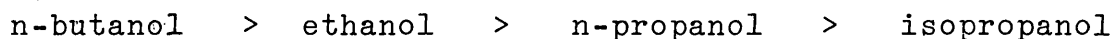


FIGURE 1.3 Temperature Dependence of the Thermodynamic Equilibrium Constant for the Dehydration of Alcohols to Olefins



The $\ln K_{eq}$ versus $1/T$ curves suggest the following:

a) The ease of ether formation by the dehydration of alcohol follows the sequence



b) The formation of ether from a branched alcohol is less favoured thermodynamically than that from its straight chain isomer.

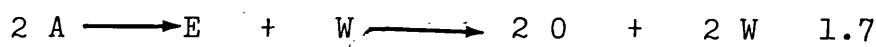
c) For these alcohols the formation of olefin would be preferred to that of ether as temperature increases, because the equilibrium constants of the reaction leading to the formation of ether are smaller.

1.4 Review of Kinetic and Product Selectivity Studies.

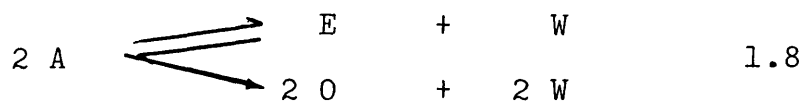
1.4.1 The Reaction Scheme.

Despite the fact that there are considerable experimental data in literature on the catalytic dehydration of alcohols, the reaction route still remains as a controversial subject (8, 23, 24). The two conflicting reaction routes (25, 26, 27) proposed in literature for the dehydration of alcohols are:

a) Consecutive reactions

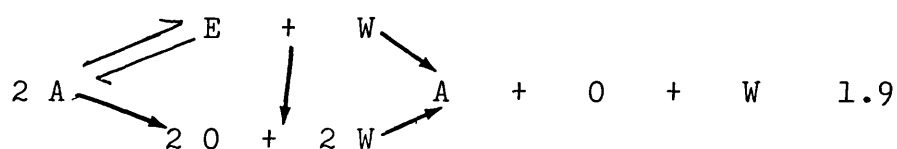


b) Simultaneous reactions



The sole reason for the choice of reaction route a) was based on the observation of a maximum in the production of ether as a function of contact time. Such maximum can occur if ether is the intermediate product. However reaction route b) can also lead to the same product distribution (27). The observed effect of the addition of ether on the rate of formation of olefin (33, 35) also favoured the latter reaction route.

Recently, a consecutive-simultaneous reaction scheme was proposed by Butt et al (32) and Knozinger and Kohne (36). The proposed scheme can be represented by



This reaction scheme can satisfactorily explain any product distribution. But it makes the dehydration reaction very complex and the scheme is of little use for design purposes.

Many workers (28, 29, 30, 31) have also reported product distribution as a function of temperature. The production of ether also goes through a maximum as the temperature increases. The product distribution appears to be the same for all alcohols except that the maximum

production of ether occurs at different temperatures. For ethanol, three regimes have been observed:

- a) At low reaction temperature, $< 250^{\circ}\text{C}$, di-ethyl ether was the principal product.
- b) In an intermediate temperature range, $250 - 350^{\circ}\text{C}$, both di-ethyl ether and ethylene were produced at about equal amounts.
- c) At high temperature, $> 350^{\circ}\text{C}$, ethylene was the only product.

On the basis of the observed product distribution an extension of the consecutive reaction was proposed (28), with the production of ether and olefin through the same intermediate product-called alkoxide. However Knozinger et al (37) have shown that dehydration of ethanol to di-ethyl ether and ethylene were not through the same intermediate.

It should be pointed out that product distribution is not necessarily a useful method for the elucidation of reaction scheme. In the analysis of product distribution (25, 26), the influence of a possible reverse reaction of formation of alcohol from ether and water had been completely neglected. That is the role of water had not been taken into consideration.

1.4.2 Kinetics and Product Selectivity.

Tables 1.2, 1.3 and 1.4 summarise the kinetic and product selectivity studies on the dehydration of ethanol, isopropanol and n-butanol, respectively.

Table 1.2 Kinetic and Product Selectivity Studies on the Dehydration of Ethanol.

Catalyst	Product	Temp. range °C	P A range atm	Model	reaction order	Controlling step	No of sites	E A Kcal gmole	Remarks	Refs
Alumina	E and O	307	0.013 to 0.14	H-W	two to zero	surface reaction	2	-	retarding species are alcohol and water	38
Resin	E	105 to 125	0 - 1.0	H-W	-	surface reaction	2	30.8	retarding components are alcohol and water	34
Alumina	E and O	138 - 220	0 - 0.04	H-W	half to zero	surface reaction	1	28 - 30	retarding species are alcohol and water	35
Alumina	E and O	205 - 307	0 - 0.2	H-W	-	surface reaction	2 and 1	25.9 10.0	retarding species are alcohol and water	32
Linde 10X, 0 13X and 5A		300 - 375		P.L	first	-	-	19, 18 and 21	acidity of catalyst was discussed.	43
Molecular sieves 3A, 4A, 5A and 13X				H-W	-	surface reaction	2	21		43
	E and O	200 - 250	low	-	-	-	-	-	product selectivity studies	45
Linde 13X	E and O	270 to 350	0.6	P.L	zero	-	-	20 and 32	product selectivity studies, assumption of zero-order kinetic.	44
Norton Zna			"	"	"	-	-	15 and 31		
Alumina			"	"	"	-	-	23 and 26		
			"	"	"	-	-	27 and 33		

E ether; O olefin; P.L Power Law; H-W Hougen-Watson.

Table 1.3 Kinetic and Product Selectivity Studies on the Dehydration of Isopropanol.

Catalyst	Prod.	Temp range °C	P _A range atm	Model	Reaction order	Controlling step	No of sites	E _A Kcal gmole	Remarks	Reference
Linde 13X powder	0	240-270	0-0.013	P.L.	first	-	-	28.4	static system, reactivity of propanols is discussed	62
Linde 13X unchanged and exchanged	0	210-277	0-0.1	P.L.	zero	-	-	33.3	continuous flow system	67
	0	110-157	"	"	"	-	-	28.6	"	67
	E	"	"	"	"	-	-	26.2	"	67
Zeolites Y and X exchanged	0	140-200	pulse technique	P.L.	first	-	-	19	activation energy over zeolite NaX, activity of zeolite is discussed.	61
Zeolites NaX and NaY	0	112-190	"	P.L.	first	-	-	22 21	22 Keal/gmole over NaX, 21 Keal/gmole over NaY	64 65
γ-Alumina	0	246	0-0.004	H-W	-	surface reaction	dual site	-	flow system	14
Resin	0 E	90-110	0-1.0	H-W	zero	surface reactions	two	28.6 24.0	no adequate correlation obtained	33
Alumina	0 E	285	0-1.0	-	-	surface reactions	-	-	mechanistic studies	13
Oxides	0 E	160-220	0.01-0.03	P.L.	less than one	-	-	26-34.2	T < 165 zero-order T > 165 fractional order	102

Table 1.4 Kinetic and Product Selectivity Studies on the Dehydration of n-Butanol.

Catalyst	Prod.	T range °C	P _A range atm	Model	Reaction order	Controlling step	No of E sites	E _A Kcal g mole	Remarks	Reference
Zeolites X	0	228	low	P.L.	first	-	-	30	reactivity of butanols was discussed.	71*
Y	0	256	low	P.L.	first	-	-	27		
γ-Alumina E	0	348-428	0.6	P.L.	zero	-	-	30.8	assumption of zero- order kinetic	73* ^e
Silica in bead form	0	205-307	1.0-7.8	H-W		surface reaction	one	16.2	data were affected by internal diffusional limitations.	74* ^e
Alumina	0	400	1.0-500	H-W	-	surface reaction	two	-		72*
Alumina	0	350 and 410	-	-	-	-	-	-	product distribution studies	75

* These authors did not resolve the isomeric butene products.

P.L. Power law; H-W Hougen-Watson; O Olefin; E ether.

^e The dehydration of ethanol and the reactivity of primary alcohols were discussed.

The power function rate expression has not been conclusively developed to account for rate data at both low and high alcohol concentrations. At low concentration the apparent order of reaction was usually found to be one. The reaction order was invariably zero or tending to zero at high alcohol concentration. The results in literature also show that the reaction order with respect to alcohol varies slightly with temperature.

Table 1.2 shows that the Hougen-Watson type of rate expression has been used to correlate the kinetic data on the dehydration of ethanol. Kinetic data on the dehydration of isopropanol and n-butanol are very limited. A rate retarding effect has been observed by many workers (38, 33, 35). This effect is believed to be due to strong adsorption of alcohol and water on the catalyst surface. The adsorption equilibrium constants were found to decrease in the following order

$$K_W > K_A > K_E \approx K_O$$

at all temperatures. Olefin and ether are the most weakly adsorbed species.

Tables 1.2, 1.3 and 1.4 also give the apparent activation energies for the dehydration reactions over different catalysts. The values of activation energies vary widely. Factors that can affect activation energies are reaction regimes, type of catalyst and alcohol.

With regard to Tables 1.2, 1.3 and 1.4, surface reaction has been consistently observed, in literature, as the controlling step.

Acid and basic sites have been used to explain the mechanism of dehydration of alcohols. Acid sites are considered by many to be responsible for the reactions, although both acidic and basic sites have also been held responsible by some.

Product selectivity of the dehydration of ethanol has been studied (44, 45). However, there is no corresponding work on the dehydration of isopropanol and n-butanol over zeolites. The variation of product selectivity over different zeolites has been attributed to the difference in pore sizes (44, 45). Pore size imposes restrictions on the diffusion or movement of reactant and/or product in out of the pores.

The reactivity of alcohols over solid catalyst has been found to be a function of the alcohol chain length (73, 74) or branching (62, 72). Increasing alcohol chain length was found to increase the rate of formation of olefin. However, its effect on the rate of formation of ether is not well understood. Increasing alcohol branching was also found to increase the rate of formation of olefin. These observations suggest that the dehydration reaction proceeds through an ionic mechanism. They also support the suggestion of increasing stability of carbonium ion formed from alcohol as a result of losing a hydroxyl group.

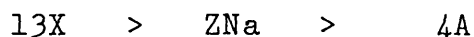
1.5 Catlysts.

Table 1.5 gives the physico-chemical properties of these catalysts. Additional information on chemical properties, physical characteristics and applications can be found in literature (80 - 86).

1.5.1 Zeolites.

Zeolites have been increasingly used as commercial catalysts because of their selectivity. Organic reactions of commercial importance which are catalysed by zeolites have been reviewed by Venuto and Landis (2) and Minachev (99). The two important physico-chemical properties to this study are pore size and acid strength.

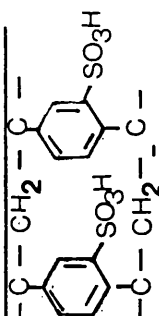
The location of catalytic sites are mainly within the pore structure. The reactivity of reactants depends on the accessibility of the reactants to the catalytic sites. But access to these sites depends on cage size and reactant dimension and structure. The order of cavity size of the zeolites used in the present work is



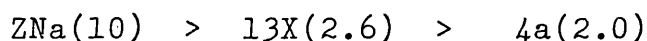
The pore structure of 13X and 4A are roughly spherical while that of ZNa is made up of tubes of elliptical sections.

Catalytic activity has been correlated with acidity (43). The acidic or basic strength of the zeolites can be measured by the ratio of SiO_2 to Al_2O_3 . Al_2O_3 and SiO_2 are on

Table 1.5 The Physico-Chemical Properties of Ion-exchangers.

Properties	13X	4A	ZNa	Cation exchange resin
Chemical formula or Structure	Na ₄₁ ·Al ₄₁ ·Si ₁₀₆ ·O ₂₉₄ ·.264 H ₂ O	Na ₁₂ ·Al ₁₂ ·Si ₁₂ ·O ₄₈ ·.27 H ₂ O	Na ₈ ·Al ₈ ·Si ₄₀ ·O ₉₆ ·.24 H ₂ O	
SiO ₂ /Al ₂ O ₃	2.6	2.0	10.0	
Nominal apperture size Å	10.0	4.2	5.7 x 7.0	
BET surface area m ² /g	359	10	103	2
Bulk density g/cc	0.67	0.74	0.68	0.85
Frame work density g/cc	1.31	1.27	1.70	-
Particle size mm	1.0 - 2.0	1.0 - 2.0	1.588 x 3.5	0.56
Binder	natural clay	natural clay	self binding	self binding
Percentage	15 - 20	15 - 20	-	-
Crytalline structure	body centre cubic	simple cubic	elliptical cylindrical	cross-linking 8% co-polymer
Physical form	spherical beads	spherical beads	1.588 mm extrudates	spherical beads

opposite sides of water when they are arranged in order of decreasing basicity. Hence the order of acidic strength of this zeolites is



where the number in the bracket is the ratio $\text{SiO}_2/\text{Al}_2\text{O}_3$.

1.5.2 Ion-exchange Resin.

Ion-exchange resins have been found (90) to be effective catalysts for some organic reactions having a low temperature activity. The operation of a catalytic reactor at low temperature does not only save energy, it also inhibits homogeneous cracking and isomerization side reactions, which are typical organic reactions at high temperatures. Ion-exchange catalyst would probably last longer because rapid deactivation of catalyst by carbon deposition is greatly reduced at low temperature. Furthermore an ion-exchange resin is particularly good for some organic reactions which are affected by equilibrium at high temperature. A typical example is the dehydration of alcohol to ether.

Ion-exchange resins are solid substances which possess exchangeable cations or anions. A typical example is the cross linked styrene-divinyl benzene (SDVB) with sulphonic acid groups (SO_3H) which are introduced to SDVB after polymerization by treatment with concentrated sulphuric acid. The structure of SDVB used for this work is shown in Table 1.5.

This type of ion-exchange resin has been used as a catalyst for the dehydration of alcohols (33, 46 - 56). Its framework is made up of a matrix consisting of an irregular macromolecular three dimensional net-work of hydrocarbon chains. The pore structure of this type of gel probably collapses on drying, since the measured BET area of dried sample is less than $2 \text{ m}^2/\text{g}$ instead of about $45 \text{ m}^2/\text{g}$ for the wet sample. The characteristics of macro-porous ion-exchange resin has been discussed by Kunin et al (91).

The sulphonic acid sites are the adsorption and catalytically active sites (34, 44, 92). Uniformity of active sites of the ion-exchange resin has been shown by many workers (34, 44, 92). This indicates the possible applicability of a Hougen-Watson type of rate expression for cation exchange resin.

1.6 Principal Conclusions in Literature.

Studies on the dehydration of alcohols over solid catalysts have been reviewed with emphasis on ethanol, isopropanol and n-butanol over ion-exchanger catalysts. The following conclusions can be made:

- a) The dehydration of alcohols proceeds almost exclusively to two principal products: ethers and olefins.
- b) Both consecutive and simultaneous reaction schemes and a combination of the two have been suggested for the dehydration reactions.

- c) A product distribution typical of two consecutive irreversible reactions has been observed with the formation of ether going through a maximum. The maximum can also occur for a simultaneous reaction scheme if the ether formation reaction is reversible.
- d) Acidic or both acidic and basic sites have been said to be responsible for the formation of olefins. But both acidic and basic sites have been suggested to be responsible for the formation of ethers.
- e) Reaction mechanisms for the dehydration of alcohols to olefins over solid catalysts have been shown to be E1 and E2 type. Factors affecting a shift in mechanism are: catalyst type, alcohol type and reaction temperature.
- f) The rate controlling step has been widely observed to be that of surface reaction.
- g) Reaction orders with respect to alcohol concentration vary between 0-2 and 0-1 for the formation of ether and olefin, respectively. However, it is generally agreed that both orders tend to zero at high alcohol concentration.
- h) Apparent activation energies for both simultaneous dehydration reactions vary widely in literature (see tables 1.2, 1.3 and 1.4). Factors affecting activation energy are: rate controlling regime, catalyst type and alcohol type

i) The order of adsorption constants for the alcohol and the main products (water, ether and olefin) decreases according to

$$K_{\text{water}} > K_{\text{alcohol}} > K_{\text{ether}} > K_{\text{olefin}}$$

The rate of the dehydration are inhibited by water and alcohol only.

j) The order of reactivity of primary alcohols and branched alcohols are

$$C_2 < C_3 < C_4 < \dots < C_n$$

and

$$\text{primary} < \text{secondary} < \text{tertiary}$$

where n is the number of carbon atoms.

CHAPTER 2

EXPERIMENTAL, APPARATUS AND OPERATION

CHAPTER 2

EXPERIMENTAL, APPARATUS AND OPERATION

2.1 Introduction

Experimental work on catalytic reactor processes is usually focused on two main aspects:

- a) The development of a reliable kinetic rate expression which can predict conversion, yield and selectivity over a wide range of reaction conditions.
- b) The development and selection of more selective, active and long-life catalyst for the reaction of interest.

The present study is devoted to these two goals for the production of olefins and ethers by the dehydration of alcohols. The activity and selectivity of zeolites (types A, Z, and X, all in sodium form) and synthetic cation exchange resin (poly styrene sulphonic) for the dehydration reactions will be systematically examined.

The vapour phase dehydration of n-butanol, iso-propanol and ethanol have been chosen for this work. By the use of zeolites, it is hoped that the influence of physico-chemical properties (acid strength and pore size) on catalytic

selectivity and activity can be established. By the use of synthetic cation exchange resin, it is hoped that favourable reaction conditions can be found for the exclusive production of ethers.

The alcohols chosen are of different molecular shape in terms of chain length and branching, so as to determine molecular shape selectivity.

The kinetic data on the dehydration reactions were obtained by using a spinning basket reactor. It is hoped that the resulting kinetic rate expressions will be free from external physical transport effects. The rate expressions for the dehydration of isopropanol over zeolite 13X will be used for the analysis of results from a catalytic fixed bed reactor. Such analysis can be the basis for investigating possible effects of internal mass and heat transfer on the catalytic dehydration of alcohol reactions.

Figure 2.1 shows a schematic diagram of the equipment which was used for both spinning and fixed bed experiments.

2.2 Selection of Reactor.

In the design of catalytic reactors, the chemical rate equation plays an important role. All physical parameters, such as effective diffusivity, effective conductivity,

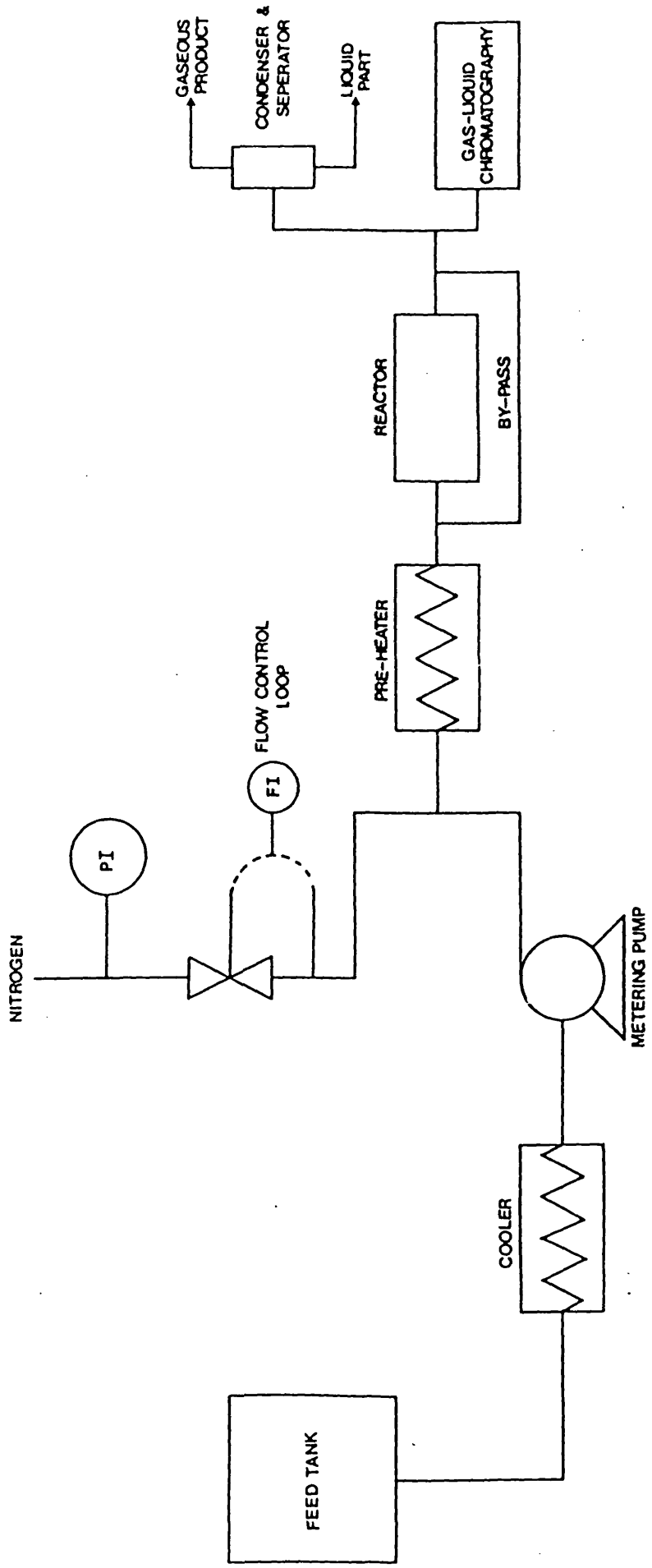
density of fluid for the reactor modelling can be estimated by using empirical correlations. But the chemical parameters, such as kinetic rate constant, adsorption equilibrium constant and/or reaction order, are always based on experimental data, collected under carefully controlled conditions, for the particular chemical reaction being considered. Rate expressions of the power function or Hougén-Watson type can be formulated from probable reaction schemes. Before they can be used for the purposes of design, they must be verified by experimentation. Only those expressions which fit the experimental data well should be used.

Kinetic data for verifying the theoretically formulated rate expressions are usually procured in a flow or static reactor system. Continuous flow reactors are usually preferred because they allow for continuous sampling of the reactor effluent. Discussions on the types of laboratory reactors for gathering kinetic data can be found in literature (105, 106, 107, 110).

The dehydration of alcohol to olefin and/or ether has been studied in differential or micro catalytic reactor (34, 73, 74), recycle fixed bed reactor (73), fluidised bed reactor (108, 109) and static type reactor (62). The reactor for this study was selected so as to eliminate external transport effects.

DILUENT FEED PREPARATION UNIT

EFFLUENT TREATMENT UNIT



LIQUID FEED PREPARATION UNIT

EVAPORATION UNIT

REACTOR UNIT

SAMPLE ANALYSIS UNIT

Fig. 2.1 Block Diagram for the Dehydration of Alcohols in Catalytic Reactors.

The type of reactor selected has little or no influence on the internal diffusional resistances. Some catalytic reactors, e.g. fluidised bed and continuous stirred gas solid reactors, permit the use of fine catalyst particles and therefore minimise internal transport resistances. But design data are best obtained with catalyst particles in their commercial form. Internal diffusional effects can be accounted for by introducing an effectiveness factor into the rate expression. The influence of internal mass and heat transfer will be assessed at all reaction conditions in this study.

The type of reactor used influences product selectivity, since selectivity depends on reactant concentration. For example, in a continuous stirred gas solid reactor with complete mixing, the inlet reactant concentration is instantaneously reduced to the outlet concentration, which is slightly smaller. Hence the selectivity for a product which has a higher dependence on reactant concentration would be reduced. The dehydration of alcohols to olefins and ethers are such examples.

In order to eliminate the effects of external mass and heat transfer, the conditions within the gas bulk must be equal to the conditions at the surface of the catalyst particles. The external concentration and temperature differences can be eliminated by using a high mass flowrate of reactant and diluent, or a high reactor

spinning speed or a continuous stirred gas solid reactor under isothermal conditions.

The two types of reactors which are suitable for collecting kinetic data under isothermal conditions are:

- a) Differential fixed bed reactor.
- b) External or internal recycle reactor.

A detailed description of reactor types will not be given here, and only the salient features of each catalytic reactor important to this investigation will be discussed.

After careful consideration of the two types of reactors mentioned above, the latter was chosen. The most striking advantage of the latter is that integral conversion can be obtained and thus a high degree of analytical precision is not required. Better discrimination of possible rate expressions can also be achieved.

2.3 Basic Principles and Features of CSGSR

The continuous stirred gas-solid reactor (CSGSR) is essentially a recycle reactor. Its recycle is internal, hence its problems do not lie within the recycle stream, as in the case of the external recycle reactor, but with its spinning devices.

At steady state, the inlet flow into the reactor vessel is instantaneously mixed with the reactants and the products that are already in the pot. The chemical reaction rate depends on the conditions within the reactor vessel. The composition of the outlet stream is the same as the composition of gas mixture in the reactor pot. Hence a well-stirred CSGSR, in principle, has ideal characteristics. This type of reactor has been employed in the study of the kinetics of homogeneous (111, 112) and heterogeneous (113-117, 120) reactions. A comprehensive table of studies on the kinetics of chemical reactions or mass and heat transfers of non-reacting mixtures using a CSGSR has been presented by Doraiswamy and Choudhary (118).

This type of reactor was first proposed, developed and used by Carberry (110). Many workers (113-117, 119) have developed and used similar, or slightly different, types of CSGSR. The basic principle and the essential features of all types of CSGSR developed, so far, are the same. The main differences lie in the way in which the catalysts are packed or held in the reactor and the mode of spinning.

Four loading arrangements have been reported (118).

- a) Four rectangular or cylindrical paddle baskets.
- b) Wire mesh circular basket

c) Catalyst impregnated on reactor wall.

d) Stationary catalyst.

There are two modes of stirring:

a) The catalyst is rotated at a high speed in circulating gas.

b) The reacting gas is forced by an impeller, attached to the tip of the stirring shaft, to flow through the stationary or impregnated catalyst. The advantages and disadvantages of loading and stirring arrangements have been fully discussed in literature (118).

Carberry (110), Brisk et al (119) and Doraiswamy and Tajbl (107) gave the following as advantages of CSGSR over other laboratory reactors.

a) Chemical kinetics can be investigated under isothermal conditions because of good heat transfer from the reactor wall to the bulk gas and catalyst, due to perfect mixing. This suggests that hot or cold spots are eliminated.

b) The external mass and heat transfer at any given flow rate can be completely eliminated by operating at high stirring speed.

c) Integral conversion is obtained in CSGSR, but the actual conversion per internal recycle pass is differential.

d) At steady state, the chemical reacting rate can be easily calculated. The rate of reaction is given by the difference between the inlet and outlet flows divided by the mass of the catalyst employed.

$$\text{Rate} = \frac{F_{in} X_{in} - F_{out} X_{out}}{W_g} \quad 2.1$$

e) The catalyst particle size can be varied over a small range without affecting the mixing properties of the gas mixture in the reactor vessel.

The following disadvantages have been observed when operating CSGSR.

a) The catalyst surface temperature cannot be measured. Hence this type of reactor is not suitable for highly exothermic or endothermic reaction, where the gas temperature in the reacting vessel may be considerably higher or lower than the catalyst surface temperature. It is suitable only for chemical reactions which are accompanied by low heat of reaction, such as the dehydration of alcohol.

b) A large ratio of free volume to catalyst volume is always involved. This can promote non-catalytic homogeneous reactions which may be taking place simultaneously with the catalytic reactions. These reactions are often not reproducible. The presence of a large surface in the reactor also enhances the rate of side reactions catalysed by the reactor surface. In the present study the presence of nickel or copper in the reactor wall can catalyse dehydrogenation reactions. Dehydrogenation of alcohols over some solid catalysts has been observed (39, 67, 101, 57) .

The stationary and impregnated catalyst types of CSGSR have larger ratio of voids to catalyst volume than those with the catalyst baskets attached to the stirring shaft. The design of CSGSR with a smaller ratio of void volume to catalyst volume approaching that which is obtained in a fixed bed reactor, would be very attractive.

c) The overall conversion, selectivity and yield in a CSGSR cannot be compared directly with the overall conversion, selectivity and yield in a fixed bed reactor.

d) The internal reactor structure (baffling arrangement), spinning speed, the flow rate and to a small extent the catalyst particle size all have influence on the mixing characteristics of gas mixture in the reactor vessel.

2.4 Experimental Equipment.

Figure 2.2 shows a schematic representation of the equipment used for the dehydration of alcohols over ion exchangers in a gas-solid spinning basket reactor. The key to the figure is given on the next page.

The equipment can be divided into five different parts:

- a) Feed preparation unit.
- b) Evaporation unit.
- c) Reactor unit.
- d) Analysis unit.
- e) Effluent treatment unit.

2.4.1 Feed Preparation Unit.

2.4.1.1 Nitrogen Supply.

High purity nitrogen was supplied from a cylinder containing no impurities detectable by Gas-Liquid Chromatographic (GLC) analysis. It was dried by passing through a column containing zeolite 13X. This prevented the nitrogen gas from carrying moisture to the reactor.

The column was constantly regenerated to avoid complete saturation of the molecular sieves.

The mass flowrate of nitrogen was metered by a mass control valve (MFC1). The valve gave a constant mass flowrate with constant inlet pressure even though the outlet pressure might vary. The inlet pressure was maintained constant by a pressure regulator (PR). The volumetric flowrate was measured by a bubble flow meter.

2.4.1.2 Alcohol Supply

The reactants (alcohols) are designated as high purity grades by British Drugs House (BDH) chemicals. Absolute ethanol was used. Their purity was higher than 99.5% as checked by Gas-Liquid chromatographic (GLC) analysis. They were used without further purification.

The alcohol was stored in a feed tank of one litre volume. The feed tank was equipped with a millimetre burette which allowed for an accurate determination of the feed rate. The alcohol was fed into the piping system by using a positive displacement metering pump, equipped with variable speed drive and 5 to 1 capsule reduction gear box.

The feed rate was determined by closing valve (V1) and the pump pumped directly from the one millimetre burette

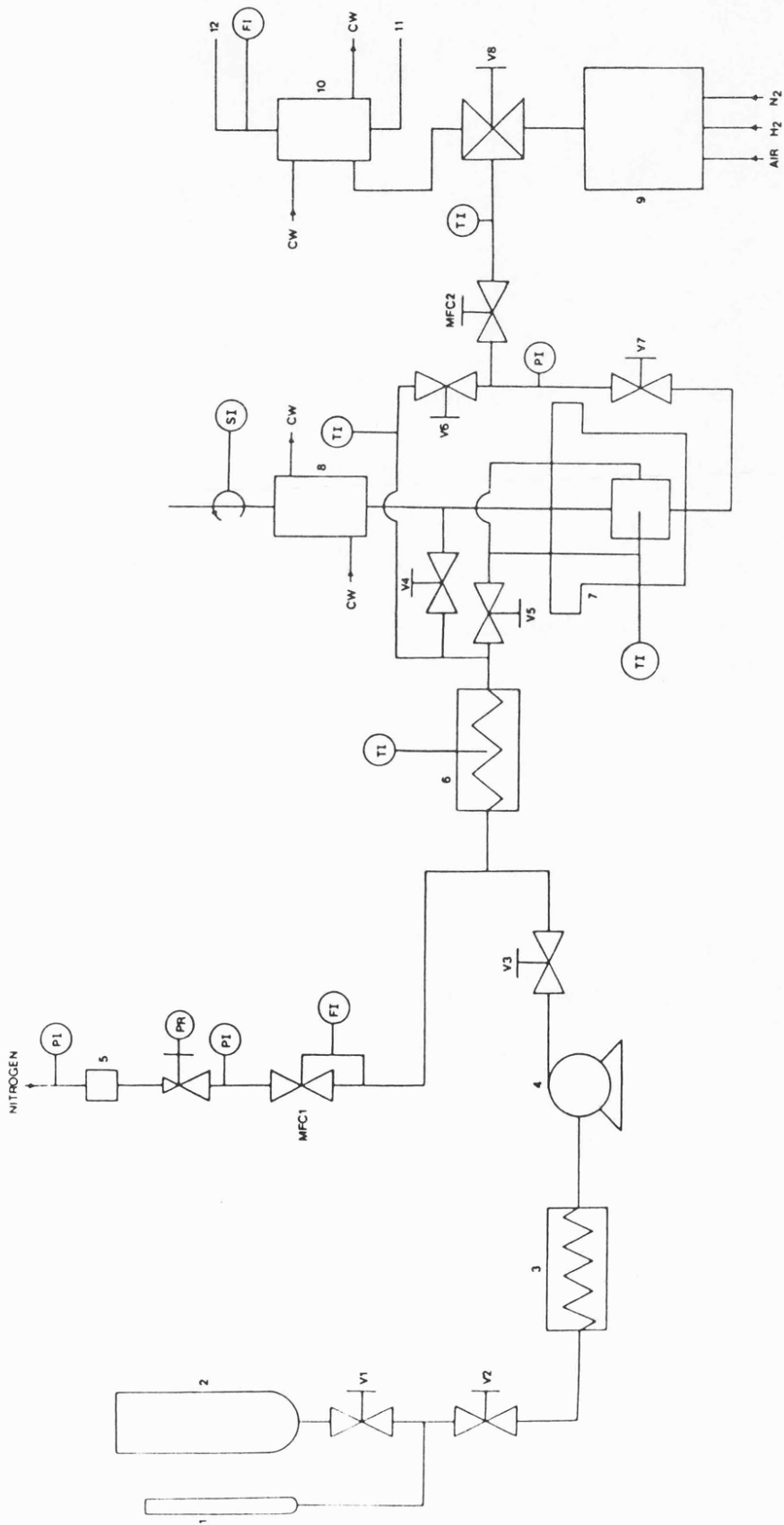


Fig. 2.2 Spinning Basket Reactor Apparatus for the Catalytic Dehydration of Alcohol.

Key to Fig.2.2

- 1 1 Millimeter burette
- 2 1 Litre feed tank
- 3 Cooler
- 4 Metering pump, manufactured by Metering Pump Limited.
- 5 Molecular sieve 13X column
- 6 Pre-heater
- 7 Spinning basket reactor, Supplied by Imperial
Chemical Industry.
- 8 Spinning drive unit
- 9 Gas-Liquid chromatograph, Manufactured by Pye Unicam
equipped with both FID dectector and amplifier.
- 10 Condenser
- 11 Condensate
- 12 Gaseous effluent
- V1-V8 Valves
- TI Temperature indicator
- PI Pressure indicator
- SI Speed indicator
- CW Cooling water
- PR Pressure regulator
- MFC Mass flowrate regulator
- FI Flowrate indicator

into the piping system. The time required to pump a chosen volume was determined with stop-clock. The feed rate was the average of at least three determined feed rates under any operating conditions. Examining a large number of feed rates determined during the experimental runs showed that the deviation from the mean was no more than 1.0%. The error was largely due to the pulsation of the metering pump.

In the suction line of the pump, the alcohol feed flowed in a coil of copper tubing immersed in cooling water in a jacketted vessel at room temperature. This prevented the vaporization of the alcohol before reaching the pump head, hence avoiding vapour locking in the pump head. The alcohol was pumped through a check valve (V_3) at the delivery line of the pump. This stopped the back flow of a mixture of vapourised alcohol and diluent-nitrogen.

2.4.2 Evaporation Unit

The alcohol feed and nitrogen were mixed at a tee-joint located close to the evaporator. The mixing of the two feed streams before the evaporator minimised the possibility of thermal cracking or decomposition of alcohol. It also enhanced the vaporization in the evaporation unit because the diluent-nitrogen was partially saturated with alcohol before entering the evaporator.

The evaporator was heated electrically. The overall resistance was about 70 ohms. The voltage supply was controlled by a voltage variac. A low current of about 3.5 Amperes was used. A thermocouple well was located at the centre of the evaporator to measure the temperature of the fluid inside the evaporator. This temperature was a few degrees higher than the temperature of the feed stream which flowed in a coil of tubing enclosed in the evaporator. The evaporator raised the temperature of the mixed feed from room temperature to nearly the reaction temperature. The temperature of the fluid in the evaporator was displayed by a Eurotherm temperature indicator. The temperature indicator displayed in whole numbers and the error in display value was about $\pm 0.5^{\circ}\text{C}$.

The line between the reactor and sampling valve (V8) was about 4 metres. This line was maintained at relatively high temperature to prevent alcohol from condensing within the piping system. Heating of the piping system was achieved by electrical heating tape. The temperatures of the piping lines and sampling loop were measured by thermocouples placed between the heating tape and the outer surface of the tube carrying the reacting fluid.

2.4.3 Reactor Unit

2.4.3.1 Continuous Stirred Gas Solid Reactor

The CSGSR used in this study was developed by Imperial Chemical Industries (ICI). It is similar to that discussed by Brisk et al (119). The difference is in the introduction of a purge line, which carries about 5% of the mixed feed stream into the reactor. Details of the reactor unit is shown in figure 2.3. The main components are reactor vessel, rotating shaft, the driving units and the catalyst basket. Figure 2.4 shows the details of the spinning baskets and chamber.

The flow of the mixture of reactant and diluent was split into three portions before entering the reactor. Two bigger portions were fed into the reactor vessel at about the same level but on opposite sides of the vessel. The smallest portion was the purge, which was fed into the reactor at a higher level along the rotating shaft. This fraction prevented the reacting fluid from flowing upward along the shaft. The purge also prevented the condensation of effluent and the deposition of carbon or polymeric products along the shaft. If carbon or polymeric products were deposited on the rotating shaft, spinning would be affected. The catalysts were held securely in a circular basket attached to the shaft. The circular basket was used to minimise the free gas volume and hence homogeneous

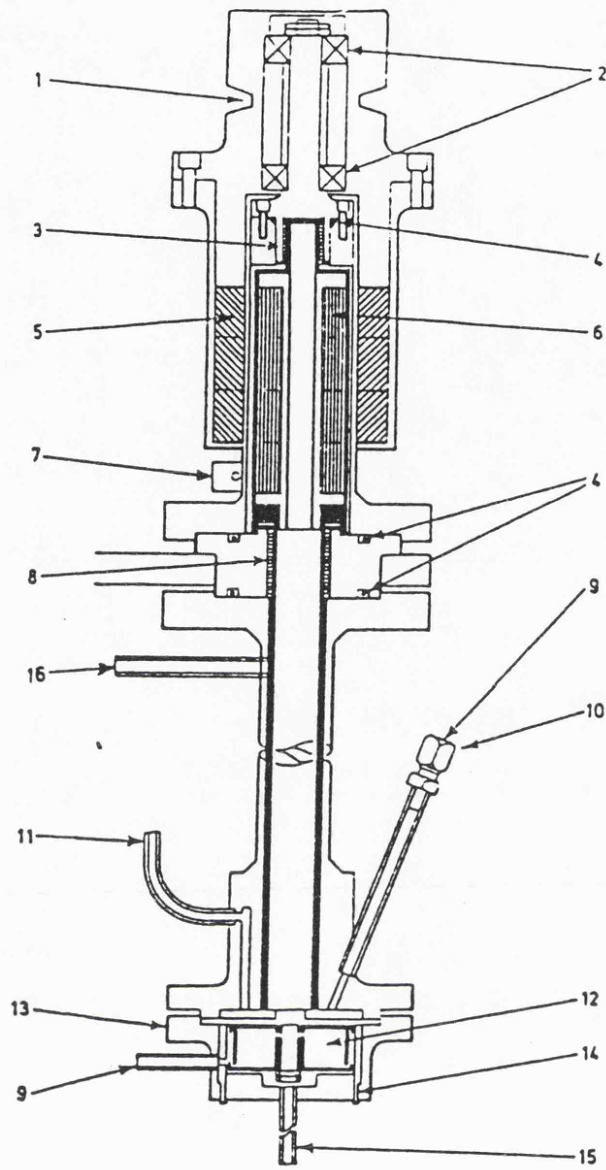
reactions, if any. The cruciform shown in figure 2.4 was not used in this study. The basket used in the present study was made of stainless steel and fine wire mesh which could hold catalysts of suitable size in place during the spinning. Catalyst of known weight was loaded evenly into the basket before an experimental run.

The total volume of the reactor was about 50 cm³ and the ratio of catalyst volume to free volume (including the voidage) varied with the type of catalyst used, but the minimum designed value was about 1:1.2.

The reactor was heated by a gas chromatograph oven with a forced circulation and built-in temperature control unit. The built-in temperature controller allowed the reactor to be maintained at constant temperature.

A thermocouple located in the reacting pot measured the fluid temperature. The catalyst bed temperature may be slightly different from that of the bulk fluid phase. The estimated temperature difference between the catalyst bed and the bulk fluid phase is less than 1°C. A stainless sheathed chromel alumel thermocouple was used. The temperature was displayed on a digital temperature indicator.

The operating reactor pressure was kept at one bar gauge. It was indicated by a pressure indicator located at the outlet of the piping system. The error in the



- | | |
|--------------------------|--------------------------|
| 1. belt drive groove | 9. thermocouples entries |
| 2. outer magnet bearings | 10. pressure tapping |
| 3. upper bearing | 11. inlet port |
| 4. O ring seals | 12. catalyst basket |
| 5. outer magnet | 13. reactor pot |
| 6. inner magnet | 14. baffles |
| 7. reed relay | 15. outlet port |
| 8. lower bearing | 16. purge point |

Fig. 2.3 Spinning Basket Reactor Including Stirrer
Drive Unit (110, 120).

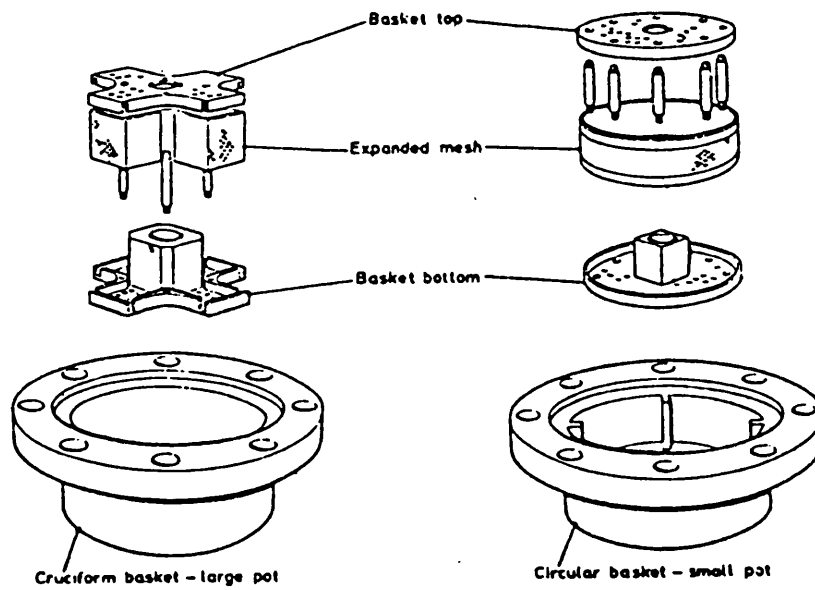


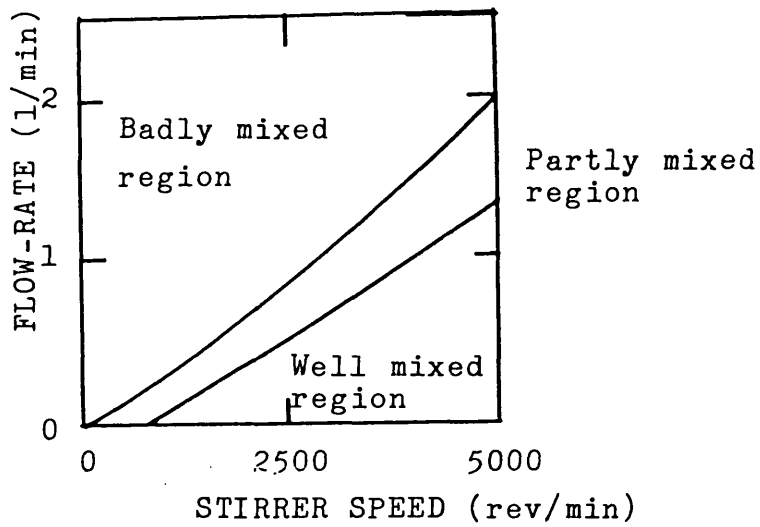
Fig. 2.4 Details of Spinning Basket Reactor Baskets and Chamber (119).

indicated pressure was less than $3.4 \times 10^3 \text{ N/m}^2$ (3%). A major advantage in operating the catalytic reactor above atmospheric pressure is that it prevents ingress of air through leaks which would result in ignition.

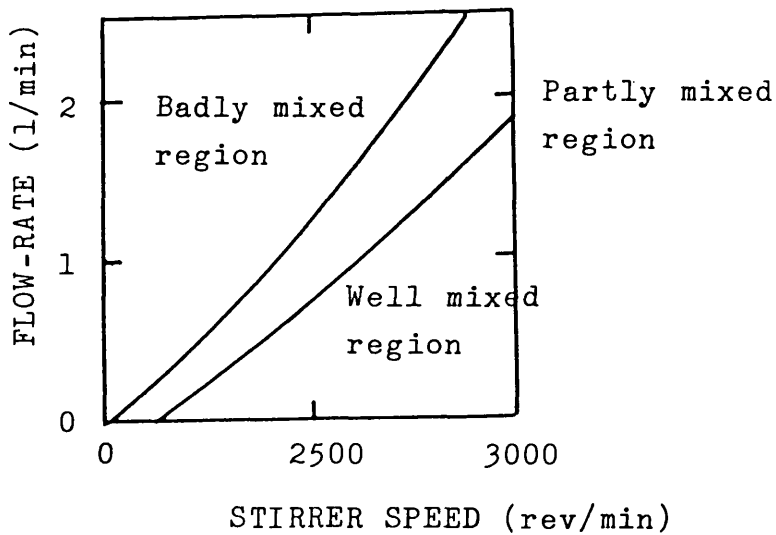
Spinning of the shaft was achieved by an electric motor which drove the outer magnet. The outer magnet spun the inner magnet at the upper section of the shaft. The magnetic coupling system prevented leakage of reactant and contamination of reactant and catalyst by the lubricating oil of the shaft. The bearing was continuously cooled by cooling water.

The selection of the spinning speed was determined in order to achieve perfect mixing and eliminate the influence of external mass and heat transfer on the rate of reaction. The latter effect could be checked by examining conversion at different spinning speeds, keeping other variables constant. Figure 2.5 shows that for a flowrate of 100 to 150 ml/min, the spinning speed should be higher than 2,000 revolutions per minute (RPM) to obtain perfect mixing and eliminate external heat and mass transfer effects. A higher spinning speed may be required if the gas flow rates are higher.

Ford and Perlmutter (116) and Santacesaria et al (94) showed that at 2,000 RPM or more, the rate of chemical reaction was not appreciably increased. This indicates



(a)



(b)

Fig. 2.5 Mixing Characteristics of Gas Mixture in the Spinning Basket Reactor Vessel (119).

a) Circular basket and small reactor.

b) Cruciform basket and large reactor.

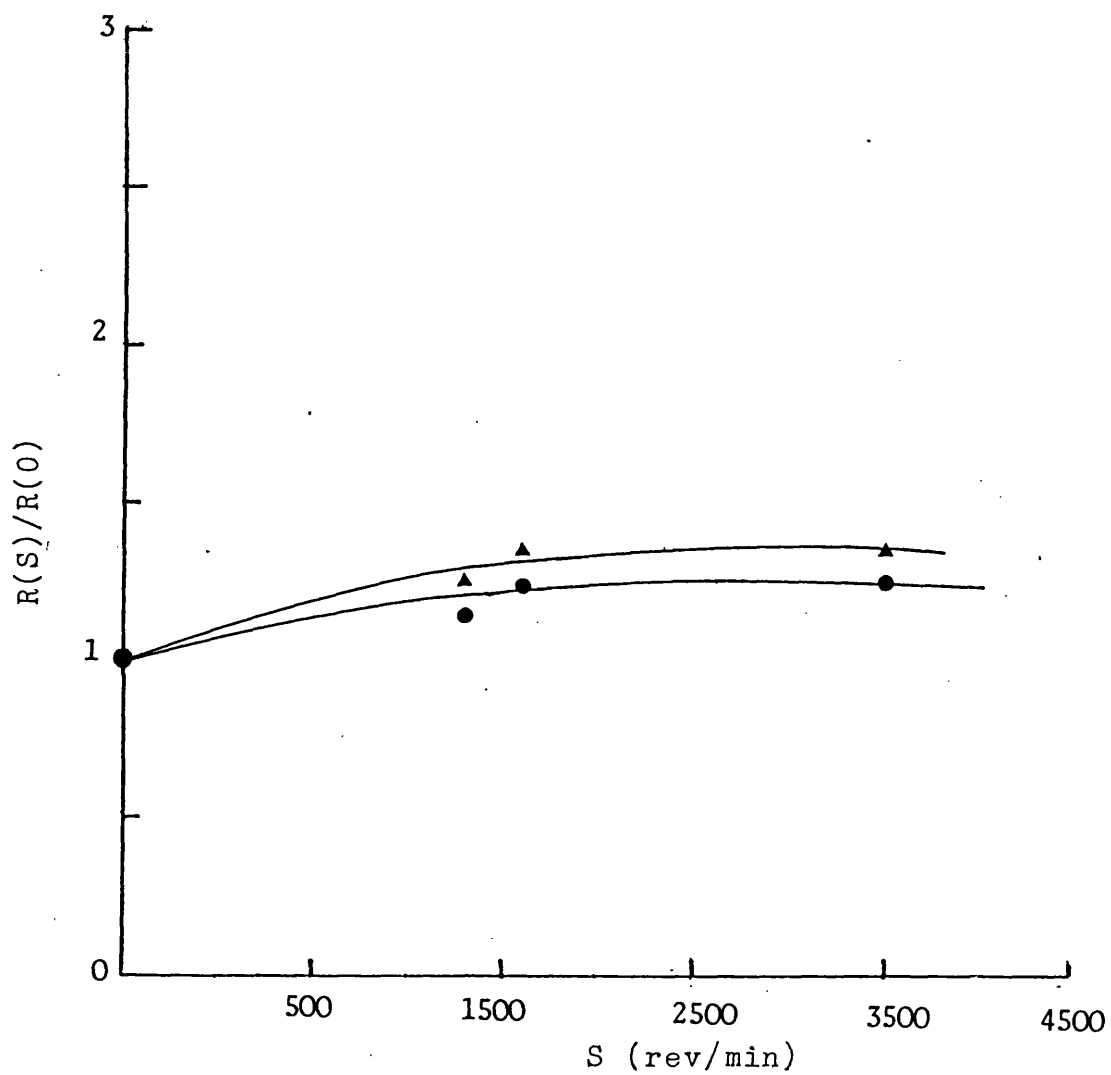


Fig. 2.6 The Influence of Spinning Speed on the Rates of Formation of Olefin (\blacktriangle) and Ether (\bullet).

that effects of external mass and heat transfer are not significant at spinning speed of 2,000 RPM or more. Figure 2.6 confirms this conclusion. The present kinetic data were gathered at spinning speeds between 2,000 and 3,000 RPM.

The spinning speed was measured by a dry reed switch at about 2cm from a small magnet mounted on the outer magnet of the spinning shaft. As the magnet passed the reed switch, a counting circuit was completed. The number of times the counting circuit was completed per minute was transformed into number of revolutions per minute. The spinning speed was controlled by a voltage regulator and displayed continuously whenever the motor was running.

2.4.3.2 Packed Tubular Reactor

Integral reactors are commonly used in kinetic experiments. There are, however, heat and mass effects which have to be accounted for. Criteria for minimising heat and mass gradients in a fixed bed reactor will be discussed in chapter 6. Only those that are considered in the design of the fixed bed reactor used for this work will be discussed briefly here.

The integral reactor used was made of stainless steel tube of 1.03 cm internal diameter by 10.0 cm long. Spherical catalysts of 1-2 mm diameter were loaded by gravity through the top.

According to Carberry and Wendel (122), if the bed length to pellet diameter ratio is greater than 50/1, axial mass transfer can be neglected. The bed length to particle diameter ratio of the reactor used in this work varied from 100/1 to 50/1, hence axial dispersion was not important. The reactor diameter to particle diameter ratio varied from 10.3/1 to 5.0/1 which yielded minimal radial heat and mass gradients.

The reactor was heated by the same oven used for the CSGSR. Two stainless sheathed chromel alumel thermocouples were located 7.00 cm apart in the catalyst bed. The average temperature in the bed was within $\pm 1^{\circ}\text{C}$ of the desired reaction temperature. Figure 2.7 shows a schematic diagram of the fixed bed reactor unit. The diluent and reactant flowed through the U-tube system. Down flow gas allowed for the preheating of the mixture to reaction temperature before flowing up through the catalyst bed.

A high flow rate of the feed was used to minimise the external mass and heat transfer effects. The effects of the external mass and heat transfer were assessed. The results of the assessment are shown in appendix 6. The assessment indicates that effects of mass and heat transfer on reaction rate were negligible.

The total operating pressure was kept at one bar gauge. Inlet pressure was indicated by a pressure indicator. The

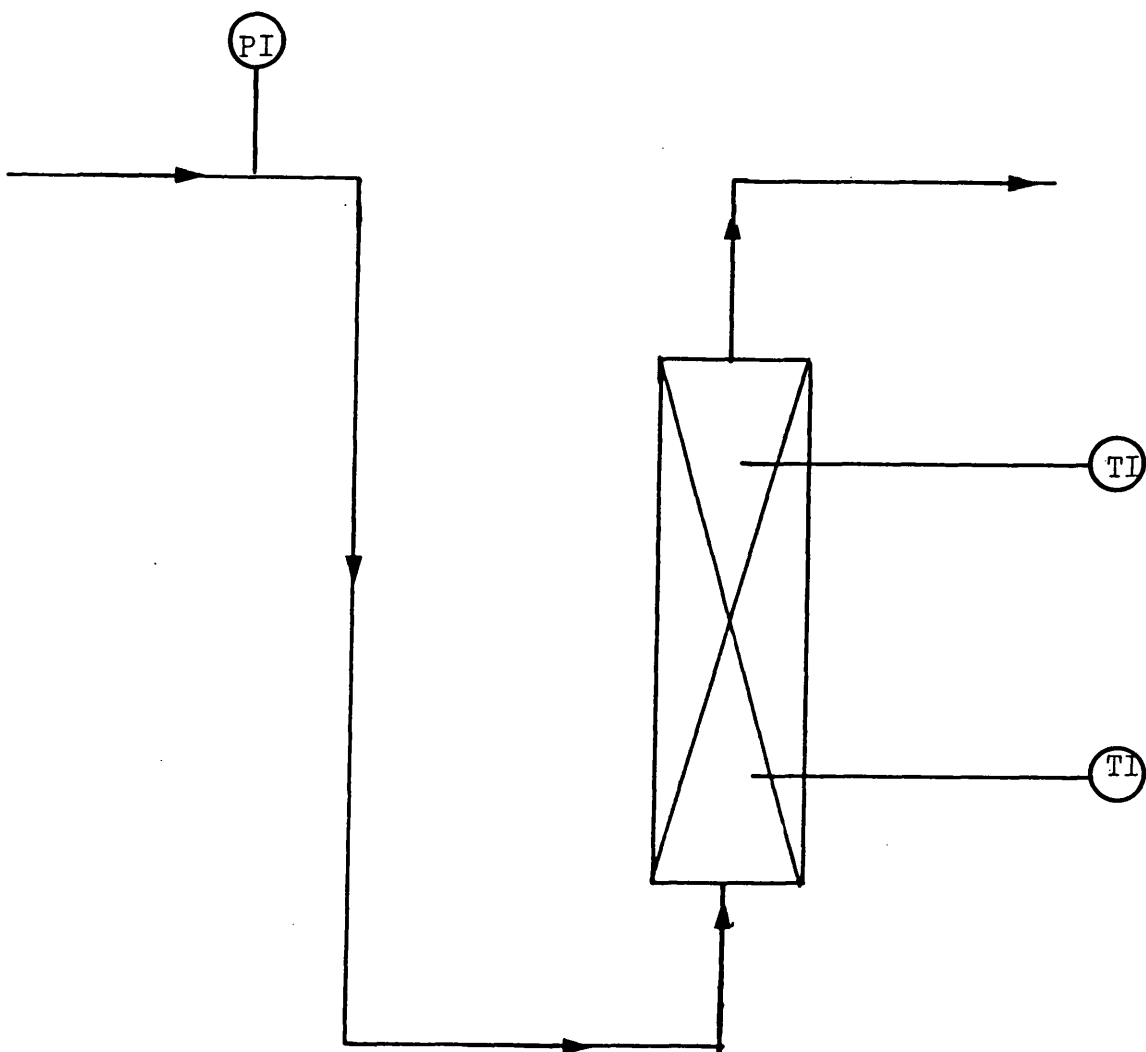


Fig. 2.7 Schematic Diagram of the Fixed Bed Reactor Unit.

PI Pressure indicator

TI Temperature indicator

error in the indicated pressure was less than $3.4 \times 10^3 \text{N/m}^2$ (3%).

2.4.4 Sample Analysis

The analysis of the products is crucial to the whole study. The composition of the products was analysed by gas chromatography. Considerable effort and time were spent in finding the most appropriate procedure of analysis.

The reactor output stream line was heated with electrical heating tape to prevent condensation of gases in the tubings prior to sampling valve V8. Gas samples were taken via a manual gas sampling valve. The valve was always at the filling position. The volume of the gas sample in the sampling loop was about 0.5 ml. When analysis was required the sampling valve was manually turned to the injection position introducing a constant volume of gas into the carrier gas which flowed into the chromatographic column. High purity nitrogen was used as carrier gas.

Three types of packing materials were used to achieve the separation of all possible products from the alcohols. Porapak Q was used for the resolution of reaction products from the dehydration of ethanol. It was packed in a 1-metre long and 4.0 mm internal diameter glass column. The column temperature was maintained at 120°C . Excellent separation of possible reaction products (propene,

di-iso-propyl ether, acetone and isopropanol) was obtained using 10 percent poly ethylene glycol on chromsorb (high performance HP) as packing material (67). A glass column of 2 metre length and 4.0 mm internal diameter was used and the column was maintained at 70°C. The resolution of the isomeric butenes produced from the catalytic dehydration of n-butanol was accomplished by a glass column of 7.3 metre length and 3.2 mm internal diameter packed with 20 percent bis (2-methoxy ethyl) adipate on chromosorb P-AW, kept at 40°C (123). It was connected in parallel with another glass column 1-metre long and 4.0 mm internal diameter packed with porapak Q. The samples for the latter column were taken directly from the reactor effluent while samples to the former were taken after the removal of condensable components and drying. A four way valve was used to direct the outputs from either column to the detector which was maintained at 250°C.

A Pye Unicam, (series 204), gas-liquid chromatograph equipped with flame ionisation detector was used. A digital integrator was used to integrate the signal from the detector. Peak area was integrated. The integrated area and retention time were printed automatically at the end of each peak. A philips recorder was connected to the output of the integrator. This enabled the determination

of the beginning and the end of an integration and also gave the base line.

Each peak was identified by injecting pure samples of all the possible components directly into the chromatographic column(s). Component peak retention time was used for identification.

The peak area of each component as a function of its number of gram-moles used was calibrated by using appropriate gas or liquid mixtures. For liquids, various mixtures were prepared and a precisely known volume was injected by a micro-syringe into the carrier gas stream. The syringe is accurate to within 1.0% of the dispensed volume. A plot of integrated area against gram-moles for each component was obtained. Linear least squares analysis was used to correlate the integrated area of a component against its gram-moles to obtain fitted expression with minimum deviation. The regressed equation was used to convert integrated area to number of gram-moles. The number of gram-moles of each component was used as the basis for the material balances around the reactor and, subsequently, for the calculation of partial pressures and reaction rates.

The chromatographic analyses were reproducible and contributed very little to final errors. Conversion was taken as the mean of at least three or more reproducible analyses. Examination of chromatographic analyses reveals

that an average error deviation from the mean is no more than 4% for each component.

2.4.5 Effluent Treatment

For safety reasons, it was desirable to minimise the amount of hydrocarbons or organic compounds emitted into the atmosphere.

After the dehydration products and unreacted alcohol had passed through the sampling valve, they were fed into a separator. This separator was cooled by air which condensed most of the condensable components. After leaving this condenser the remaining mixture was fed into a second condenser which had a cooling coil of glass of about 2 metres long. Cooling water flowed inside the glass coil while the gaseous effluent flowed counter-currently on the outside. The bottom of the condenser was connected to a flask for the collection of condensate. The condensates from both separators were removed periodically.

After the separation of the condensable products and unreacted alcohol, the gases, consisting mainly of nitrogen, were removed from the top of the condenser. The flowrate was determined by a bubble flow-meter. Mean flowrate was the average of at least two or three measured flow rates. The effluent was discharged to a fume extraction system.

2.4.6 Safety Aspects

In the design, construction and operation of the experimental equipment careful considerations were given to all possible hazards that might arise. The equipment was designed and built to conform to relevant British standards.

The properties of the materials used in the construction were carefully studied to determine their upper limits of operating conditions. The piping system was constructed of copper and stainless steel fittings. These were chosen to stand up to high temperatures and exposure to hydrogen and alcohol.

The toxicity, corrosive properties, flammability, ignition point and chemical behaviour of all reactants, possible products and gases involved in this work were thoroughly investigated. The quantity of alcohol made available to the experimental site was limited to 250 ml at any particular time, so as to reduce fire hazard and other hazards associated with alcohol.

The spinning motor belt was well guarded with plastic covering to prevent entanglement of loose clothing, long hair, etc., whilst in operation. In case of emergency, the whole system could be shut down in less than a minute. The power supply to the system was from two electrical sockets located in a conspicuous position. All wiring plugs

were provided with appropriate fuses. Shut-off valves were fitted along the hydrogen and alcohol lines.

2.4.7 Operation Procedures

The operation procedures of the experimental equipment are briefly summarised below.

- a) The empty circular basket was loaded with catalyst of a known weight.
- b) The basket and contents were firmly secured to the end of the rotating shaft by means of a nut.
- c) The reactor was covered with its lower flange carrying the outlet tubing. The shaft was turned by hand to ensure free rotation before bolting the lower plate and top plate of the reactor vessel together. There was a high temperature gasket between these plates. It fused when the reactor was heated and can only be used for one experimental run.
- d) The system was then pressurised with nitrogen to three bar gauge to test for leaks. Leaks were detected by soap solution and the rate of fall in pressure.
- e) The catalyst was then activated by heating the reactor to reaction temperature. The system was then continuously flushed with diluent, carrying with it the water liberated by the catalyst. This usually lasted at least 24 hours.

- f) The evaporator and heating tape were switched on. Cooling water for the condenser and the bearing of spinning shaft was then turned on.
- g) After the working temperature had been achieved in the reactor the metering pump was switched on. Steady state conditions were established after about half an hour.
- h) The rotating shaft was started together with the pumping of the alcohol into the piping system and the reactor. Spinning was continued throughout and was then switched off at the end of the day.
- i). For fresh catalyst, the gas sample analysis was carried out at convenient time intervals until constant activity of the catalyst was reached. The kinetic data were only collected when constant activity of the catalyst was attained. The time taken to achieve the constant activity period was dependent on the type of the catalyst. The activity of the catalyst was always checked.
- j) The change of alcohol flowrate was achieved by adjusting the stroke setting of the metering pump. Outlet pressure was then reset to one bar gauge by manual operation of the mass flowrate controller (MFC2).
- k) The gaseous product and unreacted alcohol from the reactor was sampled until reproducible results were obtained

before the operating conditions were altered.

l) When the reaction temperature was changed, steady state was checked. Usually, the alteration in reaction temperature was carried out at the end of a working day, so that steady state would be reached on the following day.

m) The shut-down procedure was as follows:

(i) The alcohol pump was switched off.

ii) The spinning motor was switched off.

iii) The heating tapes, evaporator and reactor oven were switched off.

iv) The diluent gas was allowed to flow through the system to cool and purge all unreacted alcohol and products.

Depressurization of the system was carried out gradually by opening the MFC2 valve.

v) When reactor conditions were nearly at room conditions, the inert gas was shut off. The reactor was then opened for the removal of the spent catalyst.

2.5 Selection of Reaction Conditions

For a given catalyst, the reaction temperature and partial pressure of alcohol were the two principal reaction conditions to study.

The reaction temperature was varied so as to determine the catalytic activity as a function of temperature. It

also enabled the evaluation of parameters in the rate expression which are dependent on reaction temperature. Activation energy and heats of adsorption of reactants and products can also be determined.

Early workers (28-31) investigating the dehydration of alcohols have established three temperature ranges. These have been summarized in chapter 1. On the basis of literature results and the present research objectives, the following reaction temperature ranges for the dehydration of various alcohols over zeolite catalysts were chosen.

ethanol	270-350°C
isopropanol	200-300°C
n-butanol	200-300°C

The selection of the reaction temperature for the dehydration of isopropanol and ethanol over synthetic cation exchange resin was based on results in literature. Previous workers (33, 34) collected their kinetic data on the dehydration of isopropanol and ethanol on cation exchange resin at temperatures below 125°C. It was decided to extend this limit to as high a temperature level as was permissible by the thermal stability of the catalyst. The reaction temperature range chosen for isopropanol and ethanol was 110-145°C. At least three temperature levels were used for any given catalyst and alcohol.

The variation of reactant feed pressure allowed the influence of partial pressure of alcohol in the rates of product formation and product selectivity to be determined. It also gave insight into concomitant adsorption process and reaction paths of the dehydration reactions.

The variation of alcohol partial pressure was achieved by varying the alcohol flowrate at nearly constant diluent flowrate and constant total pressure. At least five partial pressures of alcohol were used for a given reaction temperature and catalyst.

CHAPTER 3

THE MODELLING OF THE DEHYDRATION REACTION

KINETICS

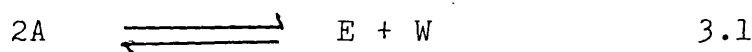
CHAPTER 3THE MODELLING OF THE DEHYDRATION REACTION KINETICS3.1 Introduction

The modelling of reaction kinetics is very important in the design and analysis of catalytic reactors. Reliable kinetic models can give accurate predictions of yields, conversion and product selectivity. Detailed reaction rate modelling techniques have been fully discussed in many text books on chemical reaction engineering (106, 107, 124, 125), papers (126, 127, 128) and reviews (121, 129).

Chemical reaction rate equations are formulated by using two classical approaches:

- a) Simple power function law
- b) Hougen-Watson method.

Consider a simple reversible chemical reaction of the form



The net power function rate expression may be written as

$$\text{Rate} = K(P_A^a - P_E^e P_W^w / K_{eq}) \quad 3.2$$

where K and K_{eq} are the forward reaction rate and the

thermodynamic equilibrium constants, respectively; a , e and w are the apparent orders with respect to A, E and W components, respectively; P_A , P_E , and P_W are the partial pressures of species A, E and W in the mixture.

If the rate controlling step of the above reaction, equation 3.1, is surface chemical reaction on dual active site, the Hougen-Watson rate expression will be of the form

$$\text{Rate} = \frac{KK_A^2 (P_A^2 - P_E P_W / K_{eq})}{(1.0 + K_A P_A + K_E P_E + K_W P_W)^2} \quad 3.3$$

where K is the forward rate constant, K_A , K_E , K_W are the adsorption constants for species A, E and W respectively and K_{eq} is the thermodynamic equilibrium constant of the reaction.

The power rate equation is simply a representation of the law of mass action. The classical Hougen-Watson approach (126) yields a hyperbolic type of expression with more parameters.

Reaction rate modelling consists of two steps (130):

a) The formulation of the rate expression based on the knowledge of the chemistry of the chemical reaction and the physical transport processes.

b) The discrimination between plausible models and the estimation of the adjustable parameters to best represent experimental data.

The model discrimination between rival models is achieved through both chemically and statistically oriented approaches. The latter approach is more versatile than the former. However the former allows one to formulate rate expressions based on the knowledge obtained from physico-chemical studies. An extensive review has been written by Mezaki and Happel (130) on the discrimination of models of rate of solid catalysed gaseous reaction. This chapter is devoted to formulating rate expressions for the catalytic dehydration of alcohols to light olefins and ethers based on the knowledge of the chemistry of the chemical reactions and physical transport processes. The statistical discrimination of the possible chemical reaction rate expressions will be discussed in chapter 4.

3.2 Transport and Kinetic Processes.

The overall process of a gaseous reaction over solid catalyst is complex and is made up of transport processes to and from the bulk of the gaseous phase and the surface or the interior of the catalyst, as well as chemical transformations on the catalyst active sites. The transport processes consist of internal and external transports, while the chemical transformation may have three consecutive steps (adsorption of reactant, chemical surface reactions, and adsorption of products). Steady state and/or equilibrium approximations are often used in kinetic analysis and the formulation of rate expressions. If one of these steps has a rate which is smaller than the rates of the other steps or

which approaches equilibrium conditions more slowly than the other steps, then that step becomes rate controlling.

In the present work, external mass and heat transfer have been minimised by careful selection of reactor and operating conditions. The kinetic data collected are therefore not controlled by external diffusion. The effects of internal mass and heat transfer will be discussed in chapter 4.

The chemical rate expressions that will be formulated below are those that describe the three chemical transformation processes on the catalyst active sites.

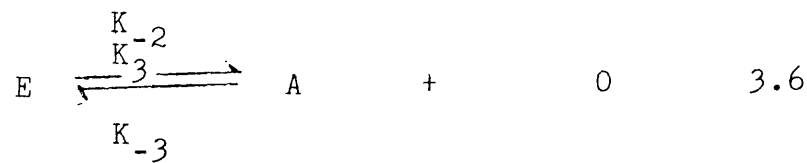
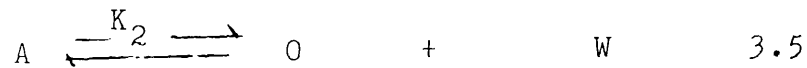
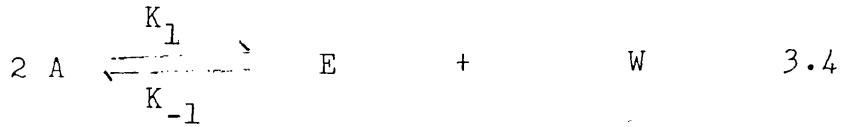
3.3 Power Function Rate Expression

Power function rate expression is normally used to correlate experimental data of homogeneous reactions. However, Weller (127, 129) has strongly recommended the use of power function rate equation to fit kinetic data of heterogeneous reaction. His arguments are:

- a) The equations are easy to use.
- b) Langmuir's adsorption theory is based on the ideality of catalytic surfaces or sites and therefore has limited applicability.
- c) Reaction rate expression produced according to the Hougen-Watson approach (126) are too complex mathematically. It requires a large amount of experimental data and mathematical work before a reliable correlation can be obtained.

3.3.1 Power Function Model.

The overall catalytic dehydration reactions can be written as



The power function rate expressions, in the absence of external mass and heat transfer effects, may be formulated as follows:

$$\text{Model 1: } R_O = K_2 P_A + K_3 P_E - K_{-2} P_O P_W - K_{-3} P_O P_A$$

This model is based on the law of mass action and assumes that the apparent orders correspond to the stoichiometric co-efficients.

$$\text{Model 2: } R_O = K_2 P_A + K_3 P_E$$

It is deduced from model 1, by neglecting the reverse chemical reactions.

$$\text{Model 3: } R_O = K_2 P_A - K_{-2} P_O P_W$$

This model is derived by assuming that reaction 3.6 does not take place. This suggests that the principal products ether and olefin are formed through a simultaneous reaction scheme.

$$\text{Model 4: } R_0 = K_{RO} P_A^a P_W^w P_U^o P_E^e$$

It is formulated on the basis that all the components compete for the active sites on the catalyst surface. The apparent orders are assumed not to correspond to the stoichiometric co-efficients.

$$\text{Model 5: } R_0 = K_{RO} P_A^a P_W^w$$

This model is deduced from the previous one. It assumes that only alcohol and water compete for the active sites on the catalyst surface.

$$\text{Model 6: } R_0 = K_{RO} P_A^a$$

This model is a further simplification of model 4. It assumes that the total active sites occupied by the products are negligible compared with that by the reactant.

Table A2.1, in appendix 2, summaries the power function rate equations derived for the formation of ether and olefin.

3.4 Hougen-Watson Approach.

In using the Hougen-Watson approach to model reaction rate, either the adsorption of reactants, or surface chemical reaction or the adsorption of product may be assumed to be the rate controlling step. This approach is an extension of the classical Langmuir-Hinshelwood kinetic theory of catalyst surface. The Langmuir-Hinshelwood is based on Langmuir adsorption isotherm theory. Surface

chemical reaction is always assumed to be the rate controlling step, while other steps are assumed to be at equilibrium. For example, the Langmuir-Hinshelwood mechanism for a bi-molecular reaction assumes that the surface chemical reaction takes place between two chemisorbed molecules. The Rideal-Eley mechanism for a bi-molecular reaction assumes that the reaction takes place between one adsorbed molecule and a second molecule from the gaseous phase. The derivation of chemical rate expression based on the Rideal-Eley mechanism still requires the application of Langmuir isotherm equations for the adsorbed reactant and products.

The Langmuir adsorption isotherm equation depends on the following assumptions:

- a) Heats and entropies of adsorption are constant for each chemisorbed species. That is, they are independent of surface coverage and the presence or absence of another adsorbed molecule on the neighbouring sites. This assumption implies catalyst surface ideality and hence uniform kinetic and thermodynamic properties.
- b) Interaction between adsorbed molecules is negligible or absent. That is, the adsorption of another molecule at the neighbouring sites does not enhance the adsorption of other molecules.
- c) Monolayer coverage of all active sites. That is one active site adsorbs one, and only one molecule. There are no multiple layers (131).

In practice, these assumptions do not necessarily hold. The variation of heat of adsorption with surface coverage is well documented and suggests interaction among adsorbed molecules (128). Boudart (128) and Weller (127, 129) have discussed extensively the applicability and limitations of the classical Langmuir-Hinshelwood theory, using simple chemical reactions to illustrate and support their arguments.

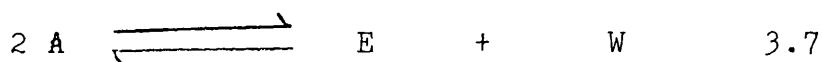
In addition to the above assumptions, the Hougen-Watson modelling approach assumes that all steps are at equilibrium except the rate controlling step. This assumption greatly simplifies the formulation of rate equations. However this assumption does not always hold at all reaction temperatures, because a step that is slow at one temperature may be fast at another. Hence it ceases to be the rate controlling step. Therefore a chemical reaction may show two rate limiting steps. Thaller and Thodos (70) have reported a chemical reaction which exhibits this type of behaviour.

Although the Hougen-Watson approach may appear to be of limited importance, it has been widely found to be useful in the analysis and design of catalytic chemical reaction and reactors. Many workers (32, 33, 34) have applied this approach to the analyses of kinetic data on the dehydration of alcohols over solid catalysts.

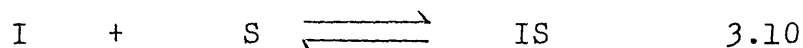
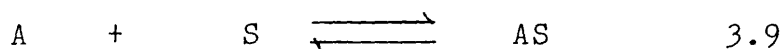
3.4.1 Reaction Steps.

The derivation of the rate equations are based on the three consecutive steps, adsorption of reactants and inerts, chemical surface reaction and desorption of products.

The overall dehydration of alcohols to ethers and olefins may be represented by two parallel reactions.



Reaction step 1: Adsorption of alcohol and inerts.

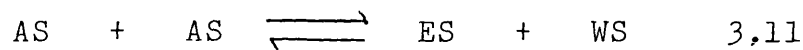


where S is the number of vacant active sites.

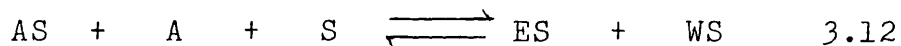
Reaction step 2: Surface chemical reaction

a) Formation of ether

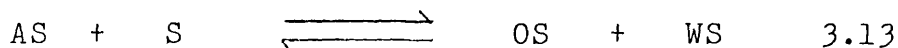
i) Via the Langmuir-Hinshelwood mechanism (LHM)



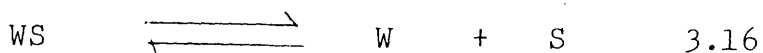
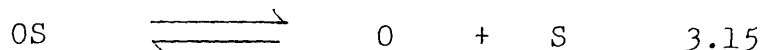
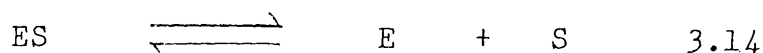
ii) Via the Rideal-Eley mechanism (REM)



b) Formation of olefin



Reaction step 3: Desorption of products



3.4.2 Equilibrium Considerations.

a) The adsorption-desorption of alcohol and inerts.

The net rates of adsorption-desorption of alcohol and inerts are given by

$$r_A = K_{aA} S C_A - K_{dA} C_{AS} \quad 3.17$$

$$r_I = K_{aI} S C_I - K_{dI} C_{IS} \quad 3.18$$

Consider that the above processes are at equilibrium, then

$$K_A = K_{aA}/K_{dA} = C_{AS}/S C_A \quad 3.18$$

$$K_I = K_{aI}/K_{dI} = C_{AS}/S C_{AI} \quad 3.19$$

where K_A and K_I are the adsorption equilibrium constants for the adsorption-desorption of alcohol and inerts, respectively.

b) The surface chemical reaction

The net rate of formation of ether, through LHM or REM is given by

$$\text{LHM} \quad R_E = K_{RE} C_{AS}^2 - K_{-RE} C_{ES} C_{WS} \quad 3.21$$

$$\text{REM} \quad R_E = K'_{RE} S C_{AS} C_A - K'_{-RE} C_{ES} C_{WS} \quad 3.22$$

The net rate of formation of olefin is

$$R_O = K_{RO} S C_{AS} - K_{-RO} C_{OS} C_{WS} \quad 3.23$$

When surface chemical reaction is at equilibrium, the net rates of formation of ether and olefin are zero. Thus one obtains

$$K_{RE} = K_{RE}/K_{-RE} = C_{ES} C_{WS}/C_{AS}^2 \quad 3.24$$

$$K'_{RE} = K'_{RE}/K'_{-RE} = C_{ES} C_{WS}/C_A C_{AS} S \quad 3.25$$

$$K_{RO} = K_{RO}/K_{-RO} = C_{OS}C_{WS}/C_{AS} \quad 3.26$$

where K_{RE} , K_{RE}' , and K_{RO} are the thermodynamic equilibrium constants for the surface chemical reaction for the formation of ether, via LHM, REM and for the formation of olefin, respectively.

c) The desorption-adsorption of ether, olefin and water.

The net rates of desorption-adsorption of ether, olefin and water are:

$$r_e = k_{aE}C_E^S - K_{dE}C_{ES} \quad 3.27$$

$$r_o = K_{aO}C_O^S - K_{dO}C_{OS} \quad 3.28$$

$$r_W = K_{aW}C_W^S - K_{dW}C_{WS} \quad 3.29$$

At equilibrium

$$K_E = K_{aE}/K_{dE} = C_{ES}/C_E^S \quad 3.30$$

$$K_O = K_{aO}/K_{dO} = C_{OS}/C_O^S \quad 3.31$$

$$K_W = K_{aW}/K_{dW} = C_{WS}/C_W^S \quad 3.32$$

where K_E , K_O and K_W are the adsorption-desorption equilibrium constants for the products ether, olefin and water respectively.

The overall equilibrium constants for the dehydration reactions, equations 3.7 and 3.8 are given by

$$K_{eq,E} = C_E C_W / C_A^2 \quad 3.33$$

$$K_{eq,O} = C_O C_W / C_A \quad 3.34$$

Substituting for C_E , C_W and C_A using equations 3.21, 3.24, 3.30 and 3.32 gives the thermodynamic equilibrium

$$\text{using LHM} \quad K_{\text{eq},E} = K_A^2 K_{RE} / K_W K_E \quad 3.35$$

$$\text{using REM} \quad K_{\text{eq},E} = K_A K'_{RE} / K_W K_E \quad 3.36$$

A similar treatment gives the overall thermodynamic equilibrium constant for the dehydration of alcohol to olefin and water, equation 3.8.

$$K_{\text{eq},O} = K_A K_{RO} / K_W K_O \quad 3.37$$

3.4.3 Adsorption of Alcohol as Rate Controlling Step.

Consider the adsorption of alcohol as the rate controlling step, all other processes are assumed to be very fast and at equilibrium. Then the overall rate of reaction is determined by the rate of adsorption of alcohol, equation 3.9.

In this work, the rates of formation of olefin and ether will be used instead of the overall rate of decomposition of alcohol. If the rates of production of ether and olefin are measured in molecules per gram of catalyst per unit time and there is no side reaction, then from the stoichiometric balance

$$R_A = 2 R_E + R_O \quad 3.38$$

a) Rate of formation of ether, via LHM.

The net rate of formation of ether is given by the difference between the rate of adsorption and that of desorption of alcohol, as in equation 3.17.

Substituting for C_{AS} , using equation 3.24, the net rate of ether formation becomes

$$R_E = K_{aA} C_A S - K_{dA} (C_{ES} C_{WS} / K_{RE})^{\frac{1}{2}} \quad 3.39$$

The uncovered active sites can be obtained by assuming that the total number of active sites remain constant in the absence of deactivation. It follows that uncovered active site is given by

$$S = S_0 - (C_{AS} + C_{ES} + C_{OS} + C_{WS} + C_{IS}) \quad 3.40$$

C_{AS} , C_{ES} , C_{OS} , C_{WS} and C_{IS} are not measurable quantities, therefore they must be eliminated and replaced by measurable quantities C_A , C_E , C_O , C_W and C_I using expressions 3.24, 3.30, 3.31, 3.32 and 3.20, the net rate of formation of ether becomes

$$R_E = \frac{K_{aA} S_0 (C_A - (C_E C_W / K_{eq,E})^{\frac{1}{2}})}{1.0 + K_E C_E + K_O C_O + (K_A^2 C_E C_W / K_{eq,E})^{\frac{1}{2}} + K_W C_W + K_I C_I} \quad 3.41$$

where $K_{eq,E}$ is already defined by equation 3.35.

Similarly the net rates of formation of ether via the REM and olefin can be written as

$$R_E = \frac{K_{aA} S_0 (C_A - C_E C_W / C_A K'_{eq,E})}{1.0 + K_E C_E + K_O C_O + K_W C_W + K_A C_E C_W / C_A K'_{eq,E} + K_I C_I} \quad 3.42$$

and

$$R_O = \frac{K_{aA} S_0 (C_A - C_O C_W / K_{eq,O})}{1.0 + K_E C_E + K_O C_O + K_W C_W + K_A C_O C_W / K_{eq,O} + K_I C_I} \quad 3.43$$

where $K'_{eq,E}$ and $K_{eq,O}$ are given by equations 3.36 and 3.39, respectively.

The above treatment can similarly be applied to the case when surface chemical reaction or desorption of product is controlling.

Tables A1.1, A1.2 and A1.3, in appendix 1, summarise the derived hyperbolic rate expressions according to Hougen-Watson approach, based on the reaction schemes given in equations 3.9 to 3.16. In the tables, the concentrations C_A , C_E , C_O , C_W and C_I have been replaced by partial pressures of the species A, E, O, W and I, respectively.

Additional rate expressions are generated by:

- a) Neglecting the influence of backward reaction.
- b) Neglecting the contribution of inerts to the adsorption term.
- c) Initial rates expressions are obtained by assuming that the partial pressures of the products are nearly zero and the adsorption equilibrium constant of inerts is very small or nearly zero. Tables A1.4 and A1.5, in appendix 1, summarise the initial rate expressions for the formation of ether and olefin, respectively.

CHAPTER 4

RESULTS AND DISCUSSION OF THE KINETIC DATA
ON THE CATALYTIC DEHYDRATION OF ALCOHOLS
IN A CSGSR

CHAPTER 4RESULTS AND DISCUSSION OF THE KINETIC DATA ON THE CATALYTIC
DEHYDRATION OF ALCOHOLS IN A CSGSR4.1 General Considerations4.1.1 Introduction

Kinetic data on the dehydration of n-butanol, isopropanol and ethanol over zeolites 13X, 4A and ZNa, all in sodium form and synthetic cation exchange resin, in hydrogen form, have been obtained for a wide range of experimental conditions. In all the experiments, the total pressure of the reactor was kept at 1-bar gauge. Pure alcohol feed diluted with inert high-purity nitrogen was used.

For each run, the rates of formation of olefin and ether were calculated using the following material balance expressions for an ideal continuous stirred tank reactor.

$$R_O = F_{A_0} X_O / W \text{ gmole/g}_c \cdot \text{hr} \quad 4.1$$

$$R_E = F_{A_0} X_E / W \text{ gmole/g}_c \cdot \text{hr} \quad 4.2$$

The mean error in the rate of formation of ether or olefin is no more than 5%.

4.1.2 Main Side Reactions.

The dehydration of alcohols (n-butanol, iso-propanol and ethanol) over zeolite 13X, 4A and ZNa catalysts yields two principal products, ether and olefin. Gas chromatograph analysis showed the formation of aldehyde from the primary alcohols or ketone from the secondary alcohol. Very little saturated paraffin was found. Aldehyde or ketone is formed by the dehydrogenation of alcohol. Saturated paraffin is produced by the hydrogenation of olefin. The experimental data were analysed in terms of the rates of formation of ether and/or olefin, instead of the overall conversion of alcohol. For each run the mass balance took into consideration the formation of aldehyde or ketone and hydrogen.

Pure alcohol was fed into the reactor system at operating conditions without catalyst. The gas chromatograph detected olefin and aldehyde or ketone, but did not detect ether. The aldehyde or ketone detected during these control runs accounted for most of these side products formed in the experiments with catalysts. This observation suggests that the bulk of aldehyde or ketone produced during the experimental runs was catalysed by the nickel and/or copper present in the reactor wall and the associated piping material. Nickel and/or copper have been found to be active catalysts for the dehydrogenation reactions (39, 40, 101). The zeolites

used may also contribute to a small extent to the formation of aldehyde or ketone, because the zeolites possess basic sites which are required for the dehydrogenation reaction.

The effect of thermal dehydration of alcohol to olefin has also been taken into account. However this effect gave less than 5% of the olefin formed under all reaction conditions.

4.1.3 Mass and Heat Transfer Effects.

The effects of external mass and heat transfer have been discussed in chapter 2. The internal mass and heat transfer effects cannot be assessed by using the Weisz and Practer (93) criterion, because of the lack of empirical correlation for the estimation of effective diffusivity in zeolite cages. The mechanism of intra-particle transport in the zeolites is not yet clear. This is because in most cases the pore size is of the same order of magnitude as the molecular dimensions. This problem has been discussed by Weisz (97).

Intra-particle effects could be checked by examining reaction rates for different particle size, keeping other variables constant. Unfortunately, the present CSGSR does not permit the use of fine catalyst particles. However the the activation energies obtained in this study compare well with those obtained from studies (62, 67) using fine zeolites. This suggests that internal diffusional limitations were minimal.

4.1.4 Mathematical Estimation of Chemical Constants.

An extensive review on the mathematical estimation of unknown parameters in chemical reaction rate equations has been given by Kittrell (121). There are two main mathematical estimation techniques:

- a) Linear least squares analysis (weighted and unweighted).
- b) Non-linear least squares analysis.

In this work both linear and non-linear least squares analyses have been used in estimating the kinetic and adsorption equilibrium constants. Theoretical aspects of linear and non-linear least squares estimation of the adjustable co-efficient can be found in the following references (55, 56, 104, 121).

The computer programmes on linear and non-linear squares analyses were made available through the South Western University Computer net-work. The non-linear programme is from the Biomedical programme package, Health Science Computing Facility, University of California, U.S.A. Details of the programme can be obtained from reference 69.

4.1.5 Preliminary Discrimination and Simplification of the Hougen-Watson Rate Expressions.

Plausible rate expressions derived according to the Hougen-Watson approach based on a simultaneous reaction scheme, and for different controlling steps, are presented

in Tables A1.1, A1.2 and A1.3, in appendix 1. Preliminary discrimination of these derived rate expressions is necessary, since not all of these rate expressions are probable. Secondly, simplification of the selected rate expressions will help to reduce the complexity of some of the rate equations. These preliminary considerations can be achieved by examining relevant data both from literature and from the present study.

a) The adsorption equilibrium constants of ether and olefin have been experimentally determined and found to be near zero (34, 100). Hence the desorption of ether or olefin cannot be the rate limiting step. The corresponding rate equations can therefore be discarded.

b) The partial pressures of ether and olefin in all the experiments are very small compared with the partial pressure of alcohol. The products $K_E P_E$, $K_O P_O$ are very much smaller than $K_A P_A$. Hence the contributions of ether and olefin to the adsorption terms can be neglected with little error involved.

c) The adsorption of nitrogen on molecular sieve is appreciable only at temperatures below 244 K (9). Under the present working conditions nitrogen should only be weakly adsorbed. Therefore the diluent contribution in the adsorption term can be neglected.

d) The equilibrium constant of the surface chemical reaction leading to the formation of olefin is high.

Hence the dehydration of alcohol to olefin can be assumed to be irreversible.

e) Although water retards the dehydration reactions, it was not necessary to consider this effect because the partial pressure of water was very low in all the experiments. The contribution of water is insignificant and can be neglected. The denominator in the Hougen-Watson rate expression, in the case the surface reaction controls, is therefore reduced to

$$(1.0 + K_A P_A)^n$$

The three remaining rate limiting steps are the desorption of alcohol, surface catalysed reaction and the desorption of water.

For the formation of olefin, if the adsorption of alcohol is the rate controlling step, then the rate of formation of olefin is given by

$$R_O = \frac{K_{aA} S_o P_A}{1.0 + K_A P_W P_O / K_{eq,0}} \quad 4.3$$

Qualitatively, this expression predicts progressive increase in the rate of formation of olefin with increasing partial pressure of alcohol. It suggests a first order reaction with respect to alcohol concentration and no alcohol retardation effect. But both behaviour were not found in the present study, therefore it was not necessary to consider this rate expression.

For the model with surface catalysed reaction as the rate controlling step, the rate of formation of olefin is given by

$$R_0 = \frac{K_R K_A S_o P_A}{(1.0 + K_A P_A)^2} \quad 4.4$$

The above expression is based on a dual site mechanism. Qualitatively, this equation predicts reaction order less than one and a depressive behaviour by alcohol. These predictions have been observed experimentally. Hence this model should be tested.

For the model with the desorption of water as the rate limiting step, the rate of formation of olefin is

$$R_0 = \frac{K_{aW} S_o K_{eq,O} P_A / P_O}{(1.0 + K_A P_A + K_{eq,O} K_W P_A / P_O)} \quad 4.5$$

Qualitatively, this equation predicts approximately zero order reaction at all partial pressures of alcohol which does not contradict experimental findings. Therefore this rate expression cannot be rejected.

4.2 Results and Discussion of the Dehydration of Alcohols over Zeolites

4.2.1 Kinetic Data.

The kinetic data on zeolites are presented in Tables A4.1 to A4.3, A4.8 to A4.10, A4.15 and A4.16.

Figures 4.1 to 4.8 illustrate the effect of partial pressure of alcohol on the rate of formation of olefin over zeolites. The dependence of the rate of formation of olefin is clearly less than first order. For the formation of butene and propene, it tends to be approximately zero-order which is typical of mono-molecular heterogeneous reactions.

Figures 4.9 to 4.11 show the influence of the partial pressure of alcohol on the rate of formation of ether over zeolites. The influence of the partial pressure of alcohol on the rate of formation of ether over zeolites 4A and ZNa was not illustrated graphically because of irregularity in the shape of the curves. For example, when the partial pressure of alcohol is low, ether was not produced, see tables A4.2, A4.3, etc or the rate at higher temperature is lower than that at lower temperature, see figures 4.10 and 4.25. This irregularity will be discussed in section 4.3.

At low temperature, the reactions are approximately zero-order. This is because chemisorption decreases

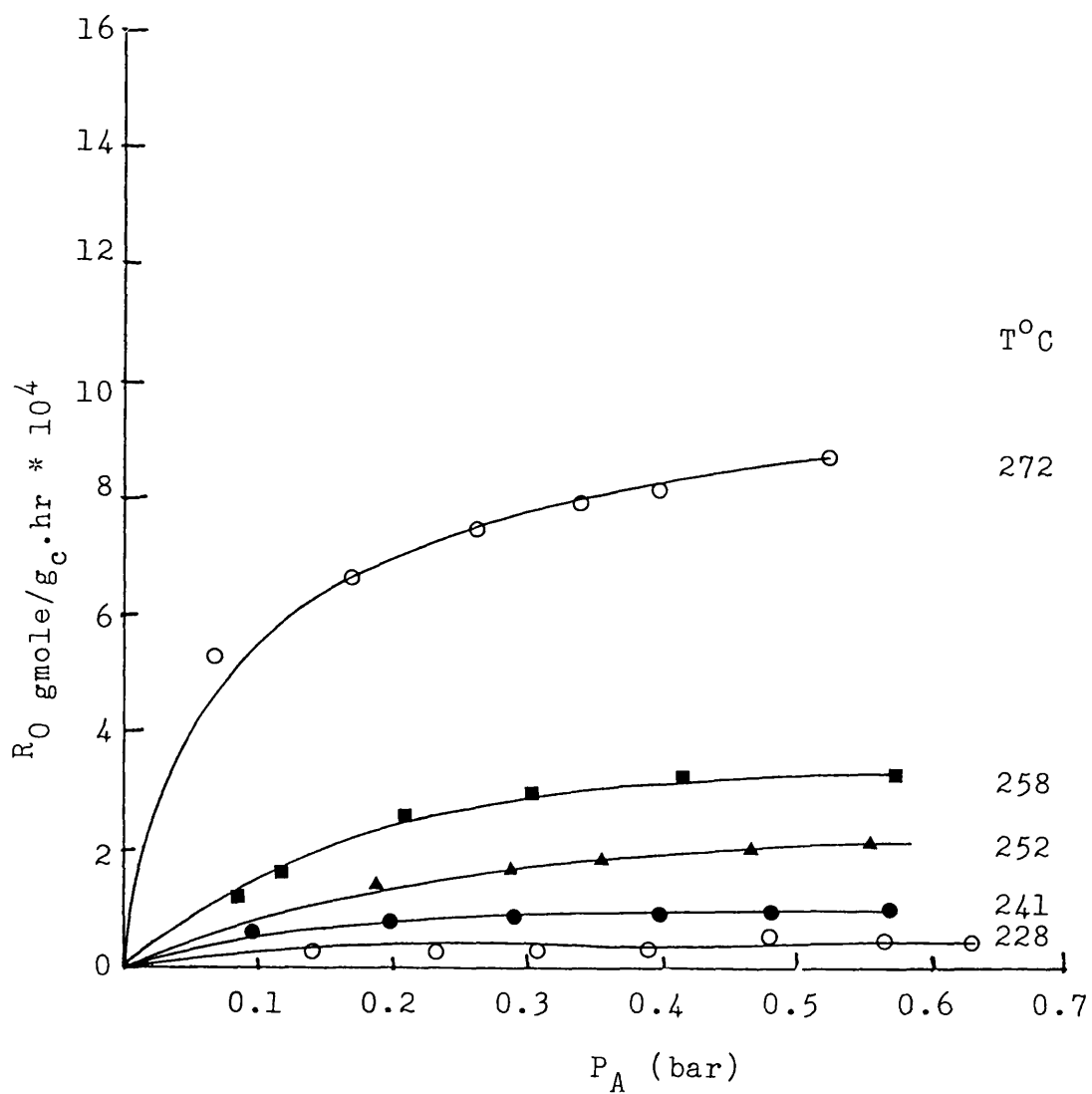


Fig.4.1 The Influence of the Partial Pressure of n-Butanol on the Rate of Formation of Butene over Zeolite 13X.

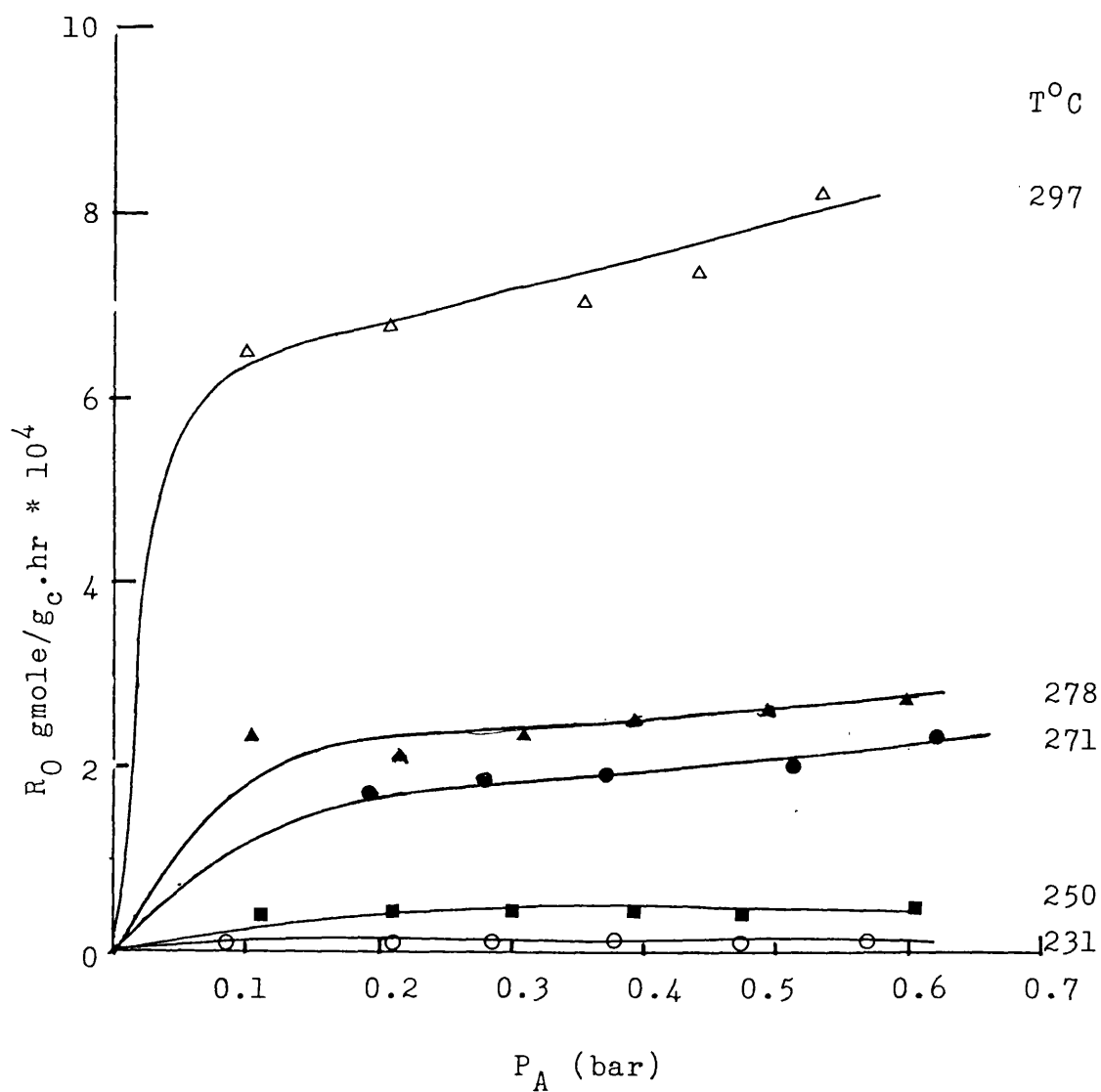


Fig. 4.2 The Influence of the Partial pressure of
n-Butanol on the Rate of Formation
of Butene over Zeolite 4A.

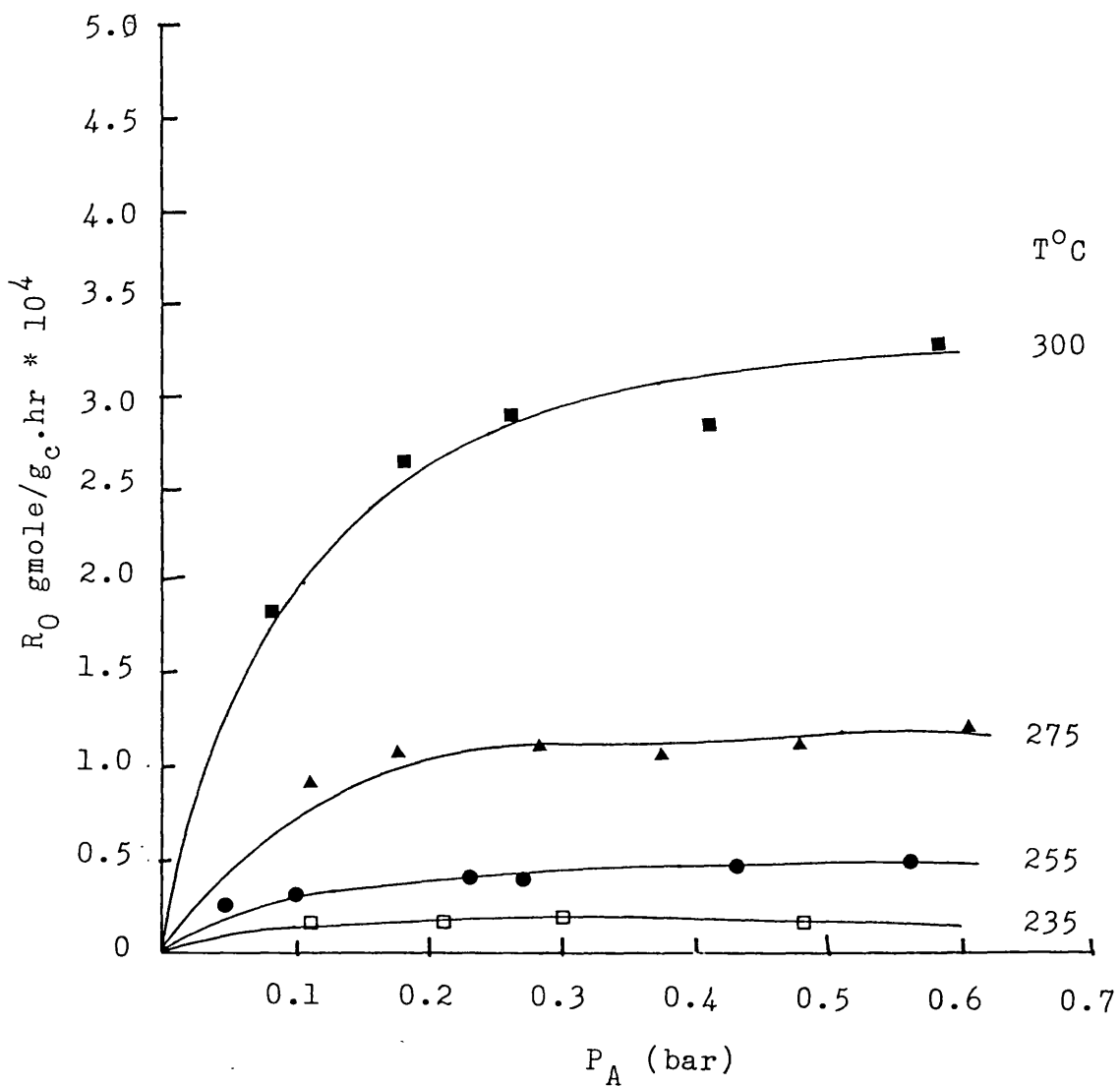


Fig. 4.3 The Influence of the Partial Pressure
of n-Butanol on the Rate of Formation
of Butene Over Zeolite ZNa.

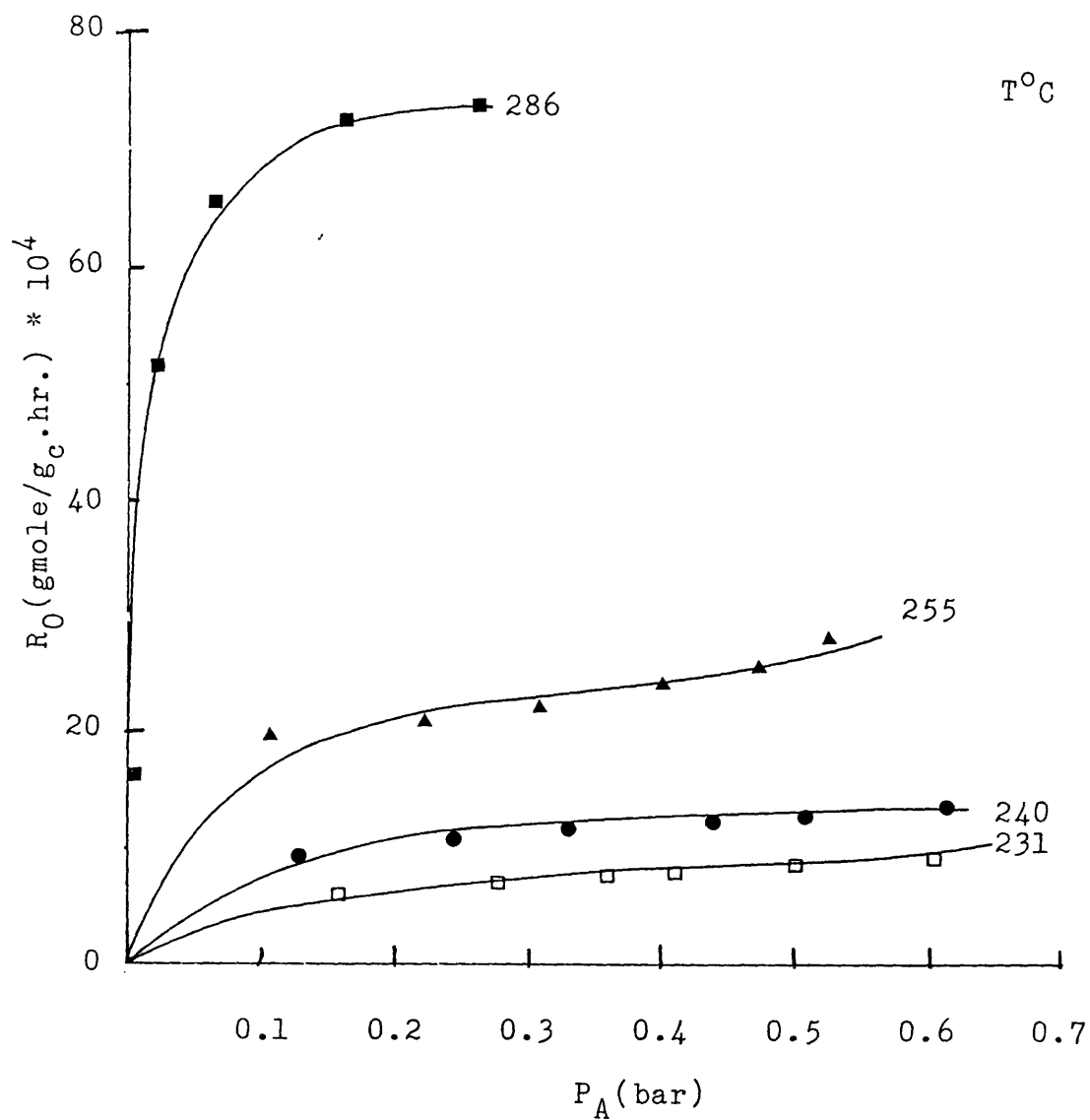


Fig. 4.4 The Influence of the Partial Pressure of Isopropanol on the Rate of Formation of Propene over Zeolite 13X.

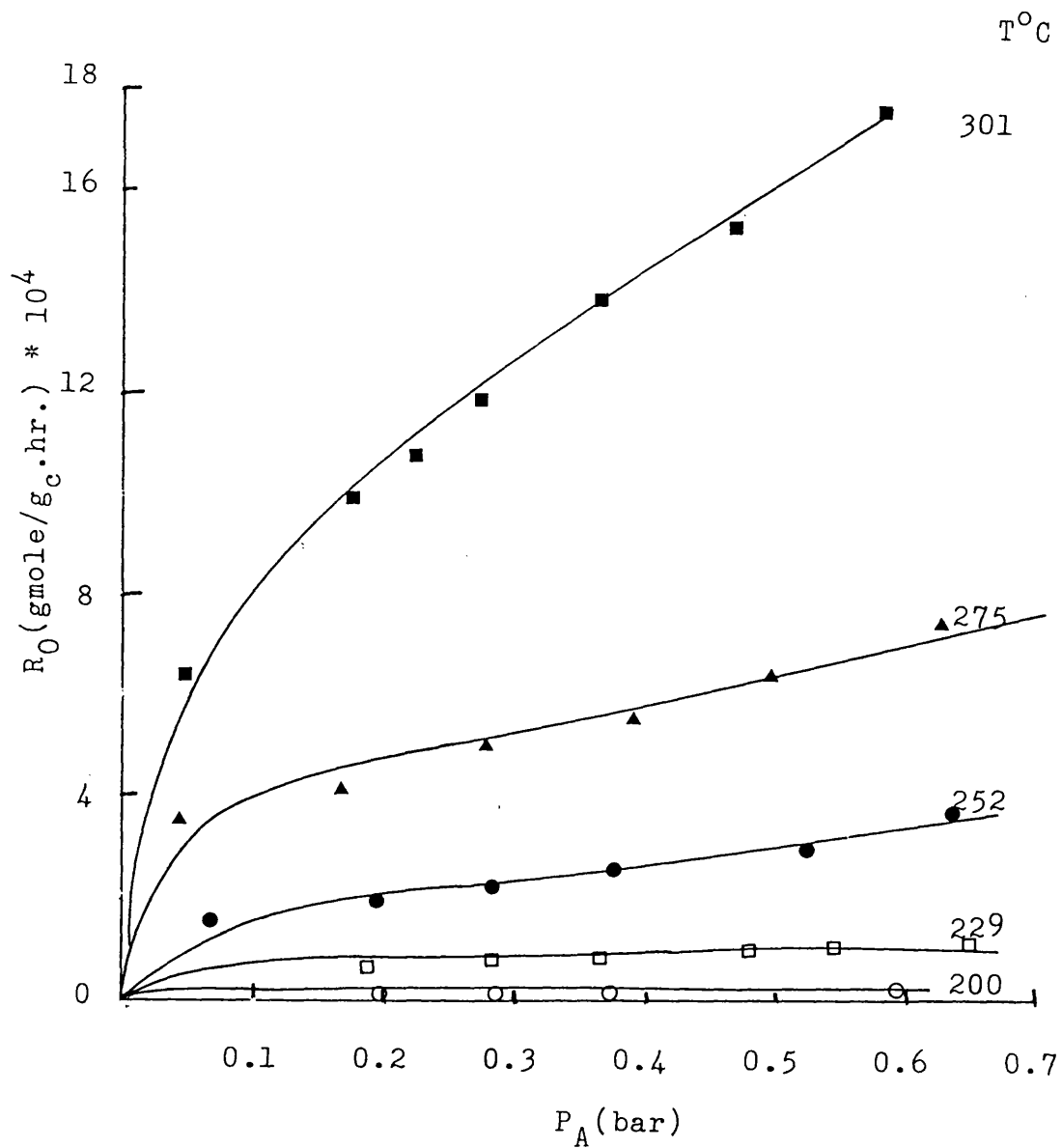


Fig. 4.5 The Influence of the Partial Pressure of Isopropanol on the Rate of Formation of Propene over Zeolite 4A.

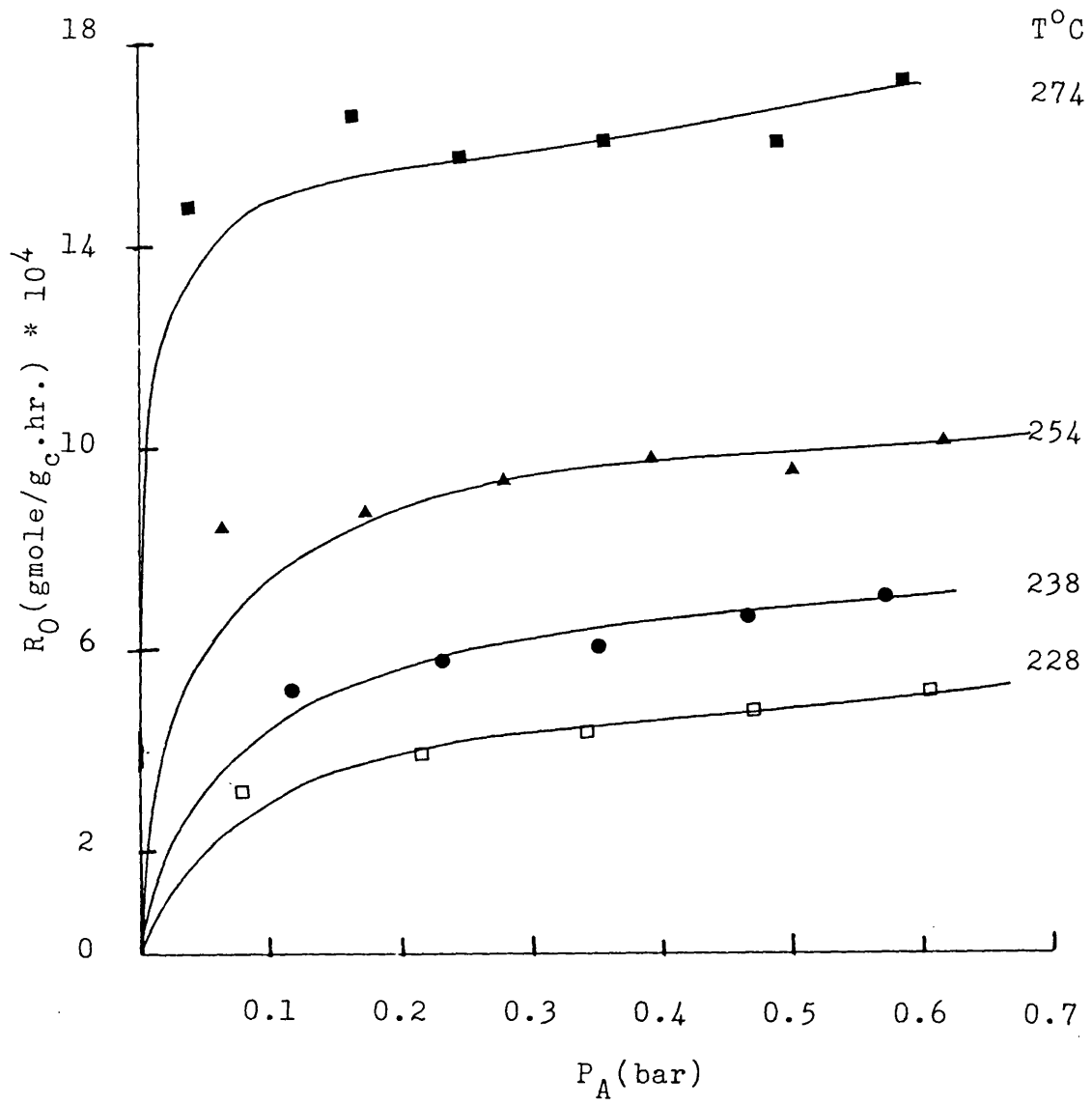


Fig. 4.6 The Influence of the Partial Pressure of Isopropanol on the Rate of Formation of Propene over Zeolite ZNa.

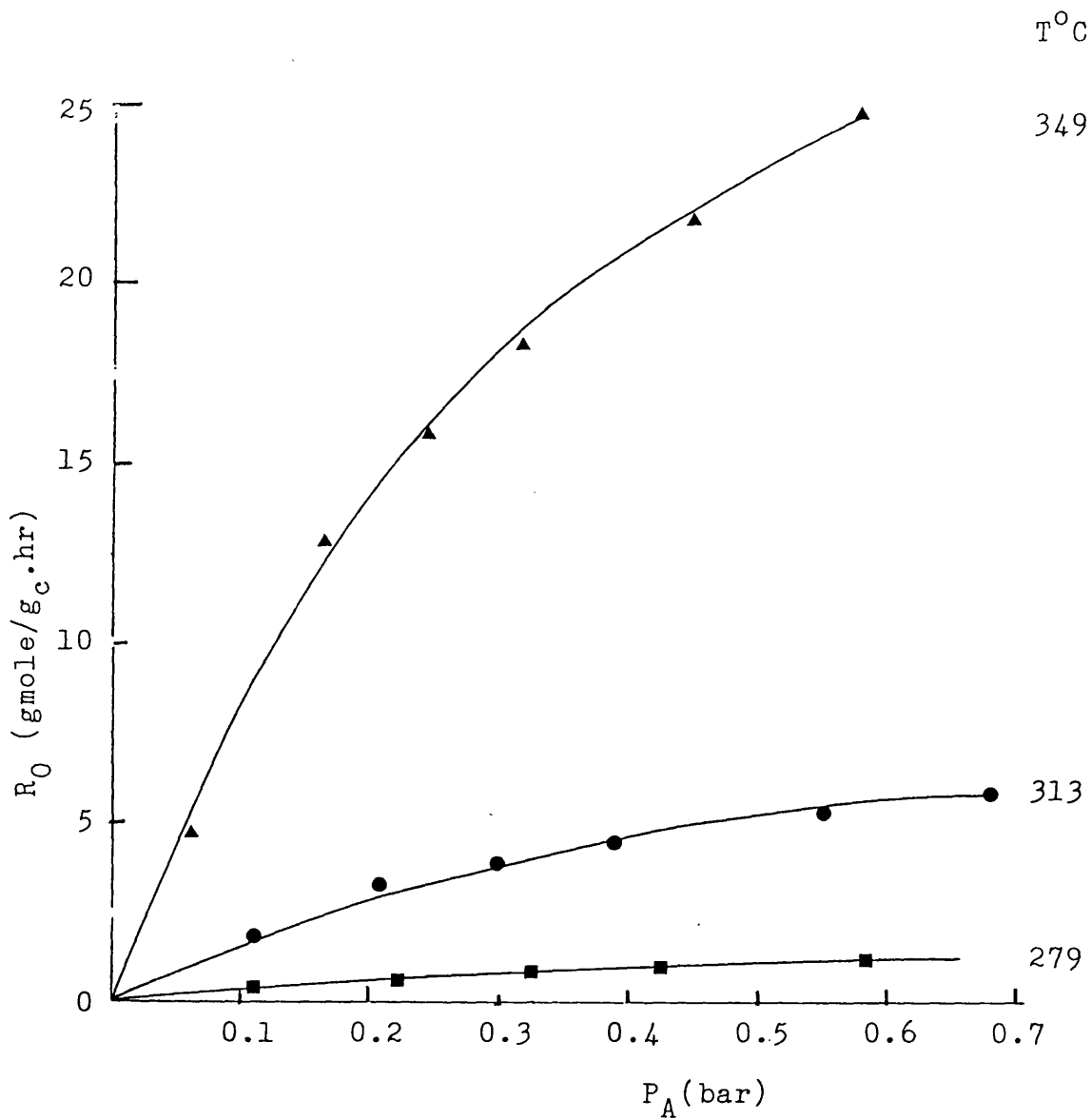


Fig. 4.7. The Influence of the Partial Pressure of Ethanol on the Rate of Formation of Ethylene over zeolite 4A.

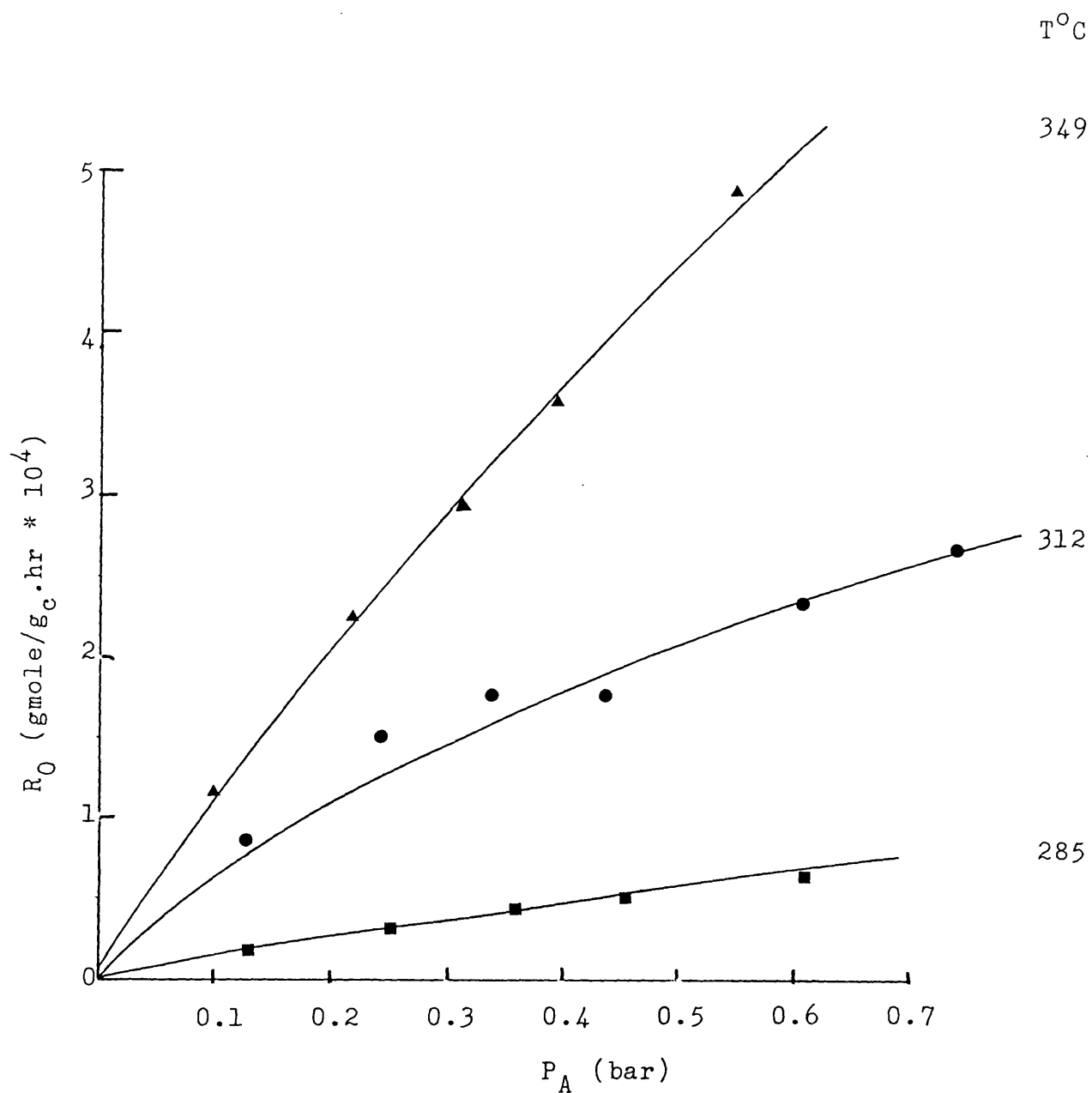


Fig. 4. 8 The Influence of the Partial Pressure of Ethanol on the Rate of Formation of Ethylene over ZNa Zeolite.

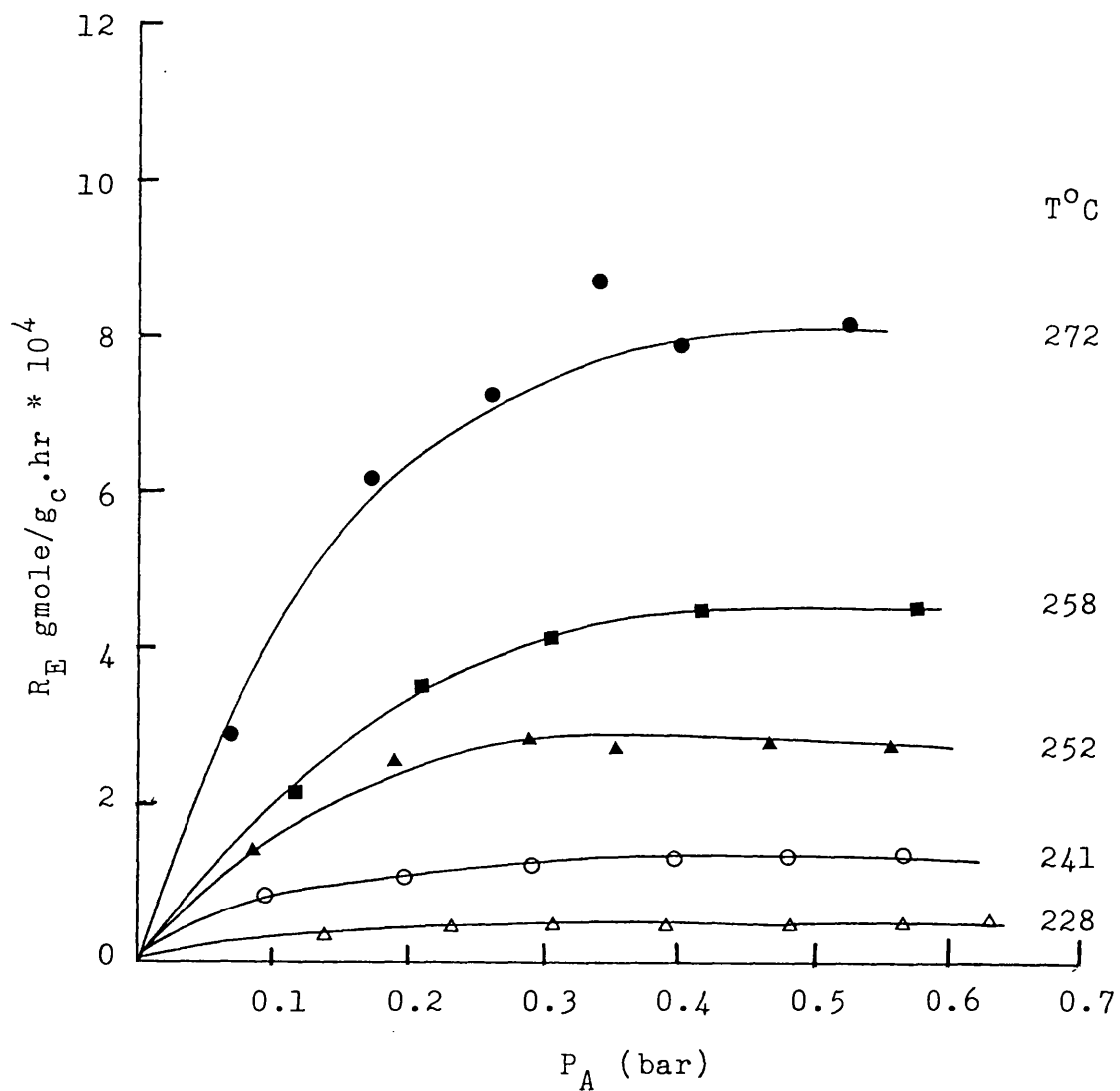


Fig. 4.9 The Influence of the Partial Pressure of
n-Butanol on Rate of Formation of
Di-n-butyl Ether over Zeolite 13X.

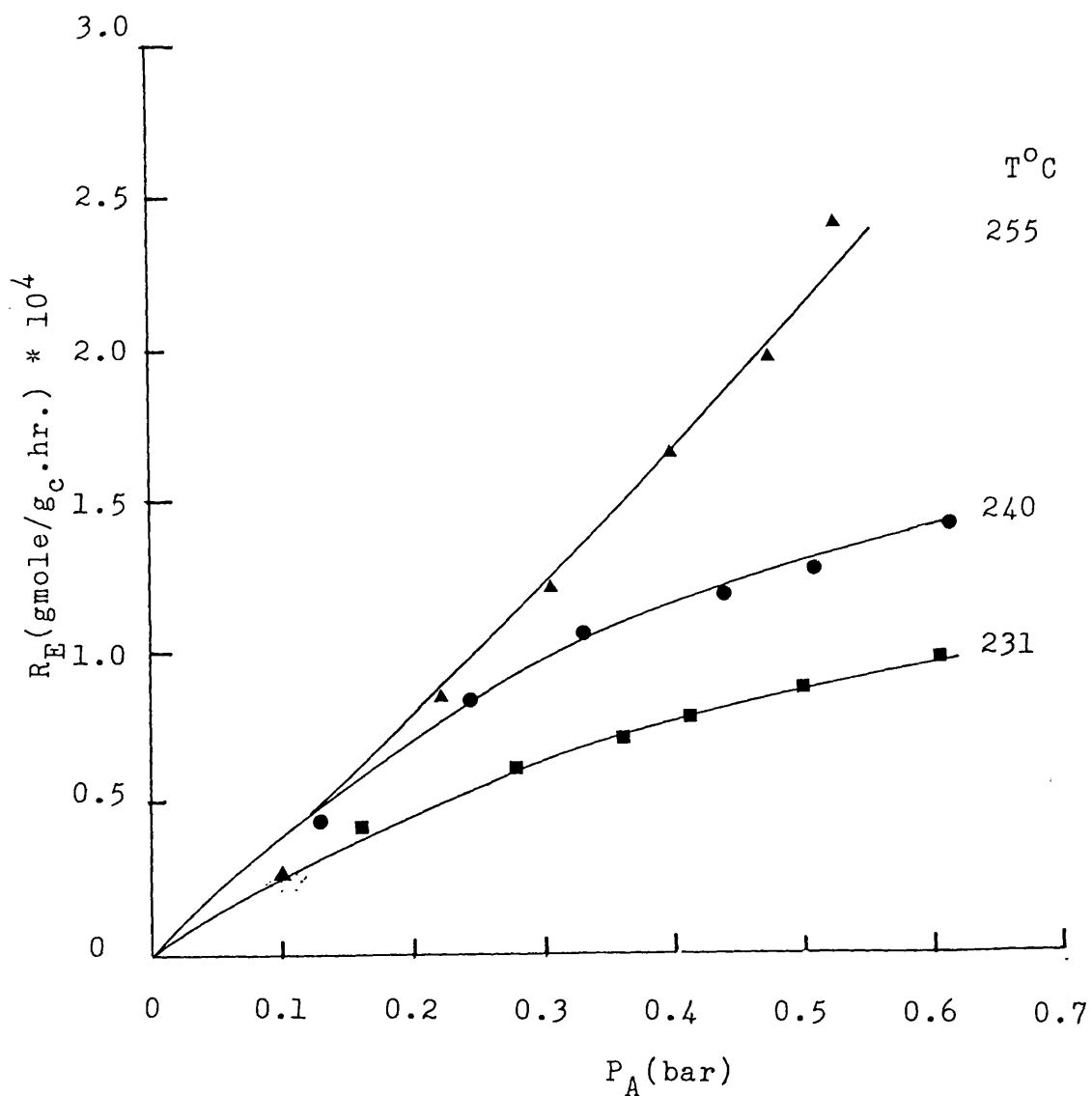


Fig. 4.10 The Influence of the Partial Pressure of Isopropanol on the Rate of Formation of Di-isopropyl Ether over Zeolite 13X.

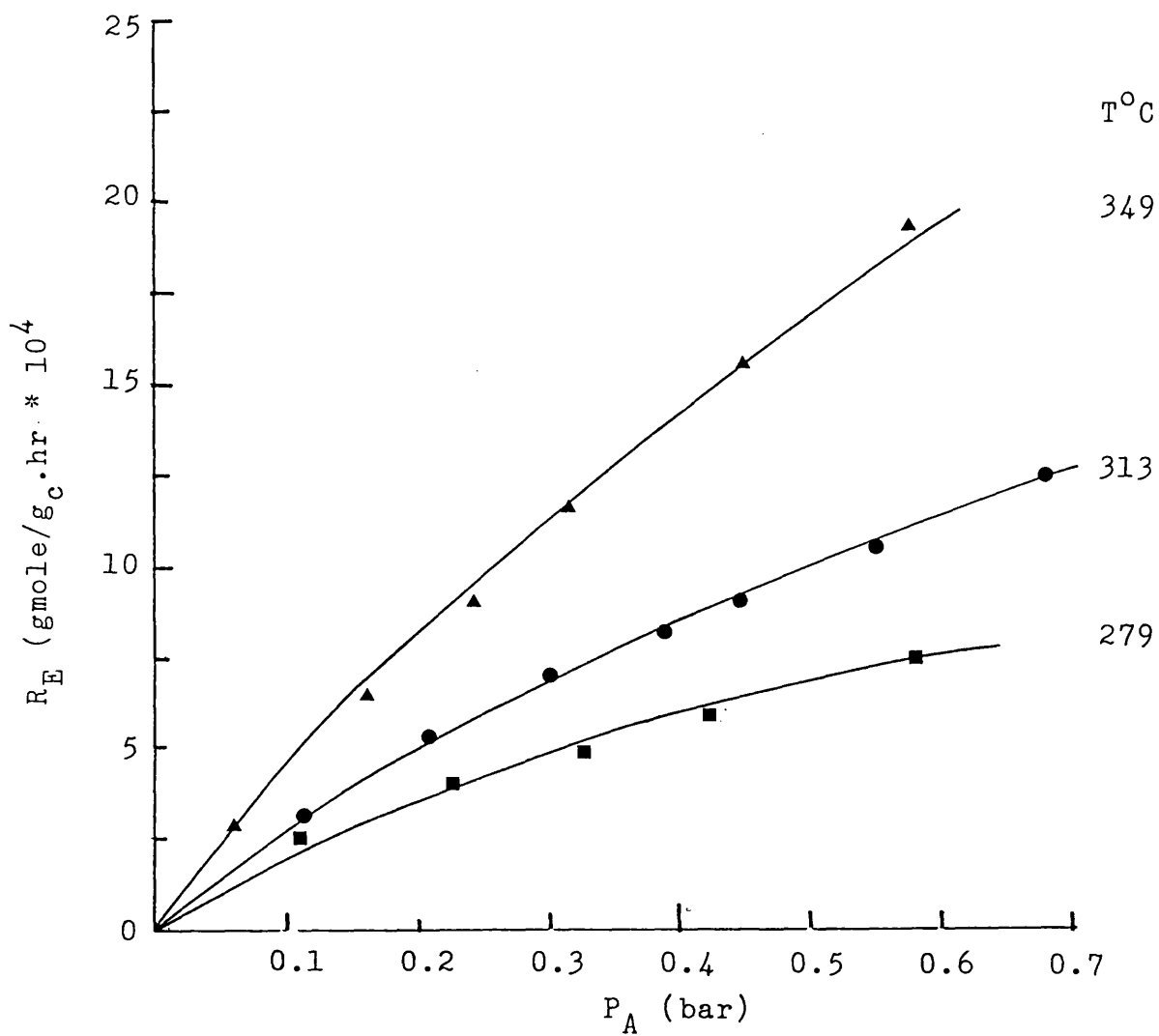


Fig. 4.11 The Influence of the Partial Pressure of Ethanol on the Rate of Formation of Di-ethyl Ether over Zeolite 4A.

with increasing temperature. The coverage of the catalyst by the reactant is nearly complete at low temperatures but not at higher temperatures. It can be seen from the shape of the curves that reaction order with respect to alcohol increases slightly with increasing reaction temperature. The value of the partial pressure of alcohol, beyond which rate of formation of ether or olefin remains constant, is found to rise with increasing temperature. This behaviour corresponds to the decrease in the adsorption of alcohol with increasing temperature.

The partial pressures of the other compounds (ether, olefin and water) are very small compared with that of alcohol. Although water has a depressive effect on reaction rate, its partial pressure is so small at all reaction temperatures that the depressive effect can be neglected. The earlier assumptions that these compounds do not contribute significantly to the rate expression are therefore justified.

4.2.2 Kinetic Expression

4.2.2.1 Empirical Power Law.

Table A2.1, in appendix 2, presents the formulated power function rate expressions for the formation of olefin and ether. The most successful candidates of these rate equations are

$$\text{for olefin formation: } R_O = K_{RO} P_A^n \quad 4.6$$

$$\text{for ether formation : } R_E = K_{RE} P_A^m \quad 4.7$$

Isothermal regression of the kinetic data shows that the reaction order with respect to alcohol concentration increases slightly with increasing reaction temperature, see table 4.1. Non-isothermal regression of the data yielded the following equation for the rate of formation of olefin.

$$R_O = A_0 \exp(-E_{A0}/R_g T) P_A^n \quad 4.8$$

A similar equation was obtained for the rate of formation of ether. The rate equations were linearised by taking the natural logarithm. All the parameters in these two equations were estimated by multi-linear least squares analysis technique. Tables 4.2, 4.3 and 4.4 give the estimated kinetic constants for the dehydration of n-butanol, isopropanol and ethanol respectively.

The t-ratio is the ratio of the estimated co-efficient and its standard deviation is also reported in the tables. A high value of t-ratio means small standard deviation, hence the confidence interval of the parameter is small. Column 7 of the tables shows the R-squared co-efficient, which is a measure of how well the regression expression fits the experimental data. All the equations gave high R-squared values. Column 8 shows the calculated F-ratio, which gives an indication of the significance of the regression. The last column shows the F-ratio from the statistical table at 95% confidence level. If the observed F-ratio exceeds the critical F-ratio at 95%

Table 4.1 Effect of Temperature on Order of Reaction.

The dehydration of ethanol to di-ethyl
ether over cation exchange resin.

Temp °C	$K \left(\frac{\text{gmole}}{\text{g}_c \cdot \text{hr} \cdot \text{bar}^n} \right) * 10^3$	n	R-squared
142	18	1.2	99
131	12	1.1	100.
120	7.0	0.91	100.

Table 4.2 Kinetic Constants for the Power Function Rate Expression.

The dehydration of n-butanol.

	1	2	3	4	5	6	7	8	9	10	
CAT	Prod.	A_0	t-ratio	E_A	t-ratio	n or m	t-ratio	R-squ.	F(K)	K	F(K)
		$\frac{\text{gmole}}{\text{g}_c \cdot \text{hr} \cdot \text{bar}^n}$		$\frac{\text{Kcal}}{\text{gmole}}$							
13X	0	$1.4 \cdot 10^{12}$	36	38	48	0.28	8.0	99	$1.2 \cdot 10^3$	32	20
	E	$4.1 \cdot 10^{10}$	17	34	23	0.38	5.8	95	$2.8 \cdot 10^2$	32	20
ZNa	0	$8.0 \cdot 10^5$	23	25	39	0.17	4.9	99	$7.7 \cdot 10^2$	22	20
	E	4.7	0.66	13	5.1	0.56	4.8	79	17	12	19
4A	0	$5.6 \cdot 10^{10}$	57	36	77	0.12	4.1	99	$3.0 \cdot 10^3$	30	20
	E	$1.7 \cdot 10^3$	5.5	20	13	0.29	5.7	95	88	12	19

Table 4.3 Kinetic Constants for the Power Function Rate Expression.

The dehydration of isopropanol.

Cat.	Prod.	1	2	3	4	5	6	7	8	9	10
		A_0	t-ratio	E_A	t-ratio	n	t-ratio	R-sq.	F(K)	K	F(K)
		$\frac{\text{gmole}}{\text{g}_c \cdot \text{hr} \cdot \text{bar}^n}$		Kcal/gmole		or					
						m					
13X	0	$1.1 \cdot 10^8$	26	26	35	0.29	14	99	$6.6 \cdot 10^2$	20	20.
	E	$1.6 \cdot 10^2$	1.9	14	5.1	0.96	9.7	88	54	15	20.
4A	0	$8.5 \cdot 10^5$	39	23	63	0.38	12	99	$2.0 \cdot 10^2$	25	20.
	E	$1.4 \cdot 10^6$	6.6	28	12	1.3	10	94	102	14	20.
ZNa	0	$2.8 \cdot 10^3$	19	16	36	0.14	6.6	99	$6.9 \cdot 10^2$	22	20.
	E	1.1	0.07	10.	8.4	0.89	16	95	$1.7 \cdot 10^2$	18	20.
Resin	0	$3.0 \cdot 10^2$	6.0	8.7	12	0.63	16	95	$1.9 \cdot 10^2$	22	20.
	E	$1.4 \cdot 10^{-4}$	5.1	-2.8	1.4	1.909	27	97	$3.6 \cdot 10^2$	22	20.

Table 4.4 Kinetic Constants for the Power Function Rate Expression.

The dehydration of ethanol.

Cat. Prod.	1 A_0	2 t-ratio	3 E_A	4 t-ratio	5 n or m	6 t-ratio	7 R-sq.	8 F(k)	9 K	10 F(k)	
	$\frac{\text{gmole}}{\text{g}_c \cdot \text{hr} \cdot \text{bar}^n}$		Kcal/gmole								
4A	0	$7.5 \cdot 10^7$	37	30	52	0.67	19	100.	$1.5 \cdot 10^2$	17	20.
E		$1.6 \cdot 10^3$	12	16	21	0.70	15	98	$3.0 \cdot 10^2$	17	20.
ZNa	0	$3.0 \cdot 10^4$	6.4	22	6.8	0.79	12	93	83	16	20.
Resin	0	$1.1 \cdot 10^{18}$	11	43	14	-0.34	2.7	95	110	15	19
E		0.88	0.12	4.1	3.9	1.	24	98	$2.8 \cdot 10^2$	15	19

confidence level by a factor greater than four, statistically significant regression is said to have been obtained (104). The results show that the regression of the kinetic data for olefin formation over all the zeolites are statistically satisfactory. The regression of the data for the formation of di-n-butyl ether over ZNa zeolites and di-iso-propyl ether over 13X zeolites did not yield very high F-ratios. Thus the power law is not suitable for representing these two sets of kinetic data. Column 9 of the tables shows the number of data points used in establishing the equations.

Orders of the simultaneous reactions are shown in column 5 of each table. The reaction order (n) for the formation of olefin is smaller than that for the formation of ether for all the alcohols over all the catalysts. This observation is in accordance with the stoichiometric equations of the reactions. If the order of reactions is restricted to integral or half integral value, then the butene and propene formation are approximately zero order over all the zeolites. The di-n-butyl ether formation over zeolites 13X and 4A are approximately zero. The di-iso-propyl ether formation reaction is approximately first order over ZNa and 4A zeolites. Both the ethylene and di-ethyl ether formation reactions show approximately half order. These reaction orders are in agreement with reported values, see tables 1.2, 1.3 and 1.4. These low values of reaction order suggest that the active sites of the catalyst are nearly

saturated with alcohol. The reaction order for the dehydration of ethanol to ethylene is higher than those for the dehydration of isopropanol and n-butanol to propene and butene respectively. The explanation is that the dehydration of ethanol was carried out at higher reaction temperatures to obtain an appreciable dehydration reaction rate. Thermodynamically adsorption decreases with increasing temperature.

The activation energies for the ether and olefin formation reactions over all the zeolites are reported in column 3 of the tables. The activation energies obtained for the formation of olefin in the present work compare very favourably with those reported in literature, see tables 1.2, 1.3 and 1.4.

Some of the activation energies estimated for the formation of ethers over all the zeolites are affected by internal diffusional limitations. The exceptions are those for the formation of di-n-butyl ether over 13X and di-isopropyl ether over 4A. This is because the ethers could not diffuse easily out of the pores. The values of the activation energies obtained are approximately half of those in literature. The value of 34 Kcal/gmole obtained for the dehydration of n-butanol to di-n-butyl ether over zeolite 13X is close to that reported by Kabel and Johanson (34). The estimated apparent activation energy for the formation of di-isopropyl ether over 4A zeolite is in good agreement with literature. An explanation for this behaviour is that all di-isopropyl ether produced on 4A zeolite are from the external surface

of the catalyst, because the crystalline pores of this zeolite are not accessible to di-iso-propyl ether.

Values of the pre-exponential factors are given in column 1 in tables 4.2, 4.3 and 4.4. The pre-exponential factor for the formation of olefin is greater than that for the formation of ether for all the zeolites. This indicates that the mobility of olefin is higher than that of ether.

The agreement between the present results (activation energies) and literature values is rather remarkable in view of the different treatment of the kinetic data and different experimental conditions used here. This agreement suggests that the reaction mechanism and the rate determining step are probably the same for these three alcohols over a wide range of reaction temperature and different catalysts.

It can be concluded that the power function rate expression can statistically represent the kinetic data on the dehydration of alcohols over zeolites in most cases.

4.2.2.2 Hougen-Watson Rate Expression.

Results in section 4.2.2.1 suggest that the active sites of the catalyst are nearly saturated with alcohol. It was therefore decided to correlate the kinetic data with the Hougen-Watson type of rate expression to determine the extent of the influence of adsorption on the various estimated parameters.

The very high activation energies obtained from the empirical power function rate expression support the previous conclusion that surface catalysed reaction is the rate controlling step and the influence of external mass and heat transfer are minimal. Statistical analysis of the present kinetic data showed that they could not be satisfactorily represented by equations 4.3 and 4.5. Only parameters relating to surface catalysed reaction as the rate determining are presented and discussed here.

4.2.2.2.1 Kinetic Expression for the Formation of Olefin.

The two rate expression derived for the dehydration of alcohol to olefin based on the assumption that surface catalysed reaction is the rate limiting step, are equations 4.9 and 4.10.

$$\text{dual site mechanism (SR2): } R_0 = \frac{K_R K_A P_A}{(1.0 + K_A P_A)^2} \quad 4.9$$

Qualitatively, this equation predicts reaction order between 1 and -1 and also the depressive behaviour of alcohol. Both predictions have been observed experimentally.

$$\text{single site mechanism (SR1): } R_0 = \frac{K_R K_A P_A}{(1.0 + K_A P_A)} \quad 4.10$$

This expression predicts qualitatively a reaction order less than 1 and a rate inhibition by alcohol concentration.

The estimated model parameters, obtained from linear regression for the dehydration of n-butanol, isopropanol and

ethanol, are presented in Tables A4.4, A4.11 and A4.17, in appendix 4, respectively.

Both correlations 4.9 and 4.10 show high R-squared co-efficients over all the zeolites at all reaction temperatures. On the basis of the R-squared co-efficients the power function rate expression compared well with the Hougen-Watson rate expressions.

The kinetic data over ZNa catalyst when fitted to model SR1 resulted in a negative adsorption co-efficient at reaction temperature 235°C. The single site model for ZNa should have therefore been rejected because of this negative adsorption co-efficient, however the non-linear analysis was still performed.

The estimated parameters through the linear analysis were used as the initial values for the non-linear analysis. Tables A4.5, A4.12 and A4.14, in appendix 4, give the estimated parameters from the non-linear analysis. There is excellent agreement between the parameters obtained from linear and non-linear analysis techniques which indicates that the kinetic data obtained are good. Table 4.5 shows the comparison of the linear with the non-linear regression method. The differences in the values are very small. Froment and Bischoff (105) have suggested that poor kinetic data may give large differences in the values obtained from the two methods. The presence of a saddle point may also result in large differences in these two values.

Table 4.5 Comparison of the Linear and Non-linear Regression Analyses.

Kinetic data on the dehydration of n-butanol over ZNa zeolite.

Model	SR1			
	SR2	Non-		Non-
Regression		Linear	Linear	Linear
Method	Linear	Linear	Linear	Linear
Temp. °C	$K_R * 10^4$	K_A	$K_R * 10^4$	K_A
	$\frac{\text{gmole}}{\text{g}_c \cdot \text{hr}}$	bar^{-1}	$\frac{\text{gmole}}{\text{g}_c \cdot \text{hr}}$	bar^{-1}
		K_A	$K_R * 10^4$	K_A
		bar^{-1}	$\frac{\text{gmole}}{\text{g}_c \cdot \text{hr}}$	bar^{-1}
			$K_R * 10^4$	K_A
			$\frac{\text{gmole}}{\text{g}_c \cdot \text{hr}}$	bar^{-1}
				$\frac{\text{gmole}}{\text{g}_c \cdot \text{hr}}$
				bar^{-1}
235	0.81	4.9	0.80	4.6
				-19
				0.15
				0.18
255	2.0	3.0	1.9	3.0
				16
				0.55
				0.52
275	4.8	2.7	4.7	2.9
				26
				1.3
				1.2
300	13	2.4	13	2.5
				14
				3.6
				3.6
				14
				1.1 10^3

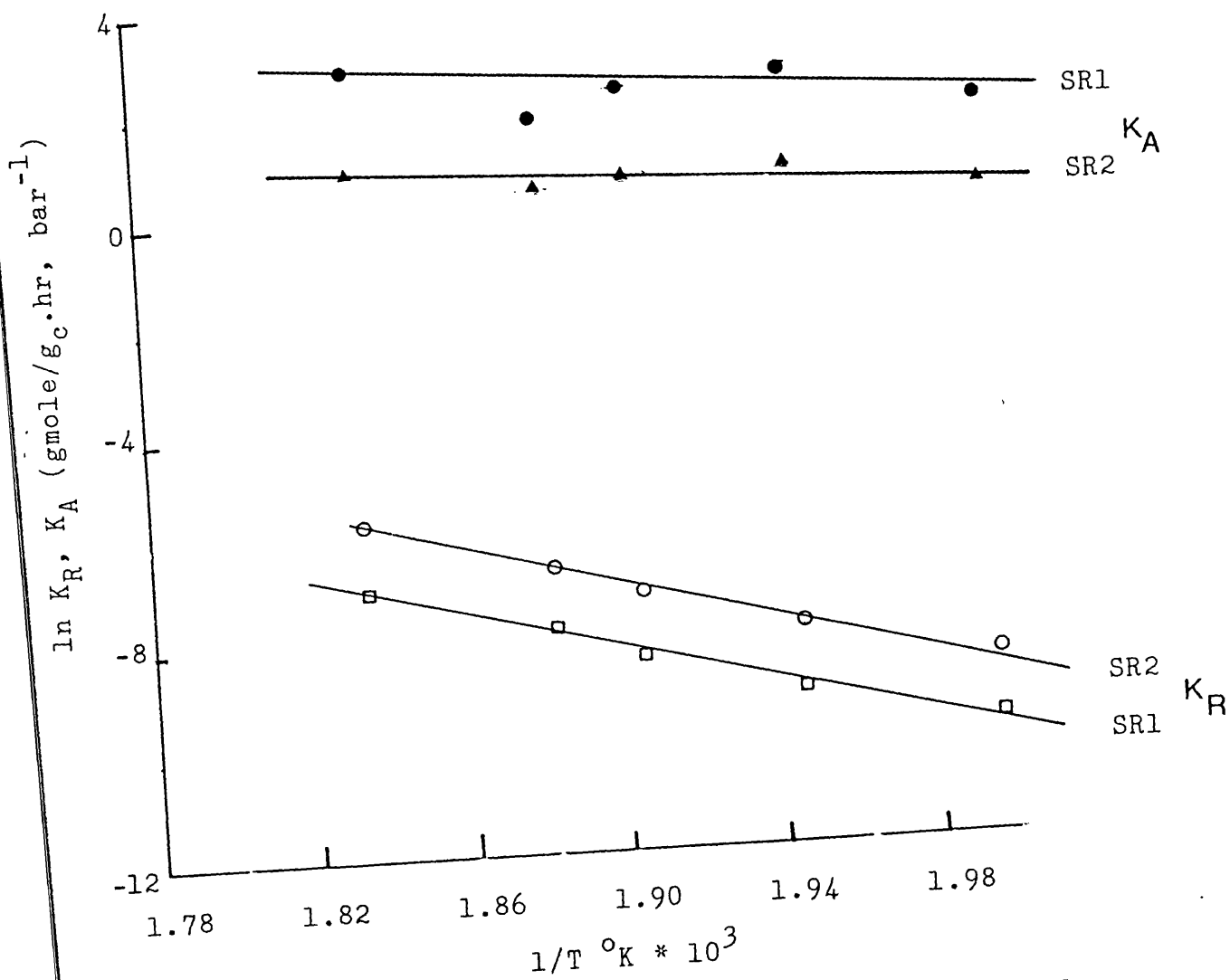


Fig. 4.12 Temperature Dependence of the Kinetic and
Adsorption Thermodynamic Equilibrium Constants.
 The dehydration of n-butanol to butene over
 zeolite 13X.

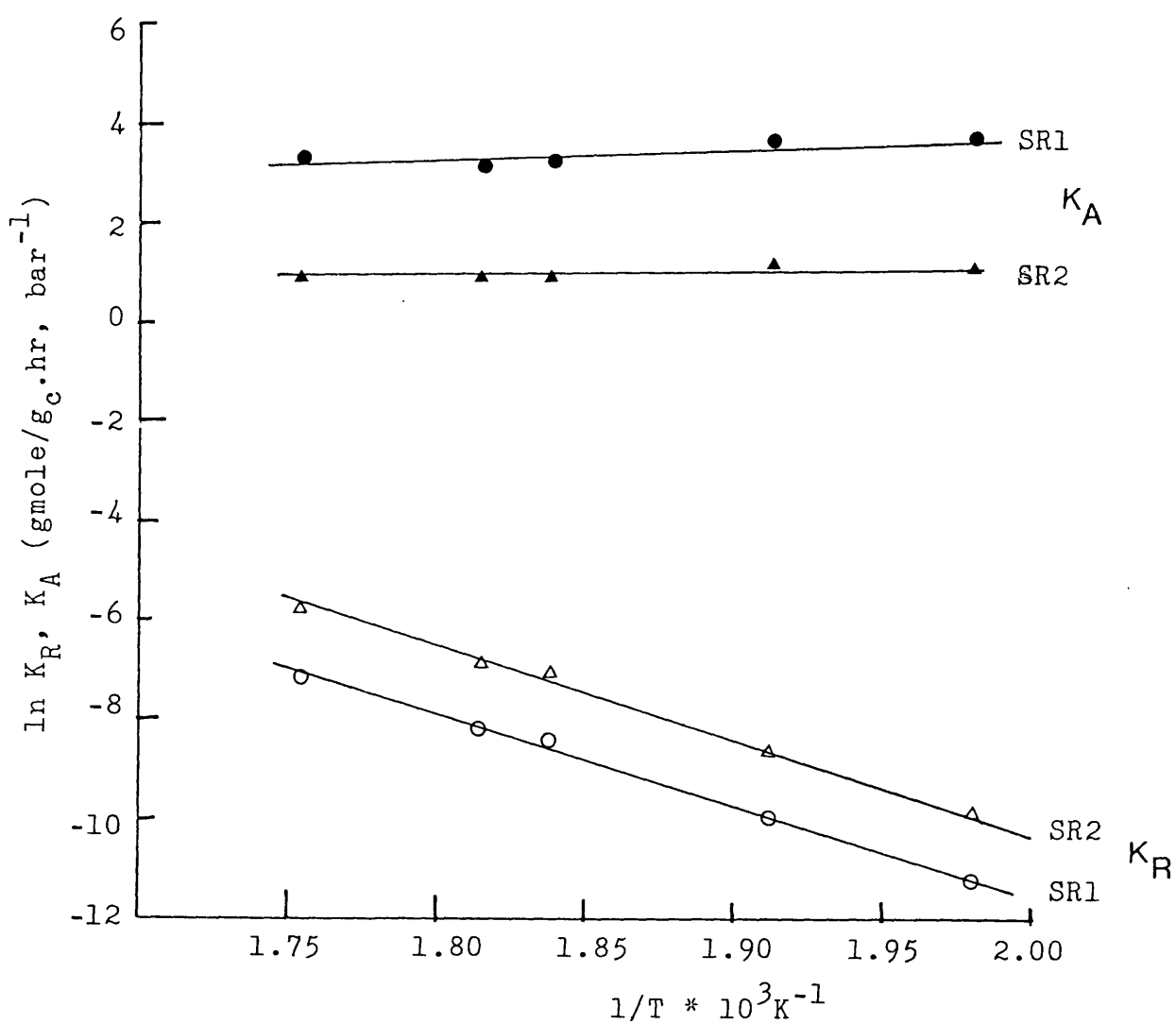


Fig. 4.13 Temperature Dependence of the Kinetic and Adsorption Equilibrium Thermodynamic Constants.

The dehydration of n-butanol to butene over zeolite 4A.

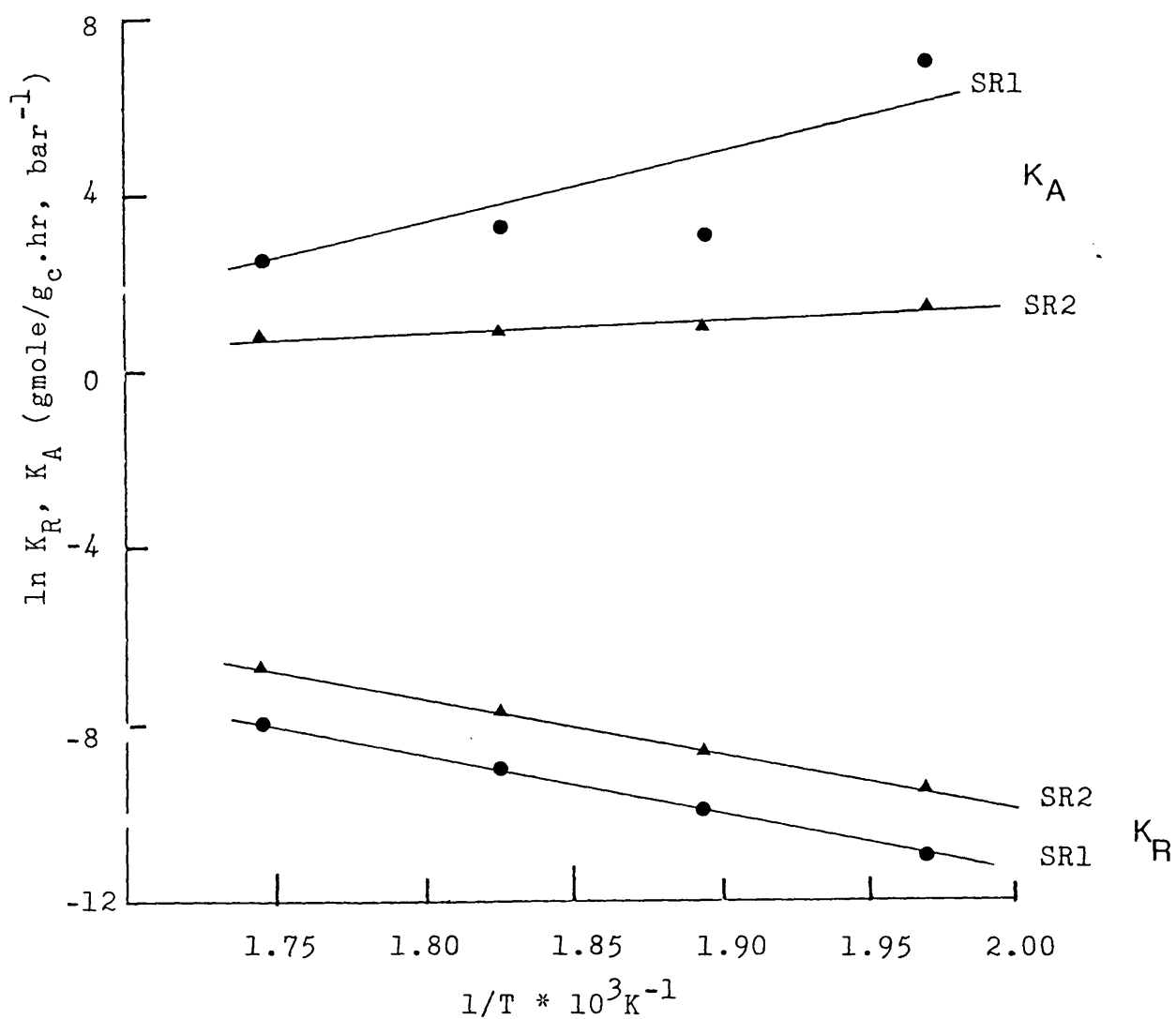


Fig. 4.14 Temperature Dependence of the Kinetic and Adsorption Thermodynamic Equilibrium Constants.
 The dehydration of n-butanol to butene over zeolite ZNa

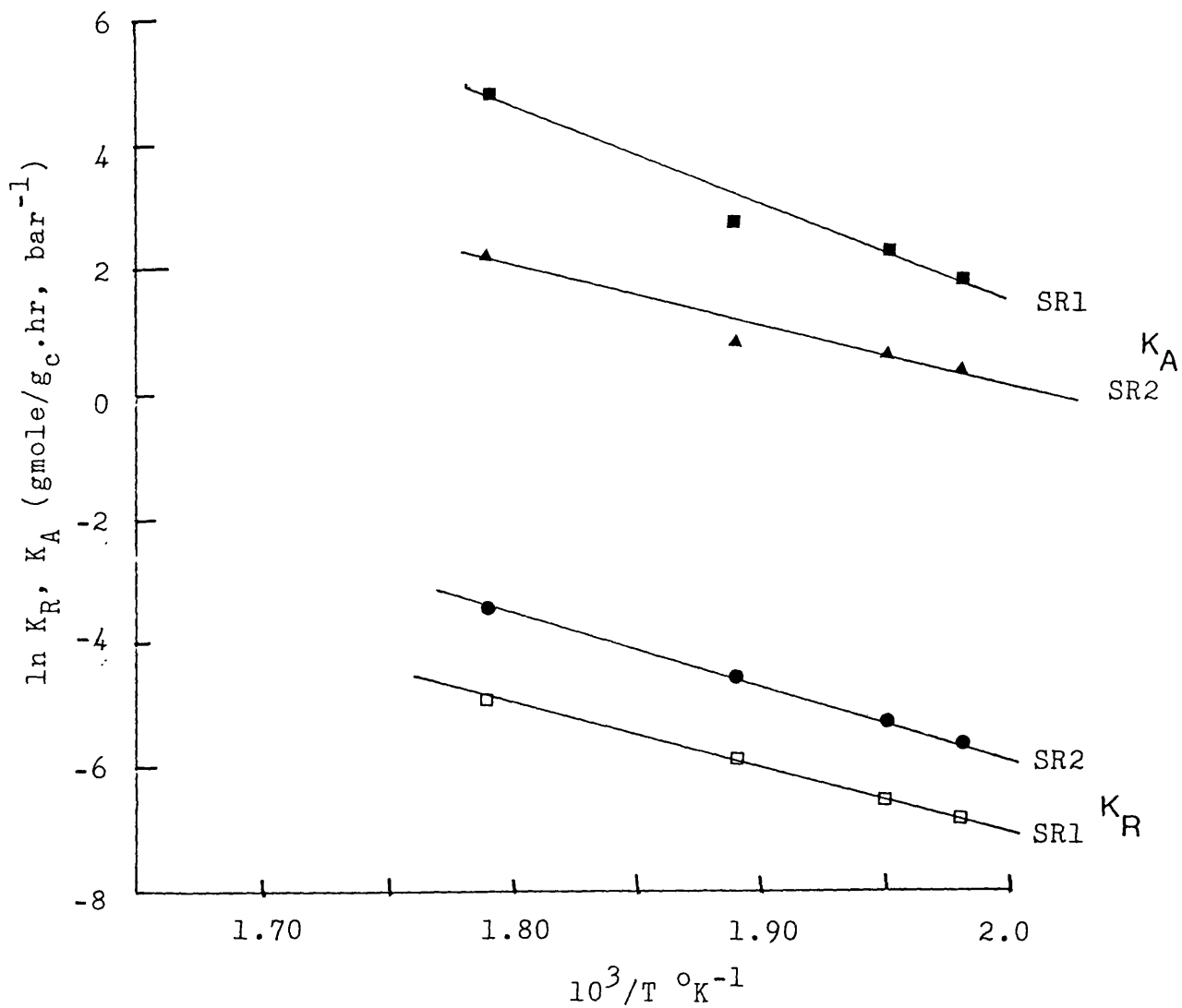


Fig. 4.15 Temperature Dependence of the Reaction Rate and Adsorption Equilibrium Constants.

The dehydration of isopropanol to propene over 13X zeolite.

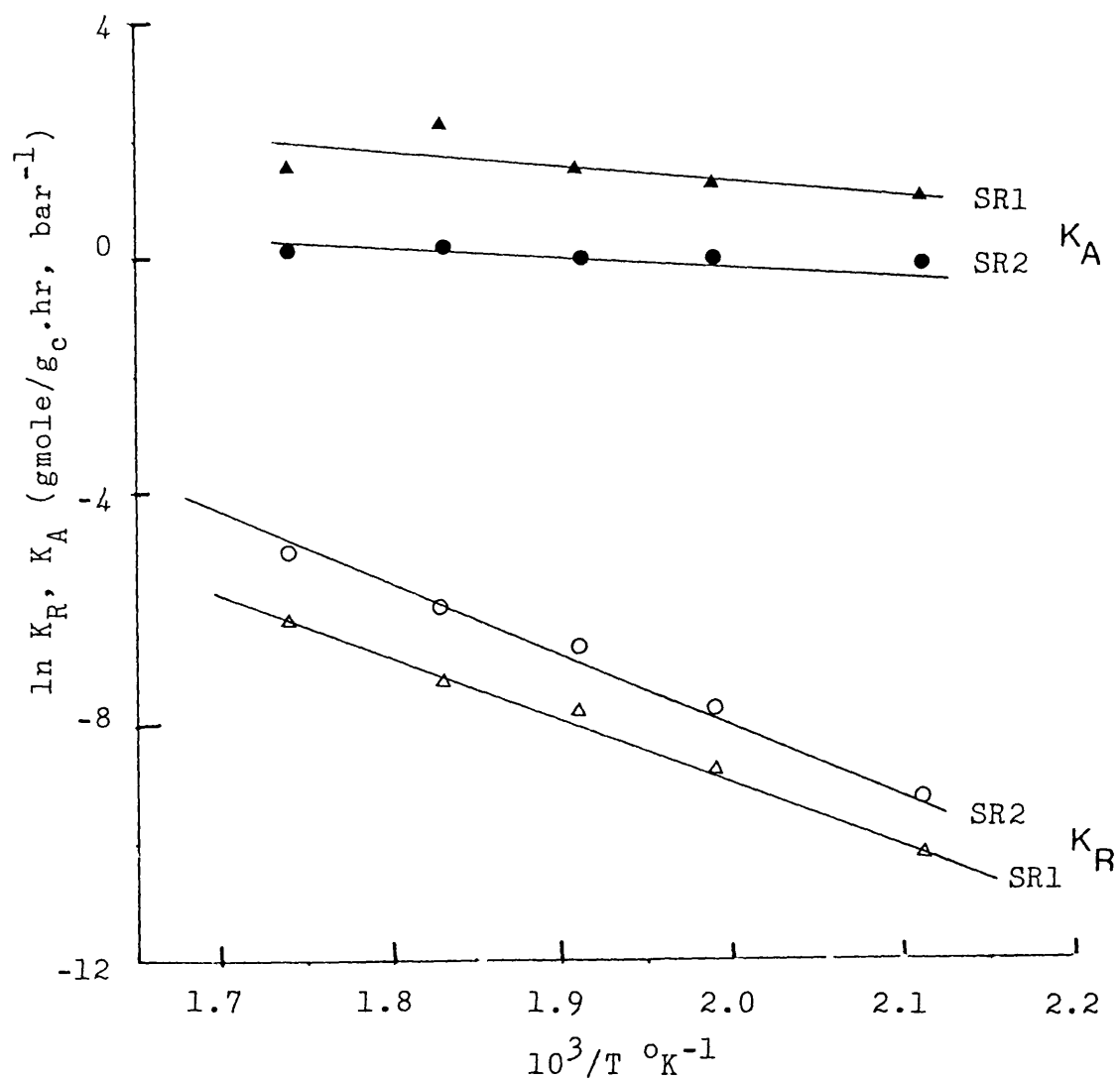


Fig. 4.16 Temperature Dependence of Reaction Rate and Isopropanol Adsorption Equilibrium Constants.

The dehydration of Isopropanol to propene over zeolite 4A.

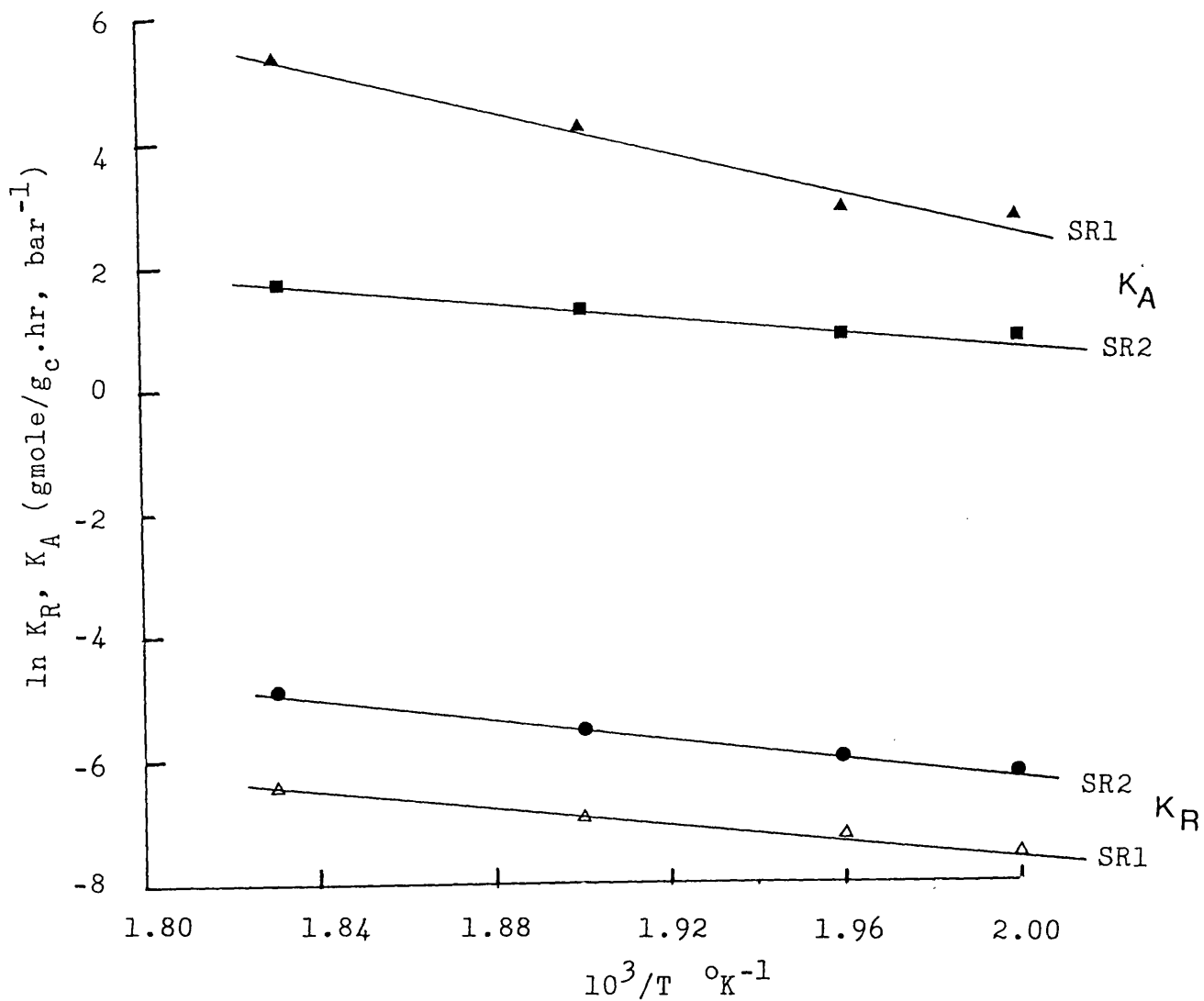


Fig. 4.17 Temperature Dependence of the Reaction Rate and Adsorption Equilibrium Constants.

The dehydration of isopropanol to propene over zeolite ZNa.

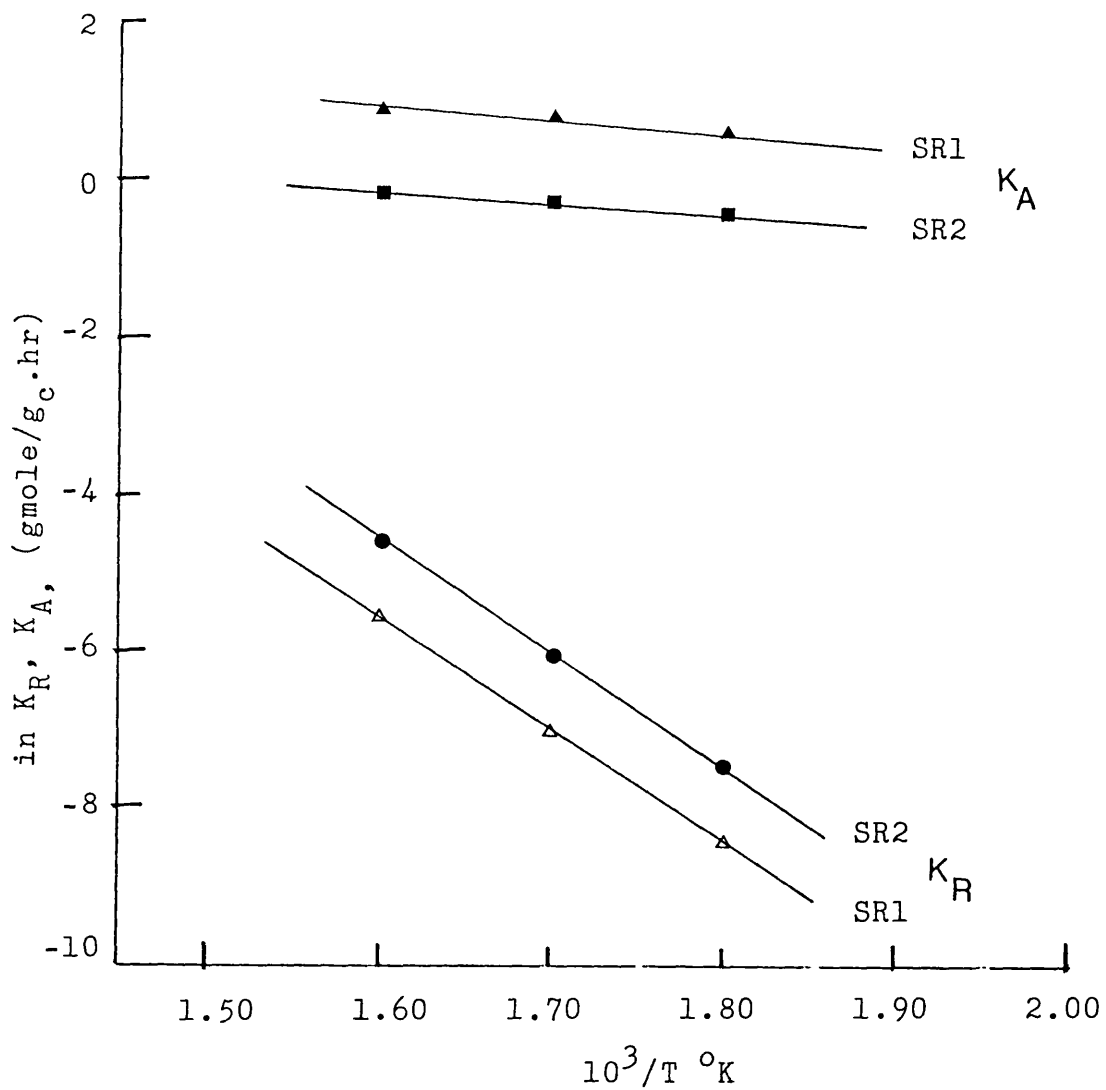


Fig. 4.18 Temperature Dependence of the Reaction Rate and Adsorption Equilibrium Constants.

The dehydration of ethanol to ethylene over zeolite 4A.

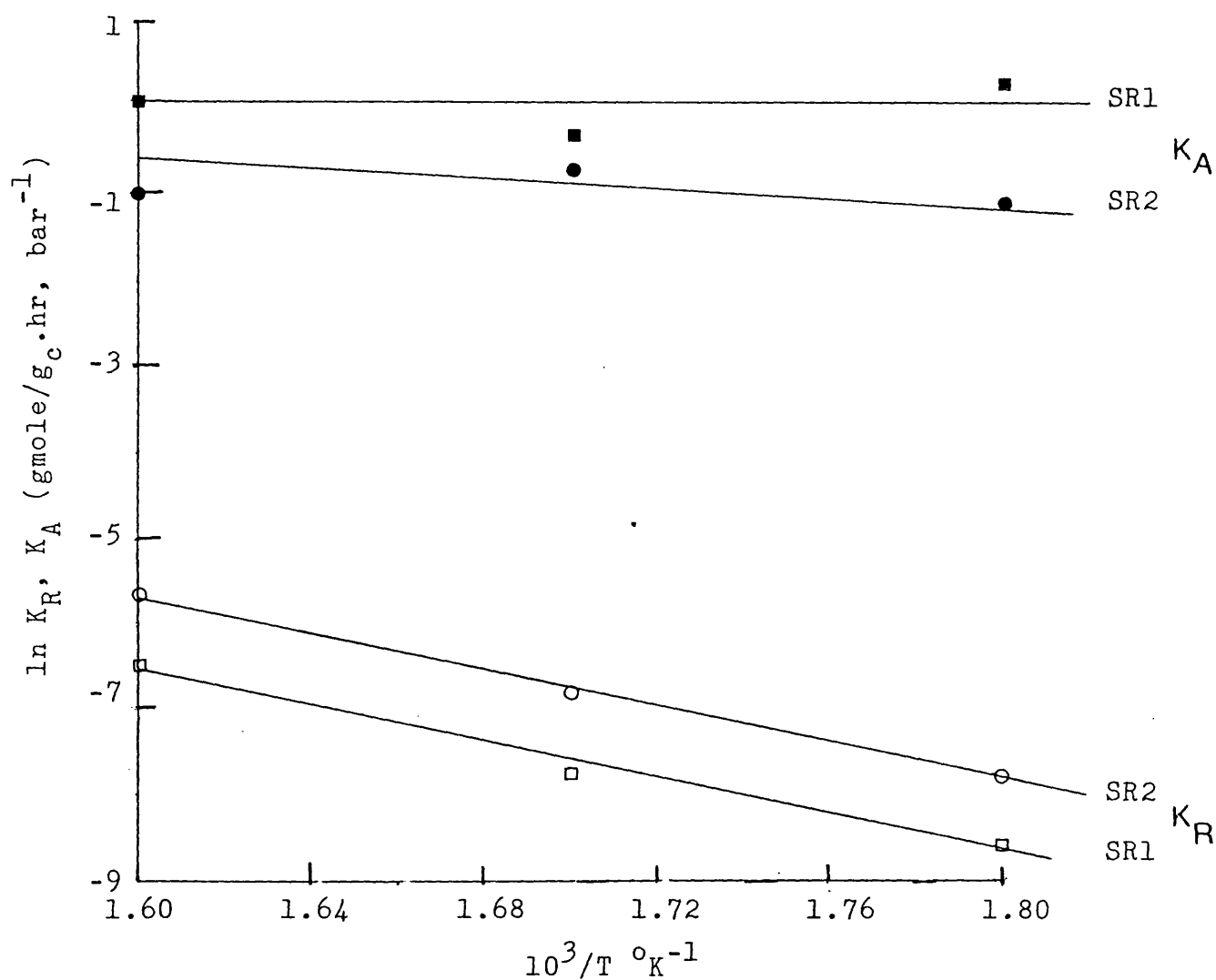


Fig. 4.19 Temperature Dependence of the Reaction Rate and Adsorption Equilibrium Constants.

The dehydration of ethanol to ethylene over zeolite ZNa.

The last column of the tables gives the sum of squares of residuals (SSR). SSR values for SR1, SR2 models are the smallest. SSR increases with temperature which can be due to the increase in the absolute values of the errors with increase in temperature. The SSR values suggest that a single site mechanism appears to be slightly superior to a dual site mechanism. But the difference between the two SSR values at any given reaction temperature is not large enough to draw any firm conclusion on the preference of one model to the other.

The temperature dependence of the kinetic and adsorption parameters are illustrated in figures 4.12 to 4.19. They are in good accordance with Arrhenius and Van't Hoff laws. The plots of the $\ln K_R$ against $1/T$ are good straight lines with high R-squared values. Deviation from a good straight line would have suggested one or more of the following:

- a) A change in the reaction regime (external mass transfer, chemically and pore diffusion controlled).
- b) A change in the rate controlling step in the chemically controlled regime.
- c) A decline in the catalyst's activity.

The straight line plots obtained here suggest that the present kinetic data were procured in only one reaction regime and the effect of phenomenon c) was minimal.

The estimated values of the pre-exponential factors, activation energies and enthalpies of adsorption of n-butanol for the zeolites are shown in tables 4.6, 4.7 and 4.8. All the parameters were estimated by linear least squares analysis technique. Activation energies obtained from the slopes of these plots agree well with those obtained from the power function rate expression. This indicates that the adsorption process has no significant effect on the apparent activation energies. The explanation is probably due to the low reaction order obtained.

The plots of $\ln K_A$ against $1/T$ are fairly linear. They obey Van't Hoff's law and have negative slopes except those in figures 4.13 and 4.14. Figures 4.13 and 4.14 show a positive slope for the adsorption plot which suggests that the adsorption of n-butanol on zeolites 4A and ZNa is exothermic. The remaining adsorption plots suggest that the adsorption of alcohols on the present zeolites is probably endothermic, indicating dissociative adsorption of alcohols. Endothermic adsorption has been found to be possible in literature (17, 132). Dissociative adsorption of alcohols suggests a carbonium ion reaction mechanism or E1 mechanism and will be fully discussed later in chapter 5.

It is interesting to note that the kinetic data over ZNa catalyst when fitted to model SRI resulted in a negative adsorption co-efficient at reaction temperature 235°C from linear analysis but resulted in positive adsorption co-efficient from the non-linear analysis technique (see table 4.5).

Table 4.6 Estimated Pre-exponential Factor, Activation Energy and Heat of Adsorption.

The dehydration of n-butanol.

Catalyst	Model	A_0 or K_{A0} gmole/gc.hr.	t-ratio	E_A or ΔH_A Kcal/gmole	t-ratio	R-squared	Eqn.*
13X	LHM	$2.6 \cdot 10^{11}$	14	36	19	99	A
		$3.2 \cdot 10^{-2}$	0.82	-6.9	1.6	45	V
	REM1	$8.3 \cdot 10^9$	6.8	29	8.2	96	A
		$3.2 \cdot 10^{-2}$	0.82	-6.9	1.6	45	V
	SR2	$6.1 \cdot 10^{11}$	18	36	22	99	A
		$8.0 \cdot 10^{12}$	2.0	6.3	1.8	53	V
	SR1	$1.1 \cdot 10^{11}$	12	35	17	99	A
		$2.1 \cdot 10^4$	1.5	8.0	1.2	31	V

Catalyst	Model	A_0 or K_{A_0} g _{mole} /g _c .hr.	t-ratio	E_A or ΔH_A Kcal/gmole	t-ratio	R-squared	* Eqn.
4A	SR2	$2.3 \cdot 10^{11}$	21	36	27	100.	A
		$4.7 \cdot 10^{-1}$	1.9	-2.0	4.5	87	V
	SR1	$8.5 \cdot 10^{10}$	20.	37	27	100.	A
		$1.5 \cdot 10^{-1}$	1.0	-5.8	2.9	74	V
ZNa	SR2	$3.1 \cdot 10^6$	54	25	83	100.	A
		$2.8 \cdot 10^{-2}$	2.7	-5.1	3.5	86	V
	SR1	$4.7 \cdot 10^6$	38	27	62	100.	A
		$5.1 \cdot 10^{-13}$	1.8	-35	2.1	68	V

* A = Arrhenius and V = Van't Hoff.

Table 4.7 Estimated Pre-exponential Factor, Activation Energy and Heat of Adsorption.

The dehydration of isopropanol.

Catalyst	Model	A_0 or K_{A0}	t-ratio	E_A or ΔH_A	t-ratio	R-squared	Eqn.*
		$\frac{\text{gmole}}{\text{bar-l}} \cdot \text{hr}$		Kcal/gmole			
13X	LHM	$1.6 \cdot 10^{15}$	4.2	44	5.2	97	A
	REM1	$1.9 \cdot 10^8$	1.4	12	3.1	91	A
	SR2	$1.3 \cdot 10^{-13}$	2.4	-32	2.6	87	V
		$2.2 \cdot 10^7$	47	23	60.	100.	A
		$2.4 \cdot 10^8$	5.7	19	5.7	94	V
	SR1	$3.8 \cdot 10^5$	18.	20.	26	100.	A
		$4.8 \cdot 10^{13}$	7.5	30.	6.8	996	V

Catalyst	Model	A_0 or K_{A_0} g mole ⁻¹ g c. hr. bar ⁻¹	t-ratio	E_A or ΔH_A Kcal/gmole	t-ratio	R-squared	* Eqn.
4A	SR2	$2.4 \cdot 10^5$	12	21	20.	99	A
		$4.6 \cdot 10^2$	2.3	4.8	1.7	50.	V
	SR1	$2.2 \cdot 10^6$	16	22	24	100.	A
		4.8	1.5	1.5	3.0	75	V
ZNa	SR2	$2.0 \cdot 10^4$	30.	16.	47	100.	A
		$2.2 \cdot 10^5$	8.6	12	7.8	97	V
	SR1	$2.3 \cdot 10^2$	8.5	13	19	100.	A
		$3.2 \cdot 10^{15}$	8.8	33	7.9	97	V

* A = Arrhenius and V = Van't Hoff.

Table 4.8 Estimated Pre-exponential Factor, Activation Energy and Heat of Adsorption.

The dehydration of ethanol.

Cat.	Model	A_0 or K_{A0} gmole/ g_c .hr/bar $^{-1}$	t-ratio	E_A or ΔH_A Kcal/gmole	t-ratio	R-squared	Eqn.*
4A	SR2	$8.9 \cdot 10^7$	48	28	36	100.	A
		5.9	45	2.4	51	100.	V
	SR1	$2.7 \cdot 10^7$	22	28	31	100.	A
		24	6.5	2.8	4.8	96	V
	LHM	71	11	12	27	100.	A
	REMI	3.2	1.1	6.7	5.3	97	A
		$4.5 \cdot 10^{-2}$	4.5	-5.6	7.0	98	V

Cat.	Model	A _o or K _{Ao} gmole/g _c .hr./bar ⁻¹	t-ratio	E _A or ΔH _A Kcal/gmole	t-ratio	R-squared	Eqn.*
ZNa	SR2	9.4 10 ⁶	9.6	27	14	100.	A
		2.0 10 ⁻³	0.67	-6.1	0.56	24	V
	SR1	6.8 10 ⁶	4.6	27	6.8	98	A
		2.6 10 ⁻³	0.50	-6.8	0.49	19	V
Resin	LHM	7.8 10 ¹⁰	33	24	38	100.	A
	REMI	3.0 10 ²	25	7.6	43	100.	A
		3.3 10 ⁻⁹	21	16	22	100.	V

* A = Arrhenius and V = Van't Hoff.

A similar observation has been reported by Kittrell et al (121).

In the present work, both dual site and single site mechanisms were found to be equally probable. It confirms the results in literature that either a dual site mechanism or a single site mechanism can be used to explain the depressing effect of alcohol on the rate of formation of olefin. Another definite agreement between this investigation and those of others is that surface catalysed reaction was found to be the rate limiting step see tables 1.2, 1.3 and 1.4.

4.2.2.2.2. Kinetic Expression for the Formation of Ether.

Three rate expressions formulated for the dehydration of alcohol to ether based on the assumption that the surface catalysed reaction is the rate controlling step will be reported. They are based on the following reaction mechanism:

a) The surface reaction may take place by a Langmuir-Hinshelwood mechanism (LHM) in which two adjacently chemisorbed alcohol molecules react to form the chemisorbed products.

The rate of formation of ether is given by

$$R_E = \frac{K_R K_A^2 (P_A^2 - P_W P_E / K_{eq})}{(1.0 + K_A P_A)^2} \quad 4.11$$

b) The surface reaction may occur by a Rideal-Eley mechanism (REMI) in which one alcohol molecule in the gas phase reacts directly with another chemisorbed alcohol

molecule in the presence of a vacant site adjacent to the chemisorbed products. The rate of formation of ether is

$$R_E = \frac{K_R K_A (P_A^2 - P_W P_E / K_{eq})}{(1.0 + K_A P_A)^2} \quad 4.12$$

c) The surface reaction may take place by a Rideal-Eley mechanism (REM2) as defined above, but not in the presence of an adjacently vacant site and only the product water is chemisorbed while the product ether goes directly into the gaseous phase. The rate of formation of ether is represented by

$$R_E = \frac{K_R K_A (P_A^2 - P_E P_W / K_{eq})}{(1.0 + K_A P_A)} \quad 4.13$$

Qualitatively, the first two expressions predict the order of reaction between 0 and 2, while the third equation predicts the order of reaction between 1 and 2. All expressions predict the depressive behaviour of alcohol but the influence is stronger with the first two equations. These rate equations were tested with the kinetic data for all the alcohols over the zeolites used. Tables A4.6, A4.13 and A4.19, in appendix 4, present the kinetic and adsorption parameters obtained from linear regression. The correlations show high R-squared values for all three models, but the third model (REM2) is less favoured at all temperatures. The R-squared co-efficients show that these models correlate the kinetic data on ether formation better than the power law. This is probably because the above expressions account for the effect of the reverse reaction

which is not included in the power function rate equation.

It should be noted that the alcohol adsorption co-efficients from model REM2 are negative. A negative adsorption co-efficient is physically meaningless, but has sometimes been ascribed to 'enhanced adsorption' (15). But the concept has not been widely accepted. Hence model REM2 should have been rejected on the basis of negative K_A . Nevertheless a non-linear analysis was performed using this model.

Results of kinetic and adsorption constants from the non-linear least squares analysis are presented in Tables A4.7, A4.14 and A4.20, in appendix 4. Model REM2 has the higher SSR values at all reaction temperatures and is inferior to the other two models, LHM and REM1. This model REM2 was therefore rejected.

Figures 4.20, 4.21 and 4.22 illustrate the temperature dependence of the kinetic and adsorption equilibrium constants. The lower plots are for the kinetic constants while the upper plot is for the adsorption constants. The plots obey the Arrhenius and Van't Hoff laws. Tables 4.6 4.7 and 4.8 summarise the estimated apparent activation energies, heat of adsorption of alcohol and pre-exponential factors over zeolites.

The activation energies obtained from the Langmuir-Hinshelwood (LHM) and Rideal-Eley (REM1) models compare well with those obtained from the empirical power function

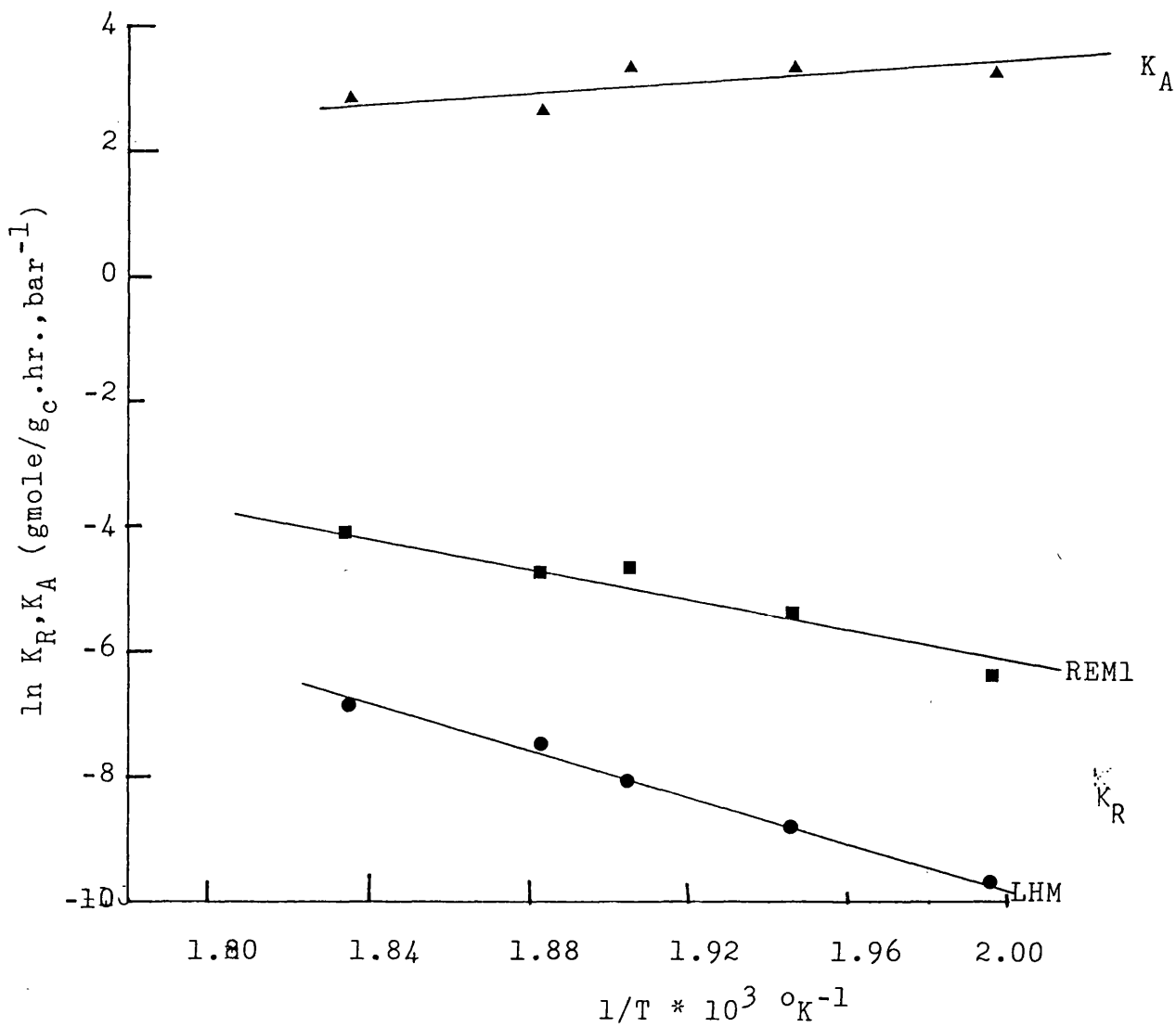


Fig. 4.20 Temperature Dependence of the Kinetic and Adsorption Equilibrium Constants.

The dehydration of n-butanol to di-n-butyl ether over 13X zeolite.

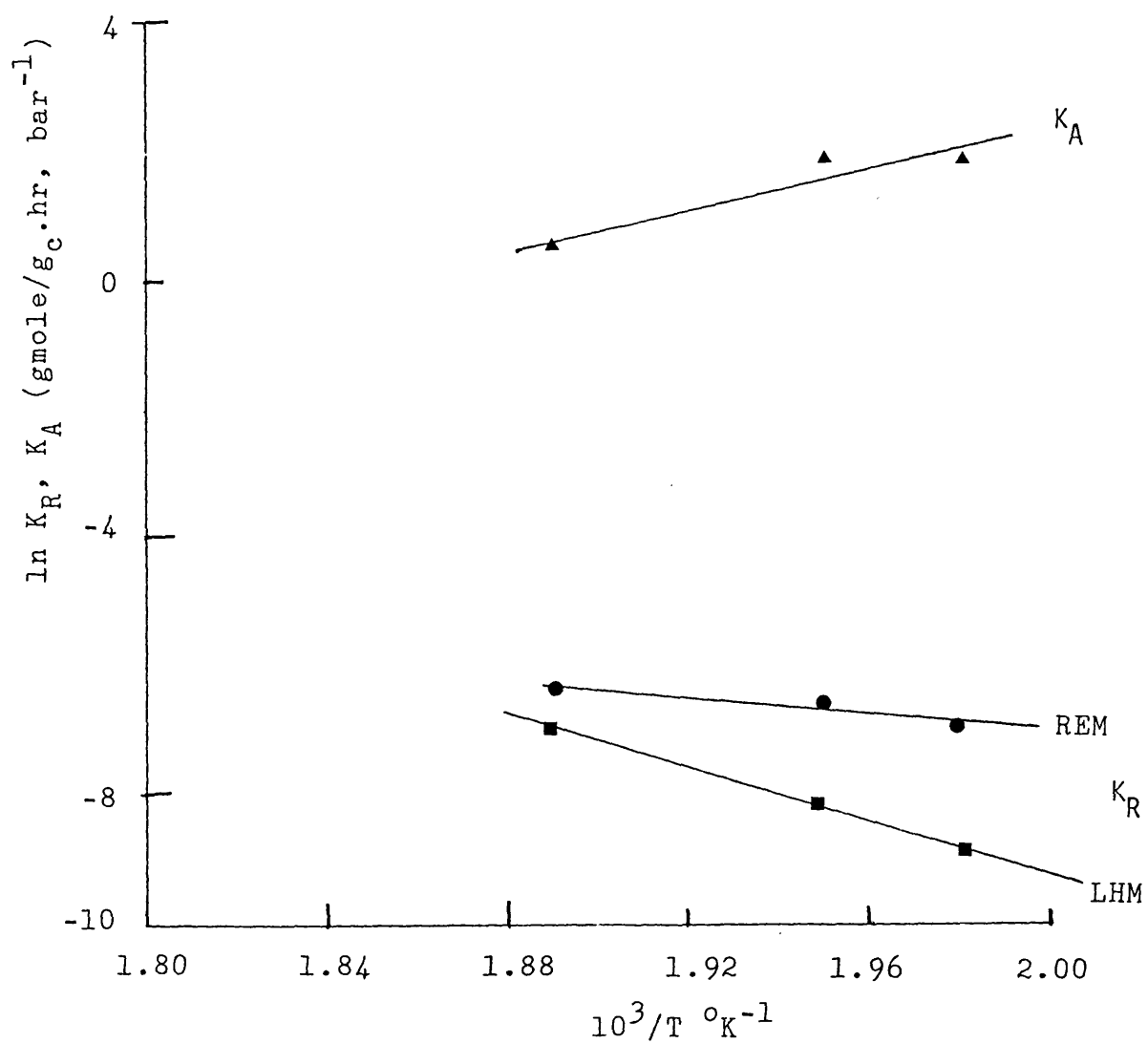


Fig. 4.21 Temperature Dependence of the Reaction Rate and Adsorption Equilibrium Constants.

The dehydration of isopropanol to di-iso-propyl ether over zeolite 13X.

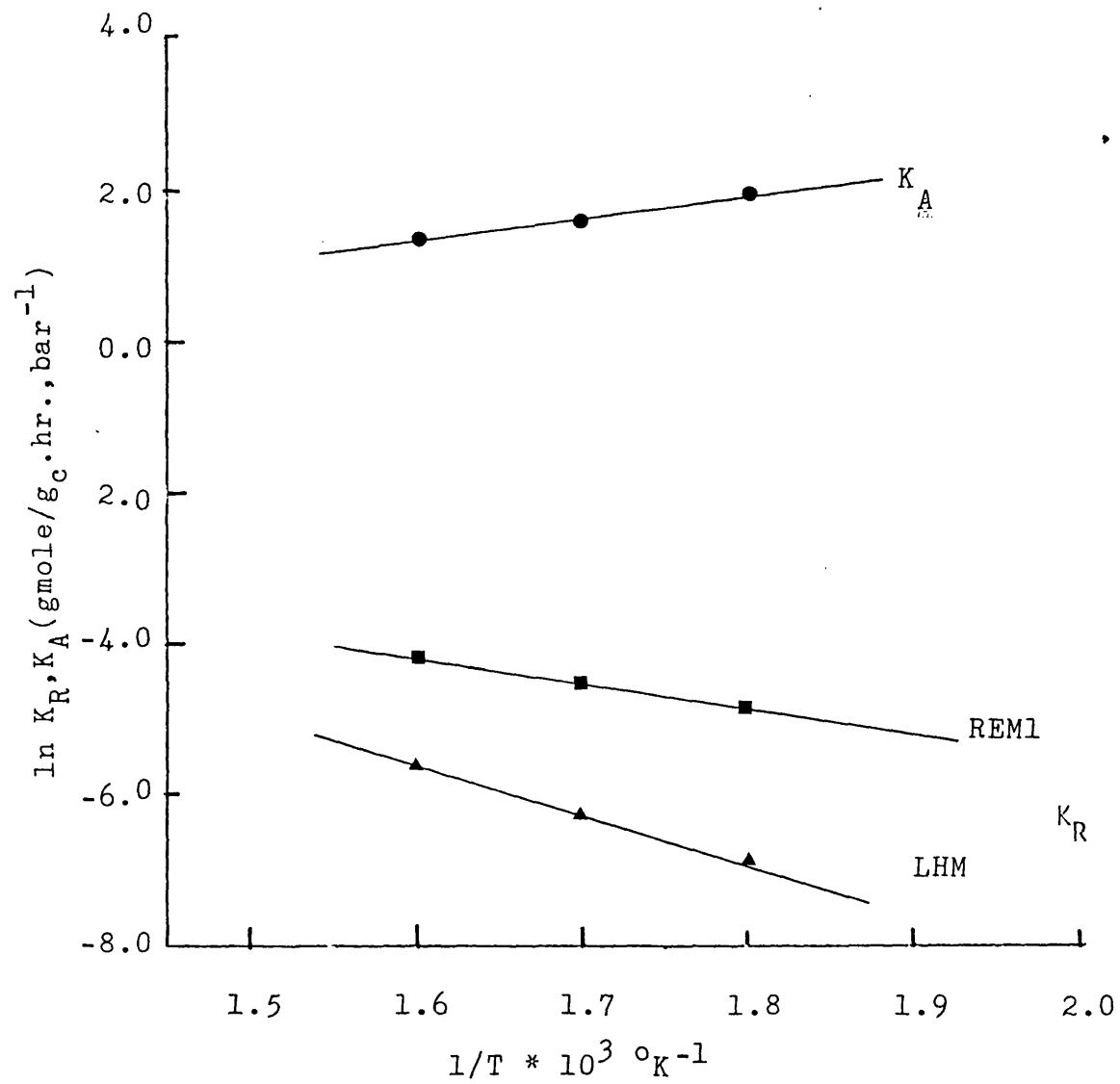


Fig. 4.22 Temperature Dependence of the Reaction Rate and Adsorption Equilibrium Constants.

The dehydration of ethanol to di-ethyl ether over zeolite 4A.

rate expression. The results have already been discussed earlier and compared with literature values. This observation suggests that the adsorption process does not greatly influence the estimated activation energy and pre-exponential factor because the reaction order tends to zero.

The heat of adsorption shows an exothermic adsorption process. The alcohol adsorption equilibrium constant decreases with increasing temperature. The absolute value of the heat of adsorption of isopropanol (32 Kcal/gmole) is greater than the heat of liquefaction of isopropanol (11 Kcal/gmole), while those of n-butanol and ethanol are smaller than their corresponding heat of liquefaction. A high value of heat of adsorption implies that the adsorption process is one of chemisorption while a low value suggests physical adsorption.

It is interesting to note that the above rate equations will predict a decline in the rate of formation of ether at high temperatures. This decline is due to the effects of the adsorption constant and the reverse reaction and will be fully explained in section 4.3.1. Also this drop in the ether formation is consistent with the shift in the equilibrium conversion as the temperature increases. Secondly, the rate expression will also predict a maximum ether production in a larger size catalytic reactor, or a static system because the effect of the reverse reaction at

high conversion of alcohol has been taken into consideration.

Theoretically the apparent activation energies and the pre-exponential factors obtained from the LHM and REM1 models are related to each other by the following expressions.

$$E_{A,HHM} = E_{A,REM1} - \Delta H_A \quad 4.14$$

and

$$A_{O,LHM} = A_{O,REM1} / K_{Ao} \quad 4.15$$

Experimental data support these relationships. For example the apparent activation energy (36 Kcal/gmole) estimated by the LHM model is practically equal to the sum of the apparent activation energy (29 Kcal/gmole) estimated by the REM2 model and the absolute heat of adsorption of n-butanol (6.9 Kcal/gmole). Thus the apparent activation energy and pre-exponential factor estimated by the Rideal-Eley mechanism model are smaller than those obtained from Langmuir-Hinshelwood mechanism model. The difference in the apparent activation energy being the heat of adsorption of the reactant.

The alcohol thermodynamic equilibrium constant for the formation of ether is found to be greater than that for the formation of olefin under the same reaction conditions and for all alcohols. This observation suggests that the alcohol dehydration reaction to form ether and olefin do not take place on the same active site.

Furthermore, it indicates that the saturation partial pressure of alcohol is higher for ether formation than for

olefin formation. This is also evident in the difference in the reaction orders and has been discussed previously. The above conclusion is in excellent agreement with the observation of Jain and Pillai (13).

It can be concluded that the LHM and REM1 models can statistically and quantitatively represent the kinetic data on the dehydration of alcohol to ether over zeolites under the reaction conditions used. The kinetic and adsorption equilibrium constants are satisfactorily correlated by Arrhenius and Van't Hoff laws, respectively. The dehydration of alcohol to both olefin and ether are surface reactions, but requiring different active sites and proceed through different transition states.

4.3 Results and Discussion of the Dehydration of Isopropanol and Ethanol over Synthetic Cation Exchange Resin.

4.3.1 Introduction

It has been shown that cation exchange resin has appreciable catalytic activity for the dehydration of alcohols (33, 34, 46, 52). Lister (90) has also reviewed some chemical reactions of industrial importance which have been studied over cation exchange resins.

Existing kinetic data on the dehydration of isopropanol (33) and ethanol (34) over synthetic cation resin are within limited temperature ranges. Hence a kinetic study of the vapour phase dehydration of isopropanol and ethanol was undertaken to extend these temperature ranges. Secondly it is hoped that favourable reaction conditions can be found for the exclusive production of ether(s).

Kinetic data were obtained for the dehydration of isopropanol and ethanol over Dowex 50-X-8 cation exchange resin. The exchange resin was in the hydrogen form, with an effective diameter of 0.56 mm. The kinetic experiments were performed in a continuous stirred gas solid reactor, kept at 1-bar gauge total pressure.

Pure alcohol feed diluted with high purity nitrogen was fed into the reactor system held under operating

conditions but without the catalyst. Gas-liquid chromatographic analysis did not detect any product, i.e. alcohol passed through the system unreacted. This indicates that there is no uncatalysed side reactions or thermal dehydration of alcohol at these operating conditions.

During the dehydration of ethanol no other product besides di-ethyl ether and ethylene was detected. This suggests that cation exchange resin catalyst does not catalyse other side reactions within the temperature range investigated. But when isopropanol was dehydrated a small amount of acetone was detected.

The activity of the catalyst was checked after the experimental runs. No deactivation of the catalyst was noticed, probably because at these low temperatures thermal cracking of alcohol or products was absent.

On the basis of careful selection of reactor spinning speed, the effects of external mass and heat transfer have been eliminated. The effects of diffusional limitations have been assessed by the criterion of Weisz and Practer (93) (appendix 3). The assessment was based on the dehydration of isopropanol over the same catalyst and reaction conditions. The results of the assessment show that internal mass and heat transfer effects are insignificant within the reaction conditions studied. Since internal diffusional effects are completely absent during the dehydration of a more reactive and bulkier isopropanol than ethanol, these effects must

be insignificant for the dehydration of ethanol. Similar conclusions have been found by Johanson et al (34, 46-47) and Gottifredi et al (33). Therefore, it is safe to assume that the kinetic data were obtained only in the reaction-controlled regime and under isothermal conditions. The high activation energies found for both dehydration reactions over cation exchange resin catalyst confirmed that external and internal diffusional limitations were minimal. These results will be presented later.

For each run, the rates of formation of ether and olefin were calculated using the material balances for an ideal continuous stirred gas solid reactor given by equations 4.1 and 4.2. The calculated rate of formation for each component has an average deviation from the mean which is less than 4%.

Preliminary runs with salt form of synthetic cation exchange resin catalyst showed that it has no activity within the reaction conditions investigated. This observation is in agreement with Gates and Johanson (47), who reported that complete replacement of hydrogen ions with metal ions resulted in no catalytic activity towards the dehydration of methanol, ethanol and t-butanol.

Tables A4.21 and A4.22, in appendix 4, summarise the kinetic data on the dehydration of isopropanol and ethanol over synthetic cation exchange resin, respectively. Figures 4.23 and 4.24 show the influence of partial pressure of isopropanol or ethanol on the rates of formation of propene or

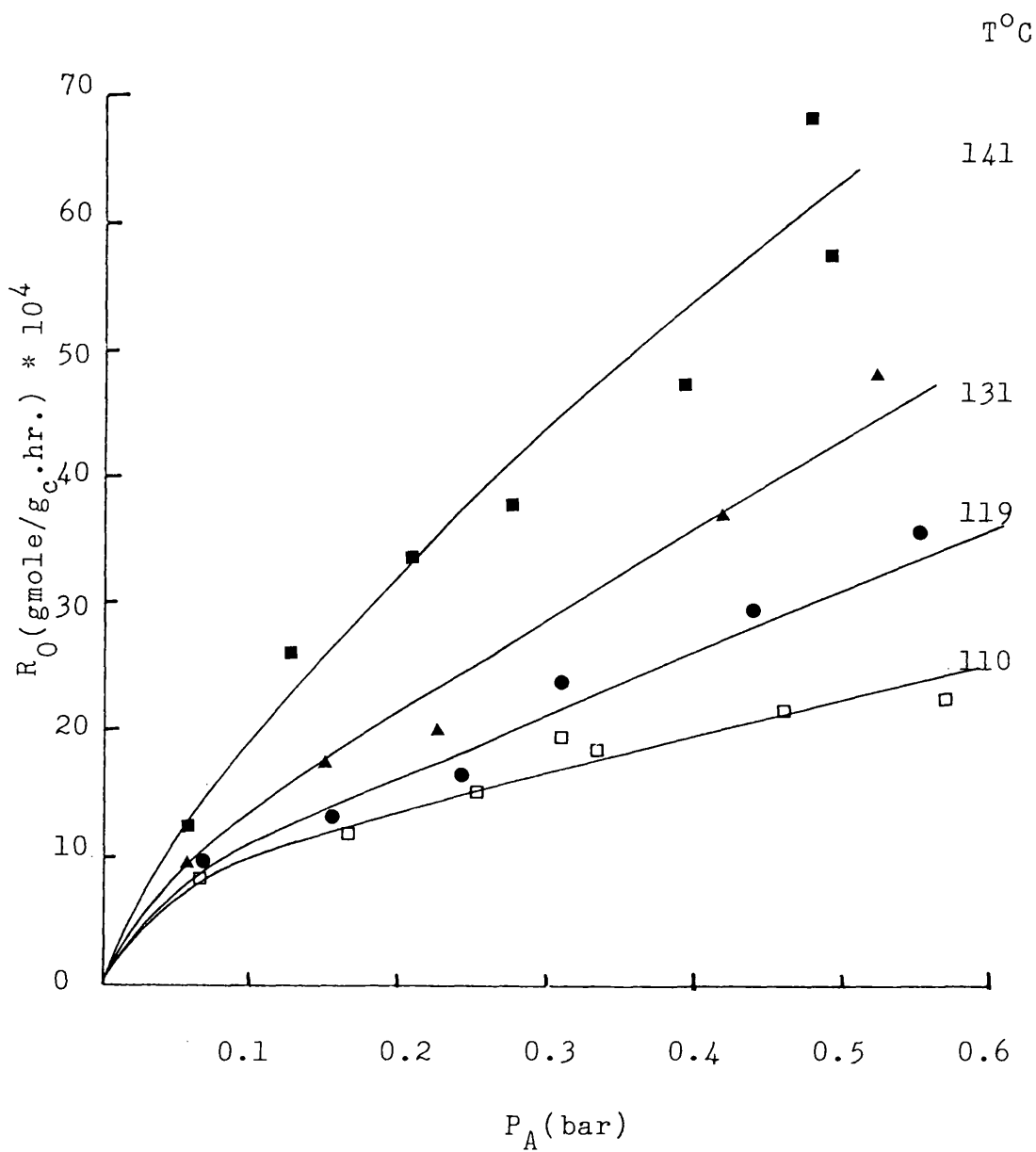


Fig. 4.23 The Influence of the Partial Pressure of Isopropanol on the Rate of Formation of Propene over Synthetic Cation Exchange Resin.

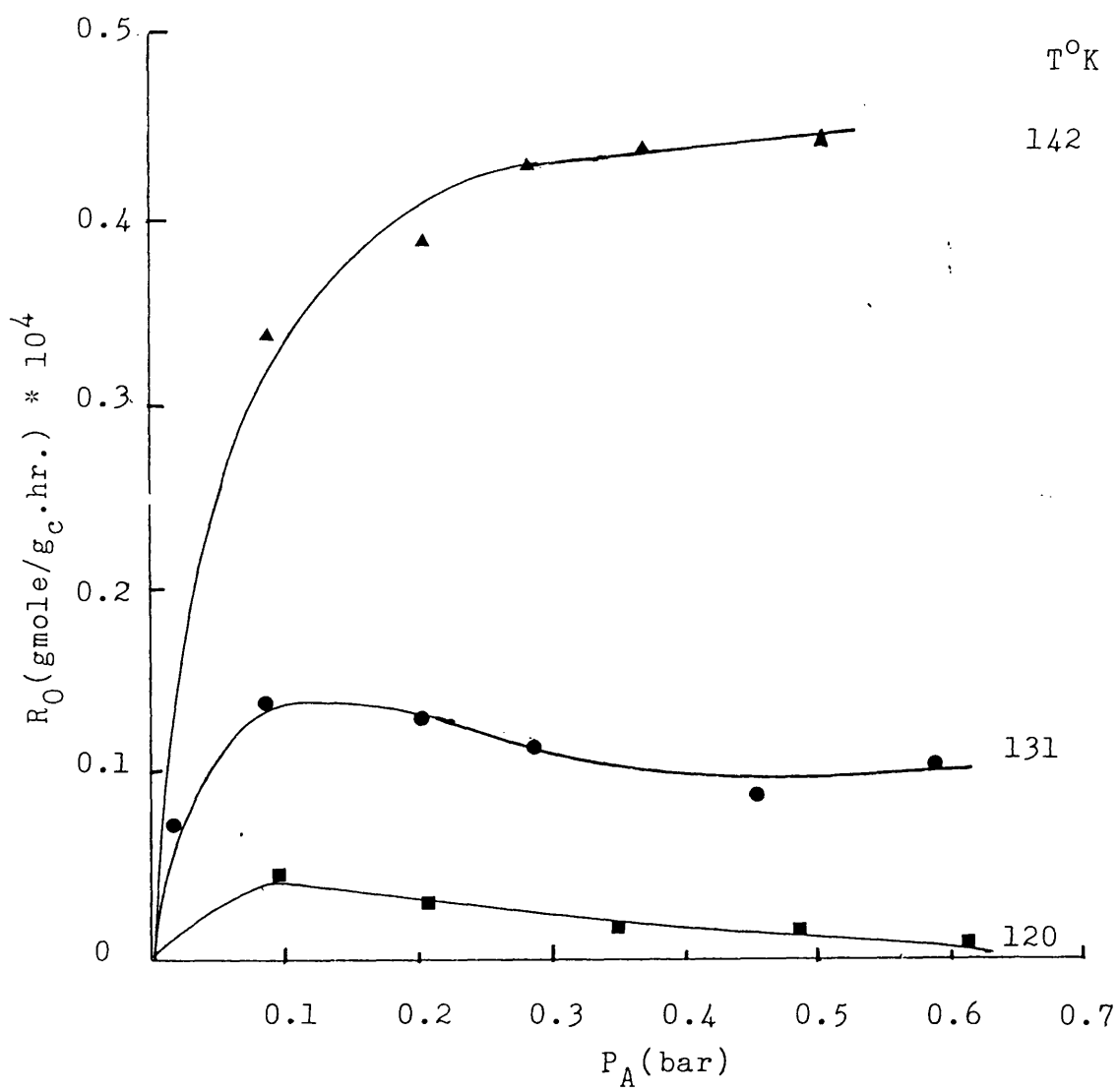


Fig.4.24 The Influence of the Partial Pressure of Ethanol on the Rate of Formation of Ethylene over Synthetic Cation Exchange Resin.

ethylene. The rate of formation of propene increases with increasing partial pressure of isopropanol. It indicates that the active sites on the catalyst are not completely saturated. It can also be seen that the order of the reaction is not zero. This observation does not agree with the results of Gottifredi et al (33), but the present experimental work was carried out at higher temperatures. It has been demonstrated experimentally that heterogeneous reaction order increases with increasing temperature, see table 4.1. At reaction temperatures, 120°C and 131°C, the rate of formation of ethylene first increases and then decreases with increasing partial pressure of ethanol. At a reaction temperature of 142°C it increases rapidly at low partial pressure, P_A below 0.3bar. Beyond this pressure the rate of ethylene formation remains virtually constant up to P_A of 0.7bar. The initial rapid increase in the rate of formation of ethylene is due to unsaturated active sites. The maximum reaction rate is obtained at P_A of approximately 0.1bar. This partial pressure was found to be dependent on temperature probably because adsorption decreases with increasing temperature. The rate of formation of ethylene remains nearly constant beyond 0.3 bar at all temperatures within the range of partial pressure of ethanol studied. This observation shows that the active sites on the catalyst are completely saturated. It suggests that further increase in ethanol concentration is not likely to increase the rate of formation of ethylene. This behaviour is expected because monomolecular heterogeneous reactions should have a tendency toward

zero-order when the concentration of the reactant increases, since the coverage of the reactant cannot exceed a single layer. Johanson et al (34, 48-50) did not report the formation of ethylene when ethanol was dehydrated over cation exchange resin. It is interesting to note, that the production of ethylene never exceed 10% of the production of di-ethyl ether under any reaction condition.

Figures 4.25 and 4.26, illustrate the effect of partial pressure of isopropanol and ethanol on the rates of formation of di-iso-propyl and di-ethyl ethers. The data on isopropanol can be represented by a single curve. Three phenomena which may explain this observation are: the effects of adsorption constant, reverse reaction and a consecutive reaction scheme.

The adsorption equilibrium constant (K_A) without dissociation decreases with increasing temperature, while the reaction rate constant (K_R) increases with increasing temperature. The rate of decrease of adsorption constant may be more than the rate of increase of the kinetic constant. In such a case, the products of the two quantities, K_R and K_A , may decrease with increasing temperature. This situation may lead to a considerable decrease in the overall rate of reaction. The decrease becomes greater when a square of the adsorption constant is involved in the numerator, as in the case for the rate of formation of ether (LHM model).

The dehydration of alcohol to ether is strongly affected by the reverse reaction. This has been discussed in chapter 1. It may also lead to lower overall reaction rate at higher temperature.

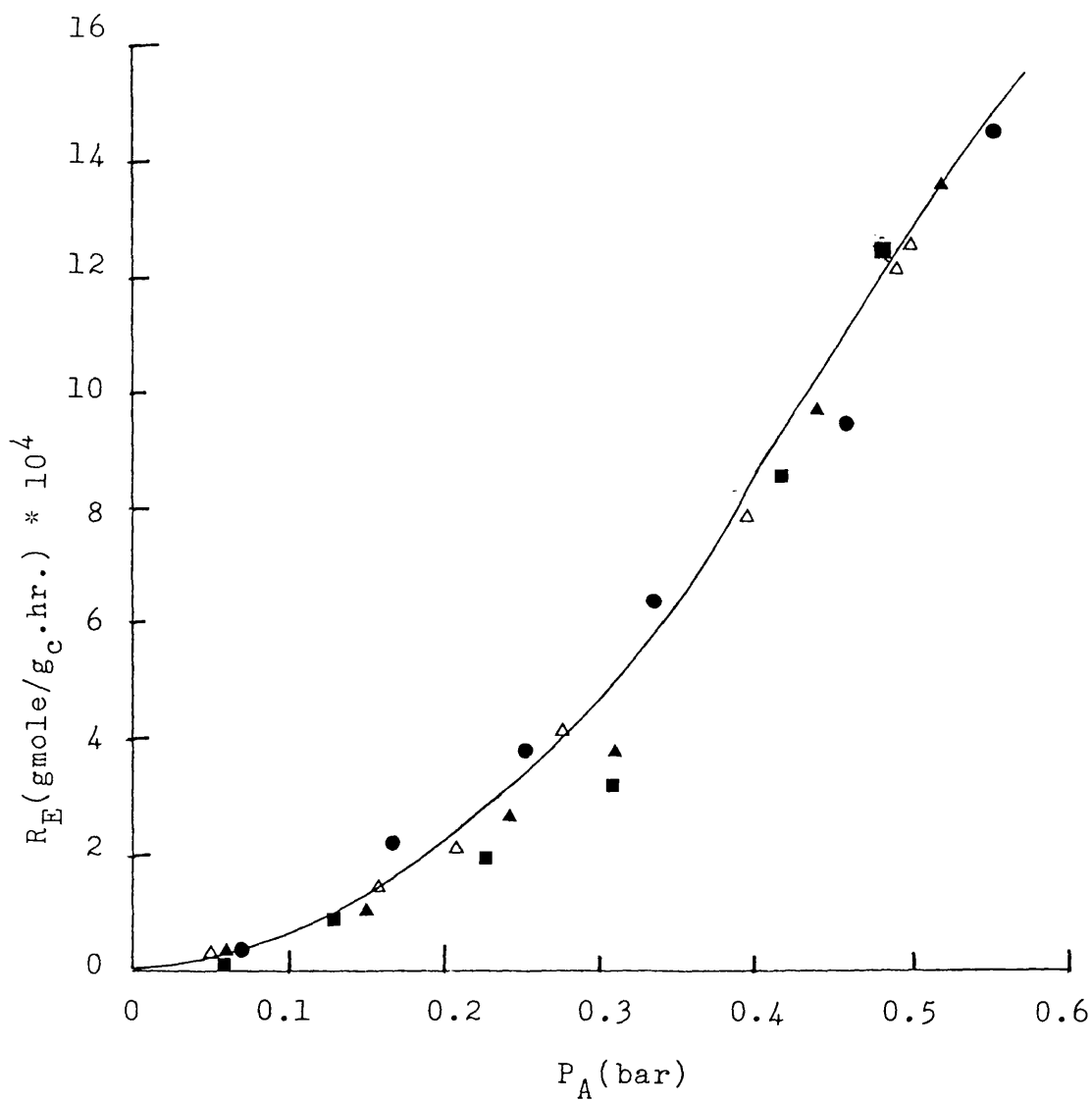


Fig. 4.25 The Influence of the Partial Pressure of Isopropanol on the Rate of Formation of Di-iso-propyl Ether over Synthetic Cation Exchange Resin.

Temp $^{\circ}\text{C}$ 141(Δ), 131(\blacksquare), 119(\blacktriangle) and 110(\bullet).

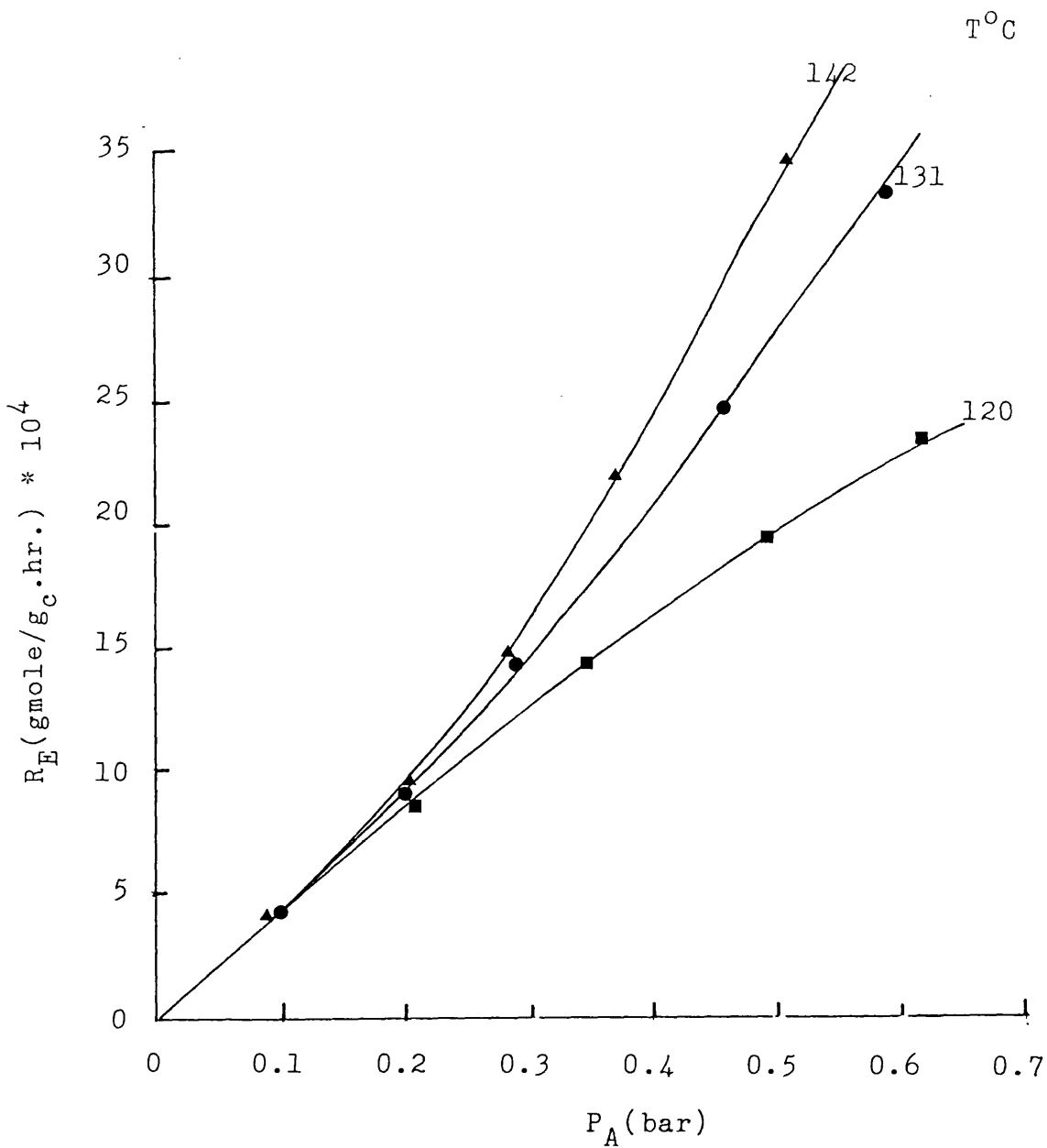
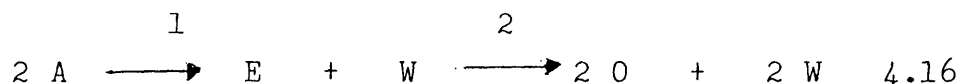


Fig. 4.26 The Influence of the Partial Pressure of Ethanol on the Rate of Formation of Di-ethyl Ether over Synthetic Cation Exchange Resin.

A consecutive reaction scheme could also explain the observed reduction in the rate of formation of di-iso-propyl ether with increasing temperature. The reaction scheme may be written as



At higher temperature, reaction step 2 takes place readily and the net amount of ether produced is small. Therefore leading to lower overall reaction rate at higher temperature.

The rate of formation of di-iso-propyl or di-ethyl ether increases progressively with increasing partial pressure of the corresponding alcohol. This observation suggests that the active sites on the catalyst have not been completely saturated. This behaviour is true in the case of the formation of propene, but not in the case of ethylene formation. This suggests that the saturation partial pressure of ethanol for the production of di-ethyl ether is higher than that for ethylene formation. A similar observation has been discussed earlier and reported by Jain and Pillai (13).

The partial pressures of the products are very small compared with the partial pressure of the reactant. The kinetic data show that the overall dehydration of isopropanol proceeds faster than the overall dehydration of ethanol over synthetic cation exchange resin at the same reaction conditions. One explanation is due to the difference in the ease of releasing the hydroxyl groups. The isopropanol could release its hydroxyl group relatively faster than ethanol because of the

effects of the two methyl groups.

There is also another very important observation about the product distribution. The dehydration of isopropanol resulted in higher yield of olefin than ether. That is, the selectivity (R_O/R_E) of olefin formation increases with branched chain alcohol. Thermodynamically the formation of propene or diethyl ether is favoured over the production of ethylene or diiso-propyl ether at the same reaction temperature. This is evident from the effect of temperature on equilibrium constant illustrated in figures 1.2 and 1.3. Hence the present observation is consistent with equilibrium behaviour.

The selectivity, R_O/R_E , decreases with increasing partial pressure of alcohols. This observation suggests that the dependence of the rate of formation of ether on P_A is higher than that of the rate of formation of olefin on P_A . A similar observation has been found earlier and reported in (67).

The present results show that the cation exchange resin catalyst is more suitable for the exclusive dehydration of ethanol to di-ethyl ether than for the dehydration of isopropanol to di-iso-propyl ether. Exclusive production of di-iso-propyl ether requires a lower reaction temperature or dehydration of isopropanol in liquid phase. Further work is required to determine favourable conditions for the exclusive production of di-iso-propyl ether.

4.3.2 Kinetic Rate Expression

4.3.2.1 Power Function Rate Expression.

The kinetic data on the dehydration of isopropanol or ethanol over synthetic cation exchange resin catalyst were regressed non-isothermally using the empirical power rate equations for the formation of olefin and ether respectively.

Tables 4.3 and 4.4 give the estimated parameters by the multi-linear least squares analysis. The R-squared co-efficients show that the power rate expression fits the kinetic data very well. The observed F-ratio exceeds the critical F-ratio from the statistical table at 95% confidence level by a factor greater than 4. It indicates that the regression of the kinetic data on the dehydration of isopropanol and ethanol to both ether and olefin is statistically significant.

The order of each reaction is shown in column 5 in Table 4.3 or 4.4. The order of reaction leading to the formation of ethylene is negative, suggesting that the only possible reaction mechanism is that of the dual-site surface reaction controlling step. The orders of the other reactions leading to formation of ethers suggest that complete saturation of the active sites with reactant was not achieved.

The activation energies for the dehydration of ethanol to ethylene and di-ethyl ether over synthetic cation exchange resin are 43 and 4.1 Kcal/gmole. The corresponding activation energies for the dehydration of isopropanol are 8.7 and -2.8 Kcal/gmole, respectively. A negative activation energy has been reported by Anderianova and Bruns (103) for the esterification of acetic acid in the vapor phase with ethanol over cation exchange resin catalyst. The values of the activation energies and pre-exponential factors for the dehydration reactions over cation exchange resin are different from those values obtained for the zeolites and those reported in literature. (see table 1.2). The possible explanations for this observation are the effects of external mass transfer and alcohol adsorption co-efficient. The former is not significant in the present experiments as has been discussed previously. The latter explanation can be demonstrated theoretically as follows.

Figure 4.23 shows that the rate of formation of olefin increases progressively with increasing partial pressure of isopropanol. The equilibrium concentration of isopropanol at low coverage can be represented by Freundlich isotherm equation of the form

$$\theta_A = K_A P_A^{1/n} \quad 4.17$$

with $0 < 1/n < 1$

If the formation of olefin occurs according to monomolecular catalytic reaction, then the rate of formation of olefin

is given by

$$R_O = K_{tO} O_A = K_{tO} K_{AO}^{1/n} P_A^{1/n} \quad 4.18'$$

Similarly the rate of formation of ether can be written as

$$R_E = K_{tE} K_{AE}^{2/n} P_A^{2/n} \quad 4.19$$

if the formation of ether takes place according to LHM model and the reverse reaction is essentially insignificant.

These derived rate expressions 4.18 and 4.19 are in agreement with the empirical power function rate equations which satisfactorily fit the experimental data on the dehydration of isopropanol over cation exchange resin.

When K_{tO} , K_{AO} , K_{tE} and K_{AE} are expressed in terms of Arrhenius and Van't Hoff temperature dependence expressions, and using the reaction orders obtained from regressing the data, the rates of formation of olefin and ether become

$$R_O = A_{OO} K_{AOO}^{0.63} \text{Exp} -(E_{AO} + 0.63 \Delta H_A)/R_g T P_A^{0.63} \quad 4.20$$

and

$$R_E = A_{OE} K_{AOE}^{1.91} \text{Exp} -(E_{AE} + 1.91 \Delta H_A)/R_g T P_A^{1.91} \quad 4.21$$

If the adsorption process was that of chemisorption without dissociation, the heat of adsorption would be comparable with or higher than the heat of liquefaction of isopropanol (10.5 Kcal/gmole). Hence equation 4.21 could yield a negative temperature co-efficient, while 4.20 yields a very small activation energy.

The deduced expressions can correctly explain the estimated pre-exponentials and activation energies obtained from the power function rate expressions. The same reason can be used to explain the correlations obtained when the kinetic data on the dehydration of ethanol were fitted with a power function rate expression.

The present results show that the power function rate equation should not be used to correlate the experimental data on the dehydration of isopropanol and ethanol over cation exchange resin, because the temperature co-efficients and pre-exponential factors are markedly affected by the adsorption process. However, the empirical power function rate expressions have been found to satisfactorily represent the kinetic data on the dehydration of isopropanol and ethanol over zeolites. This behaviour is due to low reaction orders obtained for the dehydration reactions over zeolites. The results also suggest that power function rate expression could only give the true activation energy and pre-exponential factor for a heterogeneous reaction, when its rate is completely independent of reactant concentration, that is, a zero-order reaction. Hougen-Watson type of rate equation should be used to correlate the kinetic data on cation exchange resin catalyst.

4.3.2.2 Hougen-Watson Rate Expression.

4.3.2.2.1 Rate of Formation of Olefin.

Equations 4.9 and 4.10 are the two proposed rate expressions for the catalytic dehydration of alcohol to olefin. These rate equations have been found to describe the effect of partial pressure of isopropanol and temperature on the rate of formation of propene. However, only equation 4.9 which is based on the dual site mechanism was found to explain the influence of partial pressure of ethanol and temperature on the rate of formation of ethylene. The rate expressions based on the adsorption of isopropanol or ethanol as the rate limiting step were found to be unsatisfactory. The model based on the desorption of water as the rate determining step can be discarded in the case of ethanol dehydration to ethylene, but not in the case of the dehydration isopropanol to propanol.

The estimated kinetic and adsorption constants obtained from the linear least squares analysis are presented in table A4.11. The kinetic data on the dehydration of isopropanol over synthetic cation exchange resin could not be satisfactorily correlated at all temperatures by any of these models (SR1 and SR2). This is evident in the low R-squared values at high reaction temperature. The model based on the desorption of water as the rate controlling step correlated the data adequately. However, it resulted in negative adsorption co-efficients, K_A , at all reaction temperatures. Moreover the kinetic constants at different temperatures do

not obey the Arrhenius law. This observation suggests that the rate determining step may change with increasing temperature or the rates of both surface and desorption of water may be comparable at high temperatures.

Thaller and Thodos (70) have reported that the controlling step of the catalytic dehydrogenation of sec-butanol to methyl-ethyl-ketone over brass catalyst changes with reaction temperature. At low reaction, kinetic data showed surface reaction controlling step, while at high temperature the desorption of molecularly adsorbed hydrogen appeared to be the rate limiting step.

Gottfredi et al (33) did not find a satisfactory correlation for their kinetic data on the dehydration of isopropanol over synthetic cation catalyst using the Hougen-Watson approach. A similar difficulty has been encountered by others (33). The best explanation for this difficulty is probably due to the physical adsorption of water on synthetic cation exchange resins.

The non-linear analysis was performed on the kinetic data on the dehydration of isopropanol over cation exchange resin despite the failure of the Hougen-Watson rate expressions in the linear regression. The results of the non-linear regression are presented in table A4.12.

There is poor agreement between the parameters obtained from linear and non-linear analyses based on the surface

catalysed reaction controlling rate expressions. However, there is excellent agreement between the parameters obtained from these methods, based on the desorption of water controlling rate equation. The explanation for the poor agreement between the parameters estimated from the surface reaction controlling step rate expressions could be due to two factors:

- a) A saddle point or local minimum occurs.
- b) Poor kinetic data as suggested by Froment and Bischoff (105).

The latter is not likely to be the explanation for the large differences obtained, because the same kinetic data gave no difference in the parameters obtained using the desorption of water (DEW) as the controlling rate expression.

Results of the non-linear regression of the surface catalysed reaction determining rate expression with the kinetic data reveal that there is a maximum in the plot of $\ln K_R$ versus $1/T$. The maximum occurs at high temperature. This observation suggests that there is likely a shift in the rate controlling step.

Results of the statistical analysis of the kinetic data on the dehydration of isopropanol do not allow any firm conclusion to be made about the rate limiting step. It only indicates a shift in the rate controlling step.

4.3.2.2.2 Rate of Formation of Ether.

Of the rate expressions tested, equations 4.11, 4.12 and 4.12 will be reported here. These are based on the assumption that surface catalysed reaction is the rate controlling step. These rate equations were found to predict the effects of partial pressure of isopropanol or ethanol and temperature on the rate of formation of di-iso-propyl or di-ethyl ether.

Rate expressions based on the assumption of alcohol or desorption of water is the rate determining step were found to be unsatisfactory. Linear and non-linear analyses of data yielded poor fit and unacceptable characteristics of the estimated kinetic and adsorption constants. These values will not be reported here.

4.3.2.2.2.1 Formation of Di-iso-propyl Ether.

Statistical analysis revealed the inadequacy of the rate expressions 4.11, 4.12 and 4.13 in fitting the behaviour of the kinetic data with increasing temperature. The explanation for this is probably due to an increase in the partial pressure of water as a result of higher reaction rate at higher reaction temperature.

The water adsorption term ($K_W P_W$) was added to the adsorption terms of these rate equations. Then all the data were regressed again. The regression showed an improvement, but resulted in negative adsorption co-efficients and unacceptable characteristics of the estimated constants.

Furthermore, the homogeneous rate expression given by

$$R_E = K_R(P_A^2 - P_W P_E / K_{eq,E}) \quad 4.22$$

was found to correlate the kinetic data satisfactorily. The residual mean sums of squares obtained from the above rate equation (4.22) were smaller than those obtained from the Hougen-Watson rate expressions. However, the temperature dependence co-efficient is very small, about 1.0 Kcal/gmole. This co-efficient is greatly affected by adsorption, and has been demonstrated theoretically earlier in section 4.3.2.1.

Gottfredi et al (33), the only authors, who have reported the dehydration of isopropanol over synthetic cation exchange resin had difficulties in correlating their kinetic data with Hougen-Watson rate equation. It was found that the Hougen-Watson rate expression fitted the data in a reduced range of partial pressure of water. The inadequacy of the Hougen-Watson rate equation to represent the kinetic data on the dehydration of isopropanol over synthetic cation exchange resin is probably due to the higher reactivity of isopropanol. Hougen-Watson rate equation satisfactorily correlated kinetic data on the dehydration of ethanol which has lower reactivity, over synthetic cation exchange resin as reported in (34, 46, 47) and found in the present studies. This will be discussed shortly.

It is well known that synthetic cation exchange resin has a high affinity for water. This probably explains its relatively slower desorption rate as suggested by the analysis of the kinetic data.

4.3.2.2.2.2 Formation of Di-ethyl Ether.

The estimated kinetic and ethanol adsorption constants are presented in tables A4.19 and A4.20, in appendix 4. The reaction rate constants are positive and obey the Arrhenius law.

REM2 model correlated the data adequately at two temperature levels. However, it yielded a negative ethanol adsorption co-efficient at the lowest temperature from the linear least squares analysis and a very high value from the non-linear least squares analysis. The model, REM2, is rejected on the basis of negative adsorption constant at lowest temperature.

Both REM1 and LHM satisfactorily correlated the kinetic data on the dehydration of ethanol to di-ethyl ether over cation exchange resin. The two models remain indistinguishable.

Figure 4.27 shows the temperature dependence of reaction rate and ethanol adsorption equilibrium constants obtained from models REM1 and LHM. The upper plot is for K_A while the lower plots are for K_R . The estimated pre-exponential factors, activation energies, heat of adsorption of ethanol over cation exchange resin are shown in table 4.8.

Figure 4.28 shows the plot of the experimentally observed versus calculated rates from these models, the mean relative deviation being 8.7% for all the kinetic data. The mean percentage deviation is given by

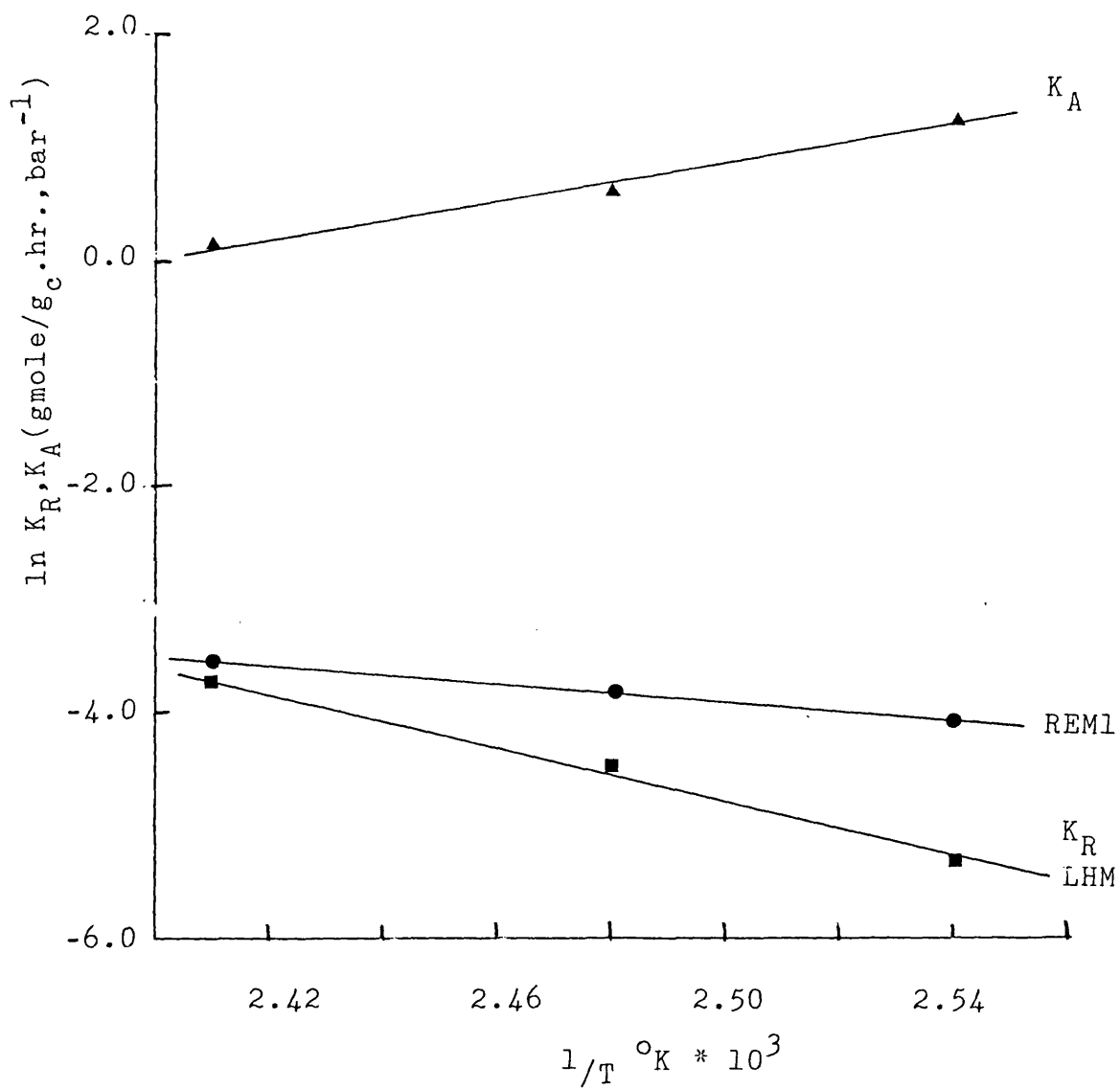


Fig. 4.27 Temperature Dependence of the Reaction Rate and Adsorption Equilibrium Constants.
 The dehydration of ethanol to di-ethyl ether over synthetic cation exchange resin.

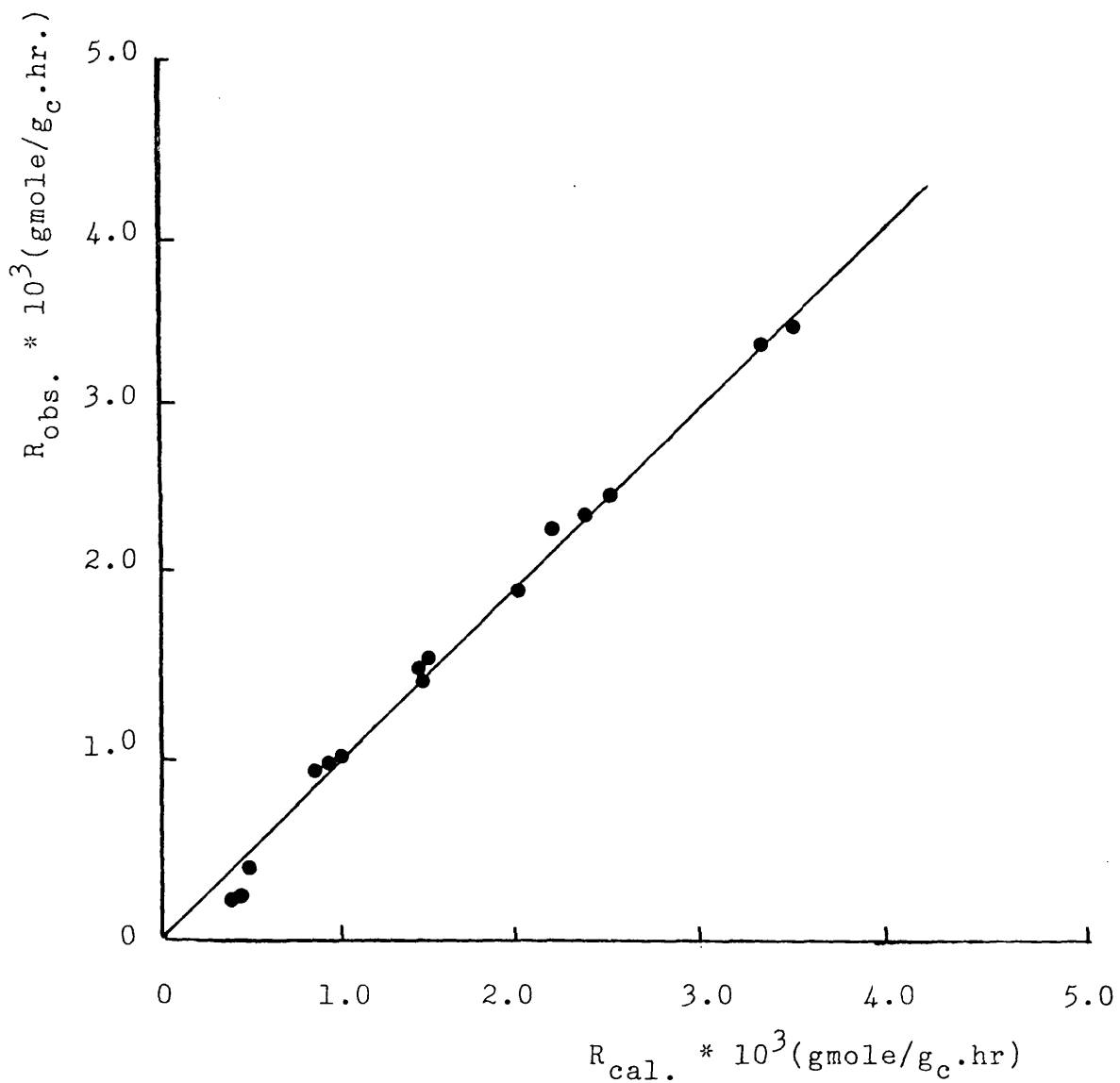


Fig. 4.28 Comparison Between Calculated and Experimental Rates.

The dehydration of ethanol to di-ethyl ether over synthetic cation exchange resin.

$$\varepsilon = \sum_{i=1}^n \left[\frac{|R_{\text{obs}}(i) - R_{\text{cal}}(i)|}{R_{\text{obs}}(i)} \right] \times \frac{100}{n} \quad 4.23$$

The relative deviation obtained from the empirical power function is 12% for all the kinetic data. This observation shows that the Hougen-Watson rate expression can correlate the kinetic data on the dehydration of ethanol to di-ethyl ether over synthetic cation exchange resin better than the power function. This is probably because the reversibility of the reaction and the depressive behaviour of ethanol are neglected by the power function rate expression.

It can be concluded that LHM and REM1 are the two models which satisfactorily represent the kinetic data on the dehydration of ethanol to di-ethyl ether over cation exchange resin. This conclusion is in perfect agreement with Kabel and Johanson (34), who have found that surface catalysed reaction is the rate limiting step for same reaction over the same catalyst in the temperature range 105°C to 125°C. This conclusion also agree with that of many others, see tables 1.2, 1.3 and 1.4.

Activation energies estimated from the slopes of the plots of logarithm of kinetic constants against the inverse of absolute temperature are 24 and 7.6 Kcal/gmole from LHM and REM1 models, respectively. It is very difficult to compare activation energies, because of different

experimental conditions. Tables 1.2, 1.3 and 1.4 show a summary of apparent activation energies for the dehydration of alcohols over solid catalysts. It is evident from these reported results that activation energies in the literature vary widely. Nevertheless, the activation energy obtained from the present kinetic analysis using the LHM model agrees with some of those reported in the literature. However, the activation energy obtained from the REML model is small compared with literature values.

The heat of adsorption of ethanol was found to be -16 Kcal/gmole. This value is negative, which implies exothermic adsorption. This is expected, since thermodynamically the rate of adsorption decreases with increasing temperature. The absolute value is very large compared with the heat of liquefaction 9.4 Kcal/gmole, suggesting that ethanol is chemisorbed on cation exchange resin. Equation 4.21 gives the deduced rate expression for the formation of di-isopropyl ether. The corresponding rate equation for the formation of di-ethyl ether, using the reaction order obtained from regressing the data is given by

$$R_E = A_{OE} K_{AOE} \text{Exp}-(E_A + \Delta H_A) / R_g T P_A \quad 4.24$$

If the heat of adsorption obtained in the present studies is used in the above expression, it can be seen that a low activation energy would be obtained. This observation confirms the previous conclusion that the estimated activation energy and pre-exponential factor obtained from empirical

power function rate equation are markedly affected by the adsorption process. The values of the heat of adsorption is in excellent agreement with Kabel and Johanson (34), who reported a value of -16.0 Kcal/gmole.

Hydrogen bonding may also be involved in the chemisorption of ethanol on synthetic resin catalyst and has been suggested by Zundel et al. (41). If this happens, it would have a considerable influence on the heat of adsorption.

The entropy of adsorption is negative, -39 cal g/mole °K. Its absolute value is less than the standard entropy of ethanol in the fluid phase 68 cal g/gmole °K. This indicates that the adsorbed ethanol molecule loses entropy on adsorption as expected.

4.4 Conclusions.

- a) Both principal products (ether and olefin) were formed when n-butanol, isopropanol and ethanol were dehydrated.
- b) Empirical power function rate expressions satisfactorily correlated the kinetic data on the dehydration of alcohols to ethers and olefin over zeolites 13X, 4A and ZNa.
- c) Activation energies have been found for each dehydration reaction.
- d) Reaction orders have been established for the dehydration reactions. Generally the reaction order for the formation of ether is higher than for the formation of olefin at the same reaction conditions.

- e) The dehydration of alcohols (n-butanol, isopropanol and ethanol) were all found to be surface reaction controlling at all reaction conditions except the dehydration of isopropanol over synthetic cation exchange resin.
- f) The dehydration reactions follow a simultaneous reaction scheme and were found to require different active sites and proceed through different transition states.
- g) Dual site mechanism (SR2) rate expression satisfactorily correlated all kinetic data on the dehydration of alcohol to olefin except those for the formation of propene over synthetic cation exchange cation resin, while the single site (SR1) mechanism fails in some cases.
- h) Langmuir-Hinshelwood mechanism (LHM) and Rideal-Eley mechanism (REMI) were found to equally fit the kinetic data on the dehydration of alcohols to ethers except those for the dehydration of isopropanol to di-iso-propyl ether over synthetic cation exchange resin. Both models remain indistinguishable. Relationship between the activation energies and pre-exponential factors from both models were deduced. These relationships were found to be valid for all dehydration of alcohols to ethers over solid catalysts employed in the present studies.
- i) Power function and Hougen-Watson rate equations satisfactorily represent the kinetic data on the catalytic dehydration of alcohols to olefin equally, however the Hougen-Watson rate expressions were superior to empirical power

function rate expressions in describing the kinetic data on the formation of ethers.

j) The alcohol adsorption and kinetic constants for the simultaneous reactions were satisfactorily correlated with the Arrhenius and Van't Hoff equations.

k) The estimated activation energy and pre-exponential factor obtained from empirical power function rate equation using data on synthetic cation exchange resin were found to be markedly affected by adsorption.

CHAPTER 5

MECHANISM, SELECTIVITY AND REACTIVITY OF ALCOHOLS
AND ACTIVITY OF ZEOLITES

CHAPTER 5MECHANISM, SELECTIVITY AND REACTIVITY OF ALCOHOLS AND
ACTIVITY OF ZEOLITES5.1 Alkene Product Distribution5.1.1 Introduction

Previous work on the catalytic dehydration of n-butanol (71-74), except that by Pine and Haag (75) has not resolved the isomeric alkene products.

The study of product distribution of alkenes from the elimination reactions of organic compounds of the forms $R_1CH_2CHXR_2$ is very helpful in shedding light on the reaction mechanism. Noller et al (11,12) have given an extensive review on elimination reactions over polar catalysts, including a section on the elucidation of reaction mechanism by examining the product distribution.

The catalytic dehydration of n-butanol over alumina was studied by Pine and Haag (75), at reaction temperatures of 350 and 410°C. It was found that some catalysts gave almost pure 1-butene while others produced mixtures of alkenes, that is 1-butene, cis-2-butene, trans-2-butene and iso-butene. At 350°C, values of the ratio of cis to trans isomers were found to lie between 0.9 to 2.3 which

were above the equilibrium value of 0.6. This indicates that some catalysts favour the formation of cis-2-butene. The preferential production of the cis-isomer is explained by the formation of an intermediate proton olefin complex. The cis- π -complexes are more stable than the trans- π -complexes, hence the formation of cis-isomer is favoured. Knozinger and Buhl (79) have observed a high cis preference during the catalytic dehydration of 2-butanol over alumina. Many authors have also reported cis preference during the catalytic elimination of haloalkanes.

The distribution of 1-butene and 2-butenes from the elimination of 1-halo-butane over lithium salts has been studied in a microcatalytic reactor at temperatures between 320-270°C (42). It was observed that the catalyst favoured the production of 1-butene above other isomers. Kladnig and Noller (76) have studied the elimination reactions of 1-chlorobutane and 2-chlorobutane over Linde 13X and 4A zeolites containing different cations at reaction temperatures between 150 and 400°C. Using the product distribution of the alkenes, the mechanism of the elimination reaction over 13X and 4A catalysts was deduced. 1-Butene was found to predominate over 2-butenes up to 200°C using 13X zeolites. Linde A with Zn^{++} cation, however, gave mainly 1-butene over the entire temperature range studied. It was concluded that NaX showed an E2 mechanism character at lower reaction temperature but the mechanism shifts to E1 type with higher

reaction temperature. For Linde A with Zn^{++} , E2 mechanism was found to apply at all reaction temperatures.

The results from elimination reactions of haloalkanes would probably be different from the dehydration reactions because the chemisorption of alcohols on catalyst is stronger than that of haloalkanes. The product distribution of alkenes from the catalytic dehydration of n-butanol was therefore studied so as to gain some insight into the reaction mechanism. Tables A5.1, A5.2 and A5.3, in appendix 5, present the alkene distribution over zeolites 13X, 4A and ZNa.

5.1.2 The Effect of the Partial Pressure of Alcohol.

Figures 5.1, 5.2 and 5.3 show the effect of the partial pressure of n-butanol on product distribution. The percentages of all the components were found to be independent of the partial pressure of n-butanol. The same behaviour was observed at all reaction temperatures. This suggests that the rate of formation of alkenes are of the same order with respect to n-butanol partial pressure.

Jewur and Moffat (78) have found that the percentage concentration of 1-butene, trans-2-butene and cis-2-butene remained the same for all the space times used during the dehydration of 2-butanol over boron phosphate.

The formation of 1-butene over 13X zeolite predominates at all alcohol partial pressures (Fig. 5.1). This indicates that 13X zeolite favours the formation of 1-butene. While for 4A zeolite with sodium ions (Fig. 5.2), the production of

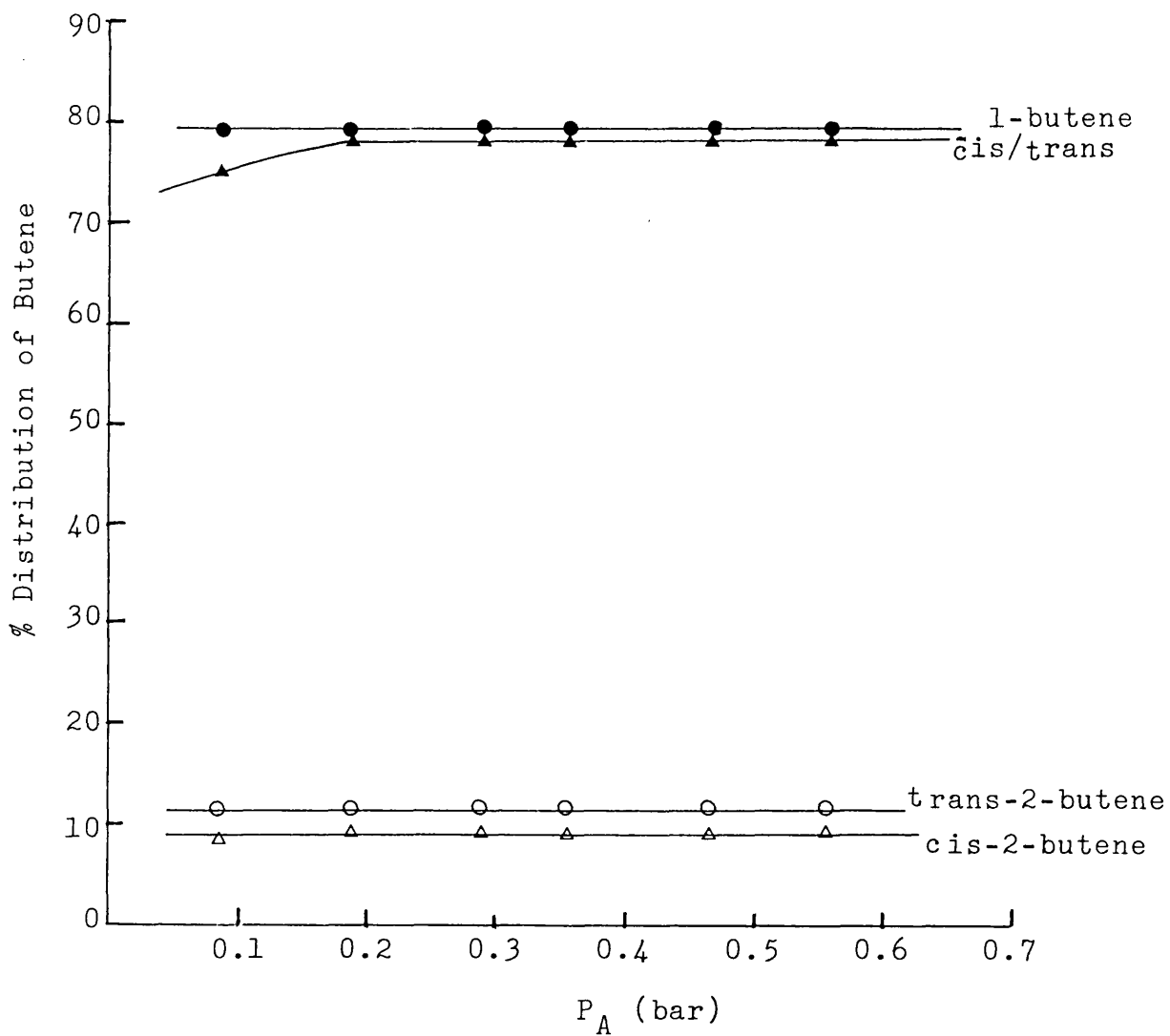


Fig. 5.1 The Effect of the Partial Pressure of n-Butanol on the Percentage Distribution of Butene Using Zeolite 13X at 252°C.

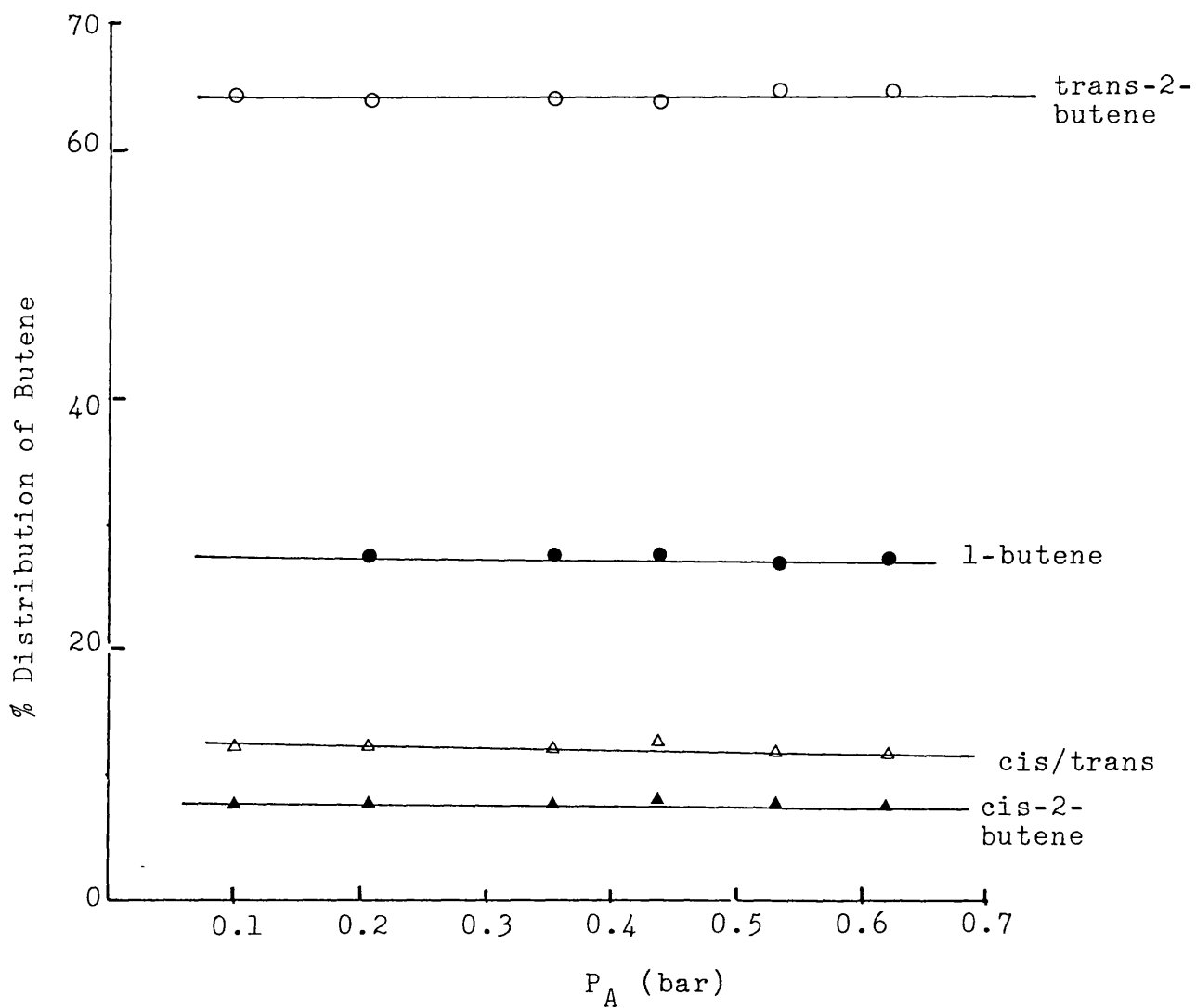


Fig. 5.2 The Effect of the Partial Pressure of n-Butanol on the Percentage Distribution of Butene Using Zeolite 4A at 297^oC.

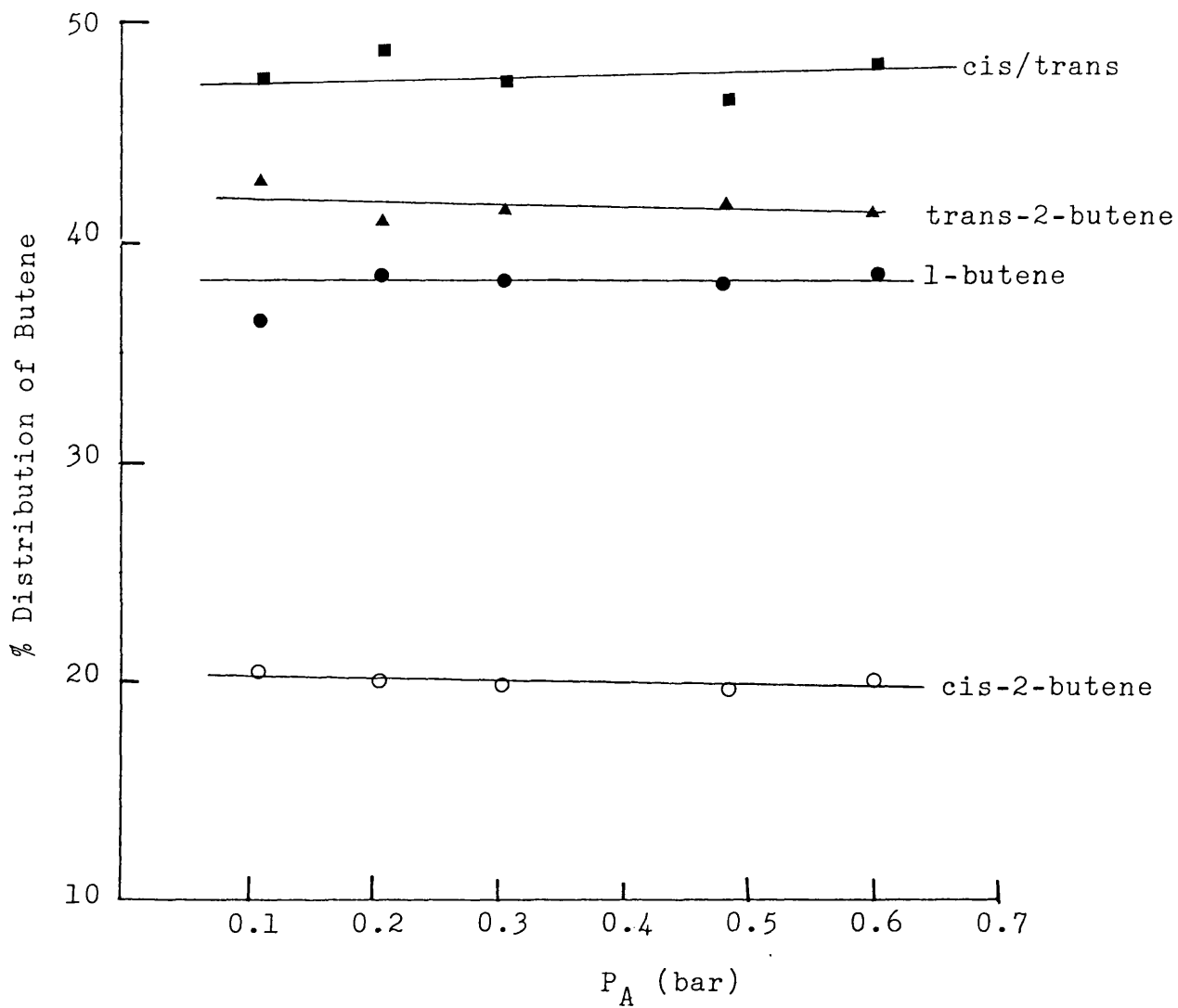


Fig. 5.3 The Effect of the Partial Pressure of n-Butanol on the Percentage Distribution of Butene Using Zeolite ZNa at 235°C.

trans-2-butene is favoured at all alcohol partial pressures. For ZNa zeolites, at 235°C, the production of trans-2-butene, predominates at all partial pressures. But at higher reaction temperatures, the percentage of 1-butene was slightly higher than that of trans-2-butene over all alcohol partial pressures.

5.1.3 The Effect of Temperature.

Figures 5.4, 5.5 and 5.6 show the effect of reaction temperature on the distribution of alkene for the zeolites 13X, 4A and ZNa respectively. The dehydration of n-butanol over these zeolites was studied between 230°C and 300°C.

For 13X zeolite, Fig. 5 shows that 1-butene isomer was the main product in the temperature range investigated. However the total percentage of the other isomers (2-butenes) increases slightly with increasing temperature. This is an indication either of the reaction mechanism shifting towards E1 type or that a Wagner-Meerwein rearrangement reaction takes place relatively faster. This will be fully discussed later.

For 4A zeolite, Fig. 4.5, trans-2-butene predominates at all temperatures. Its percentage increased with increasing reaction temperature, while the percentage of 1-butene falls sharply with increasing reaction temperature. The fraction of cis-2butene also increased with increasing reaction temperature. Increasing production of 2-alkenes with increasing reaction temperature is considered to be an important criterion for a shift of reaction mechanism from E2 to E1 type. This assumes that the dehydration reaction is taking place according to E2 type mechanism at lower reaction temperature.

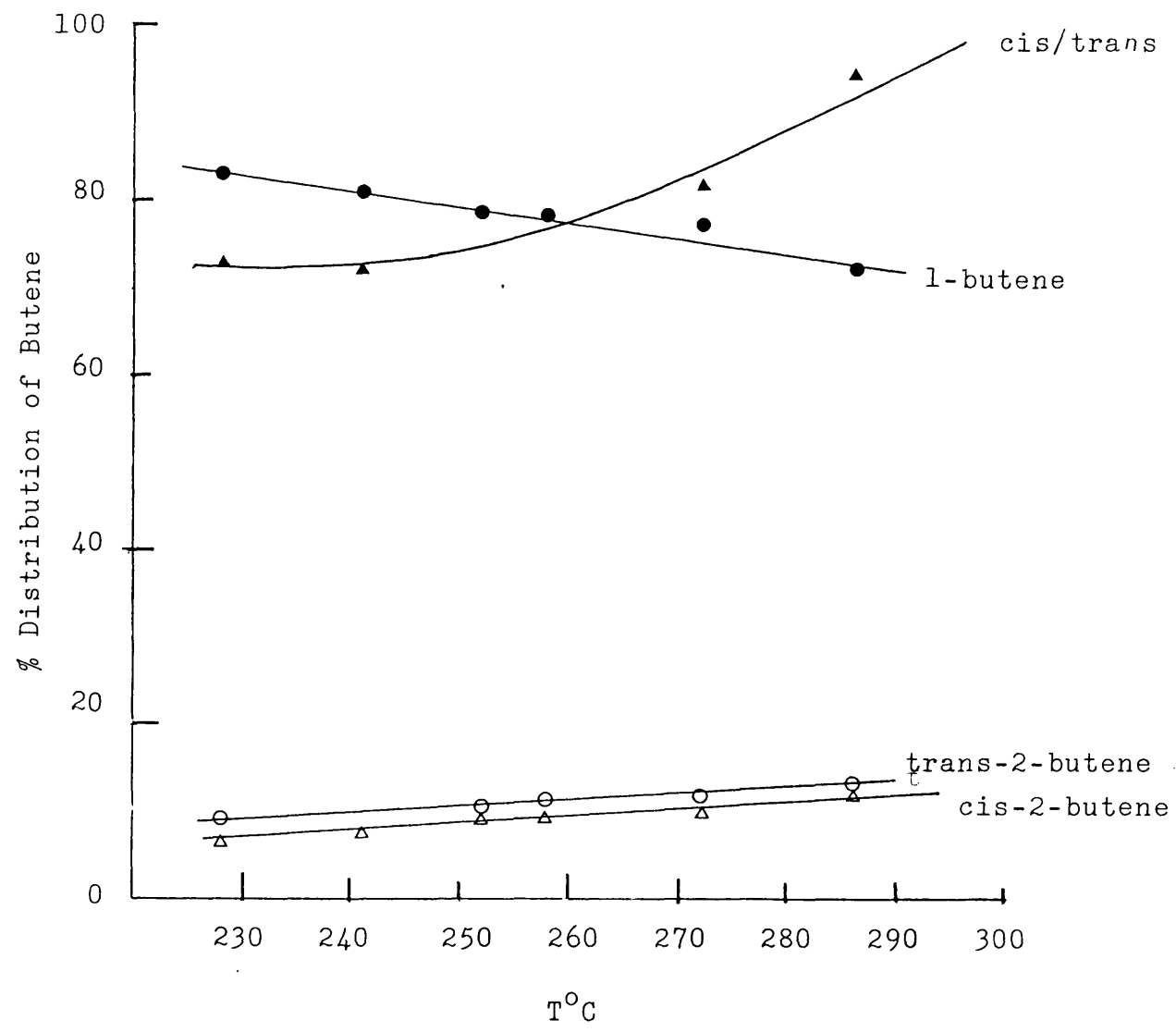


Fig. 5.4 The Effect of the Reaction Temperature on the Percentage Distribution of Butene for the Zeolite 13X.

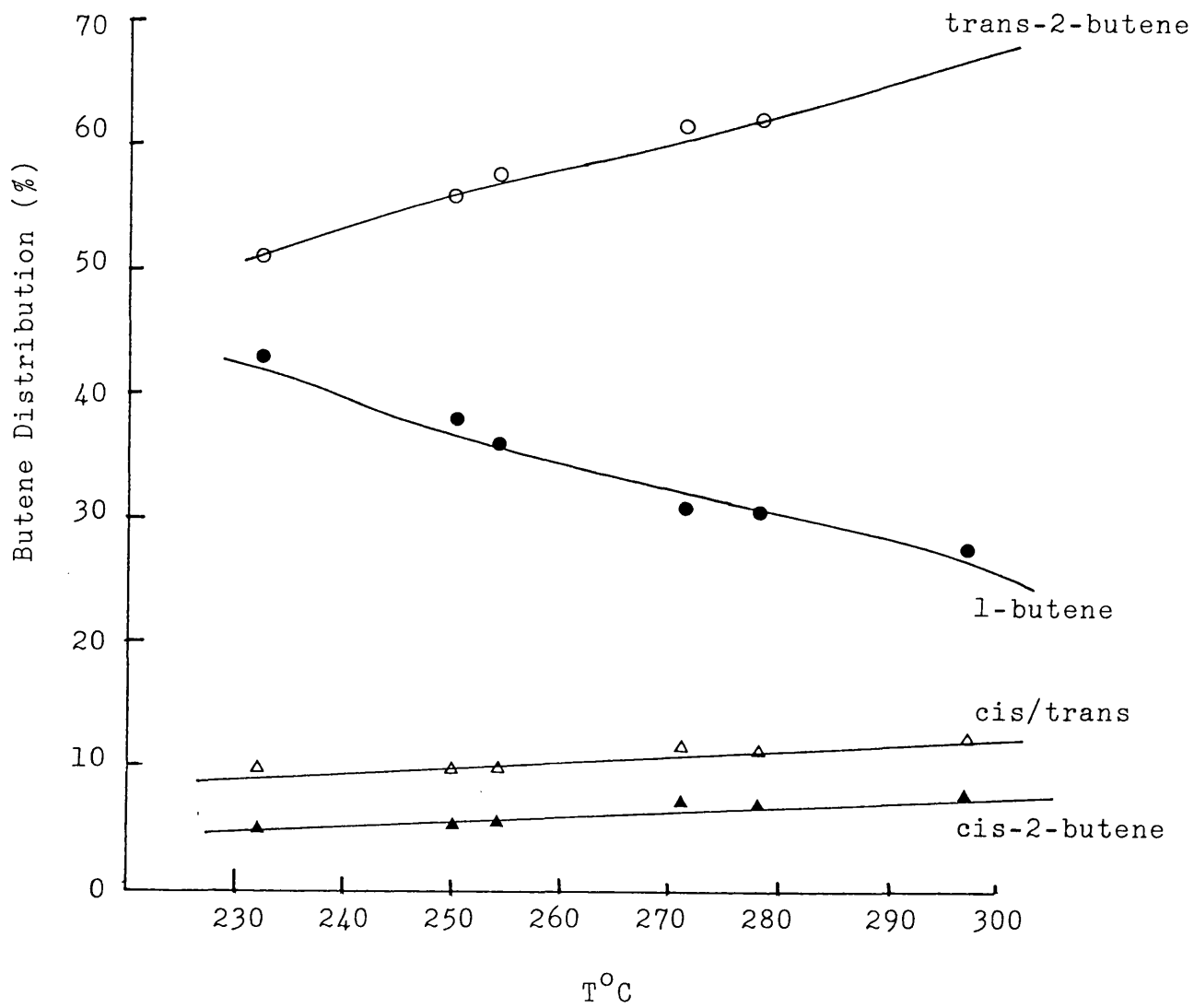


Fig. 5.5 The Effect of the Reaction Temperature on the
Percentage Distribution of Butene for the
Zeolite 4A.

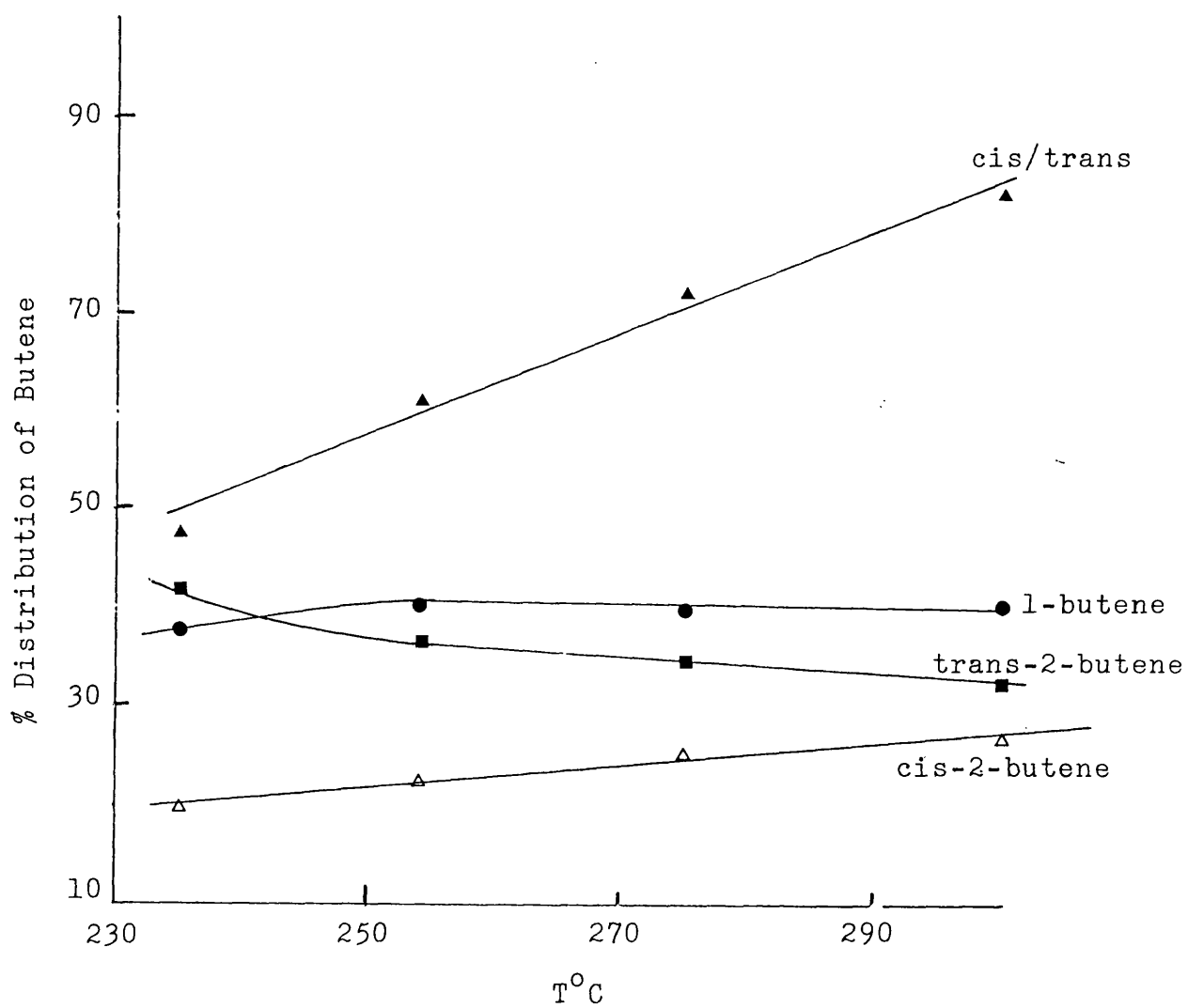


Fig. 5.6 The Effect of the Reaction Temperature on
the Percentage Distribution of Butene for
the Zeolite ZNa.

The formation of 1-butene over ZNa, figure 5.6, increases slightly from 37% at 235°C to 41% at 300°C, whereas the percentage of trans-2-butene falls slightly from 42% at 235°C to 33% at 300°C. The total percentage of 2-butenes decreases slightly from 63% at 235 to 59% at 300°C. This probably indicates either one of the following:

- a) Increasing reaction temperature does not change the mechanism of the reaction over ZNa.
- b) The catalyst selectivity towards the formation of 1-butene increases with increasing reaction temperature.

Two effects which may explain the former possibility are:

- a) The effects of reaction temperature
- b) Acidic sites on reaction mechanism

Increasing reaction temperature or acidic strength shifts the reaction mechanism towards E1 type. The number of acid sites, especially the strongest ones, may be deactivated by the increasing temperature. If this happens, the reaction mechanism shifts towards E2 type. These two effects on the changing of reaction mechanism probably balance each other, hence the reaction mechanism on ZNa zeolite becomes independent of reaction temperature.

The ratio of cis-2-butene to trans-2-butene increases with increasing reaction temperature for all the catalysts (Figures 5.4, 5.5 and 5.6). This suggests that all the catalysts are more selective towards the formation of the cis isomer.

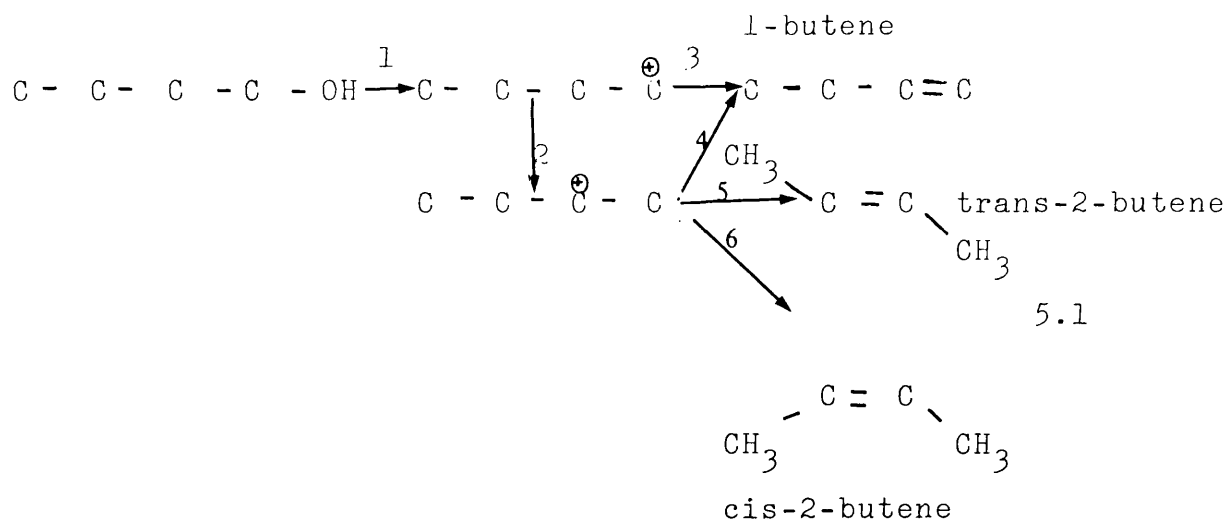
5.1.4 Discussion

5.1.4.1 Product Distribution.

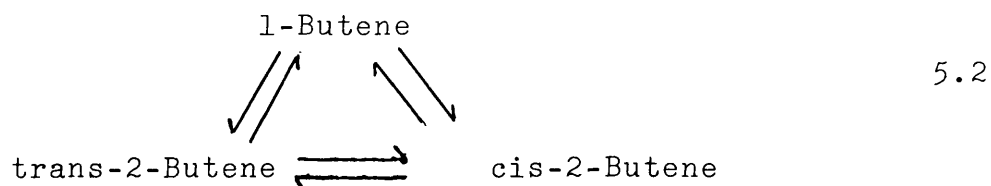
The catalytic dehydration of n-butanol to alkene isomers can take place according to three basically different mechanisms. They are called E1, E2 and E1cB mechanisms. The E1cB (cB conjugate base) will not be considered here, because it is not expected, since the catalysts employed in the present study are predominantly acidic catalysts. Only a few authors (11) have shown E1cB to be experimentally and theoretically possible for the elimination reaction.

The only mechanism that can explain the formation of the isomeric butenes from the dehydration reaction is the E1 type mechanism. E2-like mechanism only leads to the formation of 1-butene. However E2 type mechanism followed by secondary isomerization reactions of 1-butene can also lead to the formation of other isomeric products (iso-butene, cis-2-butene and trans-2-butene). The production of 2-alkenes (cis and trans) in the absence of secondary isomerization reactions therefore strongly suggests a dehydration reaction proceeding according to E1 mechanism.

The proposed dehydration reaction scheme according to E1 mechanism can be represented by



The secondary isomerization reactions can be written as



The first chemical reaction step produces 1-butyl carbonium ion by the breaking of the carbon-hydroxyl group bond. Abstraction of the hydroxyl group is believed to occur on the acidic site, while the carbonium ion is adsorbed on the basic site. This suggests that possibly both sites are responsible for the dehydration reaction.

The 1-butyl carbonium ion undergoes the Wagner-Meerwein rearrangement to form the 2-butyl carbonium ion. 1-Butene can be produced from both 1 and 2-butyl carbonium ions, while the 2-alkenes can only be produced from 2-butyl carbonium ion. This therefore suggests that production of 2-alkenes, both cis and trans, depends on the Wagner-Meerwein

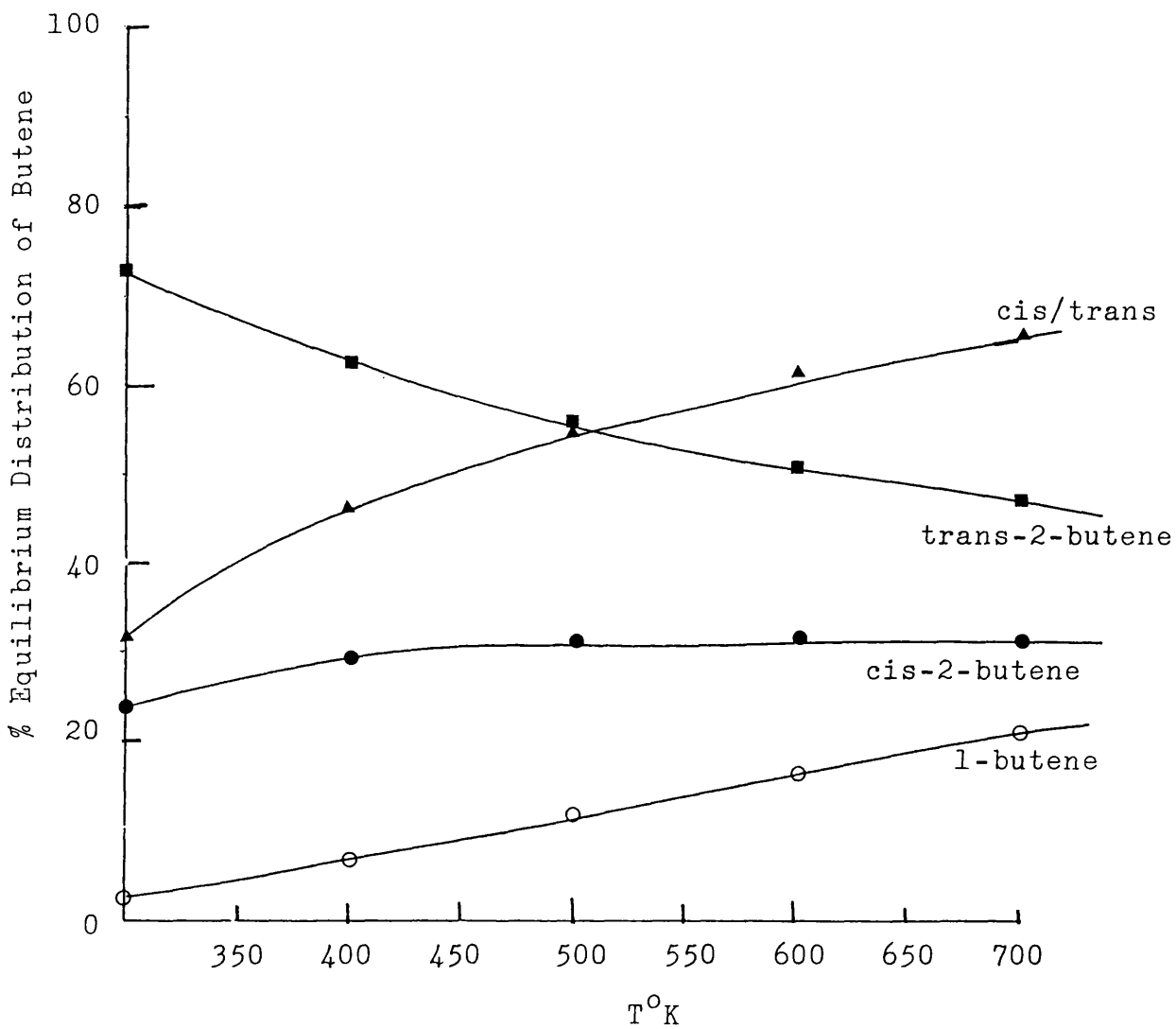


Fig. 5.7 The Temperature Dependence of the Thermodynamic Equilibrium Distribution of Butene.

rearrangement reaction. The above reaction scheme cannot lead to the production of isobutene. If isobutene is produced, it must be from the skeletal isomerization reactions of the butene. The most probable isomers are the 2-butenes. The formation of isobutene requires the migration of a methyl group from carbon 2 to carbon 3, or vice versa.

The dehydration of n-butanol to olefinic isomers is not affected by the equilibrium conditions. This has been discussed in chapter 4. Therefore, the product distribution depends on the rates of reaction steps 3, 4, 5 and 6, while the selectivity depends on the kinetics of steps 3, 4, 5 and 6 and geometrical and molecular factors. One should also bear in mind that the formation of 2-alkenes depends very much on reaction step 2. The production of 2-butyl carbonium ion can be affected greatly both by the lack of active adjacent site to the adsorbed 1-butyl carbonium ion and the rate of formation of 1-butene through reaction step 3. So far, existing reports in literature have neglected these two factors, particularly the production of 1-butene isomer from 1-butyl carbonium ion. It is believed that all alkenes are produced through the same intermediate (2-butyl carbonium ion) because this ion is more stable than 1-butyl carbonium ion. There is no convincing evidence yet to prove that 1-butene cannot be produced directly from the 1-butyl carbonium ion.

If isomerization reactions are taking place, then the product distribution would depend solely on the thermodynamic equilibrium conditions of the isomerization reactions. Figure 5.7 shows the thermodynamic equilibrium distribution of the butenes (1-butene, trans-2-butene and cis-2-butene). The thermodynamic equilibrium constants of isomerization reactions were estimated at various temperatures using the thermodynamic data (Gibbs free energy) of Stull et al (22). The thermodynamic equilibrium constants were used as the basis for the calculation of equilibrium distribution. Thermodynamically trans-2-butene is usually favoured over the other alkene isomers. At equilibrium, the composition of trans-2-butene decreases with increasing temperature while that of 1-butene and cis-2-butene increase with increasing temperature. The ratio of cis-2-butene to trans-2-butene also increases with increasing temperature. This suggests that cis-2-butene is thermally favoured. If isomerization reactions are accompanying the catalytic dehydration reaction, then reaction product distribution should follow the thermodynamic equilibrium distribution pattern.

Table 5.1 shows the comparison of experimental product distribution over zeolites 13X, ZNa and 4A with the equilibrium product distribution within the temperature range studied.

Table 5.1 Comparison of the Experimental Product Distribution with the Thermodynamic Equilibrium Product Distribution

Product	1-	trans-2-	cis-2-	
Catalyst	Butene	Butene	Butene	cis/trans
13X	above	below	below	above
ZNa	above	below	below	above
4A	above	slightly below	below	below

The percentage of 1-butene are above their thermodynamic equilibrium values at all n-butanol partial pressures and reaction temperatures for all catalysts. It can be said that isomerization reactions are absent and that the catalysts are more selective towards the formation of 1-butene. This high selectivity for 1-butene may be due to the fact that 1-butene can be produced through three different reaction routes (reaction steps 3 and 4 and E2 mechanism) while other products can only be formed through one step.

The composition of 2-butenes are below their equilibrium values at all reaction temperatures, except trans-2-butene which is nearly at its equilibrium value for 4A catalyst. In this case it is possible that secondary isomerization reactions are taking place.

The ratios of cis-2-butene to trans-2-butene are above the equilibrium values in the case of zeolites 13X and ZNa. Both catalysts clearly favour the production of cis isomer over its trans-isomer. This type of behaviour has been reported by many (11, 76-79, 159). There has been no convincing explanation given for the elimination reaction in general, in favour of cis isomer over the trans isomers.

The cis/trans ratios are below the equilibrium values in the case 4A at all reaction temperatures and partial pressures of n-butanol. This is probably due to diffusional limitations of cis-2-butene which is the most bulky group. The methyl groups are on the same side of the double bonds.

For all the catalysts used in the present studies, iso-butene was never detected under all reaction conditions. This is probably due to the fact that iso-butene cannot be produced directly from 1-butyl or 2-butyl carbonium ion or through the E2 type mechanism. The production of iso-butene involves the migration of methyl group from carbon 2 or carbon 3 in the 2-alkene products. Therefore the formation of iso-butene needs further readsorption of 2-butenes. However the 2-butenes are weakly adsorbed on the active sites of the catalyst compared with n-butanol. Therefore the readsorption of 2-butenes is highly unlikely, because 2-butenes cannot compete with n-butanol which is strongly adsorbed and present in much higher concentrations.

Secondly, the absence of iso-butene may be due to diffusional limitations because the bulky groups are attached to the same carbon atom. This however cannot explain its absence on zeolite 13X, which has large cavities.

The non-production of iso-butene is an important criterion which indicates that isomerization reactions did not occur. 2-Butenes are produced independently through the same intermediate and 1-butene is probably formed through three different routes or intermediates.

This conclusion appears to contradict with that of Pine and Haag (75), who reported the presence of secondary isomerization reactions at their working temperatures. However the present study was conducted at much lower reaction temperatures. The absence of skeletal isomerization reactions at low temperature may not be surprising, because isomerization reactions require temperatures higher than that of the dehydration reactions.

5.1.4.2 Reaction Mechanism.

There is no doubt that the type of catalyst used affects the product distribution. Two basically different properties are probably responsible for the different product distributions. These two physicochemical properties are pore geometry and the presence of acidic and basic sites.

It is well known that both acidic and basic sites are necessary for the dehydration of alcohol to olefin over solid catalysts. One site is used for the abstraction of the electronegative species or hydrogen while the other site is required for the stabilization of the carbonium ion or carbonium produced. Even in the E2-like mechanism, both sites are needed to rupture the broken bonds in the activated complex state. The stronger site probably dictates the type of mechanism or route which an elimination reaction follows. For instance, on a solid catalyst with paired basic and acidic sites, E2-type mechanism may be expected.

Zeolites are made up of essentially SiO_2 and Al_2O_3 . Al_2O_3 and SiO_2 are on the opposite sides of water respectively, if they are arranged in order of increasing acidity. Hence a zeolite with ratio of SiO_2 to Al_2O_3 greater than 1.0, would exhibit acidic properties.

Therefore, the order of acidic strength of the zeolites used in the present work is

$$\text{ZNa (10)} > \text{13X (2.6)} > \text{NaA (2.0)} \quad 5.3$$

where the number within the brackets indicates the ratio of SiO_2 to Al_2O_3 . This sequence suggests that acidic sites are predominant on these zeolites. E1-type mechanism therefore would be expected for the elimination reactions over these zeolites.

For zeolites 4A and ZNa, the E1 mechanism is preferred under all reaction temperatures. This is shown by the total percentage of 2-butenes which is equal to, or above 55% of the butene production.

For zeolite 4A, increasing temperature further increases this percentage, indicating that increasing temperature further shifts the mechanism towards E1-type. A similar change in mechanism from E2 to E1 type has been reported by Noller et al (11, 12) and Knozinger and Scheglila (77) for the elimination reactions of haloalkanes and 2-butanol.

It can be concluded that the dehydration of n-butanol over zeolites ZNa and NaA follows E1 mechanism.

The product distribution over 13X shows that 1-butene is highly favoured. This may be explained by the following:

a) Reaction step 3 is very fast and only a small amount of 1-butyl carbonium ion undergoes Wagner-Meerwein rearrangement (reaction step 2), producing small amounts of 2-butenes (cis and trans). The Wagner-Meerwein rearrangement probably requires

a vacant site which might lead to little formation of 2-butyl carbonium ion, because the active sites are nearly saturated by the reactant. This is supported by the low reaction order with respect to alcohol concentration obtained.

b) If the Wagner-Meerwein rearrangement reaction, step 2 does occur rapidly, because 1-butyl carbonium ion is less stable, as suggested by Kladnig and Noller (76) then the reaction step 4, must be very fast compared with steps 5 and 6, before zeolite 13X could become highly selective to the formation of 1-butene.

c) The preferential production of 1-butene on zeolite 13X may be due to E2 mechanism predominance. That is, most of the 1-butene is produced according to E2 mechanism. The E1 mechanism contributes much less towards the formation of 1-butene. However, the fact that 2-butenes (cis and trans) are produced in the absence of isomerization reactions suggests strongly that the dehydration reaction probably proceeds through an ionic mechanism.

The dehydration of n-butanol proceeds according to an ionic mechanism, on NaA which has the lowest $\text{SiO}_2/\text{Al}_2\text{O}_3$ ratio among the three zeolites used. An increase of the $\text{SiO}_2/\text{Al}_2\text{O}_3$ ratio in the skeleton of zeolites shifts the mechanism

for the elimination reaction further towards E1 type. This is borne out in the case of ZNa which has a much higher $\text{SiO}_2/\text{Al}_2\text{O}_3$ ratio. Therefore the dehydration of n-butanol most probably proceeds according to E1 mechanism with preferential formation of 1-butene as the principal product.

Kladnig and Noller (76) have also observed that 1-butene predominates in the elimination of 1-chlorobutane over Linde NaX, but concluded that it was an indication of the E2 type mechanism. They have not considered the fact that 1-butene can be produced through reaction step 3.

The arguments proposed above have demonstrated that 1-butene predominance may be attributed to the high activity and selectivity of 13X zeolite.

The preferential formation of 1-butene from 1-halobutane has been observed on lithium salts (11, 42). Production of 2-butenes from 1-halobutane was considered as an important indication of the elimination reaction proceeding through E1 mechanism. The argument is in agreement with that proposed here for the dehydration reaction.

5.2 The Activity of Zeolites.

The dehydration of n-butanol and isopropanol over the commercial zeolites 13X, 4A and ZNa have been carried out under nearly the same conditions to make it possible for comparison purposes. The rate of formation of olefin is used here as the variable for comparing the activity of the catalysts.

Figures 5.8 and 5.9 show the effect of a family of zeolites on the dehydration of n-butanol and isopropanol at 280°C. The order of activity is found to be

for primary alcohol: 13X > 4A > ZNa

for isopropanol: 13X > ZNa > 4A

Zeolite 13X is the most active catalyst in both cases. One factor which can explain the high activity of zeolite 13X is the highly developed surface and large cage structure.

Kinetic data by Bryant and Kranich (44) on the dehydration of ethanol over the same family of zeolites (13X, 4A and ZNa) showed a sequence of activity similar to the present one for the primary alcohols. It was found in the present study that zeolite 4A is more active than zeolite ZNa in the dehydration of ethanol. The low activity of ZNa may be due to its low basic strength, making the abstraction of hydrogen atom on β -carbon very difficult. It therefore suggests that the dehydration of alcohol on zeolites takes place by an acid-base mechanism. However

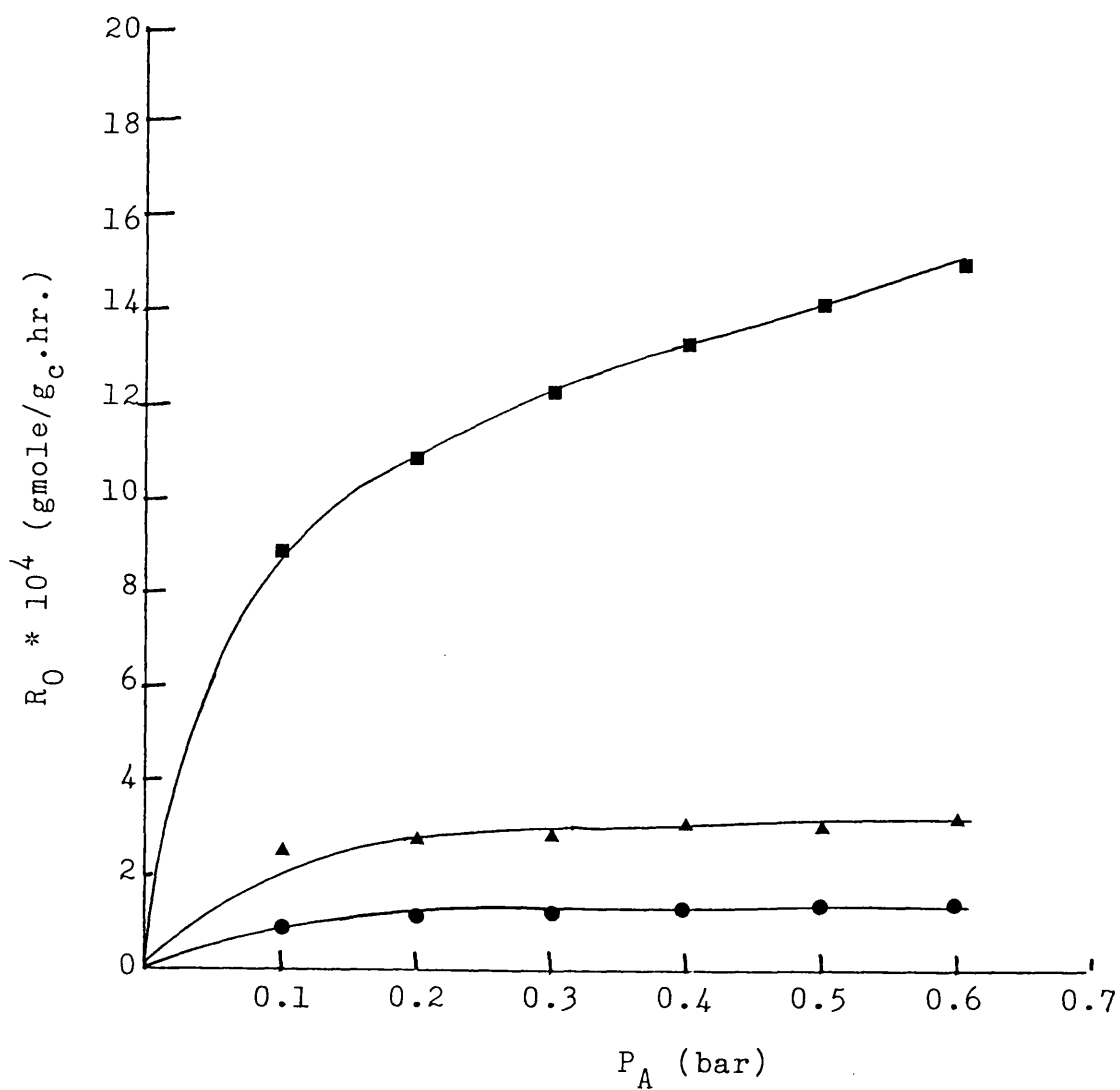


Fig. 5.8 The Effect of A Family of Zeolites.

The dehydration of n-butanol at 280°C

13X (■) 4A (▲) ZNa (●)

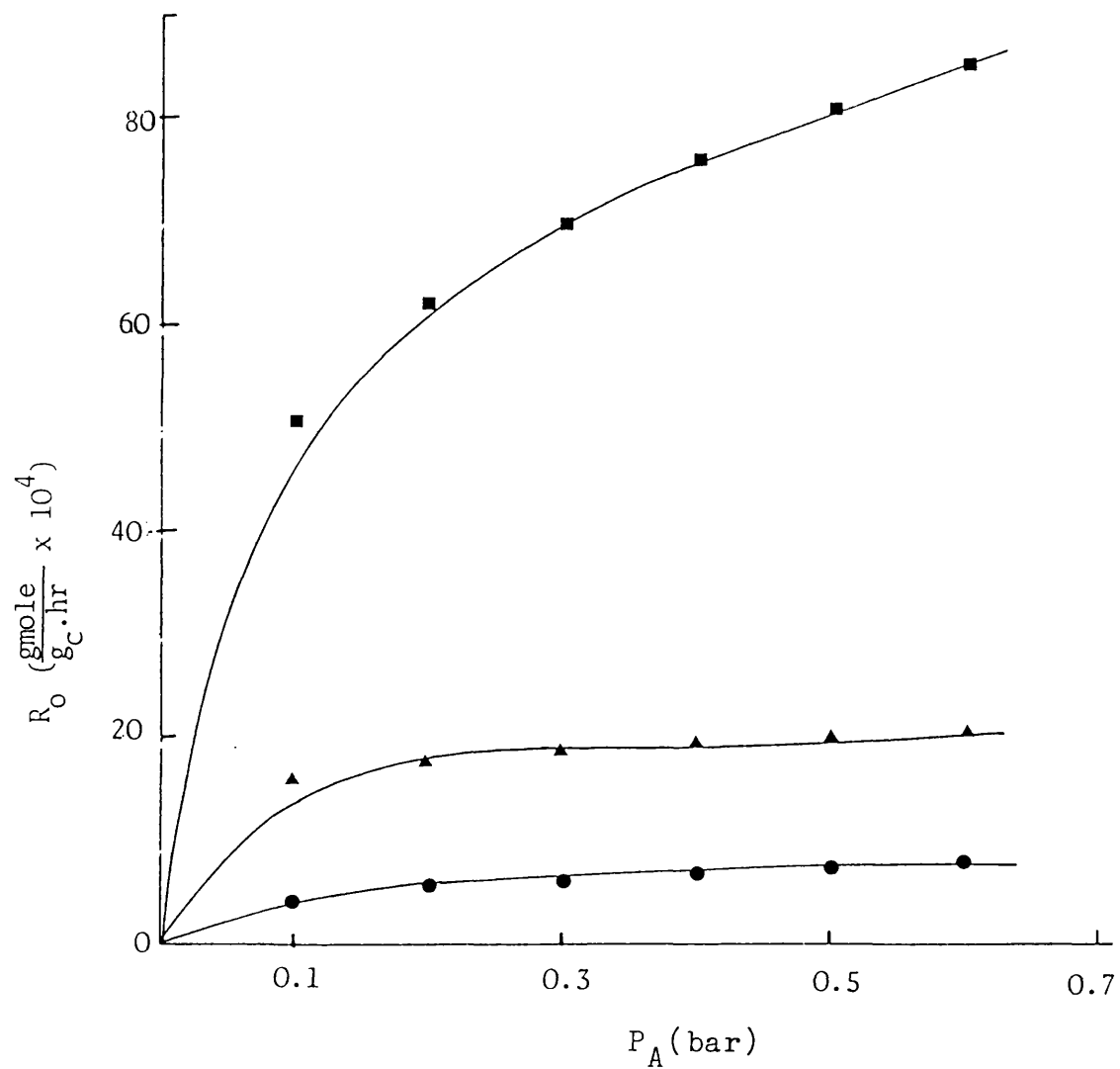


Fig. 5.9 The Effect of A Family of Zeolites.

The dehydration of isopropanol.

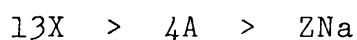
13X(■), ZNa (▲), 4A (●).

the effect of the basic sites dominates in the dehydration of n-butanol thus shifting the mechanism towards E1 type. This has been fully discussed in section 5.1.

The sequence for the primary alcohols does not correspond to that obtained for the isopropanol. In the latter case, zeolite ZNa was found to be more active than 4A. One probable explanation is that of internal diffusional effects on isopropanol in the zeolite 4A cavities. The diffusion of a branched chain alcohol is restricted in zeolite 4A, which has the smallest cages, while that of straight chain alcohols is relatively easier.

Examining the relation between the catalytic activity and the acidity strength of the catalysts suggests that there is an optimum $\text{SiO}_2/\text{Al}_2\text{O}_3$ at which the rate of dehydration of n-butanol or isopropanol is highest. The observed trend in the present study agrees with that given by Topchieva and Thoang (64, 65). Catalytic activity has also been correlated with acidity of the catalyst (43). Further work is required for a vigorous determination of the optimum acid strength for the dehydration of alcohols.

The sequence of the activation energy for the dehydration of alcohols over zeolites 13X, 4A and ZNa (tables 4.2, 4.5 and 4.7) is

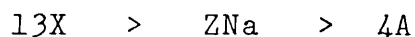


A similar sequence was found for the dehydration of ethanol

over these catalysts (44). The main reason for lower activation energy for ZNa is due to more co-ordinative interaction between the reactant and the catalyst because of high acidic strength. Activation energy is a function of the bond between the reactant and the catalyst. If a reactant is too strongly adsorbed, it depresses the rate of the reaction. But if a reactant is weakly adsorbed the reaction rate may be low.

The order of activity here does not correspond to the order of increasing activation energy or pre-exponential factor. Activation energy or pre-exponential factor estimated for the dehydration of isopropanol to form propene over ZNa is smaller than that calculated for the same reaction and under the same reaction conditions for 4A. Table 4.3 presents the results. This indicates that activation energy or pre-exponential factor is not very useful for comparing the activities of catalysts. Activation energy or pre-exponential factor could only be used if the plots of $\ln K_R$ versus $1/T$ pass through the same intercept or are parallel.

The sequence of activity of the zeolites in the production of ethers from n-butanol and isopropanol is



This order corresponds exactly to the sequence of the cage size. The significance of geometrical and molecular shapes on the production of ether will be discussed in the next sections 5.3.1 and 5.3.2.

5.3 Selectivity.

Product selectivity in multiple reactions is important industrially. Selectivity is an essential aspect of catalyst development and plays an important role in the selection of reaction conditions. Optimising product selectivity can lead to increase in process efficiency and product yield. Selectivity in catalysis has been reviewed in (95, 96, 97, 98).

5.3.1 Geometrical Shape Selectivity.

The selectivity of the simultaneous dehydration reactions is defined as the ratio of rates of formation of olefin to that of ether.

$$S = R_O/R_E$$

In the present study, selectivity was found to decrease with increasing alcohol partial pressure over all the catalysts, as shown in figure 5.10 and 5.11. This behaviour suggests that the dehydration reaction does not proceed according to a consecutive reaction scheme. If the latter had been the case, experiments using low reactant concentrations should have favoured the intermediate product ether.

The importance of cage size is clearly shown by the influence of the zeolites on selectivity. Zeolite 13X with the biggest cages has the lowest selectivity, while zeolite 4A with the smallest cages has the highest selectivity.

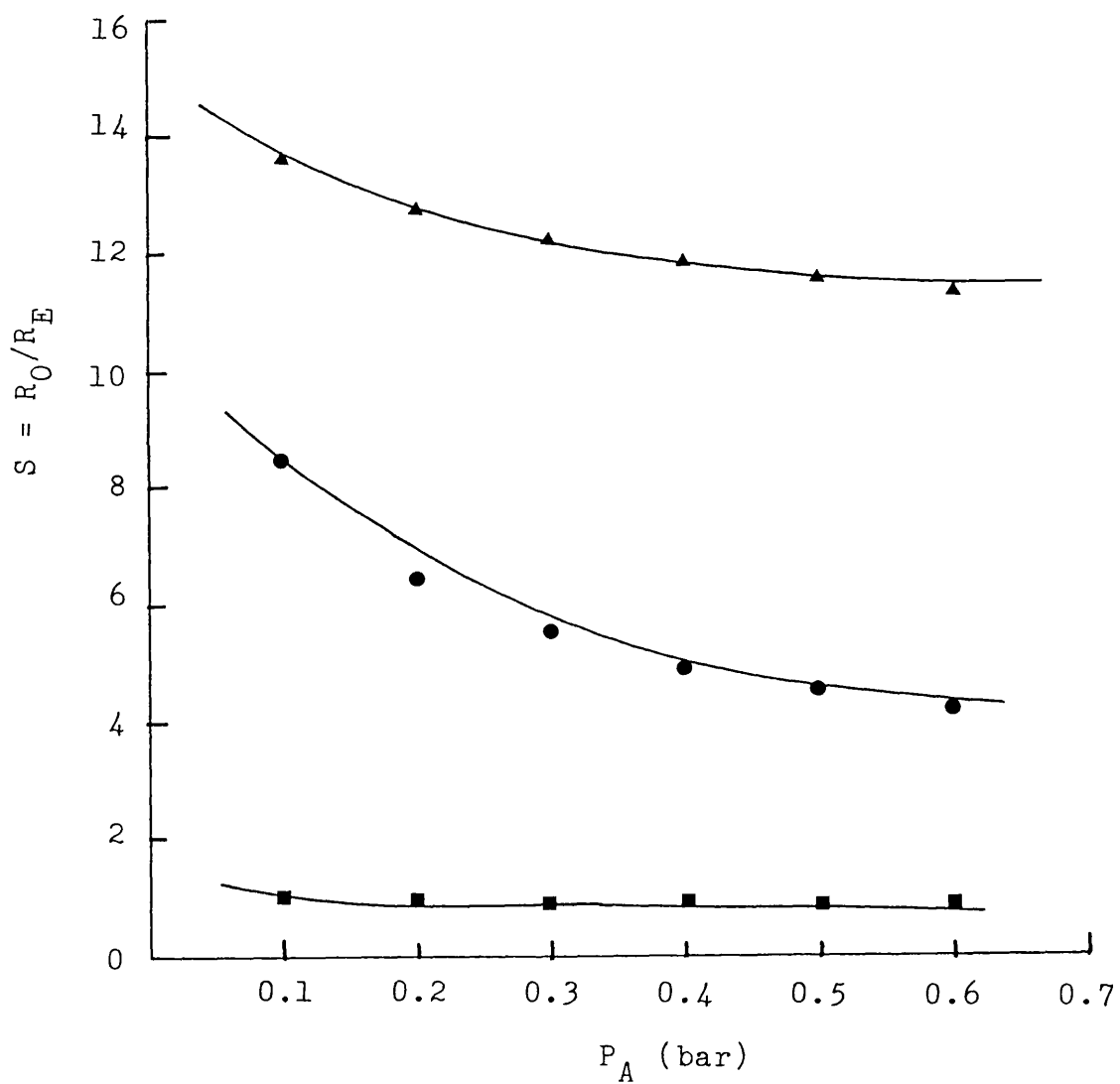


Fig. 5.10 The Effect of Partial Pressure on Selectivity.

The dehydration of n-butanol at 280°C.

4A (\blacktriangle) ZNa (\bullet) 13X (\blacksquare).

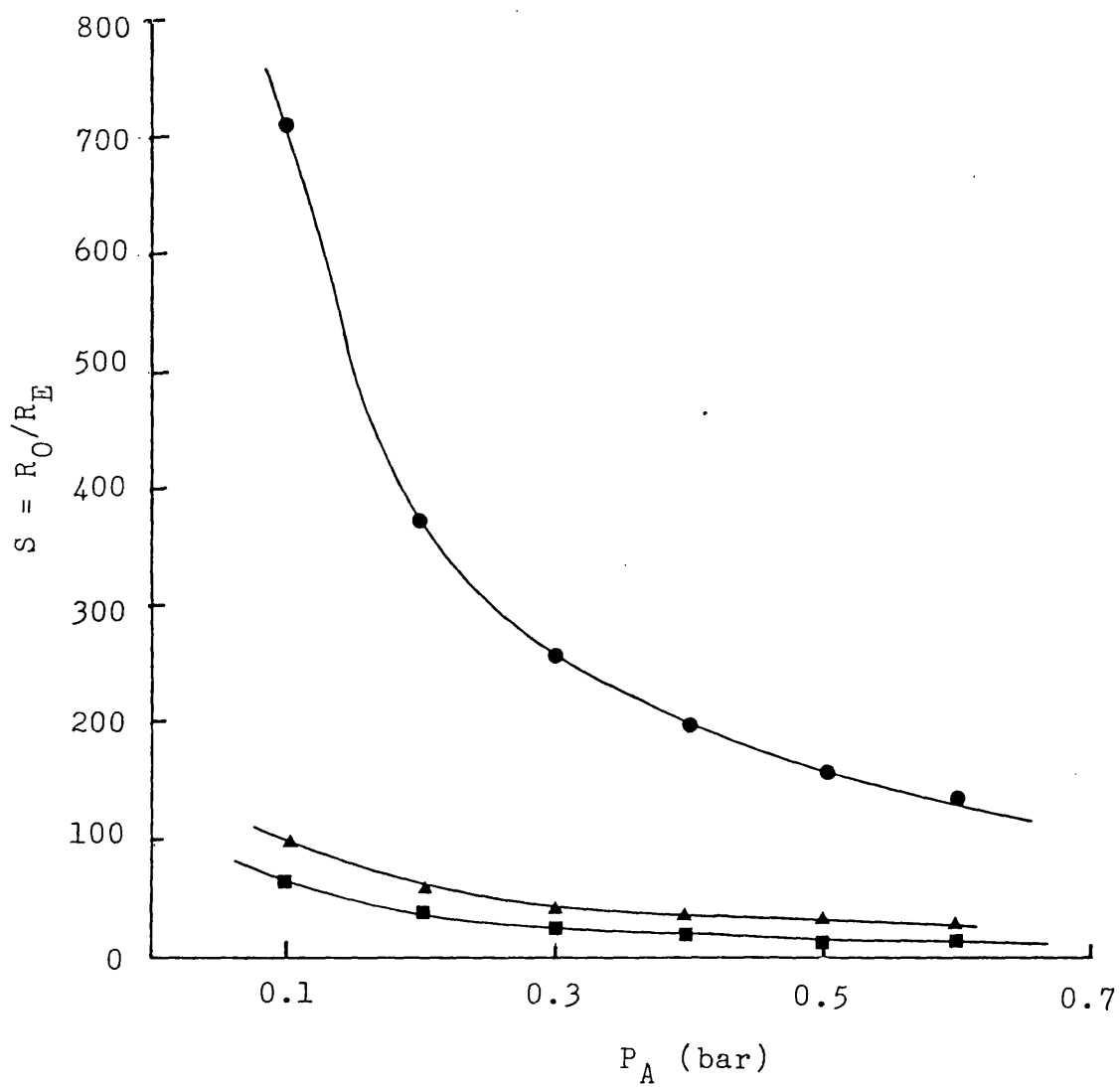


Fig. 5.11 The Effect of A Family of Zeolites on Selectivity.

The dehydration of isopropanol

13X (■) ZNa (▲) 4A (●).

ZNa which has an intermediate cage size has a selectivity between that of 13X and 4A. The selectivity under discussion is based principally on geometric factor. The trend discussed above, has been observed by Bryant and Kranich (44) and Weisz et al (87, 88, 89).

The influence of pore size on selectivity suggests that the orders of the simultaneous dehydration reactions are not the same for all the zeolites. Otherwise, the the concentration changes within the catalyst would have had no effect on selectivity.

The experimental results suggest that non-porous catalysts or those with large pores favour the production of ether, while those with smaller pores favour the formation of olefin. To achieve high selectivity for olefin, smaller pore catalyst is recommended. It should however be noted that a gain on selectivity may be offset by lower reaction rates.

5.3.2 Molecular Shape Selectivity

Weisz et al (87) have established molecular shape selectivity by dehydrating iso-butanol and n-butanol over zeolite 5A. Iso-butanol was hardly converted, while n-butanol dehydration proceeded rapidly.

Since the dehydration of n-butanol, isopropanol and ethanol over zeolites has been investigated in this work,

the influence of 'molecular shape' on selectivity can be established. The significance of product structure on selectivity is demonstrated in figures 5.10 and 5.11. The rate of production of di-iso-propyl ether over the zeolites was the lowest because this ether has the bulkiest structure. Molecular shape which is connected with intra-diffusional limitations and thermodynamic effects are possible factors that can explain this observation. The former effect plays a considerable role, because di-iso-propyl ether cannot diffuse easily even in the large cages of zeolite 13X. The alignment difficulties of the four methyl groups prevents easy diffusion out of the cages of the zeolites. The formation of di-iso-propyl ether over 4A is due to be the presence of active sites on the external surface, because the zeolite 4A cages are not accessible to di-iso-propyl ether. The presence of active sites on the external surface of zeolite 4A and others has been used to explain the formation of bulky molecules (2). The present results show that the straight chain ethers can move faster than branched chain ethers out of the cages of the zeolites.

Thermodynamically the formation of di-iso-propyl ether is least favoured. This is evident from the dependence of the thermodynamic equilibrium constant on the inverse of absolute temperature. Figure 1.2 illustrates

that the formation of di-n-butyl ether is thermodynamically favoured over that of di-ethyl ether. However the experimental results in tables A4.2 and A4.15 show that di-ethyl ether is produced more readily than di-n-butyl ether. This is because the diffusion of ether with longer chain length is more restricted within the zeolite cages. Molecular shape selectivity is therefore evident in the dehydration of n-butanol, isopropanol and ethanol.

5.3.3 Thermal Selectivity

Olefin selectivity was found to increase with increasing temperature. Figure 5.12 illustrates this influence which is called thermal selectivity. The results are in agreement with the shift in equilibrium conversion with increasing temperature.

The results show that the selectivity over zeolite 4A or ZNa shows stronger dependence on reaction temperature than the selectivity over zeolite 13X. This can be explained by the internal diffusional limitations on ether in zeolite type A or Z. Similar influence of reaction temperature has been observed and discussed by Bryant and Kranich (44).

The experimental observations suggest higher temperature should be used for the production of olefin and lower temperature for the production of ether.

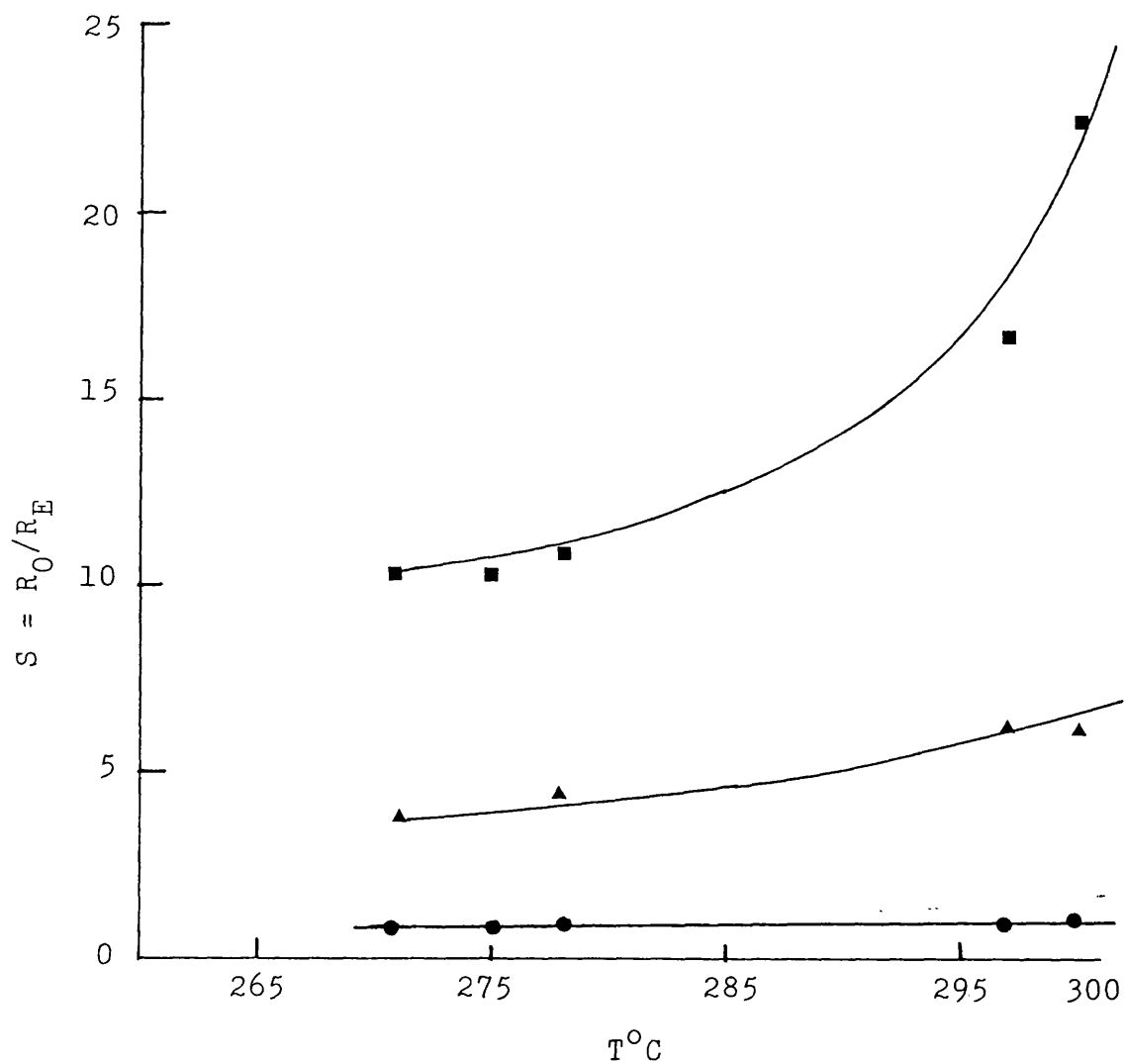


Fig. 5.12 Effect of Temperature and Catalyst Type on Selectivity.

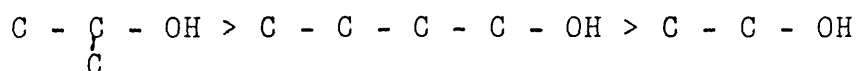
The dehydration of n-butanol

4A (■) ZNa (▲) 13X (●).

5.4 Reactivity of Alcohols

The alcohols studied belong to two different families. 1-Butanol and ethanol are primary alcohols, whereas isopropanol is a secondary alcohol. So far, nothing has been reported in the literature on this combination of alcohols. It is not yet clear whether a branched chain alcohol with n carbon atoms is more reactive than a straight chain alcohol with $n + 1$ carbon atoms. The present investigation therefore, provides experimental evidence to support theoretical predictions on the degree of reactivity of these alcohols.

As discussed previously, the rate of reaction was selected as the most useful variable for comparing the reactivity of reactants or the activity of catalysts. Figure 5.13 shows the effect of dehydrating *n*-butanol, isopropanol and ethanol over zeolite 4A. A similar trend was observed over zeolite 13X or ZNa. Thus the order of reactivity of alcohols is

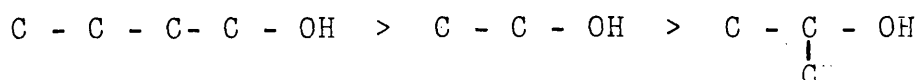


It is well known that longer chain alcohol is more reactive than shorter chain alcohol (11, 73) and branched chain alcohol is more reactive than straight chain alcohol (11, 62, 63).

The high reactivity of isopropanol is due to the effect of the substituted methyl groups on the hydroxyl group attached to the first or α -carbon atom. The reactivity of *n*-butanol is greater than that of ethanol because of the

effects of long alkyl group. Investigation on the elimination of haloalkane over TiC oxide catalyst revealed the same reactivity trend (11).

The sequence of the estimated activation energy is



for all the zeolites used. This order shows that the activation energy increases with alkyl chain length in primary alcohols and decreases with branched alcohol. The activation energy corresponds to the order of decreasing acidity of the hydrogen atom on β -carbon atom. It suggests that the abstraction of the hydrogen atom from the β -carbon atom is the rate determining step of the activated complex state. This has also been used to explain the different activities of the zeolites in section 5.2. A similar trend has been observed for the dehydration of primary alcohols (74), or primary, secondary and tertiary alcohols (11) and elimination of haloalkanes over TiC oxide catalyst (11). Stauffer and Kranich (73) found that activation energy is practically independent of alcohol chain length. The present results do not support this conclusion.

The present observation indicates that the most reactive alcohol has the least activation energy, while the least reactive has an intermediate activation energy. Thus demonstrating why activation energy is not a useful variable for comparing reactivity. The reactivity and activation

sequences can be explained by an inductive effect.

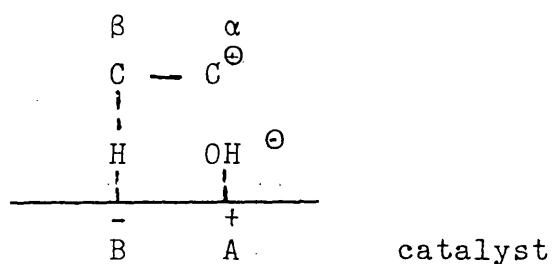
Consider the aliphatic alcohols, the alkyl chain length has two effects on the abstraction of hydroxyl group from α -carbon atom and hydrogen atom from β -carbon atom. The inductive effect of the alkyl chain length decreases the electron density of the hydroxyl group favours strong interaction between the hydroxyl group and acidic sites on the catalyst surface, which probably leads to alcohol dissociation.

The reaction mechanism for the dehydration of alcohol to form olefin may therefore be E1 type. It is also consistent with the shift in mechanism from E2 to E1 type when the reactant changes from shorter chain alcohol to longer chain alcohol or primary to tertiary alcohols. The kinetic analysis in chapter 4 also suggests that the dehydration of alcohol to olefin proceeds according to ionic mechanism. The product distribution of the alkenes from the dehydration of n-butanol over zeolites 4A and ZNa has demonstrated that the dehydration of n-butanol to butenes takes place according to E1-mechanism. In the case of the dehydration of n-butanol to olefin over zeolite 13X, the mechanism is E1 type, however E2 type mechanism cannot be precluded entirely.

Alkyl chain length also decreases the acidity strength of the hydrogen atom on the β -carbon atom. The higher the acidity, the lower the energy is required for the abstraction of the hydrogen atom from the β -carbon by the

basic site on the catalyst surface. Hence longer alkyl chain length results in higher activation energy. This is indeed the case found in the present study.

The proposed transition state may therefore be represented as



This proposed transition state requires two sites, basic and acidic. This is consistent with the dual site mechanism of the Hougen-Watson rate expression which has been found to correlate the present kinetic data on the dehydration of alcohols to olefins over zeolites satisfactorily.

It can be hypothesised that the dehydration of alcohols to olefins over zeolites requires an intermediate adsorbed species in which an alcohol molecule is probably bonded to both acidic and basic sites. The present results show that E1 type reaction mechanism is favoured because the acidic sites are stronger than the basic sites. However, both sites are still required for the dehydration reaction to olefin.

De-Mourgues et al (102) have concluded that acid sites are definitely involved in the dehydration of isopropanol over oxide catalysts but basic sites help the reaction. The present work supports this conclusion. Experimental data of Topchieva and Tkhoang (64) show that the dehydration of

isopropanol over both zeolites and alumino-silica gels occurs by an acid-base mechanism. Dzisko et al (59) suggested that the dehydration of isopropanol is entirely a function of the acidic strength of the catalysts. This suggestion is not supported by the present experimental results.

Compensation effect is exhibited by the family of zeolites (13X, 4A and ZNa) used in the dehydration of primary alcohols and isopropanol. Figure 5.14, a plot of $\ln A_0$ versus E_A , shows that two parallel lines can be drawn. The first straight line passes through the points connecting all the primary alcohols for the family of zeolites, while the second straight line connects the points for isopropanol for the same catalysts.

The following expressions have been deduced from a linear squares analysis

for primary alcohols: $\ln A_0 = -12 + 1.04 E_A$
with R-squared value of 100%.

for isopropanol: $\ln A_0 = -8 + 1.000 E_A$
with R-squared value of 96%

It is evident from these relationships that the straight lines are indeed parallel. The slope of 1.0 probably suggests a mechanism involving one hydroxyl group for the formation of olefin.

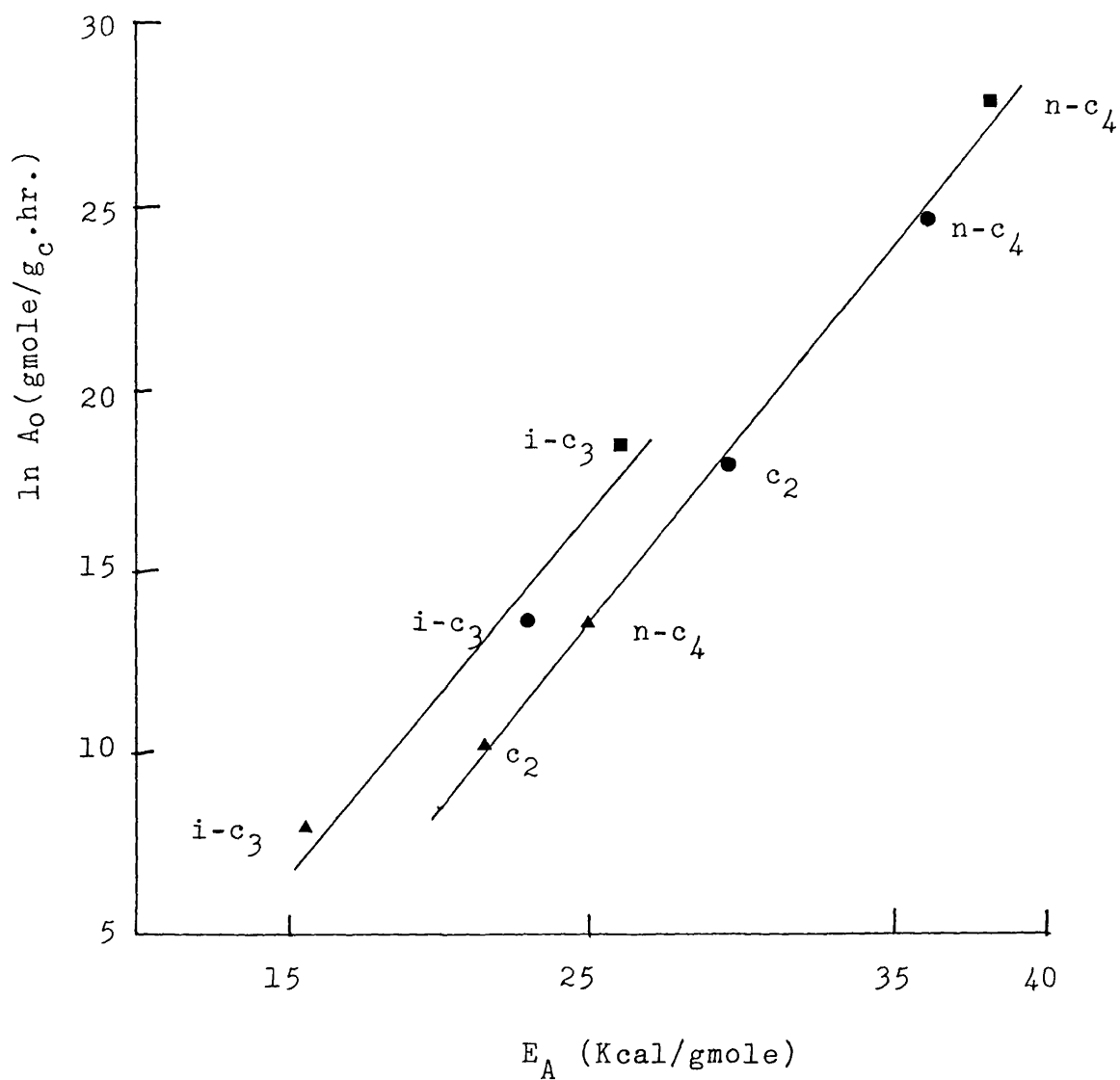


Fig. 5.14 The Compensation Effect.

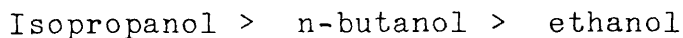
The dehydration of primary and secondary alcohols over a family of zeolites.

13X (■) 4A (●) ZNa (▲).

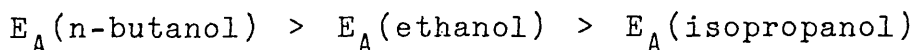
5.5 Conclusions

- a) The percentage distribution of butenes (1-butene, cis-2-butene and trans-2-butene) was found to be practically independent of the partial pressure of n-butanol at a given reaction temperature.
- b) 'Cis preference' was observed on zeolites 13X and ZNa.
- c) The dehydration of n-butanol to butenes over the zeolites used was found to proceed through E1 mechanism, although E2 type mechanism cannot be precluded entirely for the case of zeolite 13X.
- d) The predominance of E1 type mechanism increases with increasing reaction temperature.
- e) The sequence of activity for the dehydration of straight chain alcohols is
- $$13X > 4A > ZNa$$
- for branched chain alcohol is
- $$13X > ZNa > 4A$$
- The activity pattern of the zeolites was explained in terms of the surface area, crystalline pore size and acid and base strengths.
- f) The influence of crystalline pore size on selectivity has been clearly demonstrated.
- g) Molecular shape selectivity is demonstrated by the dehydration of isopropanol, n-butanol and ethanol.

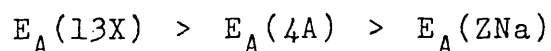
h) The pattern of reactivity of the alcohols is



i) The sequence of the activation energy for the dehydration of isopropanol, n-butanol and ethanol over the zeolites investigated is



j) The order of activation energy for the dehydration of alcohol over the zeolites used is



k) Compensation effect expressions are proposed which can correlate the activation energy and pre-exponential factor for the dehydration of primary alcohols (n-butanol and ethanol) and isopropanol over the zeolites examined.

l) It is proposed that the dehydration of alcohols to olefins proceeds through an intermediate species in which the hydroxyl group is bounded to an acidic site and the hydrogen on β -carbon is attached to the basic site, (acid-base mechanism). However, the effect of the acidic site predominates, hence leading to complete abstraction of hydroxyl group on the acid site. The rate determining step of the activated transition state is the abstraction of hydrogen atom from the β -carbon. The present proposal satisfactorily explains the activity and activation energy sequences.

CHAPTER 6

MODELLING OF CATALYTIC BED REACTOR

CHAPTER 6MODELLING OF CATALYTIC PACKED BED REACTOR6.1 Introduction

Many catalytic chemical reactions of industrial importance are performed in fixed bed reactors. In the last two decades, the design of tubular packed bed reactor has been extensively studied. According to Froment (60), the mathematical description of continuous fixed bed reactor at steady state can be classified as shown in table 6.1.

Table 6.1 Classification of Packed Bed Reactor Models

		Models	
		Pseudo-Homogeneous	Heterogeneous
		$T = T_s; C = C_s$	$T \neq T_s; C \neq C_s$
One dimensional	A1	Ideal plug flow	B1 A1 + gradients at the phase boundary of catalyst pellet.
	A2	A1 + axial dispersion term	B2 B1 + axial dispersion
Two dimensional	A3	A1 + radial dispersion term	B3 B1 + radial dispersion term
	A4	A3 + axial dispersion term	B4 B3 + axial dispersion term

The advantages and disadvantages of these models have been fully discussed in (60, 106).

In this work, the pseudo-homogeneous models are used because of their simplicity and the substantially shorter time required for computing. The rate expressions which satisfactorily correlate the kinetic data on the dehydration of isopropanol over 13X was chosen as the basis for simulating conversion in a fixed bed reactor. Experimental work was undertaken using an integral fixed bed reactor. This provided conversion data for comparison with the simulated results of conversion. The present chapter shows the comparison between the mathematical simulation and the experimental data. The comparison should give some indication on the usefulness of the rate expressions obtained in chapter 4 for fixed bed reactor design.

6.2 Mathematical Description of Catalytic Packed Bed Reactor.

A cylindrical packed bed reactor with continuous plug flow of gaseous reactants is considered here. The catalyst pellets are taken as point sources within the reactor. Both axial and radial variations of concentration and temperature are to be evaluated, giving rise to a two dimensional pseudo-homogeneous model. The following assumptions are taken in order to make the model as simple as possible.

a) The effective diffusivities of heat and mass in the radial and axial directions throughout the reactor length are averaged.

- b) The heat transfer co-efficient and temperature at the wall throughout the entire bed length are taken to be constant.
- c) An average bed porosity is assumed.
- d) Heat capacity and heat of reactions, fluid density, velocity and mean molecular weight throughout the bed length are taken to be constant.
- e) Although the catalyst activity may vary with time and axial position. Such variations are neglected.

The steady state material or energy balance consists of four terms: longitudinal bulk flow, radial dispersion, axial dispersion and a reaction term. The transient behaviour of packed bed reactor have been extensively discussed by Kobayashi and Kobayashi (63) and Balmer et al (68) but is not considered in this work. At steady state, the mass and energy balances, in the dimensionless form, for component, i , in the reaction fluid in a cylindrical tubular packed reactor, according to two-dimensional pseudo-homogeneous model with axial mixing are as follows:

Mass balance

$$\frac{\partial Y_i}{\partial Z} - \frac{a_1}{X} \frac{\partial}{\partial X} \left(X \frac{\partial Y_i}{\partial X} \right) + b_1 \frac{\partial^2 Y_i}{\partial Z^2} = C_1 \beta_i R_i \quad 6.1$$

Energy balance

$$\frac{\partial \theta}{\partial Z} - \frac{a_2}{X} \frac{\partial}{\partial X} \left(X \frac{\partial \theta}{\partial X} \right) + b_2 \frac{\partial^2 \theta}{\partial Z^2} = C_2 \sum_{i=1}^n \beta_i \Delta H_i R_i \quad 6.2$$

with boundary conditions

$$\text{at } Z = 0; Y_i = 0.0; \theta = 1.0; 0 \leq X \leq 1.0$$

$$\text{at } X = 0; \frac{\partial Y_i}{\partial X} = \frac{\partial \theta}{\partial X} = 0.0 \quad 0 \leq Z \leq 1.0$$

$$\text{at } X = 1.0; \frac{\partial Y_i}{\partial X} = 0.0; \quad \frac{\partial \theta}{\partial X} = B_i(\theta - \theta_w) \quad 0 \leq Z \leq 1.0$$

where $Y = C/C_0$; $\theta = T/T_0$; $Z = l/l_0$; $X = 2r/d_t$

R_i is in the dimensionless form, given by

$$R_i = R_i(Y_1, Y_2, Y_3, \dots, Y_n, \theta)$$

$$a_1 = \frac{4d_p l_0}{d_t^2 Bo_{m,r}} \quad a_2 = \frac{4d_p l_0}{d_t^2 Pe_{h,r}}$$

$$b_1 = \frac{d_p}{l_0 Bo_{m,a}} \quad b_2 = \frac{d_p}{l_0 Pe_{h,a}}$$

$$c_1 = \frac{l_0 R_g T_0 \rho_b}{UP A_0} \quad c_2 = \frac{l_0 \rho_b}{G_m C_p T_0}$$

$$B_i = \alpha_w d_t / 2\lambda_{e,r} \quad \beta_i = \beta(K_{Ri}, K_{Ai}, P_{A0})$$

where $Bo_{m,r}$ and $Bo_{m,a}$ are the Peclet numbers for the radial and axial effective diffusions, respectively and $Pe_{h,r}$ and $Pe_{h,a}$ are the Peclet numbers for the radial and axial effective conductivities. They are given by

$$Bo_{m,r} = Ud_p / D_{e,r} \quad Bo_{m,a} = Ud_p / D_{e,a}$$

$$Pe_{h,r} = \frac{G_m C_p d_p}{\lambda_{e,r}} \quad Pe_{h,a} = \frac{G_m C_p d_p}{\lambda_{e,a}}$$

6.3 Chemical Reaction Rates, R_i .

The modelling of the catalytic dehydration of alcohols has been discussed in chapter 3. The analyses of results and the discrimination of rate expressions have been discussed extensively in chapter 4. The rate equations based on a simultaneous reaction scheme, with surface reaction as the rate controlling step, have been found to satisfactorily correlate the kinetic data on the dehydration of isopropanol to propene and di-iso-propyl ether. The equations are given by

$$R_O = \frac{K_{RO}K_{AO}P_{AO}(1.0 - 2X - Y)}{(1.0 + P_{AO}K_{AO}(1.0 - 2X - Y))^2} \quad 6.3$$

$$R_E = \frac{K_{RE}K_{AE}^2P_{AO}^2(1.0 - 2X - Y)^2 - (y + X)Y/K_{eq,E}}{(1.0 + P_{AO}K_{AE}(1.0 - 2X - Y))^2} \quad 6.4$$

where $X = P_E/P_{AO}$ and $Y = P_O/P_{AO}$.

The variation of the co-efficients K_{RE} , K_{RO} , K_{AE} , K_{AO} and $K_{eq,E}$ with temperature have been determined by linear regression analysis within the temperature range studied. Table 4.7 summarises the values of estimated parameters in the Arrhenius and Van't Hoff equations.

6.4 Solution of the Mathematical Model.

The two-dimensional pseudo-homogeneous model for the catalytic dehydration of isopropanol to form propene and di-iso-propyl ether yields a set of three non-linear parabolic partial differential equations, PDE, with three sets of boundary conditions, two for the mass balance, one for each component and one for the energy balance.

The experimental data used here for testing the model have been gathered in an isothermal laboratory reactor. The wall temperature was maintained constant by means of circulating air. The wall temperature throughout the bed length can be considered constant. The thermocouples located at the top and bottom of the bed showed essentially the same temperature. Therefore the reactor was taken to be under isothermal conditions. The isothermal models were solved so that the results are compared with predictions.

6.4.1 Ideal Plug Flow Model.

The model assumes that the effects of the axial and radial dispersion terms are not significant. The resulting model is given by

$$\frac{dY}{dZ} = C_1 \beta_O R_O(Y_O, Y_E) \quad 6.5$$

$$\frac{dY}{dZ} = C_1 \beta_E R_E(Y_O, Y_E) \quad 6.6$$

where β_0 and β_E are given by

$$\beta_0 = K_{RO} K_{AO} P_{Ao} \quad 6.7$$

$$\beta_E = K_{RE} K_{AE}^2 P_{Ao}^2 \quad 6.8$$

It can be seen that the model consists of a set of first order ordinary differential equations with initial values given by

$$\text{at } Z = 0 \quad Y_0 = Y_E = 0 \quad 6.9$$

The equations were solved using the fourth order Runge - Kutta - Merson method (58). The truncation error incurred is $16/15 (Y_{n+1,h} - Y_{n+1,h/2})$, where h is the step size.

6.4.2 One-Dimensional Plug Flow with Axial Dispersion Term

This model assumes that the effect of the radial term is not important. The resulting expressions are

$$\frac{dY_0}{dZ} + b_2 \frac{d^2 Y_0}{dZ^2} = C_1 \beta_0 R_0(Y_0, Y_E) \quad 6.10$$

$$\frac{dY_E}{dZ} + b_2 \frac{d^2 Y_E}{dZ^2} = C_1 \beta_E R_E(Y_0, Y_E) \quad 6.11$$

Initial boundary conditions are

$$\text{at } Z = 0, \quad Y_0 = Y_E = 0.0 \quad 6.12$$

$$\frac{dY_0}{dZ} = \frac{dY_E}{dZ} = 0.0 \quad 6.13$$

The model yields a set of second order ordinary differential equations. The solution was obtained by converting them to a set of first order ordinary differential equations by substitution.

$$\text{Let } \frac{dY_0}{dZ} = W \quad 6.14$$

$$\text{and } \frac{dY_E}{dZ} = X \quad 6.15$$

Equations 6.11 and 6.12 become

$$\frac{dY_0}{dZ} = W \quad 6.16$$

$$b_2 \frac{dW}{dZ} = -W + C_1 \beta_0 R_0(Y_0, Y_E) \quad 6.17$$

$$\frac{dY_E}{dZ} = X \quad 6.18$$

$$b_2 \frac{dX}{dZ} = -X + C_1 \beta_E R_E(Y_0, Y_E) \quad 6.19$$

Initial boundary conditions are

$$\text{at } Z = 0, \quad Y_0 = Y_E = W = X = 0 \quad 6.20$$

The solution of the four simultaneous first order ordinary differential equations was again obtained by Runge-Kutta-Merson method.

6.4.3 Two-Dimensional Pseudo Homogeneous Model

This model accounts for the effect of the radial dispersion term. However the influence of the axial dispersion term has been neglected. The solution of the last model reveals that the axial dispersion term has practically no effect on the concentration profile. The mathematical expressions are

$$\frac{\partial Y_0}{\partial Z} - \frac{a_1 \partial}{X \partial X} \left(X \frac{\partial Y_0}{\partial X} \right) = C_1 \beta_0 R_0(Y_0, Y_E) \quad 6.21$$

$$\frac{\partial Y_E}{\partial Z} - \frac{a_1 \partial}{X \partial X} \left(X \frac{\partial Y_E}{\partial X} \right) = C_1 \beta_E R_E(Y_0, Y_E) \quad 6.23$$

Boundary conditions are

$$\text{at } Z=0 \quad Y_0 = Y_E \quad 6.24$$

$$\frac{\partial Y_0}{\partial X} = \frac{\partial Y_E}{\partial X} = 0 \quad \text{at } 0 \leq X \leq 1.0 \quad 6.25$$

The radial term is expressed in central finite difference form. Therefore the radial term at the grid point (n,m) for component i can be written as

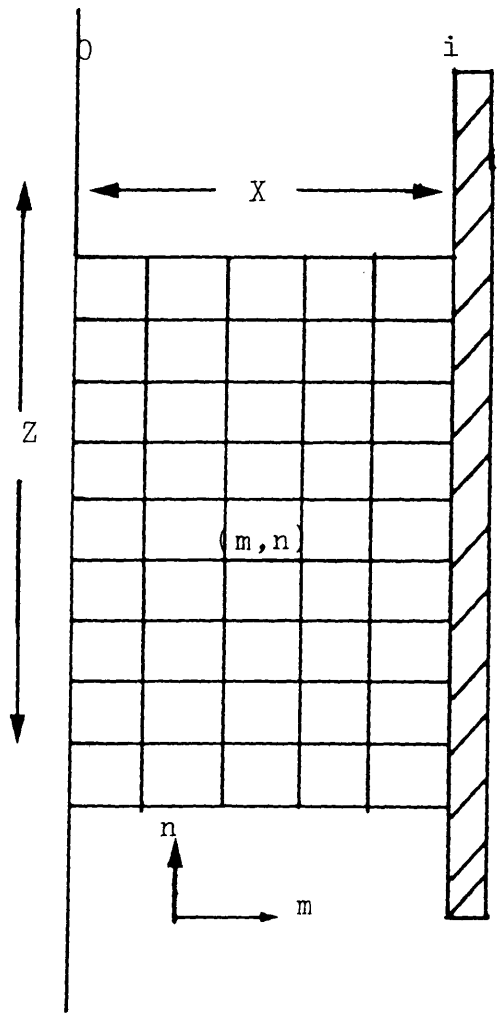


Figure 6.1 Grid Used in Finite Difference

$$\frac{a_1 \partial}{X \partial X} \left(X \frac{\partial Y_i}{\partial X} \right) = \frac{a_1 (Y_{i,n,m+1} + Y_{i,n,m-1} - 2 Y_{i,n,m})}{\Delta X^2}$$

$$\frac{a_1 (Y_{i,n,m+1} - Y_{i,n,m-1})}{\Delta X^2} \quad 6.26$$

Figure 6.1 shows the grid used in the solution of equations 6.21 and 6.23. The truncation errors for the central finite difference formulae for the first and second derivatives at grid point (m,n) are $f''(Y_{i,n,m})\Delta X/2$ and $f^{4'}(Y_{i,n,m})\Delta X^2/12$ respectively. Altogether there are $2(i+1)$ simultaneous ordinary differential equations. They were solved using fourth order Runge-Kutta-Merson integration method.

6.5 Results and Discussion.

The predicted conversions from an isothermal integral catalytic bed reactor were simulated by using pseudo-homogeneous isothermal models.

The solution of the one-dimensional plug flow model with axial dispersion yields practically the same average concentration profile as the one-dimensional ideal plug flow model. This suggests that axial back mixing is insignificant. The ratio of the bed length to the diameter of the particle gives a value which is greater than the ratio suggested for neglecting the axial mass term by Carberry (122).

The solution of the two-dimensional pseudo-homogeneous model yielded essentially the same average conversion profile as the one-dimensional ideal plug flow model. The two-dimensional model gave the average conversion as a function of the radial position at various axial positions. These are practically flat. The flat profile, is probably due to the assumptions of flat inlet concentration and velocity profiles and isothermal conditions considered. The two-dimensional pseudo-homogeneous model is therefore reduced to the one-dimensional ideal plug flow model, because strong heat effects do not exist in the fixed bed reactor.

Only the results from the two-dimensional pseudo-homogeneous isothermal model are presented and discussed. Table A6.1, in appendix 6, shows the comparison between the predictions of the model and the experimental data. Some typical results are presented in Figures 6.2, 6.3 and 6.4. Table A6.2, in appendix 6, shows the values of the estimated parameters used.

The experimental results show fair agreement with the predictions of the model at high temperature, while at low reaction temperatures agreement was poor. The magnitude of the discrepancies between the predicted and the experimental results are not excessive in view of uncertainties in the assumptions made and in the values of the estimated parameters. One important source of uncertainty is the validity of the assumption of isothermal conditions. For example, the

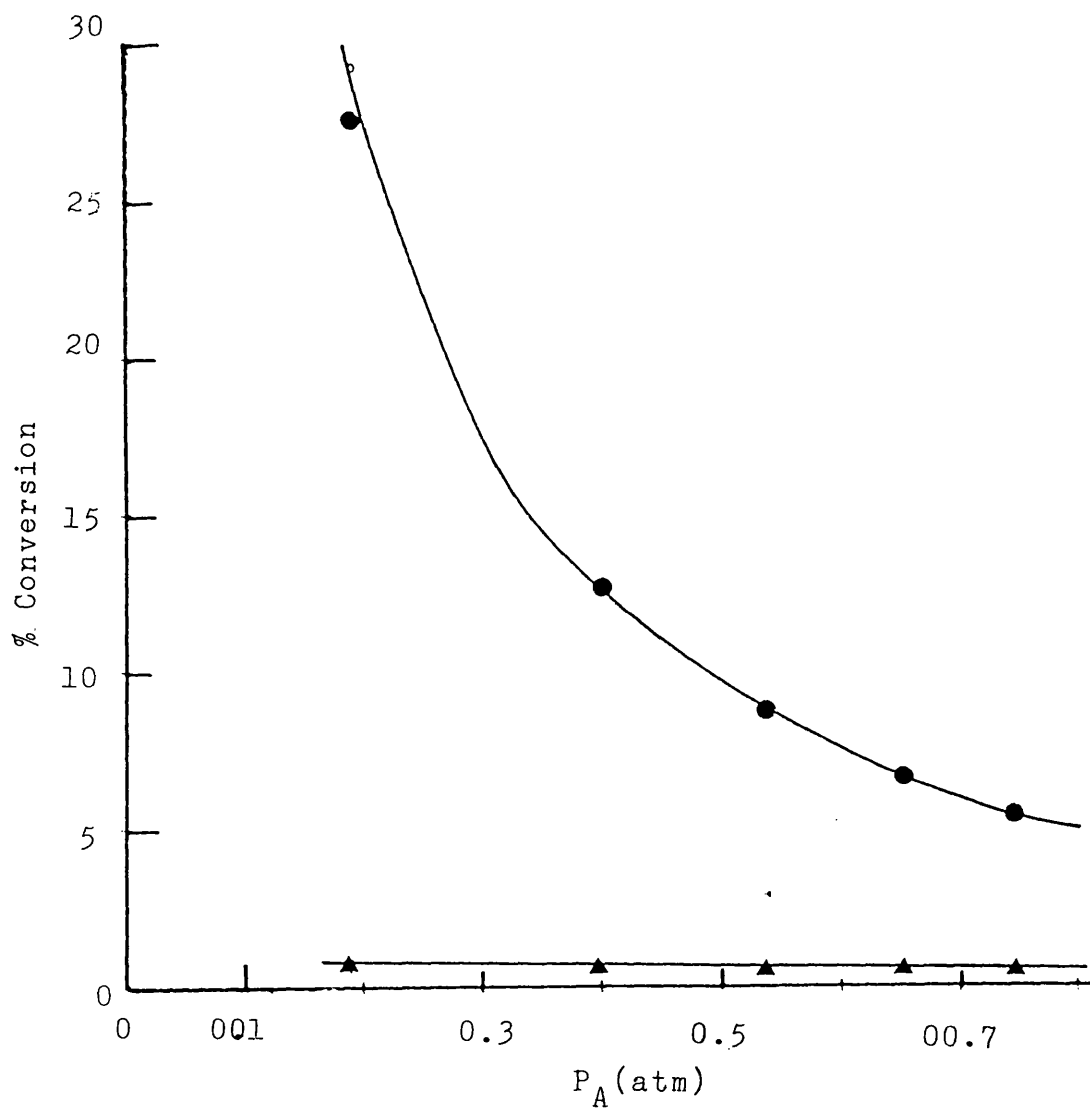


Fig. 6.2 Comparison Between Predicted and Experimental Conversions.

Temp. 268°C ; propene (●) and di-iso-propyl ether (▲).

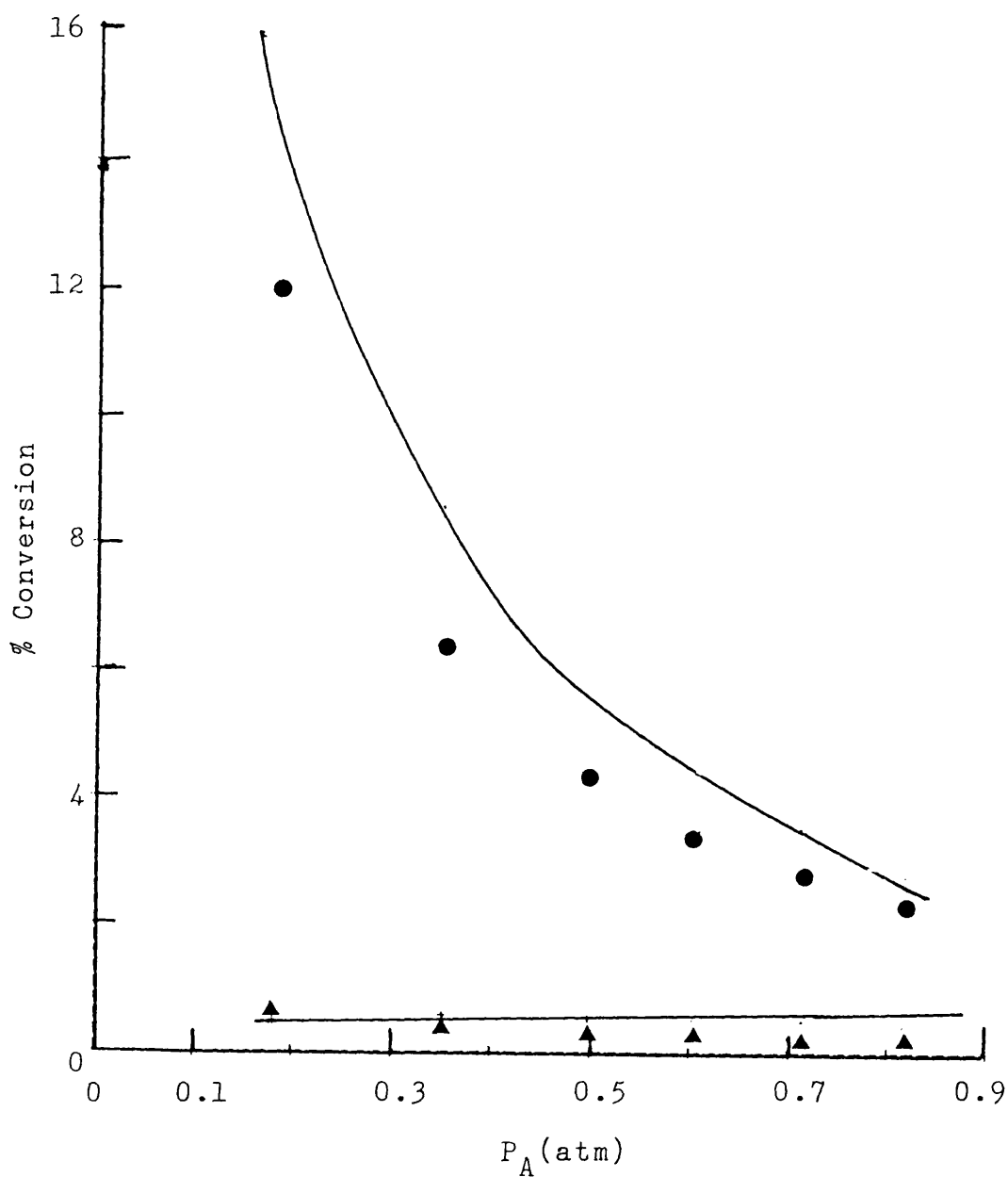


Fig. 6.3 Comparison Between Predicted and Experimental Conversions.

Temp. 254°C ; propene (●) and di-iso-propyl ether (▲).

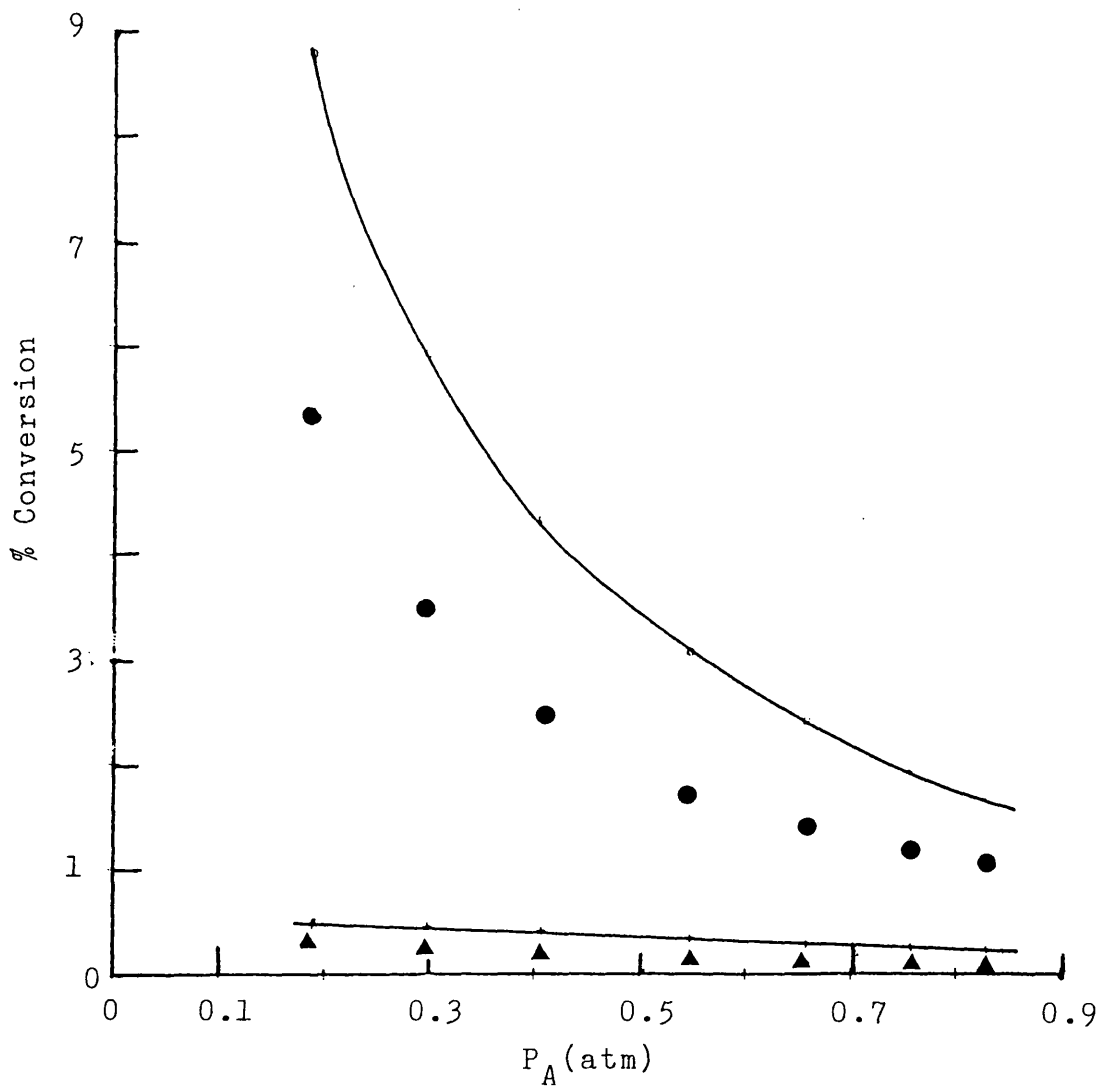


Fig. 6.4 Comparison Between Predicted and Experimental Conversions.

Temp. 242°C; propene (●) and di-iso-propyl ether (▲).

temperature measured by the thermocouple may be higher than that of the bulk of the gas passing through the centre of the reactor, leading to over prediction of conversion.

Smith (66) used the radial dispersion model for theoretical prediction of conversions. Error in the order of 25% were reported between the experimental and predicted average conversions. It has been shown in (66) that poor results may be obtained when incorrect inlet temperature and concentration profiles are used in the radial dispersion model.

The inclusion of temperature effects could be important in testing models more rigorously, especially if the reactions are accompanied with high heat effects. Such study requires a packed bed reactor designed with facilities for measuring the fluid concentration and temperature at various axial and radial positions. Further work is required to test the adequacy of the reaction rate expressions obtained in predicting conversion in a fixed bed reactor. On the whole, the present test of the rate equations may be considered satisfactory in view of the uncertainties in the assumptions.

6.6 Summary.

This chapter discusses the simulation of conversions from an isothermal integral catalytic bed reactor by using pseudo-homogeneous isothermal models and compares the simulated and the experimental conversions.

The predictions of the models at high temperatures agree fairly well with the experimental results, but at low temperatures poor agreement was found. An explanation for this discrepancy is the uncertainties in the assumptions made and in the values of the estimated parameters. Further work is required to test the applicability of the rate expressions in fixed bed reactors.

CHAPTER 7

CONCLUSIONS AND RECOMMENDATIONS.

CHAPTER 7CONCLUSIONS AND RECOMMENDATIONS.7.1 Conclusions.

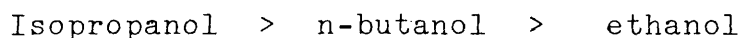
a) The dehydration of n-butanol, isopropanol and ethanol over zeolites 13X, 4A and ZNa yields both olefin and ether. At lower temperatures, using cation exchange resin Dowex 50-X-8 as catalyst, isopropanol dehydrates to propene and di-iso-propyl ether while ethanol gives mainly di-ethyl ether.

b) Empirical power function rate expressions for simultaneous formation of olefin and ether were found to correlate the rate data for both reactions over all the catalysts covering a wide range of alcohol concentrations.

c) The kinetic data have also been satisfactorily correlated by Hougen-Watson type of expressions, equations 4.9 and 4.10 for the formation of olefin and equations 4.11 and 4.12 for the formation of ether, based on surface reaction controlling rate. Kinetic and adsorption parameters in the rate equations have been correlated as functions of reaction temperature.

d) The catalytic activity and product selectivity of the zeolites and activation energies have been found to relate to the acidic strength of catalyst and crystalline pore size.

e) The order of reactivity of the alcohols is:



f) Compensation effect between activation energy and pre-exponential factor has been found for the alcohols and zeolites studied. Empirical correlations have been established to describe this compensation effect.

g) Dehydration of n-butanol over zeolites was found to proceed according to carbonium ion (E1) mechanism with the exception of 13X, where E2 mechanism cannot be precluded.

h) The preferential formation of Cis-2-butene over that of trans-2-butene has been observed over zeolites 13X and ZNa but not zeolite 4A.

i) At a given temperature, the percentage distribution of butenes (1-butene, cis-2-butene and trans-2-butene) was found to be practically independent of the partial pressure of n-butanol.

j) Reaction conditions for the exclusive production of di-ethyl ether over synthetic cation exchange resin have been found.

k) For the dehydration of isopropanol over zeolite 13X, the rate expression obtained from the kinetic analysis was applied to simulate the behaviour of a fixed bed reactor. The simulated results agree fairly well with experimental ones.

7.2 Recommendations.

Further work is required to determine

- a) The exact acid strength of the zeolites and the optimum acid strength for the dehydration of alcohols.
- b) The reaction conditions for the exclusive production of di-iso-propyl ether over cation exchange resin.
- c) The effect of introducing reaction products into the feed on the product distribution of butenes and
- d) The effect of introducing water into the feed.

It is also recommended that the rate expressions obtained be more extensively tested by experimental studies using fixed bed reactors.

APPENDIX 1

HOUGEN-WATSON TYPE RATE EQUATION

Table A1.1 Hougen-Watson Type Chemical Rate Expression.

Formation of ether via Langmuir-Hinshelwood mechanism (LHM)

Controlling Step	Rate Expression	Model No.
Adsorption of alcohol	$\frac{K_{aA}S_0(P_A - (P_W^P/K_{EQ,E})^{\frac{1}{2}})}{1.0 + K_{E^R}P_E + K_{W^P}P_W + (K_A^2/K_{EQ,E^P}P_E^P)^{\frac{1}{2}} + K_{O^P}P_O + K_{I^P}P_I}$	LHM1
Adsorption of alcohol without inert term	$\frac{K_{aA}S_0(P_A - (P_W^P/K_{EQ,E})^{\frac{1}{2}})}{1.0 + K_{E^P}P_E + K_{W^P}P_W + (K_A^2/K_{EQ,E^P}P_E^P)^{\frac{1}{2}} + K_{O^P}P_O}$	LHM2
Adsorption of alcohol without inert term and backward reaction	$\frac{K_{aA}S_0^P P_A}{1.0 + K_{E^P}P_E + K_{W^P}P_W + K_{O^P}P_O + (K_A^2/K_{EQ,E^P}P_E^P)^{\frac{1}{2}}}$	LHM3
Surface reaction (2 active sites)	$\frac{S_0^2 K_R K_A (P_A^2 - P_{E^P} P_{W^P} / K_{EQ,E})}{(1.0 + K_{E^P}P_E + K_{O^P}P_O + K_A P_A + K_{W^P}P_W + K_{I^P}P_I)^2}$	LHM4

Controlling Step	Rate Expression	Model No.
Surface reaction without inert term	$\frac{S_{O_R}^2 K_A^2 (P_A^2 - P_{E,W} P_{EQ,E})}{(1.0 + K_{E,E} P_E + K_{O,P_0} + K_{A,P_A} + K_{W,P_W})^2}$	LHM5
Surface reaction without inert term and backward reaction	$\frac{S_{O_R}^2 K_A^2 P_A^2}{(1.0 + K_{E,E} P_E + K_{O,P_0} + K_{A,P_A} + K_{W,P_W})^2}$	LHM6
Desorption of water	$\frac{K_{aW} S_{O_R} (K_{EQ,E} P_{A,E}^2 - P_W)}{1.0 + K_{O,P_0} + K_{E,E} P_E + K_{A,P_A} + K_{W^{K_{EQ,E}} P_E^2} + K_{I,P_I}}$	LHM7
Desorption of water without inert term	$\frac{K_{aW} S_{O_R} (K_{EQ,E} P_{A,E}^2 - P_W)}{1.0 + K_{O,P_0} + K_{E,E} P_E + K_{A,P_A} K_{W^{K_{EQ,E}} P_E^2}}$	LHM8

Controlling Step	Rate Expression	Model No.
Desorption of water without inert term and backward reaction	$\frac{K_{aW} S_O K_{EQ, E} P_A^2 / P_E}{1.0 + K_{O} P_O + K_{E} P_E + K_A P_A + K_W K_{EQ, E} P_A^2 / P_E}$	LHM9
Desorption of Ether	$\frac{K_{aE} S_O (K_{EQ, E} P_A^2 / P_W - P_E)}{1.0 + K_{O} P_O + K_W P_W + K_A P_A + K_E K_{EQ, E} P_A^2 / P_W + K_I P_I}$	LHM10
Desorption of Ether without inert term	$\frac{K_{aE} S_O (K_{EQ, E} P_A^2 / P_W - P_E)}{1.0 + K_{O} P_O + K_W P_W + K_A P_A + K_E K_{EQ, E} P_A^2 / P_W}$	LHM11
Desorption of Ether without inert term and backward reaction	$\frac{K_{aE} S_O K_{EQ, E} P_A^2 / P_W}{1.0 + K_{O} P_O + K_W P_W + K_A P_A + K_E K_{EQ, E} P_A^2 / P_W}$	LHM12

Table A1.2 Hougen-Watson Type EChemical Rate Expression.

Formation of ether through Rideal-Eley mechanism REM)

Controlling Step	Rate Expression	Model No.
Adsorption of alcohol	$\frac{K_{aA}S_O(P_A - P_{E^*P}/P_A/K'_{EQ,E})}{1.0 + K_{E^*P} + K_{O^*P} + K_A/K'_{EQ,E}P_{E^*P}/P_A + K_{W^*P} + K_{I^*P}}$	REM1
Adsorption of alcohol without inert term	$\frac{K_{aA}S_O(P_A - P_{E^*P}/P_A/K'_{EQ,E})}{1.0 + K_{E^*P} + K_{O^*P} + K_A/K'_{EQ,E}P_{E^*P}/P_A + K_{W^*P}}$	REM2
Adsorption of alcohol without inert and backward reaction	$\frac{K_{aA}S_O P_A}{1.0 + K_{E^*P} + K_{O^*P} + K_A/K'_{EQ,E}P_{E^*P}/P_A + K_{W^*P}}$	REM3

Controlling Step	Rate Expression	Model No.
Surface reaction	$\frac{S_O^2 K_A^1 K_A (P_A^2 - P_{E,W} P_{E,Q,E})}{(1.0 + K_{E,E} P_E + K_{A,P_A} + K_{O,P_O} + K_{W,P_W} + K_{I,P_I})^2}$	REM4
2 active sites		
Surface reaction	$\frac{S_O^2 K_A^1 K_A (P_A^2 - P_{E,W} P_{E,Q,E})}{(1.0 + K_{A,P_A} + K_{E,P_E} + K_{O,P_O} + K_{W,P_W})^2}$	REM5
2 active sites without inert term		
Surface reaction	$\frac{S_O^2 K_A^1 K_A P_A^2}{(1.0 + K_{A,P_A} + K_{E,P_E} + K_{O,P_O} + K_{W,P_W})^2}$	REM6
2 active sites without inert term and backward reaction		
Surface reaction	$\frac{S_O K_A^1 K_A (P_A^2 - P_{W,E} P_{E,Q,E})}{1.0 + K_{A,P_A} + K_{O,P_O} + K_{W,P_W} + K_{I,P_I}}$	REM7
1 active site (AS + A \rightleftharpoons WS + E)		

Controlling Step	Rate Expression	Model No.
Surface reaction, 1 active site without inert term	$\frac{S_0 K_A' K_A (P_A^2 - P_W P_E / K_{EQ, E}^1)}{1.0 + K_A P_A + K_O P_O + K_W P_W}$	REM8
Surface reaction, 1 active site, without inert term and back- ward reaction	$\frac{S_0 K_A' K_A}{1.0 + K_A P_A + K_O P_O + K_W P_W}$	REM9
Desorption of water	$\frac{K_{aW} S_0 (K_{EW}^1 P_E^2 / P_E - P_W)}{1.0 + K_A P_A + K_E P_E + K_O P_O + K_{EQ, E}^1 / K_W P_A^2 / P_E + K_I P_I}$	REM10
Desorption of water without inert term	$\frac{K_{aW} S_0 (K_{EQ, E}^1 P_E^2 / P_E - P_W)}{1.0 + K_A P_A + K_E P_E + K_O P_O + K_W K_{EQ, E}^1 P_A^2 / P_E}$	REM11

Controlling Step	Rate Expression	Model No.
Desorption of water without inert term and backward reaction	$\frac{K_{aW} S_{O_{EQ}} K'_{EA} P_A^2 / P_E}{1.0 + K_{A} P_A + K_{E} P_E + K_{O} P_O + K_{W} K'_{EQ} P_A^2 / P_E}$	REM12
Desorption of ether	$\frac{K_{aE} S_{O_{EQ}} (K'_{EA} P_A^2 / P_W - P_E)}{1.0 + K_{A} P_A + K_{O} P_O + K_{W} P_W + K_{EQ} K_{EA} P_A^2 / P_W + K_{I} P_I}$	REM13
Desorption of ether without inert term	$\frac{K_{aE} S_{O_{EQ}} (K'_{EA} P_A^2 / P_W - P_E)}{1.0 + K_{A} P_A + K_{O} P_O + K_{W} P_W + K_{EQ} K_{EA} P_A^2 / P_W}$	REM14
Desorption of ether without inert term and backward reaction	$\frac{K_{aE} S_{O_{EQ}} K'_{EA} P_A^2 / P_W}{1.0 + K_{A} P_A + K_{O} P_O + K_{W} P_W + K_{EQ} K_{EA} P_A^2 / P_W}$	REM15

Table A1.3 Hougen-Watson Type Chemical Rate Expression.

Formation of olefin

Controlling Step	Rate Expression	Model
Adsorption of alcohol	$\frac{K_{aA} S_O (P_A - P_{O^P_W} / K_{EQ, O})}{1.0 + K_{E^P_E} + K_{O^P_O} + K_{W^P_W} + K_A K_{EQ, E} P_{O^P_W} + K_{I^P_I}}$	1
Desorption of alcohol without inert term	$\frac{K_{aA} S_O (P_A - P_{O^P_W} / K_{EQ, O})}{1.0 + K_{E^P_E} K_{O^P_O} + K_{W^P_W} + K_A / K_{EQ, O} P_{O^P_W}}$	2
Adsorption of alcohol without inert and backward reaction	$\frac{K_{aA} S_O P_A}{1.0 + K_{E^P_E} + K_{O^P_O} + K_{W^P_W} + K_A / K_{EQ, O} P_{O^P_W}}$	3

Controlling Step	Rate Expression	Model
Surface reaction 2 active sites	$\frac{K_{R_{O_A}} S^2 K_A (P_A - P_{O_E} P_{E_{Q,0}} / K_{E_{Q,0}})}{(1.0 + K_{E_E} P_E + K_{A_P A} + K_{O_P O} + K_{W_P W} + K_{I_P I})^2}$	4
Surface reaction 2 active sites without inert term	$\frac{K_{R_{O_A}} S^2 K_A (P_A - P_{O_E} P_{E_{Q,0}} / K_{E_{Q,0}})}{(1.0 + K_{E_E} P_E + K_{A_P A} + K_{O_P O} + K_{W_P W})^2}$	5
Surface reaction 2 active sites without inert term and backward reaction	$\frac{K_{R_{O_A}} S^2 K_A P_A}{(1.0 + K_{E_E} P_E + K_{A_P A} + K_{O_P O} + K_{W_P W})^2}$	6
Surface reaction 1 active site ($AS \rightleftharpoons O + WS$)	$\frac{K_{R_{O_A}} S K_A (P_A - P_{O_E} P_{E_{Q,0}} / K_{E_{Q,0}})}{1.0 + K_{A_P A} + K_{W_P W} + K_{E_P E} + K_{I_P I}}$	7

Controlling Step	Rate Expression	Model
Surface reaction 1 active site without inert term	$\frac{K_R S_O K_A (P_A - P_O P_E / K_{EQ, O})}{1.0 + K_A P_A + K_W P_W + K_E P_E}$	8
Surface reaction 1 active site, without inert and backward reaction	$\frac{K_R S_O K_A P_A}{1.0 + K_A P_A + K_W P_W + K_E P_E}$	9
Desorption of water	$\frac{K_{aW} S_O (K_{EQ, O} P_A / P_O - P_W)}{1.0 + K_O P_O + K_E P_E + K_A P_A + K_{EQ, O} K_W P_A / P_O + K_I P_I}$	10
Desorption of water without inert term	$\frac{K_{aW} S_O (K_{EQ, O} P_A / P_O - P_W)}{1.0 + K_O P_O + K_E P_E + K_A P_A + K_{EQ, O} K_W P_A / P_O}$	11

Controlling Step	Rate Expression	Model No.
Desorption of water without inert and backward reaction	$\frac{K_{aW} S_0 K_{EQ,0} P_A / P_0}{1.0 + K_A P_A + K_{O} P_0 + K_{E} P_E + K_{EQ,0} K_{W} P_A / P_0}$	12
Desorption of olefin	$\frac{K_{a0} S_0 (K_{EQ,0} P_A / P_W - P_0)}{1.0 + K_A P_A + K_{E} P_E + K_{W} P_W + K_{EQ,0} K_{E} P_A / P_0 + K_{I} P_I}$	13
Desorption of olefin without inert term	$\frac{K_{a0} S_0 (K_{EQ,0} P_A / P_W - P_0)}{1.0 + K_{E} P_E + K_A P_A + K_{W} P_W + K_{EQ,0} K_{E} P_A / P_0}$	14
Description of olefin without inert term and backward reaction	$\frac{K_{a0} S_0 K_{EQ,0} P_A / P_W}{1.0 + K_{W} P_W + K_{E} P_E + K_A P_A + K_{EQ,0} K_{E} P_A / P_0}$	15

Table A1.4 Initial Rate for the Formation of Ether

Controlling Step	Initial Rate Expression	Model No.
Adsorption of alcohol	$K_{aA} S_O P_A$	AR1
Surface reaction 2 active sites	$\frac{K_R S_O^2 K_A^2 P_A^2}{(1.0 + K_A P_A)^2}$	LHM
Surface reaction 2 active sites	$\frac{K_R' S_O^2 K_A P_A^2}{(1.0 + K_A P_A)^2}$	REM1
Surface reaction 1 active site	$\frac{K_R S_O K_A P_A^2}{1.0 + K_A P_A}$	REM2
Desorption of water	$K_{aW} S_O$	DR1
Desorption of ether	$K_{aE} S_O$	DR2

Table A1.5 Initial Rate for the Formation of Olefin.

Controlling Step	Initial Rate Expression	Model No.
Adsorption of alcohol	$K_{aA} S_O P_A$	AR01
Surface reaction 2 active sites	$\frac{K_R K_A S_O^2 P_A}{(1.0 + K_A P_A)^2}$	SR2
Surface reaction 1 active site	$\frac{K_R K_A S_O P_A}{1.0 + K_A P_A}$	SR1
Desorption of water	$K_{aW} S_O$	DR01
Desorption of olefin	$K_{aO} S_O$	DR02

APPENDIX 2

POWER FUNCTION RATE EXPRESSION

Table A2.1 Power Function Rate Expression

Model	Rate of Formation of	
	Ether	Olefin
1	$K_1 P_A^2 + K_{-3} P_A P_O$ $- K_{-1} P_E P_W - K_3 P_E$	$K_2 P_A + K_3 P_E$ $- K_{-2} P_O P_W - K_{-3} P_O P_A$
2	$K_1 P_A^2 - K_3 P_E$	$K_2 P_A + K_3 P_E$
3	$K_1 (P_A^2 - P_E P_W / K_{eq})$	$K_2 (P_A - P_O P_W / K_{eq})$
4	$K_{RE} P_A^a P_W^b P_O^c P_E^e$	$K_{RO} P_A^a P_W^b P_O^c P_E^e$
5	$K_{RE} P_A^a P_W^b$	$K_{RO} P_A^a P_W^b$
6	$K_{RE} P_A^a$	$K_{RO} P_A^a$

APPENDIX 3

EFFECTS OF INTRA-PARTICLE MASS AND HEAT TRANSPORT

APPENDIX 3

Effect of intra-particle mass and heat transport on the dehydration of isopropanol over cation exchange resin.

Weisz and Practer (93) criterion for the assessment of the importance of intra-particle mass transport in solid catalysed chemical reactions, is given by

$$\phi = \frac{R_{obs} R_o^2 \rho_b}{D_e C_{Ao}} \ll 1.0$$

The relationship for the temperature difference, for component, i, between the external catalyst surface and at the centre of the catalyst is given by

$$T_c - T_s = \frac{D_e (-\Delta H_R) (P_{is} - P_{ic})}{\lambda_e R_g T_S \alpha_i}$$

α_i is the stoichiometric co-efficient of the reactant.

In the present case $\alpha_i = 1.0$.

Reaction Conditions:

Reaction rate $8.2 \cdot 10^{-3}$ gmole/g_c.hr at 0.49 atm

R_o 0.028 cm

T 414 K

ρ_b 0.8 gm/cc

P_t 2 atm

Molecular weight of reactant 60

Molecular weight of diluent (N_2) 28

Parameters.

D_e	$1.1 \cdot 10^{-2} \text{ cm}^2/\text{s}$
λ_e	$5.0 \cdot 10^{-3} \text{ cal/cm s K}$
ΔH_R	$12 \cdot 10^3 \text{ cal/gmole}$
C_A	$4.2 \cdot 10^{-5} \text{ gmole /cc.}$

Weisz and Practer parameter.

$$\begin{aligned} \phi &= \frac{8.2 \cdot 10^{-3} \times 0.028^2 \times 0.8}{1.1 \cdot 10^{-2} \times 3.6 \cdot 10^3 \times 4.2 \cdot 10^{-5}} \\ &= 3.1 \cdot 10^{-3} \end{aligned}$$

Maximum Temperature Difference.

It is assumed that the concentration at the centre is zero.

$$\text{i.e. } P_{ic} = 0$$

$$\begin{aligned} \Delta T_{\max} &= \frac{1.1 \cdot 10^{-2} \times 12 \cdot 10^3 \times 4.2 \cdot 10^{-5}}{5.0 \cdot 10^{-3}} \\ &= \underline{1.1 \text{ K}} \end{aligned}$$

The results of the above calculations show that interanal mass and heat transfer effects are insignificant within the reaction conditions studied.

APPENDIX 4

TABLES OF EXPERIMENTAL KINETIC DATA AND

ESTIMATED PARAMETERS

Table A4.1 Kinetic Data on the Dehydration of n-Butanol over 13X Zeolite.

Total pressure 1 bar gauge.

Mass of catalyst 4.78g, 4.42g*

T	V _A	V _{N₂}	P _A	P _O	P _E	P _W	R _O	R _E	S
°C	cc/hr	cc/min	bar	bar	bar		gmole/g _c .hr * 10 ⁴		R _O /R _E
228	2.14	119	0.14	0.0010	0.0011	0.0021	0.34	0.37	0.91
	3.70	120.	0.23	0.0009	0.0014	0.0023	0.32	0.50	0.64
	5.07	120.	0.31	0.0008	0.0014	0.0022	0.22	0.52	0.60
	6.76	120.	0.39.	0.0009	0.0013	0.0022	0.34	0.52	0.66
	6.77	118	0.48	0.0014	0.0013	0.0027	0.57	0.53	1.1
	11.0	120.	0.57	0.0011	0.0012	0.0023	0.48	0.52	0.91
	12.9	121	0.63	0.0010	0.0012	0.0022	0.44	0.58	0.76

T °C	V _A cc/hr	V _{N₂} cc/min	P _A	P _O bar	P _E	P _W	R _O gmole/g _c .hr * 10 ⁴	R _E	S R _O /R _E
241	1.48	119	0.093	0.0020	0.0027	0.0047	0.65	0.89	0.72
	3.15	119	0.20	0.0023	0.0032	0.0055	0.80	1.1	0.72
	4.83	119	0.29	0.0024	0.0034	0.0058	0.87	1.3	0.69
	7.05	120.	0.40	0.0024	0.0035	0.0059	0.93	1.3	0.67
	9.04	121	0.48	0.0024	0.0034	0.0058	1.0	1.4	0.72
	11.2	121	0.57	0.0024	0.0032	0.0056	1.1	1.4.	0.74
252*	1.45	120.	0.85	0.0034	0.0052	0.0096	1.3	1.5	0.81
	3.12	120.	0.19	0.0040	0.0069	0.011	1.5	2.6	0.57
	4.95	120.	0.29	0.0041	0.0072	0.011	1.6	2.9	0.57
	6.35	122	0.36	0.0045	0.0065	0.011	1.9	2.8	0.68
	8.80	121	0.47	0.0045	0.0063	0.011	2.0.	2.8	0.71
	11.0	121	0.56	0.0044	0.0059	0.010	2.1	2.8	0.75

T °C	V _A cc/hr	V _{N₂} cc/min	P _A	P _O bar	P _E	P _W	R _O gmole/g _c .hr	R _E * 10 ⁴	S R _O /R _E
258	2.01	121	0.12	0.0050	0.0064	0.011	1.7	2.1	0.78
	3.74	120	0.21	0.0073	0.010	0.017	2.6	3.6	0.73
	5.61	122	0.30	0.0078	0.011	0.019	3.0	4.1	0.71
	8.03	121	0.42	0.0080	0.011	0.091	3.3	4.5	0.73
	12.0	122	0.57	0.0072	0.0098	0.017	3.2	4.5	0.73
272*	1.38	122	0.068	0.015	0.011	0.026	5.3	2.9	1.8
	3.45	123	0.17	0.017	0.016	0.033	6.6	6.2	1.1
	5.28	124	0.26	0.018	0.018	0.036	7.5	7.3	1.0
	6.97	124	0.34	0.018	0.017	0.038	8.0	8.8	0.91
	8.23	124	0.40	0.018	0.018	0.038	8.2	8.0	1.0
	11.4	124	0.52	0.018	0.017	0.085	8.7	8.2	1.0
286	1.83	122	0.04	0.034	0.019	0.043	1.2	6.3	1.8
	3.16	124	0.094	0.040	0.031	0.071	1.5	11	1.3

Table A4.2 Kinetic Data on the Dehydration of n-Butanol over 4A Zeolite.

Total pressure 1 bar gauge.

Mass of catalyst 6.11g*, 4.88g.

T °C	V _A cc/hr	V _{N₂} cc/min	P _A	P _O	P _E	P _W	R _O gmole/g _c .hr*10 ⁴	R _E	S R _C /R _E
232*	1.25	118	0.08	0.0004	-	0.0004	0.12	-	-
	3.17	118	0.21	0.0004	-	0.0004	0.12	-	-
	4.52	118	0.29	0.0004	-	0.0004	0.12	-	-
	6.33	118	0.38	0.0005	-	0.0005	0.14	-	-
	8.42	118	0.48	0.0004	-	0.0004	0.13	-	-
	10.7	117	0.57	0.0004	-	0.0004	0.13	-	-

T °C	V _A cc/hr	V _{N₂} cc/min	P _A	P _O bar	P _E	P _W	R _O gmole/g _C .hr.*10 ⁴	R _E	S R _O /R _E
250*	1.62	118	0.11	0.0016	-	0.0016	0.42	-	-
	3.32	118	0.21	0.0016	-	0.0016	0.44	-	-
	4.83	119	0.30	0.0016	-	0.0016	0.46	-	-
	6.72	120	0.39	0.0015	-	0.0015	0.46	-	-
	8.49	119	0.48	0.0014	-	0.0014	0.45	-	-
	11.7	118	0.60	0.0014	-	0.0014	0.50	-	-
	271	1.28	118	0.081	0.0055	-	0.0055	1.7	-
	3.05	119	0.19	0.0056	-	0.0056	1.9	-	-
	4.56	119	0.28	0.0056	-	0.0056	2.0	-	-
	6.37	118	0.37	0.0054	-	0.0054	2.0	-	-
	9.60	119	0.51	0.0057	0.0005	0.0062	2.3	0.20	12
	12.4	119	0.62	0.0053	0.0005	0.0058	2.3	0.23	11

T °C	V _A cc/hr	V _{N₂} cc/min	P _A	P _O bar	P _E	P _W	R _O gmole/g _c .hr.*10 ⁴	R _E	S
278*	1.61	120.	0.10	0.0082	-	0.0082	2.1	-	-
	3.41	119	0.21	0.0085	-	0.0085	2.4	-	-
	5.30	122	0.31	0.0086	0.0007	0.0093	2.5	0.20	13
	7.00	123	0.39	0.0084	0.0007	0.0091	2.6	0.21	12
	9.39	123	0.49	0.0082	0.0007	0.0089	2.7	0.24	12
	12.1	122.	0.60	0.0078	0.0007	0.0085	2.8	0.26	11
297	1.92	121	0.099	0.020	0.0009	0.021	6.5	0.30	22
	3.78	122	0.21	0.019	0.0010	0.020	6.8	0.35	20.
	5.66	122	0.35	0.019	0.0010	0.020	7.1	0.35	20
	8.36	122	0.44	0.018	0.0010	0.019	7.4	0.41	18
	10.8	122	0.52	0.019	0.0012	0.020	8.3	0.48	17
	13.1	120	0.62	0.019	0.0012	0.020	8.5	0.51	17

Table A4.3 Kinetic Data on the Dehydration of n-Butanol over ZNa Zeolite

Total pressure 1 bar gauge.

Mass of catalyst 5.17g

T °C	V _A cc/hr	V _{N₂} cc/min	P _A	P _O	P _E	P _W	R _O	R _E	S
			bar				gmole/g _c .hr * 10 ⁴		R _O /R _E
235	1.64	122	0.11	0.0006	-	0.0006	0.18	-	-
	3.18	120.	0.21	0.0006	-	0.0006	0.19	-	-
	4.93	120.	0.30	0.0006	-	0.0006	0.21	-	-
	8.73	120.	0.48	0.0004	-	0.0004	0.18	-	-
	11.7	120.	0.60	0.0004	-	0.0004	0.15	-	-
255	0.66	121	0.046	0.0009	-	0.0009	0.29	-	-
	1.43	120.	0.10	0.0012	-	0.0012	0.35	-	-
	3.58	120.	0.23	0.0012	-	0.0012	0.42	-	-
	4.27	121	0.27	0.0012	-	0.0012	0.42	-	-
	7.56	120.	0.43	0.0013	0.0004	0.0017	0.48	0.15	3.2
	10.7	120.	0.56	0.0013	0.0005	0.0018	0.51	0.20	2.6

T	V _A	V _{N₂}	P _A	P _O	P _E	P _W	R _O	R _E	S
°C	cc/hr	cc/min	bar	bar			gmole/g _c .hr * 10 ⁴		R _O /R _E
275	1.65	120.	0.11	0.0030	-	0.0030	0.92	-	-
	2.72	120.	0.18	0.0034	0.0004	0.0038	1.1	0.14	7.5
	4.66	122	0.28	0.0030	0.0005	0.0035	1.1	0.18	6.3
	6.84	121	0.37	0.0030	0.0005	0.0035	1.1	0.20	5.4
	8.76	121	0.48	0.0030	0.0007	0.0037	1.1	0.29	3.9
	12.1.	121	0.61	0.0029	0.0008	0.0037	1.2	0.20	6.0
300	1.22	120	0.078	0.0071	0.0006	0.0077	1.9	0.18	10
	2.91	121	0.18	0.0082	0.0005	0.0087	2.7	0.18	15.
	4.26	122	0.25	0.0086	0.0007	0.0093	2.9	0.25	12
	7.30	121	0.41	0.0078	0.0013	0.0091	2.9	0.49	5.9
	11.6	121	0.58	0.0080	0.0013	0.0093	3.3	0.54	6.2

Table A4.4 Kinetic and Adsorption Thermodynamic
Constants from Linear Regression Analysis.

The dehydration of n-butanol.

Butene Formation

Model	T ^o C	$K_R \left(\frac{\text{gmole}}{\text{g}_c \cdot \text{hr}} \right)$	$K_A (\text{bar}^{-1})$	R-squared	Catalyst
		* 10 ⁴			
SR2	228	1.8	1.4	76	13X
	241	4.0	2.2	98	
	252	8.0	2.1	96	
	258	13.	1.6	99	
	272	34	2.9	96	
SR1	228	0.61	5.2	77	13X
	241	1.2	11	99	
	252	2.5	8.9	99	
	258	4.3	6.8	98	
	272	9.6	16	100.	
SR2	232	0.55	3.0	99	4A
	250	2.0	2.8	98	
	271	9.2	2.5	95	
	278	11	2.5	98	
	297	33	2.5	95	
SR1	232	0.14	29	99	4A
	250	0.51	33	99	
	271	2.5	16	99	
	278	3.0	19	99	
	297	9.1	15	98	

Model	T ^o C	$K_R \left(\frac{\text{mole}}{\text{g} \cdot \text{hr}} \right) * 10^4$	$K_A (\text{bar}^{-1})$	R-squared	Catalyst
SR2	235	0.81	4.9	99	ZNa
	255	2.0	3.0	96	
	275	4.8	2.7	98	
	300	13	2.4	88	
SR1	235	0.15	-19	96	ZNa
	255	0.55	16	99	
	275	1.3	26	99	
	300	3.6	14	99	

Table A4.5 Kinetic and Adsorption Thermodynamic
Constants from Non-linear Regression Analysis.

The dehydration of n-butanol

Butene Formation

Model	T°C	$K_R \frac{\text{gmol}}{\text{hr} \cdot \text{g}_c} \times 10^4$	S.DEV. $\times 10^4$	$K_A (\text{bar}^{-1})$	S.DEV.	SSR 10^{10}	CAT.
SR2	228	1.9	0.28	1.3	0.62	1.0	13X
	241	4.0	0.16	2.2	0.34	1.0	
	252	8.0	0.43	2.0	0.39	3.0	
	258	13	0.32	1.6	0.12	1.0	
	272	33	1.4	2.7	0.48	52	
SR1	228	0.59	0.15	6.3	5.2	1.0	13X
	241	1.2	0.04	12	2.0	<0.5	
	252	2.4	0.15	11	2.6	1.0	
	258	4.4	0.37	6.3	1.7	3.0	
	272	9.4	0.30	17	2.7	8.0	
SR2	232	0.55	0.03	3.3	0.72	<0.5	4A
	250	2.0	0.07	3.1	0.47	<0.5	
	271	9.0	0.55	2.7	0.65	9.0	
	278	11	0.40	2.7	0.42	5.0	
	297	32	1.8	2.7	0.61	104.	
SR1	232	0.14	0.01	46	25	<0.5	4A
	250	0.49	0.01	44	13	<0.5	
	271	2.4	0.01	28	11	2.0	
	278	2.9	0.07	24	4.0	<0.5	
	297	8.4	0.47	29	13	29	

Model	T °C	$K_R \frac{\text{gmole}}{\text{gc hr}}$ *10 ⁴	S.DEV. * 10 ⁴	$K_A (\text{bar}^{-1})$	S.DEV.	SSR 10 ¹⁰	CAT
SR2	235	0.80	0.03	4.5	0.49	< 0.5	ZNa
	255	1.9	0.12	3.0	0.66	< 0.5	
	275	4.7	0.15	2.9	0.37	1.0	
	300	13	0.56	2.5	0.38	6.0	
SR1	235	0.18	0.01	17 10 ²	0	< 0.5	ZNa
	255	0.52	0.02	23	5.0	< 0.5	
	275	1.2	0.04	30	8.3	< 0.5	
	300	3.6	0.20	14.	3.4	2.0	

Table A4.6 Kinetic and Adsorption Thermodynamic
Constants from Linear Regression Analysis.

The dehydration of n-butanol over
 zeolite 13X.

Ether Formation

Model	T ^o C	$K_R \frac{\text{mole}}{\text{g}_c \text{hr}}$ * 10 ⁴	$K_A (\text{bar}^{-1})$	R-squared
LHM	228	0.62	29	100.
	241	1.6	30	100
	252	3.2	37	100.
	258	5.6	18.	100.
	272	10.	20.	100.
REM1.	228	18.	29	100.
	241	48	30	100.
	252	116	37	100.
	258	102.	18	100.
	272	209	20	100.
REM2	228	0.74	-7.0	97
	241	2.2	-8.8	96
	252	4.4.	-8.8	96
	258	6.8	-8.5	95
	272	15	-11	93

Table A4.7 Kinetic and Adsorption ThermodynamicConstants from Non-linear Regression Analysis.

The dehydration of n-butanol over zeolite
13X

Ether Formation

Model	T°C	$K_{Rg_c} \frac{\text{gmole}}{\text{hr}}$ * 10 ⁴	S.DEV. * 10 ⁴	K_A (bar ⁻¹)	S.DEV.	SSR 10 ¹⁰
LHM	228	0.63	0.03	28	6.0	< 0.5
	241	1.6	0.04	31	3.0	< 0.5
	252	3.4	0.21	30	8.0	4.0
	258	5.9	0.43	15	3.1	6.0
	272	11	0.77	18	4.0	29
REM1	228	17	3.0	28	0.0	< 0.5
	241	48	3.9	31	3.0	< 0.5
	252	99	22	30	8.0	4.0
	258	90	12	15	3.0	6.0
	272	2 10 ²	30	18	4.0	29
REM2	228	1.1	0.15	60 10 ²	0	3.0
	241	3.2	0.46	35 10 ³	0	18
	252	6.9	1.1	26 10 ³	0	95
	258	10	1.5	76 10 ²	0	1.5 10 ²
	272	21	2.7	49 10 ²	0	4.6 10 ²

Table A4.8 Kinetic Data on the Dehydration of Isopropanol over 13X Zeolite.

Total pressure 1-bar gauge.

Mass of catalyst 6.74g.

T	V _A	V _{N₂}	P _A	P _O	P _E	P _W	R _O	R _E	S
°C	cc/hr	cc/min	bar	bar	bar		gmole/g _c .hr.*10 ³		R _O /R _E
231	2.38	123	0.16	0.025	0.0017	0.026	0.62	0.042	15
	4.19	123	0.28	0.026	0.0023	0.029	0.70	0.062	11.
	5.60	123	0.36	0.027	0.0026	0.030	0.77	0.072	11
	6.49	121	0.41	0.028	0.0027	0.031	0.81	0.078	10.
	8.34	122	0.50	0.028	0.0028	0.031	0.87	0.088	9.9
	10.8	122	0.60	0.028	0.0029	0.030	0.93	0.096	9.7

T °C	V _A cc/hr	V _{N₂} cc/min	P _A	P _O bar	P _E	P _W	R _O gmole/g _c .hr.*10 ³	R _E	S
240	2.14	123	0.13	0.039	0.0018	0.040	0.96	0.044	22
	3.91	123	0.24	0.041	0.0032	0.044	1.1	0.085	13
	5.42	123	0.33	0.042	0.0038	0.046	1.2	0.11	11
	7.38	122	0.44	0.042	0.0040	0.046	1.2	0.12	10.
	8.85	123	0.51	0.041	0.0041	0.045	1.3	0.13	10.
	11.4	124	0.61	0.040	0.0042	0.045	1.4	0.14	9.7
255	2.38	127	0.11	0.077	0.0010	0.078	2.0	0.025	79
	4.26	127	0.22	0.076	0.0031	0.080	2.1	0.086	25
	5.83	128	0.31	0.076	0.0042	0.080	2.2	0.12	18
	7.85	130	0.40	0.077	0.0053	0.08	2.4	0.17	15
	9.56	132	0.47	0.076	0.0058	0.082	2.6	0.20	13
	10.9	130.	0.52	0.081	0.0069	0.087	2.9	0.24.	12

T °C	V _A cc/hr	V _{N₂} cc/min	P _A	P _O	P _E bar	P _W	R _O gmole/g _c .hr.*10 ³	R _E	S R _O /R _E
286	0.86	124	0.0017	0.070	-	0.070	1.7	-	-
	2.87	135	0.018	0.19	-	0.19	5.2	-	-
	4.31	141	0.062	0.22	0.0004	0.22	6.6	0.011	6.2 10 ²
	6.38	146	0.16	0.22	0.0017	0.22	7.3	0.036	2.0 10 ²
	8.48	148	0.26	0.21	0.0021	0.21	7.4	0.077	97

Table A4.9 Kinetic Data on the Dehydration of Isopropanol over 4A Zeolite.

Total pressure 1-bar gauge.

Mass of catalyst 8.64g.

T °C	V _A cc/hr	V _{N₂} cc/min	P _A	P _O bar	P _E	P _W	R _O gmole/g _c .hr.*10 ³	R _E	S R _O /R _E
200	2.40	119	0.20	0.0008	-	0.0008	0.015	-	-
	3.68	118	0.29	0.0008	-	0.0008	0.017	-	-
	5.09	119	0.37	0.0009	-	0.0009	0.019	-	-
	9.36	119	0.59	0.0010	-	0.0010	0.025	-	-
229	2.34	120.	0.19	0.0036	-	0.0036	0.069	-	-
	3.74	120.	0.28	0.0040	-	0.0040	0.082	-	-
	5.04	120.	0.36	0.0042	-	0.0042	0.089	-	-
	7.21	121	0.43	0.0044	-	0.0044	0.10	-	-
	8.44	120.	0.54.	0.0046	-	0.0046	0.11	-	-
	10.9	121	0.65	0.0045	-	0.0045	0.12	-	-

T °C	V _A cc/hr	V _{N₂} cc/min	P _A	P _O	P _E bar	P _W	R _O gmole/g _c .hr.*10 ³	R _E	S R _O /R _E *10 ²
252	0.81	121	0.065	0.0088	-	0.0088	0.16.	-	-
	2.51	120.	0.19	0.010	0.00003	0.010	0.19	0.0005	3.9
	3.86	121	0.28	0.010	0.00004	0.010	0.23	0.0008	2.8
	5.50	122	0.38	0.012	0.00004	0.012	0.26.	0.0008	3.3
	8.32	123	0.52	0.013	0.00004	0.013	0.30.	0.0011	2.8
	11.0	123	0.63	0.014	0.00004	0.014.	0.38	0.0014	2.7
275	0.92	122	0.045	0.015.	0.00000	0.015	0.35	0.0000	-
	2.34	120.	0.17	0.022	0.00006	0.022	0.42.	0.0013	3.2
	4.09	123	0.28	0.024.	0.00010	0.024	0.51	0.0020	2.5
	6.04	123.	0.39	0.025	0.00010	0.025.	0.56.	0.0024	2.4
	8.14	124	0.49	0.027	0.00012	0.027	0.64.	0.0029	2.2
	11.3	125	0.62	0.027	0.00015	0.027.	0.75	0.0038	2.0

T °C	V _A cc/hr	V _{N₂} cc/min	P _A	P _O bar	P _E	P _W	R _O gmole/g _c .hr.*10 ³	R _E	S
									R _O /R _E
301	1.03	120.	0.050	0.036	0.00002	0.036	0.65	0.0003	2.2 10 ³
	2.95	123	0.17	0.050	0.0003	0.050	1.0	0.0041	2.5 10 ²
	3.75	124.	0.22.	0.052.	0.0003	0.052.	1.1	0.0056	1.9 10 ²
	4.61	125	0.27	0.056	0.0003	0.056	1.2	0.0066	1.8 10 ²
	6.41	127	0.36.	0.060	0.0004	0.060	1.4	0.0096	1.5 10 ²
	8.61	128	0.47	0.061	0.0005	0.062	1.5	0.012.	1.3 10 ²
	11	129	0.58	0.064	0.0003	0.064.	1.8	0.014.	1.2 10 ²

Table A4.10 Kinetic Data on the Dehydration of Isopropanol over ZNa Zeolite.

Total pressure 1-bar gauge.

Mass of catalyst 7.90g.

T °C	V _A cc/hr	V _{N₂} cc/min	P _A	P _O	P _E	P _W	R _O gmole/g _c .hr.*10 ³	R _E	S R _O /R _E
228	1.09	114	0.079	0.017	0.0003	0.018	0.33	0.0063	52
	2.87	115	0.21	0.019	0.0006	0.020	0.40	0.014	29
	4.81	115	0.34	0.020	0.0008	0.021	0.44	0.018	24
	7.15	117	0.47	0.020	0.0009	0.021	0.48	0.023	22
	9.91	116	0.60	0.020	0.0009	0.021	0.53	0.026	20.
238	1.64	113	0.11	0.028	0.0006	0.028	0.53	0.012	46
	3.29	116	0.23	0.028	0.0010	0.029	0.58	0.021	28
	5.13	117	0.35	0.027	0.0012	0.028	0.61	0.027	23
	7.32	118	0.47	0.027	0.0014	0.02	0.67	0.033	21
	9.46	118	0.57	0.027	0.0014	0.028	0.71	0.038	19

T °C	V _A cc/hr	V _{N₂} cc/min	P _A	P _O bar	P _E	P _W	R _O gmole/g _c .hr*10 ³	R _E	S R _O /R _E
254	1.26	116	0.063	0.044	0.0002	0.044	0.85	0.0049	1.7 10 ²
	2.70	117	0.17	0.043	0.0010	0.044	0.88	0.02	43
	4.34	119	0.28	0.042	0.0016	0.044	0.95	0.034	28
	6.23	119	0.39	0.041	0.0018	0.045	1.0	0.045	22
	8.24	118	0.50	0.038	0.0018	0.040	0.97	0.048	20.
	10.9	119	0.62	0.037	0.0020	0.039	1.0	0.054	19
274	1.29	115	0.036	0.073	0.0000	0.073	1.5	0.0000	0
	3.13	120 _a	0.16	0.077	0.0009	0.07	1.7	0.020	83
	4.21	116	0.25	0.072	0.0016	0.074	1.6	0.034	47
	6.10	118	0.36	0.068	0.0021	0.070	1.6	0.051	32
	8.50	117	0.49	0.063	0.0024	0.065	1.6	0.063	26
	10.9	120 _a	0.58	0.06	0.0026	0.074	1.7	0.078	22

Table A4.11 Kinetic and Adsorption Thermodynamic
Constants from Linear Regression Analysis.

The dehydration of isopropanol.

Olefin Formation

Model	T ^o C	K _R ($\frac{\text{gmole}}{\text{g}_c \cdot \text{hr}}$) * 10 ⁴	K _A (bar ⁻¹)	R-squared	Catalyst
SR2	231	36	1.5	97	13X
	240	52	2.0	97.	
	255	104	2.3	94	
	286	3.7 10 ²	12	96	
SR1	231	12	6.1	99	13X
	240	16	10.	99.	
	255	32	11	94	
	286	76	1.3 10 ²	100.	
SR2	200	1.0	0.97	92	4A
	229	4.7	1.1	98	
	252	13	1.5	83	
	275	26	2.1	87	
	301	63	1.7	89	

Model	T ^o C	K _R ($\frac{\text{gmole}}{\text{g}_c \cdot \text{hr}}$) * 10 ⁴	K _A (bar ⁻¹)	R-squared	Catalyst
SR1	200	0.38	2.9	94	4A
	229	1.6	3.7	99	
	252	4.5	4.6	89	
	275	8.4	7.4	94	
	301	22	5.4	95	
SR2	228	20	2.4	96	ZNa
	238	27	2.4	97	
	254	43	3.4	97	
	274	76	4.4	96	
SR1	228	5.8	12	99	ZNa
	238	7.8	14	99	
	254	10	41	100	
	274	17	96	100	
SR2	141	3.0 10 ²	0.76	80	Resin
	131	2.2 10 ²	0.66	51	
	119	1.5 10 ²	0.77	50	
	110	88	1.5	92	
SR1	141	1.2 10 ²	1.9	80	Resin
	131	98	1.4	49	
	119	67	1.7	62	
	110	31	4.6	96	

Model	T°C	$K_R \left(\frac{\text{gmole}}{\text{g}_c \cdot \text{hr}} \right)$	$K_A (\text{bar}^{-1})$	$K_W (\text{bar}^{-1})$	R-squared
		* 10 ⁴			
DEW	141	1.0	-5.5	0.034	99
	131	0.62	-5.4	0.034	100.
	119	0.80	-7.0	0.060	100.
	110	1.0	-9.5	0.098	100.

Table A4.12 Kinetic and Adsorption Thermodynamic
Constants from Non-linear Regression Analysis.

The dehydration of isopropanol.

Olefin Formation.

Model	T°C	$K_R \left(\frac{\text{gmole}}{\text{g}_c \cdot \text{hr}} \right)$	S.DEV.	K_A	S.DEV.	SSR	CAT
		$* 10^4$	$* 10^4$	(bar ⁻¹)		$* 10^8$	
SR2	231	36	1.7	1.5	0.24	0.25	13X
	240	52	2.0	2.0	0.32	0.88	
	255	103	5.8	2.4	0.59	8.7	
	286	$3.2 \cdot 10^2$	29.	9.9	2.5	$1.5 \cdot 10^2$	
SR1	231	11	0.66	6.9	1.4	0.10	13X
	240	15	0.61	12.	2.5	0.22	
	255	29.	2.3	16	7.1	3.8	
	286	75	1.4	$1.4 \cdot 10^2$	16	3.5	
SR2	200	1.0.	-	0.97	-	-	4A
	229	4.7	0.20	1.1	0.12	0.00	
	252	14	2.6	1.1	0.46	0.22	
	275	27	5.1.	1.3	0.71	1.6	
	301	68	7.1.	1.2	0.31	2.1	
SR1	200	0.38	-	2.9	-	-	4A
	229	1.6	0.08	3.7.	0.50	0.00	
	252	4.1	0.95	4.7	2.7	0.17	
	275	7.4	1.3	11	7.8	1.1	
	301	22	2.8	5.0.	1.6	1.4	

Model	T ^o C	K _R ($\frac{\text{gmole}}{\text{g}_c \cdot \text{hr}}$) * 10 ⁴	S.DEV. * 10 ⁴	K _A (bar ⁻¹)	S.DEV.	SSR *10 ⁸	CAT
SR2	228	20.	1.3	2.4	0.59	0.35	ZNa
	238	27	1.4	2.5	0.52	0.44	
	254	42.	2.7	3.9	0.84	2.1	
	274	77.	7.6	5.9	1.6	11	
SR1	228	5.5	0.31	17	4.8	0.08	ZNa
	238	7.4	0.40	19	6.1	0.11	
	254	10.	0.24	74	24	0.13	
	274	17	0.31	2.2 10 ²	97	0.33	
SR1	141	1.6 10 ²	1.0	1.3	-	28	Resin
	131	9.0 10 ²	4.1 10 ²	0.11	0.50	14	
	119	1.4 10 ²	1.1 10 ²	0.59	0.57	7.4	
	110	32	-	4.2	-	1.5	
SR2	141	3.7 10 ²	1.4 10 ²	0.52	0.29	29	Resin
	131	1.9 10 ³	9.1 10 ³	0.049	0.24	14	
	119	3.2 10 ²	2.4 10 ²	0.26	0.23	7.0	
	110	93	8.0	1.2	0.24	2.1	

Model	T°C	$K_R (\frac{g_{mole}}{g_c \cdot hr})$ * 10 ⁴	S.DEV. * 10 ⁴	$K_A (bar^{-1})$	S.DEV.	$K_W (bar^{-1})$ * 10 ²	S.DEV. * 10 ²	SSR * 10 ⁸	Catalyst.
DEW	141	1.0	0.28	-5.4	2.0	3.4	1.5	13	Resin
	131	0.61	0.22	-4.9	2.3	3.0	1.8	3.0	
	119	0.85	0.27	-7.3	3.0	0.3	0.30	0.83	
	110	1.0	0.15	-9.4	3.0	9.7	0.28	0.16	

Table A4.13 Kinetic and Adsorption Thermodynamic
Constants from Linear Regression Analysis.

The dehydration of isopropanol over
Zeolite 13X

Ether Formation

Model	T°C	$K_R \left(\frac{\text{gmole}}{\text{g}_c \cdot \text{hr}} \right)$ * 10 ⁴	$K_A (\text{bar}^{-1})$	R-squared	Catalyst
LHM	231	1.5	6.9	100.	13X
	240	2.2	6.6	100.	
	255	9.1	1.9	99	
REM1	231	10.	6.9	100.	13X
	240	15	6.6	100.	
	255	18	1.9	99	
REM2	231	1.4	-10.	99	13X
	240	2.1	-12	98	
	255	4.7	8.7	98	

Table A4.14 Kinetic and Adsorption Thermodynamic
Constants from Non-linear Regression Analysis.

The dehydration of isopropanol over
 Zeolite 13X

Ether Formation

Model	T°C	$K_R \left(\frac{\text{gmole}}{\text{g}_c \cdot \text{hr}} \right)$	S.DEV.	K_A	SSR	CAT
		* 10 ⁴	* 10 ⁴	(bar ⁻¹)	*10 ¹⁰	
LHM	231	1.5	0.06	6.9	<0.5	13X
	240	2.2	0.07	6.7	<0.5	
	255	10.	2.27	1.8	<0.5	
REM1	231	10.	0.36	6.9	<0.5	13X
	240	15	0.45	6.7	<0.5	
	255	18	0.59	1.8	1.0	
REM2	231	1.8.	0.11	8.1 10 ³	1.0	13X
	240	2.6.	0.16	4.1 10 ³	3.0	
	255	5.4	0.44	9.7	<0.5	

Table A4.15 Kinetic Data on the Dehydration of Ethanol over 4A Zeolite.

Total pressure 1-bar gauge.

Mass of catalyst 5.00g.

T °C	V _A cc/hr	V _{N₂} cc/min	P _A	P _O	P _E	P _W	R _O	R _E	S
				bar			gmole/g _c .hr.*10 ³		R _O /R _E
349	0.91	122	0.062	0.015	0.0090	0.024	0.48	0.29	1.6
	2.52	126	0.16	0.035	0.018	0.053	1.3	0.65	2.0
	3.84	128	0.24	0.041	0.023	0.064	1.6	0.91	1.8
	5.17	130.	0.32	0.043	0.027	0.071	1.8	1.2	1.6
	7.88	133	0.45	0.046	0.032	0.078	2.2	1.6	1.4
	10.9	133	0.58	0.047	0.037	0.083	2.5	1.9	1.3

T	V _A	V _{N₂}	P _A	P _O	P _E	P _W	R _O	R _E	S
°C	cc/hr	cc/min	bar	bar	bar	g mole/g _c .hr.*10 ³	g mole/g _c .hr.*10 ³	R _O /R _E	
313	1.22	120.	0.11	0.0058	0.010	0.016	0.19	0.32	0.56
	2.53	120.	0.21	0.0094	0.016	0.025	0.33	0.54	0.61
	3.81	122	0.30	0.011	0.019	0.030	0.40	0.70	0.57
	5.17	122	0.39	0.011	0.021	0.032	0.45	0.82	0.55
	8.0	122	0.55	0.012	0.024	0.035	0.53	1.1	0.51
	10.89	124	0.68	0.012	0.025	0.037	0.59	1.3	0.47
279	1.21	119	0.11	0.0014	0.0081	0.0096	0.043	0.26	0.16
	2.53	120.	0.22	0.0021	0.012	0.014	0.072	0.41	0.18
	3.85	120.	0.33	0.0024	0.014	0.016	0.090	0.50	0.18
	5.24	120.	0.42	0.0026	0.015	0.018	0.10	0.60	0.17
	8.04	122	0.58	0.0028	0.017	0.020	0.13	0.75	0.17

Table A4.16 Kinetic Data on the Dehydration of Ethanol over ZNa Zeolite.

Total pressure 1-bar gauge

Mass of catalyst 5.86g.

T °C	V _A cc/hr	V _{N₂} cc/min	P _A	P _O bar	P _E	P _W	R _O gmole/g _c .hr.*10 ³	R _E	S R _O /R _E
349	1.04	124	0.10	0.0046	-	0.0046	0.12	-	-
	2.46	123	0.22	0.0080	0.0030	0.011	0.23	0.091	2.6
	3.76	123	0.31	0.010	0.0048	0.015	0.29	0.16	2.0
	5.01	123	0.39	0.012	0.012	0.018	0.36	0.23	1.8
	7.99	125	0.55	0.014	0.013	0.026	0.49	0.49	1.1

T	V _A	V _{N₂}	P _A	P _O	P _E	P _W	R _O	R _E	S
°C	cc/hr	cc/min	bar	bar			gmole/g _c .hr*10 ³		R _O /R _E
312	1.26	121	0.13	0.0034	-	0.0034	0.088	-	-
	2.59	122	0.24	0.0052	-	0.0052	0.15	-	-
	3.80	122	0.34	0.0058	-	0.0058	0.18	-	-
	5.08	120.	0.44	0.0057	-	0.0057	0.18	-	-
	7.99	121	0.61	0.0066	-	0.0066	0.24	-	-
	10.8	121	0.74	0.0068	-	0.0068	0.27	-	-
285	1.24	118	0.13	0.0008	-	0.0008	0.020	-	-
	2.54	119	0.25	0.0012	-	0.0012	0.034	-	-
	3.88	118	0.36	0.0016	-	0.0016	0.045	-	-
	5.17	118	0.46	0.0018	-	0.0018	0.053	-	-
	7.76	119	0.61	0.0020	-	0.0020	0.067	-	-

Table A4.17 Kinetic and Adsorption Thermodynamic
Constants from Linear Regression Analysis.

The dehydration of ethanol.

Olefin Formation.

Model	T ^o C	K _R ($\frac{\text{gmole}}{\text{g}_c \cdot \text{hr}}$) * 10 ³	K _A (bar ⁻¹)	R-squared	Catalyst
SR1	349	4.6	2.1	96	4A
	313	0.98	2.2	98	
	279	0.23	2.1	99	
SR2	349	12	0.80	98	4A
	313	2.6	0.79	99	
	279	0.57	0.78	98	
SR2	349	3.5	0.34	82	ZNa
	312	1.1	0.72	92	
	285	0.42	0.38	98	
SRL	349	1.6	1.3	83	ZNa
	312	0.44	1.9	93	
	285	0.19	1.1	98	

Table A4.18 Kinetic and Adsorption Thermodynamic
Constants from Non-linear Regression Analysis.

The dehydration of ethanol.

Olefin Formation.

Model	T°C	$K_R \left(\frac{\text{gmole}}{\text{g}_c \cdot \text{hr}} \right)$	S.DEV.	K_A	SDEV	SSR	CAT
		* 10^3	* 10^3	(bar ⁻¹)		* 10^8	
SR1	349	4.2	0.29	2.6	0.35	0.39	4A
	313	0.95	0.050	2.4	0.25	0.01	
	279	0.24	0.016	1.9	0.23	0.00	
SR2	349	11	0.53	0.90	0.09	0.39	4A
	313	2.6	0.10	0.80	0.07	0.20	
	279	0.60	0.040	0.71	0.08	0.00	
SR1	349	2.4	0.91	0.46	0.21	0.02	ZNa
	312	0.44	0.066	1.9	0.54	0.02	
	285	0.20	0.019	0.80	0.10	0.00	
SR2	349	5.3	1.9	0.21	0.09	0.02	ZNa
	312	1.2	0.04	0.65	0.15	0.02	
	285	0.46	0.042	0.34	0.04	0.00	

Table A4.19 Kinetic and Adsorption Thermodynamic
Constants from Linear Regression Analysis.

The dehydration of ethanol.

Ether Formation.

Model	T°C	$K_R \left(\frac{\text{gmole}}{\text{g}_c \cdot \text{hr}} \right)$ * 10 ³	$K_A (\text{bar}^{-1})$	R-squared	Catalyst
LHM	349	3.1	5.6	98	4A
	313	1.9	5.5	99	
	279	1.1	7.6	99	
REM	349	18	5.6	98	4A
	313	11	5.5	99	
	279	8.1	7.6	99	
REM2	349	3.3	-33	100	
	313	1.7	-15	100	
	279	1.2	-14	100	
LHM	142	16	2.3	91	Resin
	131	11	2.9	96	
	120	7.8	4.4	99	

Model	T°C	$K_R \left(\frac{\text{gmole}}{\text{g}_c \cdot \text{hr}} \right)$	$K_A (\text{bar}^{-1})$	R-squared	Catalyst
		* 10 ³			
REM1	142	25	2.3	91	Resin
	131	23	2.9	95	
	120	19	4.4	99	
REM2	142	7.9	9.3	96	Resin
	131	6.0	23	99	
	120	3.8	-44	100.	

Table A4.20 Kinetic and Adsorption Thermodynamic
Constants from Non-linear Regression Analysis.

The dehydration of ethanol.

Ether Formation.

Model	T°C	$K_R \left(\frac{\text{gmole}}{\text{g}_c \cdot \text{hr}} \right)$	S.DEV.	K_A	S.DEV.	SSR	CAT
		$* 10^3$	$* 10^3$	(bar ⁻¹)		$* 10^8$	
LHM	349	3.8	0.47	4.2	0.69	0.71	4A
	313	2.0	0.18	5.1	0.75	0.28	
	279	1.1	0.13	7.4	1.6	0.18	
REM1	349	16	0.82	4.2	0.69	0.71	4A
	313	10.	0.65	5.1	0.75	0.28	
	279	8.0	0.88	7.4	1.6	0.18	
LHM	142	25	0.80	1.2	0.23	1.4	Resin
	131	12	0.23	1.9	0.35	1.3	
	120	5.0	0.59	3.5	0.55	0.74	
REM1	142	29	2.5	1.2	0.29	1.4	Resin
	131	23	5.7	2.0	0.35	1.3	
	120	18	0.80	3.5	0.55	0.74	
REM2	142	9.8	1.3	4.5	1.6	1.1	Resin
	131	6.2	0.28	17	6.1	0.46	
	120	4.0	0.07	$1.5 \cdot 10^2$	0	0.41	

Table A4.21 Kinetic Data on the Dehydration of Isopropanol over Cation Exchange Resin.

Total pressure 1-bar gauge.

Mass of catalyst (dry basis) 2.97g.

T °C	V _A cc/hr	V _{N₂} cc/min	P _A	P _O	P _E	P _W	R _O gmole/g _C .hr.*10 ³	R _E	S
			bar						R _O /R _E
141	0.97	123	0.058	0.023	0.0002	0.024	1.3	0.013	94
	2.26	126	0.13	0.045	0.0016	0.047	2.6	0.092	28
	3.71	129	0.21	0.055	0.0034	0.058	3.4	0.21	15
	5.11	130	0.28	0.058	0.0066	0.063	3.8	0.41	9.2
	7.90	134	0.39	0.064	0.011	0.075	4.8	0.78	6.1
	10.6	134	0.49	0.072	0.013	0.085	5.8	1.2	4.8
	10.7	135	0.48	0.084	0.015	0.10	6.9	1.2	5.5

T °C	V _A cc/hr	V _{N₂} cc/min	P _A	P _O bar	P _E	P _W	R _O gmole/g _c .hr.*10 ³	R _E	S R _O /R _E
131	0.88	119.	0.057	0.019	0.0002	0.019	0.98	0.0097	101
	2.36	124	0.15	0.031	0.0018	0.033	1.8	0.11	19
	3.54	124	0.23	0.034	0.0033	0.037	2.0	0.20	10
	5.05	125	0.31	0.038	0.0050	0.043	2.4	0.32	7.6
	7.86	127	0.42	0.052	0.012	0.064	3.7	0.86	4.3
	11	132.	0.52	0.060	0.017	0.077	4.8	1.	3.6
119	1.03	123	0.067	0.018	0.0007	0.019	0.98	0.038	25
	2.35	124	0.16	0.023	0.0026	0.026	1.3	0.15	9.0
	3.76	125	0.24	0.028	0.0045	0.032	1.7	0.27	6.1
	5.01	125.	0.31	0.030	0.0060	0.036	2.0	0.38	5.2
	8.00	125.	0.44	0.042	0.014	0.056	3.0	0.97	3.1
	11	127	0.55	0.046	0.019	0.065	3.6	1.5	2.5

T °C	V _A cc/hr	V _{N₂} cc/min	P _A	P _O bar	P _E	P _W	R _O gmole/g _c .hr.*10 ³	R _E	S
110	0.96	120.	0.064	0.017	0.0008	0.017	0.87	0.043	20.
	2.41	121	0.17	0.021	0.0035	0.025	1.2	0.23	5.3
	3.89	123	0.25	0.026	0.0064	0.032	1.5	0.39	4.0
	5.50	125	0.33	0.029	0.0099	0.039	1.9	0.64	2.9
	8.07	125	0.46	0.031	0.014	0.044	2.2	0.95	2.3
	10.9	124	0.57	0.030	0.019	0.049	2.3	1.5	1.5

Table A4.22 Kinetic Data on the Dehydration of Ethanol over Cation Exchange Resin.

Total pressure 1-bar gauge.

Mass of catalyst (dry basis) 3.22g.

T °C	V _A cc/hr	V _{N₂} cc/min	P _A	P _O	P _E bar	P _W	R _O gmole/g _c .hr.*10 ³	R _E	S R _O /R _E
142	1.00	123	0.089	0.0006	0.0080	0.0088	0.034	0.41	0.08
	2.40	120	0.20	0.0008	0.018	0.019	0.039	0.96	0.04
	3.68	121	0.28	0.0008	0.026	0.027	0.043	1.5	0.03
	5.05	122	0.37	0.0008	0.036	0.037	0.044	2.2	0.02
	7.89	124	0.51	0.0007	0.050	0.051	0.044	3.5	0.01
131	0.95	121	0.085	0.0002	0.0084	0.0086	0.014	0.41	0.03
	2.36	122	0.20	0.0002	0.017	0.017	0.013	0.92	0.02
	3.62	122	0.29	0.0002	0.025	0.025	0.012	1.4	0.01
	6.42	123	0.45	0.0002	0.038	0.038	0.0089	2.5	0.004
	9.22	123	0.59	0.0002	0.046	0.046	0.011	3.3	0.003

T °C	V _A cc/hr	V _{N₂} cc/min	P _A	P _O	P _E bar	P _W	R _O gmole/g _c .hr.*10 ³	R _E	S R _O /R _E
120	1.04	121	0.090	0.0001	0.0088	0.0090	0.0046	0.44	0.011
	2.38	121	0.21	0.0001	0.016	0.016	0.0033	0.87	0.004
	4.40	122	0.35	0.0001	0.025	0.025	0.0019	1.5	0.001
	6.76	123	0.49	0.00002	0.030	0.030	0.0012	2.0	0.001
	9.22	123.	0.62	0.00002	0.033	0.033	0.0010	2.4	0.001

APPENDIX 5

THE PERCENTAGE DISTRIBUTION OF BUTENE

Table A5.1 The Percentage Distribution of butene
Using Zeolite 13X.

T °C	P _A bar	% 1-Butene	% Trans- 2-Butene	% cis 2-Butene	% Cis Trans
228	0.14	87	7.9	5.2	66
	0.24	83	10.	7.0	71
	0.31	83	10.	6.9	68
	0.39	83	10.	7.4	77
	0.48	83	10.	7.3	75
	0.57	84	9.2	7.3	79
	0.63	84	10.	7.9	76
Mean		84	10.	7.0	73
241	0.93	82	10.	7.8	75
	0.20	81	11	7.7	70.
	0.29	80.	11	8.3	73
	0.40	83	10.	7.4	74
	0.48	81	11	7.8	72
	0.57	81	11	8.1	73
Mean		81	11	7.9	73

T °C	P _A bar	% 1-Butene	% Trans 2-Butene	% Cis- 2-Butene	% Cis Trans
252	0.085	80.	12	8.8	73
	0.19	79	12	10.	83
	0.29	79	12	10.	83
	0.36	79	12	10.	83
	0.47	79	12	10.	83
	0.56	79	12	9.4	80.
Mean		79	12	9.3	78
258	0.12	80.	12	8.3	69
	0.21	78	12	9.7	81
	0.30	79	12	9.6	81
	0.42	78	12	9.6	81
	0.57	79	12	9.3	80.
	Mean		79	12	9.6
272	0.068	77	13	11	85
	0.17	78	12	10.	83
	0.26	78	12	10.	83
	0.34	78	12	10.	83
	0.40	78	12	10.	83
	0.52	78	12	10.	83
Mean		78	12	10.	83

T	P _A	%	% trans-	% cis-	$\frac{\% \text{ cis}}{\text{trans}}$
°C	bar	1-butene	2-butene	2-butene	
286	0.049	72	14	14	100.
	0.094	73	13	13.	100.
Mean		73	14	13	100.

T	P _A	%	% Trans-	% Cis-	<u>Cis</u> <u>Trans</u>
°C	bar	1-butene	2-butene	2-butene	
271	0.081	30.	63	7.1	0.11
	0.19	31	62	7.3	0.12
	0.28	31	62	7.2	0.12
	0.37	31	62	7.4	0.12
	0.51	32	61	7.3	0.12
	0.62	32	61	7.3	0.12
Mean		31	62	7.3	0.12
278	0.10	30.	64	6.4	0.10
	0.21	30.	63	6.5	0.10
	0.31	30.	63	6.9	0.11
	0.39	31	62	7.0	0.11
	0.49	31	62	7.5	0.12
	0.60	31	62	7.0	0.11
Mean		31	62	7.1	0.11
297	0.099	27	64	8.0	0.13
	0.21	28	64	8.1	0.13
	0.35	28	64	8.0	0.12
	0.44	28	64	8.2	0.13
	0.53	27	65	7.8	0.12
	0.62	27	65	7.7	0.12
Mean		28	65	8.0	0.12

Table A5.3 The Percentage Distribution of Butene
Using Zeolite ZNa.

T	P _A	%	% trans-	% cis-	<u>cis</u>
°C	bar	1-butene	2-butene	2-butene	<u>trans</u>
235	0.11	37	43	20.	0.48
	0.21	39	41	20.	0.49
	0.30	38	42	20.	0.48
	0.48	38	42	20.	0.47
	0.60	39	42	20.	0.48
Mean		38	42	20.	0.48
254	0.046	41	36	23	0.65
	0.098	40.	36	23	0.63
	0.27	41	37	22	0.60
	0.43	40.	37	22	0.60
	0.56	40.	38	22	0.59
Mean		41	37	23	0.61
275	0.11	40.	34	25	0.74.
	0.18	40.	35	25	0.72
	0.28	40.	35	24	0.72
	0.37	40.	35	25	0.71
	0.48	40.	35	25	0.72
	0.61	40.	35	25	0.71
Mean		40.	35	25	0.72

Table A5.2 The Percentage Distribution of Butene
Using Zeolite 4A.

T °C	P _A bar	% 1-Butene	% Trans- 2-Butene	% Cis- 2-Butene	$\frac{\text{Cis}}{\text{Trans}}$
232	0.088	44	51	5.0	0.098
	0.21	44	51	4.7	0.092
	0.29	43	51	5.5	0.10
	0.38	43	52	5.1	0.098
	0.48	43	52	5.3	0.10
	0.57	43	52	5.3	0.10
Mean		43	51	5.2	0.10
250	0.11	38	57	5.3	0.093
	0.21	38	56	5.5	0.098
	0.30	38	56	5.6	0.099
	0.39	38	56	5.5	0.098
	0.48	38	56	5.6	0.099
	0.60	38	56	6.0	0.11
Mean		38	56	5.6	0.10

T	P _A	%	% trans-	% cis-	<u>cis</u>
°C	bar	1-butene	2-butene	2-butene	trans
300	0.078	41	32	27	0.85
	0.18	40.	33	27	0.83
	0.26	40.	33	27	0.83
	0.41	41	33	27	0.82
	0.58	41	33	27	0.82
Mean		41	33	27	0.83

APPENDIX 6

EFFECTS OF EXTERNAL MASS AND HEAT TRANSPORT

Appendix 6Effects of External Mass and Heat Transport

Effects of external mass and heat transport on the dehydration of isopropanol over zeolite 13X in a fixed bed reactor.

Froment and Bischoff (105) gave the expressions for the the external concentration and temperature differences as

$$\frac{\Delta P_A}{P_{fA}} = \frac{R(P_{As}, T_s) \bar{M} Sc^{2/3}}{S_{ex} \phi G_{mA} j_d}$$

$$\Delta T = \frac{R(P_{As}, T_s) \bar{M} Pr^{2/3}}{S_{ex} \phi G_{mA} \bar{C}_p j_h}$$

where ϕ is the sphericity. For spherical pellet $\phi = 1.0$

Reaction Conditions.

Temperature	268 °C
Weight of catalyst	7.70 g
Conversion to propene	28 %
Conversion to di-iso-propyl ether	0.77 %
Partial pressure of isopropanol	0.18 bar
Mass flowrate of isopropanol	$8.4 \cdot 10^{-4}$ g/s
Mass flowrate of nitrogen	$38 \cdot 10^{-4}$ g/s

Average rate of dehydration reaction	$5.4 \cdot 10^{-7} \text{ gmole/g}_c\text{s}$
Heat capacity C_p	$0.25 \text{ cal/gmole } ^\circ\text{K}$
EXternal surface area of catalyst	$32 \text{ cm}^2/\text{g}$

Mass flowrate per unit cross sectional area of the reactor.

$$A_R = \pi d_t^2 / 4 = \pi (1.03)^2 / 4 = 2.6$$

$$G_{mA} = 46 \cdot 10^{-4} / 2.6 = 18 \cdot 10^{-4} \text{ g/cm}^2\text{s}$$

Reynolds number Re_p (see table 6.3)

$$Re_p = \frac{1.6 \cdot 10^3 G_m}{1.6 \cdot 10^3 \times 46 \cdot 10^{-3}}$$

$$7.6$$

Chilton - Colborn factors

For mass transfer, the Chilton-Colborn factor is given by

$$j_d = 0.84 Re^{-0.51} \quad \text{for } Re < 190$$

$$= 0.84 (7.6)^{-0.51}$$

$$J_d = 0.3$$

The Chilton-Colborn factor, for the heat transfer is related to its mass transfer factor by

$$j_h = 1.076 j_d$$

$$= 0.32$$

Schmidt number Sc .

$$Sc. = \frac{\mu}{\rho_f D_{mA}}$$

The mean density of the fluid is given by

$$\bar{\rho}_f = \frac{\bar{M} P_t}{R_g T}$$

$$\begin{aligned} &= \frac{31 \times 2}{82 \times 541} \\ &= 1.4 \times 10^{-3} \text{ g/cm}^3 \end{aligned}$$

$$\text{Viscosity, } \mu = 1.7 \times 10^{-4} \text{ g/cm s}$$

The molecular diffusivity of isopropanol in the mixture is $5.5 \times 10^{-2} \text{ cm}^2/\text{s}$.

Therefore Schmidt number = 2.2

Heat of reaction ΔH_R is $12 \times 10^3 \text{ cal/gmole}$

Hence

$$\frac{\Delta P_A}{P_{fA}} = \frac{5.3 \times 10^{-7} \times 31 \times (2.2)^{2/3}}{32 \times 2.9 \times 10^{-3} \times 0.30}$$

$$\frac{\Delta P_A}{P_{fA}} = 10^{-3} = 0.10 \%$$

and

$$\Delta T = \frac{5.4 \cdot 10^{-7} \times 12 \cdot 10^3 \times 0.7^{2/3}}{0.25 \times 32 \times 2.9 \times 0.32}$$

$$\Delta T = 0.71^{\circ}\text{K} = 0.71^{\circ}\text{C}$$

The Prandtl number is assumed to be 0.7. This is true for most gas mixtures.

The results of the assessment show that the effects of external mass and heat transfer on the dehydration of isopropanol over zeolite 13X is insignificant under the reaction conditions investigated.

Table A6.1 The Comparison Between the Predictions of
the Model and the Experimental Data.

Mass of Catalyst 7.70g^{*}, 5.06g.

Flowrate of Nitrogen at 268, 254 and 242°C 200 cc/min

Flowrate of Nitrogen at 277, 257 and 239°C 220 cc/min

Flowrate of Nitrogen at 278, 262 and 243°C 460 cc/min.

T °C	V _A cc/hr	P _A bar	X _O			X _E		
			Expt.	Pred.	%Dev.	Expt.	Pred.	% Dev.
268 [*]	3.27	0.18	28	29	-5.8	0.77	0.34	56
	9.28	0.40	13	13	0.0	0.71	0.56	21
	13.8	0.54	9.0	8.7	2.8	0.57	0.59	-3.5
	18.2	0.65	7.3	6.7	8.1	0.48	0.59	-22
	22.4	0.75	6.1	5.5	10	0.40	0.57	-43
254 [*]	3.68	0.18	12	17	-38	0.56	0.46	18
	7.90	0.35	6.4	8.7	35	0.39	0.55	41
	12.2	0.50	4.4	5.8	-41	0.29	0.52	-79
	16.2	0.61	3.5	4.5	-29	0.24	0.48	-100
	20.6	0.71	2.8	3.5	-26	0.19	0.44	-131
	25.8	0.82	2.3	2.9	-22	0.19	0.39	-144
278	11.3	0.23	10.4	10	4	0.35	0.11	2.2 10 ²
	16.1	0.25	7.8	8.4	-8.4	0.31	0.11	2.8 10 ²
	21.7	0.39	6.2	5.2	17	0.28	0.15	87
	28.4	0.48	5.1	4.0	22	0.23	0.17	35

T °C	V _A cc/hr	P _A bar	X _O			X _E		
			Expt.	Pred.	% Dev.	Expt.	Pred.	% Dev.
242*	3.85	0.19	5.4	8.8	64	0.28	0.47	-68
	6.48	0.30	3.5	6.0	-70	0.21	0.45	-1.1 10 ²
	9.45	0.41	2.5	4.4	-75	0.16	0.40	-1.5 10 ²
	14.0	0.55	1.7	3.1	-79	0.12	0.33	-1.8 10 ²
	18.2	0.66	1.4	2.4	-70	0.10	0.28	-1.8 10 ²
	22.5	0.76	1.2	2.0	-65	0.09	0.24	-1.7 10 ²
	26.2	0.83	1.1	1.7	-59	0.08	0.22	-1.8 10 ²
262	11.4	0.23	3.9	5.4	-38	0.17	0.15	35
	14.2	0.27	3.3	4.4	-31	0.16	0.16	0
	18.3	0.34	2.7	3.3	-19	0.13	0.17	-31
	22.9	0.41	2.3	2.5	-12	0.12	0.17	-42
	28.2	0.48	2.0	2.0	0	0.10	0.17	-70
243	11.2	0.23	1.2	2.2	-87	0.063	0.14	-1.1 10 ²
	14.1	0.28	0.95	1.9	-95	0.053	0.13	-1.5 10 ²
	18.2	0.34	0.76	1.5	-100	0.044	0.13	-1.8 10 ²
	24.0	0.43	0.62	1.2	-90	0.036	0.11	-1.1 10 ²
	28.3	0.49	0.55	1.0	-82	0.032	0.10	1.2 10 ²
277*	11.3	0.42	14	15	2	1.1	0.46	43
	11.1	0.42	16	15	9	0.87	0.46	47
	28.4	7.3	7.3	5.9	20	0.54	0.52	4

T °C	V _A cc/hr	P _A bar	X _O			X _E		
			Expt.	Pred.	% Dev.	Expt.	Pred.	% Dev.
357*	13.6	0.49	4.3	5.9	-35	0.34	0.49	-44
	16.8	0.57	3.9	4.7	-35	0.35	0.47	-34
	19.4	0.63	3.5	4.2	-20	0.28	0.45	-61
	22.5	0.70	3.1	3.2	-4	0.26	0.40	-54
	25.4	0.75	2.7	3.3	-21	0.23	0.41	-78
	28.4	0.81	2.6	2.9	-13	0.22	0.39	-56
239*	16.8	0.58	1.1	2.2	-99	0.068	0.23	-1.4 10 ²
	19.5	0.64	0.94	1.9	-102	0.059	0.21	-1.6 10 ²
	22.6	0.70	0.91	1.7	-85	0.07	0.19	-1.7 10 ²
	25.1	0.76	0.84	1.5	-80	0.068	0.18	-1.7 10 ²
	28.4	0.82	0.76	1.4	-56	0.068	0.16	-1.4 10 ²

Table A6.2 The Values of the Estimated Parameters.

Molecular weight of isopropanol	60 g/mole
Density of isopropanol	0.79 g/cc
Density of nitrogen at room conditions	$1.2 \cdot 10^{-3}$ g/cc
Viscosity of the mixture	$1.7 \cdot 10^{-4}$ g/cms
Diameter of reactor	1.03 cm
Particle diameter	0.15 cm
Bulk density	0.67 g/cc
Density of the material	2.0 g/cc
Density of the pellet	1.3 g/cc
Porosity of the bed	0.66
External surface area of the pellet	32 cm ² /g
Pelect Number for the radial diffusion	10
Radial effective diffusivity	$1.1 \cdot 10^{-2} U_s \text{ cm}^2/\text{s}$
Pelect Number for the axial diffusion	1.5
Axial effective diffusivity	$0.1 U_s \text{ cm}^2/\text{s}$
Reynolds Number ($Re_p = \frac{G_m d_p}{\epsilon \mu A_c}$)	$1.6 \cdot 10^3 G_m$

REFERENCES

REFERENCES.

1. Pine, H. and Manassen, J.
Advances in Catalysis, 1966, 16, 49.
2. Venuto, P. B. and Landis, P. S.
Advances in Catalysis, 1968, 18, 259.
3. Emmett, P. H. (Ed. Winfield, M. E.)
Catalysis, 1960, 7, 93.
4. Rudham, R. and Stockwell, A.
Catalysis, 1977, 1, 87. The Chemical Society.
London.
5. John, C. S. and Scurell, M. S.
Catalysis, 1977, 1, 154. The Chemical Society, London.
6. Knozinger, H.
Advances in Catalysis, 1976, 25, 184.
7. Russell, R. W.
Hydrocarbon Processing, May, 1980, 223.
8. Winter, O. and Eng, M.
Hydrocarbon Processing, Nov., 1976, 125.
9. Hersh, C. K.
"Molecular Sieves", 1961, 79.
Reinhold Publishing Co-operation.
10. Banthorpe, D. V.
"Elimination Reactions", 1963.
Elsevier, Amsterdam, Holland.

11. Noller, H. and Kladnig, W.
Cat. Review-Sci. and Eng., 1976, 13, 149.
12. Noller, H. Andreu, P. and Hunger, M.
Angew. Chem. (int. edn.), 1971, 3, 172.
13. Jain, J. R. and Pillai, C. N.
J. Catalysis, 1970, 9, 322.
14. Leaute, R and Lana, I. G. D.
J. Catalysis, 1979, 60, 460.
15. Gerai, S. V., Ruzhkova, E. U. and Gorokhovatsky, Ya. B.
J. Catalysis, 1973, 28, 341.
16. Perona, J. J. and Thodos, G.
AIChE J., 1957, 3, 230.
17. Thomas, J. M.
J. of Chem. Educ., 1961, 38(3), 138.
18. Knozinger, H., Kochloefl, K. and Meye, W.
J. Catalysis, 1973, 28, 69.
19. Thomke, K. and Noller, H.
Proceedings of the 5th Int. Congr. on Catalysis,
1973, 3, 1183, Elsevier, Amsterdam.
20. Thomke, K.
Proceedings of the 6th Int. Congr. on Catalysis,
1976, 303, Elsevier, Amsterdam.
21. Kabel, R. L. and Johanson, L. N.
J. Chem. Eng. Data, 1961, 6, 496.
22. Stull, D. R., Westrum, Jr. E. F. and Sinke, G. C.
'The Chemical Thermodynamic of Organic Compounds',
John Wiley and Sons, N. Y. 1969.

23. Kochar, N. K., Merims, R. and Padia, A. S.
Chem. Eng. Progr., June, 1981, 66.
24. Irani, R. K., Kulkarni, B. D., Doraiswamy, L. K.
and Hussain, S. Z. Ind. Eng. Chem. Proc. Des, Dev.,
1982, 21, 192.
25. Alvarado, M.
J. Amer. Chem. Soc., 1928, 50, 790.
26. Balaceanu, J. C. and Jungers, J. C.
Bull Soc. Chim., Belg., 1951, 60, 476.
(Source: Chem. Abstr., 1953, 47, 2683c)
27. Brey, W. S. and Krieger, K. A.
J. Amer. Chem. Soc., 1949, 71, 6637.
28. Kimura, T., Watanabe, M., Kikuchi, E. and Morita, Y.
Bulletin of Sci. and Eng. Res. Lab., Waseda
University, 1975, 69, 35.
29. Topchieva, K. V. and Yun-Pin, K.
Zh. Fiz. Khim., 1955, 29(10), 1854.
30. Bennet, D. E. R. and Ross, R.A.
J. Chem. Soc., 1968, A, 1524.
31. Yoshida, S., Akimotu, K., Koshimidzu, Y. and Tarama, K.
Int. Chem Res., Kyoto University, 1975, 53, No 2.
32. Butt, J. B., Bliss, H. and Walker, C.A.
AIChE J., 1962, 8, 42.
33. Gottifredi, J. C., Yeraman, A. A. and Cunningham, R. E.
J. Catalysis, 1968, 12, 245.
34. Kabel, R. L. and Johanson, L. N.
AIChE J., 1962, 8, 621.

35. Figueras, F., Nohl, A., De-Mourgues, L. and Tranbonze, Y. Trans. of the Faraday Soc., 1971, 67, 1155.
36. Knozinger, H. and Kohne, R.
J. Catalysis, 1966, 5, 264.
37. Knozinger, H., Ress, E. and Buhl, H.
J. Catalysis, 1968, 12, 121.
38. De-Boer, J. H., Fahim, R. B., Linsen, B. G., Visseren, W. J. and De-Vleesschauwer, W. F. N. M.
J. Catalysis, 1967, 7, 163.
39. Pines, H. and Simonik, J.
J. Catalysis, 1972, 24, 220.
40. Gele, R.L., Haber, J. and Stone, F. S.
J. Catalysis, 1962, 1, 32.
41. Zundel, G., Noller, H. and Schwab, G. M.
Z. Electrochem., 1962, 66, 225.
42. Noller, H., Rosa-Brusin, M. and Andreu, P.
Angew. Chem. Int. Edn., 1967, 6, 170.
43. Krishnaprasad, T.N. and Ravindram, M.
Hungarian J. of Ind. Chem., 1977, 5, 13.
44. Bryant, D. E. and Kranich, W. L.
J. Catalyst, 1967, 8, 8.
45. Ralek, M. and Gruber, O.
Proceedings on the 3rd Int. Congress on Catalysis,
1964, 2, 1302, Elsevier, Amsterdam, Holland.
46. Gates, B. C. and Johanson, L. W.
AIChE J., 1971, 17, 981.
47. Gates, B. C. and Johanson, L. W.
J. Catalysis, 1969, 14, 69.

48. Kabel, R.L.
AIChE J., 1968, 14, 358.
49. Hsu, S.M. and Kabel, R.L.
AIChE J., 1974, 20, 713.
50. Hsu, S.M. and Kabel, R.L.
J. Catalysis, 1974, 33, 74.
51. Thornton, R. and Gates, B.C.
J. Catalysis, 1974, 34, 275.
52. Gates, B.C. and Schwab, G.M.
J. Catalysis, 1969, 15, 430.
53. Health, H.W. Jr, and Gates, B.C.
AIChE J., 1972, 18, 321..
54. Gates, B.C., Wisnovskas, J.S. and Health, H.W. Jr.
J. Catalysis, 1972. 24. 320.
55. Kittrell, J.R., Mezaki, R. and Watson, C.C.
Ind. Eng. Chem. 1965, 57, (12). 18.
56. Lapidus, L. and Peterson, T.I.
AIChE J., 1965, 11, 891..
57. Franckaerts, J. and Froment, G. F.
Chem. Eng. Sci., 1964, 19, 807..
58. Carnahan, B., Luther, H. A. and Wilkes, J. O.
"Applied Numerical Methods", 1969.
John Wiley and Sons.
59. Dzisko, V. A., Borisova, M. S., Kotsarenko, N. S.
and Kusnatsova, E. V.
Kinetics and Catalysis, USSR, Engl. Transl., 1962, 3, 633.

60. Froment, G. F.
Proceedings of fifth European Symp. on Chemical
Reaction Engineering, 1972, A5.1.
61. Stone, F. S. and Agudo, A. L.
Z. Phy. Chem., Frankfurt, 1969, 64, 161.
62. Butler, J. D., Poles, T. C. and Wood, B. T.
J. Catalysis, 1970, 16, 239.
63. Kobayashi, H. and Kobayashi, M.
Cat. Rev.-Sci. and Eng., 1974, 10(2), 139.
64. Topchieva, K. V. and Tkhoang, H. S.
Kinetics and Catalysis, USSR, 1973, 14, 398.
65. Topchieva, K. V. and Tkhoang, H. S.
Kinetics and Catalysis, USSR, 1973, 14, 1491.
66. Young, L. C. and Finlayson, B. A.
Ind. Eng. Chem. Fund., 1973, 12(4), 412.
67. Gentry, S. J. and Rudham, R.
J. Chem. Soc. Trans. Faraday, I, 1970, 70, 1685.
68. Baiker, A., Cascnova, R. and Richaz, W.
German Chem. Eng. J., 1980, 3, 112.
69. Dixon, W. J. and Brown, M. B.
"Biomedical Computer Programs"
University of California Press, 1979.
70. Thaller, L. H. and Thodos, G.
AIChE J., 1960, 3, 369.
71. Gryaznova, Z. V., Ermilova, M. M., Tsitsishvili, G. V.,
Androwiashvilli, T. G. and Krupennikova, Yu. A.
Kinetics and Catalysis, USSR, 1969, 10, 1099.

72. Maurer, J. F. and Sliepcevich, C. M.
AIChE. Progr., Symp. Series, 1952, 48(4), 31.
73. Stauffer, J. E. and Kranich, W. L.
Ind. and Eng. Chem. Fund. 1962, 1(2), 107.
74. Miller, D. N. and Kirk, R. S.
AIChE J., 1962, 8(2), 183.
75. Pines, H. and Haag, W. D.
J. Amer. Chem. Soc., 1960, 82, 2471.
76. Kladnig, W. and Noller, H.
J. Catalysis, 1973, 29, 385.
77. Knozinger, H. and Scheglila, A.
J. Catalysis, 1970, 29, 252.
78. Jewur, S. S. and Moffat, J. B.
J. Catalysis, 1979, 59, 167.
79. Knozinger, H. and Buhl, H.
Z. Phy. Chem. N. F., 1969, 63, 199.
(Source: Reference No 11)
80. Rabo, J. A.
'Zeolite Chemistry and Catalysis', Collection of
Papers on the Int. Conference on Zeolite., 1976,
ACS., Washington, D. C.
81. Breek, D. W.
'Zeolite Molecular Sieve, Structure, Chemistry
and Use', 1974, John Wiley, N. Y.
82. Mays, R. L. and Pickert, P. E.
'Molecular Sieve, Zeolite Catalysts and their
Properties and Applications', Int. Conference
on Molecular Sieves at London, 1967, Soc. of Chem.,
London.

83. Turkenich, J.
Cat. Review-Sci. and Eng., 1968, 1, 1.
84. Gould, R. F.
'Molecular Sieve, Zeolites I and II, Synthesis,
Structure, General Properties and Catalysts', 1971,
ACS, Washington, D. C.
85. Sand, L. B. and Mumpton, F. A.
'Natural Zeolites', Papers Presented at Zeolite
Int. Conference at Tucson, Arizona, June, 1976.
86. Roberts, C. W.
Paper Presented at Symp. on 'The Properties and
Applications of Zeolites' at The City University, 1979.
87. Weisz, P. B., Frilette, V. J., Maatman, R. W. and
Mower, E. B. J., Catalysis, 1962, 1, 307.
88. Weisz, P. B. and Friletter, V. J.
J. phy. Chem., 1960, 44, 382.
89. Frilette, V. J., Weisz, P. B. and Golden, R. L.
J. Catalysis, 1962, 1, 301.
90. Lister, B. A. J.
The Ind. Chemist, 1956, July, 257.
91. Kunin, R., Frisch, N. W., Fisher, S. A., Metzner,
E. F. and Oline, J. A., Ind. Eng. Chem Prod. Res.
and Develop., 1962, 1, 140.
92. Berranch, L.
Cat. Rev.-Sci. and Eng., 1977, 16(1), 1.
93. Weisz, P. B. and Practer, C. D.
Advances in Catalysis, 1954, 6, 143.

94. Santacesaria, E., Morbidelli, M. and Carra, S.
Chem. Eng. Sci., 1981, 36, 909.
95. Csicserry, S. M.
Amer. Chem. Soc. Monogr., 1976, 171, 80.
96. Chen, N. Y. and Weisz, P. B.
Chem. Eng. Prog. Symp. Series, 1967, 63, 73.
97. Weisz, P. B.
Chem. Tech., 1973, 3, 498.
98. Imelik, B., Naccache, C., Taarit, Y. B.,
Vedrine, J. C., Coudurier, G. and Polaiiaud, H.
"Catalysis by Zeolites", Proceedings of an Int. Symp.,
Ecully., pp6, 1980, Elsevier, Amsterdam, 1980.
99. Minachev, Kh. M.
"Application of Zeolites in Catalysis", The first All-
Union Conference on Molecular Sieves in Catalysis, Nov
Nov. 1976, Akademiai Kiado, Budapest, 1979.
- 100 Haering, E. R.
"Dynamic Adsorption and Desorption Studies of
t-Butyl Alcohol, Water and Iso-butylene", Ph.D
Thesis, 1966, The Ohio State University, USA.
- 101 Coulson, J. M. and Richardson, J. F.
"Chemical Engineering", Vol.3, Pergamon Press, 1979.
102. De-Mourgues, L., Peyron, F., Trambouze, Y. and Pettre, M . .
J. Catalysis, 1967, 7, 117.
103. Andrianova, T. I. and Bruns, B. P.
Kinetika i Kataliz, 1960, 1(3), 440.
104. Draper, n. R. and Smith, H.
"Applied Regression Analysis", John Wiley and Sons, 1966.

105. Froment, F. G. and Bischoff, K. B.
"Chemical Reactor Analysis and Design", John Wiley
John Wiley and Sons, NY, 1980.
106. Rase, H. F.
"Chemical Reactor Design for Process Plant",
John Wiley and Sons, NY, 1977.
107. Doraiswamy, L. K. and Tajbl, D. G.
Cat. Rev. Sci. and Eng., 1974, 10(2), 177.
108. Magee, T. R. A.
"The Catalytic Dehydration of Alcohol in Fluidised Bed",
Ph.D. Thesis, The Queen's University of Belfast, 1975.
109. Zen'Kovich, I. A. and Topchieva, K. V.
Int. Chem. Eng., 1972, 12(3), 469.
110. Carberry, J. J.
Ind. Chem. Eng., 1964, 56(11), 39.
111. Hammett, L. P.
J. Amer. Chem. Soc., 1948, 70, 3444.
112. Denbigh, K. G.
Trans. Faraday Soc., 1944, 40, 352.
113. Tajbl, D. G., Simons, J. B., and Carberry, J. J.
Ind. and Eng. Chem. Fund., 1966, 5, 171.
114. Tajbl, D. G.
Can. J. Chem. Eng., 1969, 47, 154.
115. Tajbl, D. G.
Ind. Eng. Chem. Proc. Des. Develop., 1969, 8(3), 364.
116. Ford, F. E. and Perlmutter, D. D.
Chem. Eng. Sci., 1964, 19, 371.
117. Trifiro, T., Banfi, C., Caputo, G., Forzahi, P.
and Pasquon, I.
J. Catalysis, 1973, 30, 393.

118. Choudhary, V. R. and Doraiswamy, L. K.
Ind. Eng. Chem. Proc. Des. Develop., 1972, 11(3), 420.
119. Brisk, M. L., Day, R. L., Jones, M. and Warren, J. B.
Trans. Instn. Chem. Engrs., 1968, 46, T3.
120. Partner, M. R. C.
"A Study of Catalytic Reforming"., Ph.D. Thesis,
1977, Bath University, Bath, U.K.
121. Kitrell, J. R.
Advances in Chem. Eng., 1970, 8, 97.
122. Carberry, J. J. and Wendel, M. A.
AIChE J., 1963, 9(1), 129.
123. Mindrup, R.
J. of Chrom. Sci., 1978, 16, 380.
124. Thomas, J. M. and Thomas, W. J.
"Introduction to the Principles of Heterogeneous
Catalysis", London, Academic Press, 1967.
125. Hougen, O. A. and Watson, K. M.
"Chemical Process Principles", Part III, John
Wiley and Sons, N. Y., 1953.
126. Yang, K. H. and Hougen, O. A.
Chem. Eng. Progr., 1950, 46(3), 146.
127. Weller, S. W.
AIChE J., 1956, 2, 59.
128. Boundart, M.
AIChE J., 1956, 2, 62.
129. Weller, S. W.
Adv. Chem. Ser., 1975, 148, 26.
130. Mezaki, R. and Happel, J.
Cat. Rev.-Sci. and Eng., 1969, 3, 241.

131. Brunauer, S., Emmett, P. H. and Teller, E.
J. Amer. Chem. Soc., 1938, 60, 309.
- 132 De-Boer, J. H.
Advances in Catalysis, 1957, 9, 472.